uOttawa

L'Université canadienne
Canada's university

FACULTÉ DES ÉTUDES SUPÉRIEURES ET POSTOCTORALES

uOttawa

L'Université canadienne
Canada's university

FACULTY OF GRADUATE AND POSDOCTORAL STUDIES

Brian David Melanson
AUTEUR DE LA THÈSE / AUTHOR OF THESIS

Ph.D. (Cellular and Molecular Medicine)
GRADE / DEGREE

Department of Cellular and Molecular Medicine
FACULTÉ, ÉCOLE, DÉPARTEMENT / FACULTY, SCHOOL, DEPARTMENT

Post-transcriptional Regulation of DNA Damage Binding Protein 2 and the Identification of a Novel mRNA Stability Determinant

TITRE DE LA THÈSE / TITLE OF THESIS

Bruce McKay
DIRECTEUR (DIRECTRICE) DE LA THÈSE / THESIS SUPERVISOR

CO-DIRECTEUR (CO-DIRECTRICE) DE LA THÈSE / THESIS CO-SUPERVISOR

Christina Addison

Jocelyn Côté

Martin Holcik

Chow Lee
U. of Northern British Columbia

Gary W. Slater
Le Doyen de la Faculté des études supérieures et postdoctorales / Dean of the Faculty of Graduate and Postdoctoral Studies

Post-transcriptional regulation of DNA Damage Binding protein 2 and the identification of a novel mRNA stability determinant

Brian D Melanson

Thesis submitted to the
Faculty of Graduate and Postdoctoral Studies
In partial fulfillment of the requirements
For the PhD degree in Cellular and Molecular Medicine

Cellular and Molecular Medicine
Faculty of Medicine
University of Ottawa

Your file Votre référence
ISBN: 978-0-494-73902-0
Our file Notre référence
ISBN: 978-0-494-73902-0

Chapter 1: Preliminary Pages

1.1 Authorization for use of published figures and tables

1. Figure 1 was reproduced and adapted with permission from: Tyrrell, R.M., *Activation of mammalian gene expression by the UV component of sunlight--from models to reality.* Bioessays, 1996. **18**(2): p. 139-48.

   License Number: 2411031237396
   License date: Apr 16, 2010
   Licensed content publisher: John Wiley and Sons
   Licensed content publication: BioEssays
   Portion used: Figures / tables
   Number of figures / tables: 1
   Requestor type: Student
   Type of Use: Thesis / Dissertation

2. Figures 2A, 4B and 5B were reproduced and adapted from: Latonen, L. and M. Laiho, *Cellular UV damage responses--functions of tumor suppressor p53.* Biochim Biophys Acta, 2005. **1755**(2): p. 71-89.

   License Number: 2411040954520
   License date: Apr 16, 2010
   Licensed content publisher: Elsevier
   Licensed content publication: Biochimica et Biophysica Acta - Reviews on Cancer
   Portion used: Figures / tables
   Number of figures / tables: 3
   Requestor type: Student
   Type of Use: Thesis / Dissertation

3. Figure 2B was reproduced and adapted with permission from: Sugasawa, K., *UV-induced ubiquitylation of XPC complex, the UV-DDB-ubiquitin ligase complex, and DNA repair.* J Mol Histol, 2006. **37**(5-7): p. 189-202.

   License Number: 2411041421614
   License date: Apr 16, 2010
   Licensed content publisher: Springer
   Licensed content publication: Journal of Molecular Histology
   Portion used: Figures / tables
   Number of figures / tables: 1
   Requestor type: Student
   Type of Use: Thesis / Dissertation

4. Figure 3 was reproduced and adapted from: Sugasawa, K., *Xeroderma pigmentosum genes: functions inside and outside DNA repair.* Carcinogenesis, 2008. **29**(3): p. 455-65. Published by Oxford University Press.

> This publication does not require permission for academic uses. "The person using Carcinogenesis Online may view, reproduce or store copies of articles comprising the journal provided that the articles are used only for their personal, non-commercial use." (http://carcin.oxfordjournals.org/misc/terms.dtl)

5. Table 1 was reproduced and adapted with permission from: Hanawalt, P.C. and G. Spivak, *Transcription-coupled DNA repair: two decades of progress and surprises.* Nat Rev Mol Cell Biol, 2008. **9**(12): p. 958-70.

> License Number: 2411061483536
> License date: Apr 16, 2010
> Licensed content publisher: Nature Publishing Group
> Licensed content publication: Nature Reviews Molecular Cell Biology
> Portion used: Figures / tables
> Number of figures / tables: 1
> Requestor type: Student
> Type of Use: Thesis / Dissertation

6. Figures 4A and 5A were reproduced and adapted from: Ljungman, M., *Dial 9-1-1 for p53: mechanisms of p53 activation by cellular stress.* Neoplasia, 2000. **2**(3): p. 208-25. Published by Neoplasia Press.

> This publication does not require permission for academic uses. "Transmission, reproduction, or reuse of protected material, beyond that allowed by the fair use principles of the copyright laws, requires the written permission of the copyright owners." (http://www.ncbi.nlm.nih.gov/pmc/about/copyright.html)

7. Table 2 was adapted with permission from: Raghavan, A. and P.R. Bohjanen, *Microarray-based analyses of mRNA decay in the regulation of mammalian gene expression.* Brief Funct Genomic Proteomic, 2004. **3**(2): p. 112-24. Published by Oxford University Press.

> Thank you for your email dated 17 April 2010 requesting permission to reprint the above material. Our permission is granted without fee to reproduce the material. Use of the above is restricted to reproduction of 1 table in a Thesis to the University of Ottawa available in print/electronic format only, to be used only in the English language. This permission is limited to this particular use and does not allow you to use it elsewhere or in any other format other than specified above.

8. Figure 7 was reproduced and adapted from: Kedersha, N., et al., *Stress granules and processing bodies are dynamically linked sites of mRNP remodeling.* J Cell Biol, 2005. **169**(6): p. 871-84. Published by the Rockefeller University Press.

   This publication does not require permission for academic uses: "Third parties may reuse our content for noncommercial purposes without specific permission as long as they provide proper attribution "
   (http://www.rupress.org/site/misc/permissions.xhtml)

9. Figure 8 was reproduced with permission from: Keene, J.D., *RNA regulons: coordination of post-transcriptional events.* Nat Rev Genet, 2007. **8**(7): p. 533-43.

   License Number: 2411081219004
   License date: Apr 16, 2010
   Licensed content publisher: Nature Publishing Group
   Licensed content publication: Nature Reviews Genetics
   Portion used: Figures / tables
   Number of figures / tables: 1
   Requestor type: Student
   Type of Use: Thesis / Dissertation

10. Figure 10A was reproduced and adapted with permission from: Gannon, J.V. and D.P. Lane, *Protein synthesis required to anchor a mutant p53 protein which is temperature-sensitive for nuclear transport.* Nature, 1991. **349**(6312): p. 802-6.

    License Number: 2411030027174
    License date: Apr 16, 2010
    Licensed content publisher: Nature Publishing Group
    Licensed content publication: Nature
    Portion used: Figures / tables
    Number of figures / tables: 1
    Requestor type: Student
    Type of Use: Thesis / Dissertation

1.2 Abstract

UV light is a potent inducer of the p53 tumour suppressor, a transcription factor that positively regulates a large number of UV-responsive transcripts. However, UV light also induces RNA polymerase-blocking DNA lesions in a stochastic manner. This poses a challenge to the coordinated regulation of UV-responsive gene expression. We previously reported a UV dose-dependent shift in the spectrum of p53 induced target genes towards smaller genes with fewer and smaller introns. Here, we report that the DDB2 transcript is induced more strongly than other similar sized p53 target genes (FAS or MDM2) following UV exposure. The preferential induction of DDB2 mRNA is not due to the expression of a cryptic internal promoter. Instead, the DDB2 transcript was found to be unstable prior to UV exposure and its half-life was increased significantly in a UV dose-dependent manner. UV light did not affect the stability of the FAS or MDM2 mRNAs. Cis-acting elements within the 3'UTR of transiently expressed transcripts often target labile mRNAs for rapid degradation. The DDB2 3'UTR induced a rapid increase in mRNA turnover of an EGFP reporter gene that was also observed at the protein level. Using this reporter system, we localized a destabilizing element within a 49 nucleotide region, and have termed this the 3'UTR DDB2 destabilizing element (3'DDE). Structural analysis of the 3'DDE predicted the presence of distinct structural features. Mutational analysis of these structures further isolated a minimal 14nt region that is required to elicit rapid mRNA turnover. Given the role of DDB2 in nucleotide excision repair, we suggest that its post-transcriptional regulation contributes to recovery from UV-induced DNA damage. In addition to DDB2, we found that the mRNA of p53 target-genes are generally short-lived. We propose that this phenomenon has evolved as a method to keep p53-mediated pro-apoptotic and anti-survival stress responses in check.

1.3 Table of Contents

1.4 List of Tables

1.5 List of Figures

Chapter 2 Introduction

Chapter 3 Materials and Methods

Chapter 4 Results

Chapter 5 Discussion

Chapter 7.1 Appendix I: Supplemental data

1.6 List of abbreviations

3'/5'UTR - 3' or 5' untranslated region

3'DDE - 3'UTR DDB2 destabilizing element

6-4PP - 6-4 photoproduct

ACP2- lysosome acid phosphatase 2

Act D - actinomycin D

AMD - ARE-mediated decay

ARE - AU-rich element

ARE-BP - ARE-binding protein

BER - base excision repair

CDK - cyclin-dependent kinase

CHX - cycloheximide

CPD - cyclobutane pyrimidine dimer

CUG-BP1 - CUG-binding protein 1

d2EGFP - destabilized enhanced green fluorescent protein

DDB1/2 - DNA damage binding protein 1 and 2

Dox - doxycycline

FACS - fluorescence activated cell sorting

FL Ins - full-length insert

GG-NER - global genomic nucleotide excision repair

HeLa TO - HeLa Tet-off cells

HR - homologous recombination

HT29-tsp53 - temperature sensitive p53-expressing HT29 colorectal carcinoma cells

-Ins - minus insert

IR - ionizing radiation

IRE - iron response element

MAPK - mitogen-activated protein kinase

miRNA - micro RNA

MMR - mismatch repair

ncRNA - non-coding RNA

NER - nucleotide excision repair

NHEJ - nonhomologous end-joining

NMD - nonsense-mediated decay

PTC - premature termination codon

RBP - RNA binding protein

RISC - RNA-induced silencing complex

RNApolII - RNA polymease II

RNP - ribonuclear protein complex

ROS - reactive oxygen species

RT-PCR - reverse transcriptase polymerase chain reaction

SLmut - stem-loop mutant

SSmut - single-stranded mutant

TC-NER - transcription-coupled nucleotide excision repair

TFIIH - transcription factor IIH

TLS - translesion synthesis

TTP - tristetraprolin

XP - xeroderma pigmentosum

1.7 Acknowledgments

Many people have offered me technical assistance, support, guidance, and understanding over the long years of my graduate work. I extend my sincere gratitude to all of them, and anyone I have left off this list.

I would like to thank Paul Oleynik from the Flow Cytometry Facility of StemCore Laboratories at the Ottawa Genomics Innovation Center in Ottawa, ON for his highly valued assistance in generating the EGFP-enriched HeLa cell lines used in this work.
I also offer my gratitude to my Ph.D. Advisory committee of Drs. Douglas Grey, Martin Holcik and Barbara Vanderhyden. Without your careful guidance and advice, this project would not have succeeded. To my fellow lab members both past and present, especially Jeff Hamill, Lawton Stubbert, Jennifer Smith and Christine MacKinnon-Roy, thank you is not enough for making my time in the lab as rewarding and enjoyable as possible (and for the always invigorating coffee-breaks). My thesis supervisor, Dr. Bruce McKay has been an exemplary mentor who has always made himself available and open to discussion. His support and unyielding vision have truly been the driving force of this research project.

My family, and especially my father have been there for me when things looked bleak, encouraging me to push on. I hope you know just how much your support and pride in me have helped me persevere and accomplish all I have done over these years.

Finally, to my wife Isabelle, who has taken the brunt of the many sacrifices the pursuit of a PhD degree entails, there are no words to express my gratitude. For putting up with the endless weekends spent in the lab, the financial burden I have been all these years and the dishevelled mess I have become over the last few months of writing this, I promise you, it will all be worth it. I love you.

Chapter 2 Introduction

2.1 Ultraviolet Light

Of all potential environmental mutagens, ultraviolet light is the most prevalent in our daily lives. Humans are constantly bombarded with ultraviolet radiation from the sun. UV light can induce various forms of cellular damage, most seriously DNA damage. If these DNA lesions are allowed to propagate through DNA replication, harmful oncogenic mutations can arise leaving us prone to UV-induced skin cancers. Fortunately, we have evolved a series of defences to impede UV light from causing DNA damage, repair damage that is incurred or destroy cells that have sustained more damage than repair mechanisms can cope with. This section will give an overview of the biological implications of UV light. Its physical attributes, the molecular damage it induces, and cellular responses will be discussed.

2.1.1 Physical properties

UV light is divided into three categories, sorted by its wavelength. UVA: 315-380nm, UVB: 280-315nm and UVC: 190-280nm. The energy content is inversely proportional to wavelength, making UVC the most harmful of the three. The Earth's atmosphere blocks UVC and most UVB, making approximately 90% of the UV light that reaches the planet's surface UVA. All three categories have the ability to cause cellular damage and alter transcriptional events (Figure 1). As the ozone layer is depleted, the

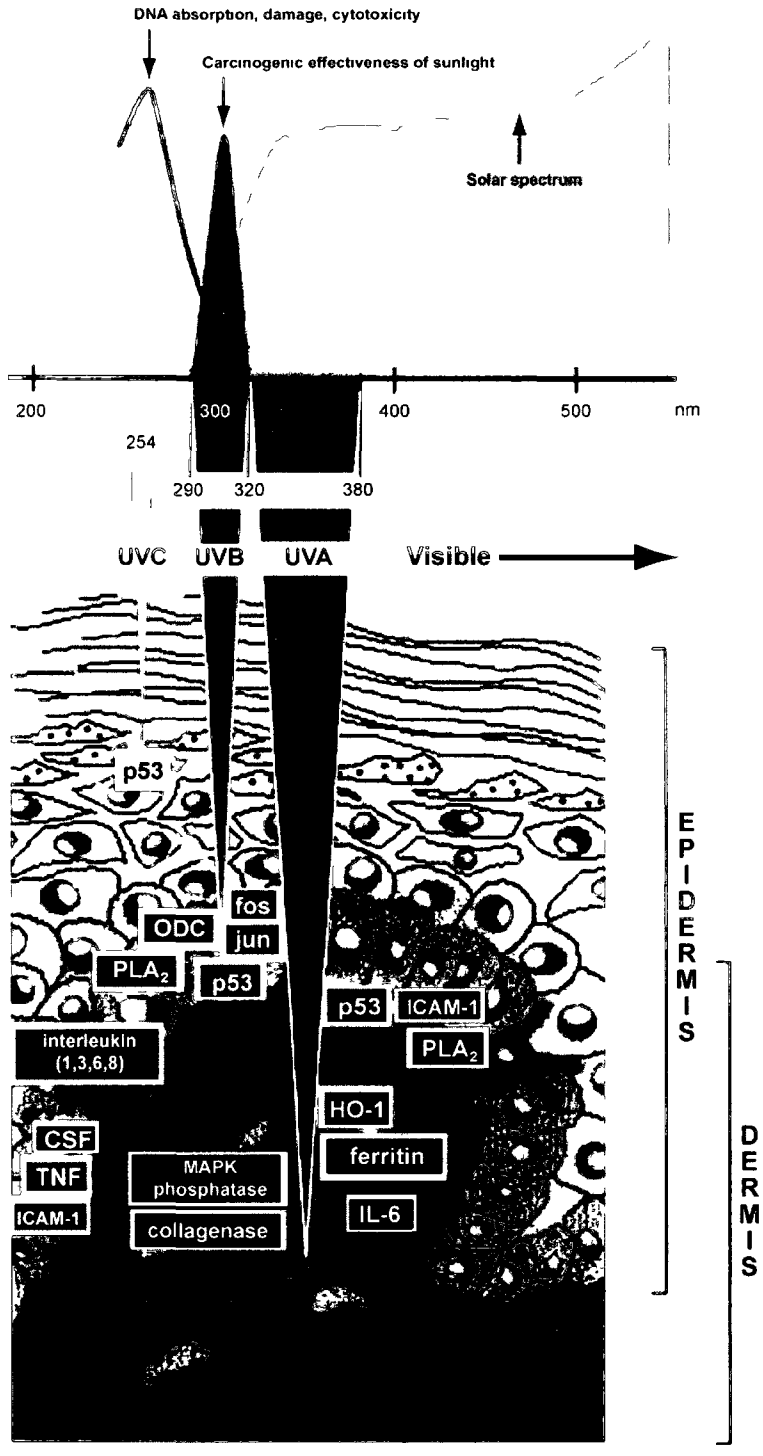

Figure 1. Solar UV spectrum and gene activation in the skin. The spectrum of solar radiation incident at the earth's surface is shown together with a representation of the transmission of its component UV wavelength ranges through human skin. ODC, ornithine decarboxylase; PLA_2, phospholipase 2; CSF, colony stimulating factor; TNF, tumor necrosis factor; CAM-I, intracellular adhesion molecule; HO-1, heme oxygenase 1; MAPK phosphatase, mitogen activated protein kinase phosphatase. Adapted from [2].

importance of protecting against the lower wave-length UV may become more important [1]. UVA and B exposure leads to oxidative damage through the creation of reactive oxygen species (ROS). They can also induce DNA-protein cross links and a limited amount of DNA damage. Because the rate of molecular absorption by photosensitive molecules of UV light increases with energy content, the depth of tissue transmission by UV is proportional to wavelength. This means UVA can penetrate deepest into dermal tissues, where it elicits a wide range of transcriptional responses and generates ROS [2]. On the other hand, UVB and especially UVC are readily absorbed by DNA and so they are particularly efficient at inducing DNA damage (Figure 2a). Because UVC is not part of the spectrum of solar irradiation that reaches the Earth's surface, its efficacy in studying physiological or pathological effects of sunlight exposure is limited. However, due to the ability of UVC to rapidly induce DNA lesions without the oxidative reactants UVA and UVB can generate, and its easy delivery using a germicidal 254nm UV bulb, UVC is often used as a model mutagen for studying DNA damage and repair *in vitro* [2].

2.1.2 UV light, DNA damage and cancer

In humans, moderate UV light exposure causes tanning or sunburn, but less benign consequences are also common. Repeated or prolonged exposure has been associated with local and systemic immunosuppression [3], viral activation [4] and most importantly, skin cancer. Non-melanoma skin cancer is one of the most commonly diagnosed cancers. In the United States, over one million cases occur every year, accounting for 30% of all cancer diagnoses in that country. World-wide incidence rates have been climbing steadily for 50 years [5, 6]. The combination of changing demographics of developed countries toward an

A

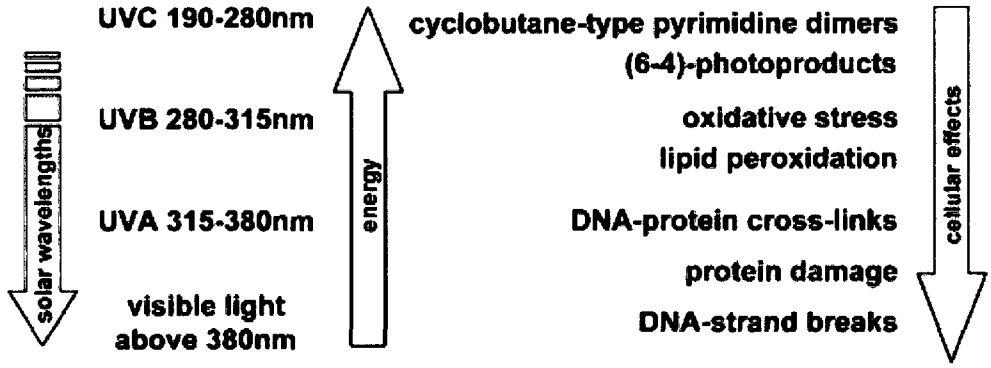

B

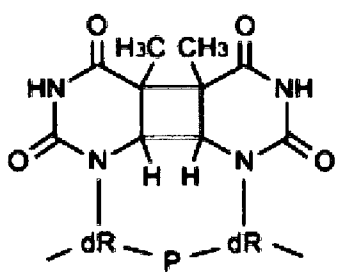

cyclobutane pyrimidine dimer
(CPD)

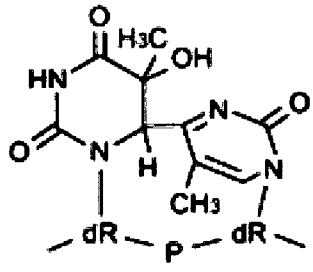

6-4 photoproduct
(6-4PP)

Figure 2. Physical attributes of UV radiation and types of damage. (A) UV light is divided into three wavelength areas (UVA, UVB, and UVC). The damage that UV radiation inflicts on cellular chromophores depends on its wavelength, which is inversely correlated to its energy content Reproduced from [1]. (B) Chemical structure of the two major UV-induced photolesions, CPDs and 6-4PPs. Red bonds, location of dimers. Adapted from [10].

older population and global warming and ozone depletion will likely drive the impact of skin cancer even higher in the decades to come.

The physiological damage caused by UV light can contribute to all types of skin cancer including basal cell carcinomas, squamous cell carcinomas and cutaneous melanomas [7]. The effects of UV light cause cancer in a number of ways. UV light-induced DNA damage needs to be repaired to avoid deleterious mutations. The location and repair efficiency of these lesions are the most important factors regulating UV light-induced transformation. When neoplastic transformation occurs as a result of environmental insults such as excessive UV light exposure, it is probable that mutations have occurred in genes that either normally suppress tumour growth or control cellular proliferation. The p53 tumour suppressor for example has been found to be mutated in over 50% of cancers. As soon as a deleterious mutation in a potential oncogene occurs against a p53 mutated background, the risk for neoplasia dramatically increases [8].

The majority of direct UV-induced DNA lesions are caused by UVB and UVC radiation. UVA-mediated DNA damage is an indirect effect of intracellular ROS generation which in turn causes oxidative damage to DNA bases such as the formation of 8-oxo-G. This miscoding lesion leads to G to T transversions following DNA replication [9]. The most common UVB and UVC-induced DNA lesions are manifested as dimers between adjacent pyrimidine bases. Two forms of pyrimidine dimers are formed; cyclobutane pyrimidine dimers (CPDs) and 6-4 photoproducts (6-4PPs). As the name suggests, CPDs form a 4-member ring between pyrimidines. The bonds are formed between the 5 and 6 positions of adjacent bases. 6-4PPs contain a stable link between the 4 and 6 position of neighbouring pyrimidines [10] (Figure 2b). CPDs are formed at

significantly higher levels than 6-4PPs and are the major lesion responsible for mutagenesis of mammalian DNA [11].

If these lesions are not properly repaired before the cell can replicate its DNA or the repair is error-prone, mutations are either propagated in future cell divisions and/or the protein encoded is mutated or non-functional. Certain polymerases (i.e. DNA polymerase η) are able to bypass lesions by inserting an adenine opposite to the site of damage. This usually results in a C to T transition which has been described as a "UV signature" mutation[12]. While this process is subjected to a proofreading mechanism, mutations are still common [7, 13].

2.1.3 Cellular responses to UV radiation

Nearly all living organisms are exposed to UV light at some or all stages of their life cycle. It is not surprising then, that many cellular responses have evolved to cope with the destructive effects of ultraviolet light. These responses fall into three main categories: 1) repair of damaged DNA, 2) induction of various signalling cascades, and 3) changes in transcription and post-transcriptional regulation [1].

2.1.3a DNA repair

Immediately following UV-induced DNA damage, repair mechanisms are activated. In lower organisms, the photolyase enzyme begins the repair process, while in higher eukaryotes, the most prominent repair mechanism is nucleotide excision repair (NER). It is activated following the recognition of helix distorting lesions. If this lesion is in a non-transcribed area of the genome, the global genomic NER (GG-NER) pathway is

activated. If a stalled RNA polymerase has encountered a lesion in the transcribed strand of DNA, the transcription coupled NER (TC-NER) pathway in engaged [14]. The repair of DNA damage will be considered in future sections, and will not be addressed here.

2.1.3b Signalling cascades

In the face of UV light-induced DNA damage, mammalian cells must decide their fate. Ultimately, an organism needs to do what is required to prevent harmful mutations from being propagated to daughter cells upon DNA replication and cell division. Depending on the amount of damage, cells will either go into cell cycle arrest and repair their damaged DNA before resuming regular cell growth, or they will initiate signalling cascades that result in death by apoptosis [1]. Immediately following ionizing radiation (IR) or UV exposure, the ensuing DNA damage is recognized by the PI-3-kinase related ataxia telangiectasia-mutated (ATM) or ataxia telangiectasia-related (ATR) proteins, respectively. These phosphorylate several G1/S checkpoint proteins, which sets off a signalling cascade that leads to the inactivation of the cyclin E/Cdk2 complex required to drive the cell cycle. Simultaneously, the Cdk inhibitor p21 is activated which further suppresses the cyclin E/Cdk2 complex. Thus, prolonged cell cycle arrest is achieved (reviewed in [1]).

UV light also provokes cellular responses independently of its ability to damage DNA. Cell surface cytokine and growth factor receptors are activated by UV light which activate, among other things, the p38 MAPK (mitogen-activated protein kinase) pathway. The generation of ROS also contributes to MAPK activation. Together, these pathways lead to the activation of transcription factors such as AP1, NFκB and p53 (p53's role in

mediating cellular responses to UV light will explored in detail in a future section). These transcription factors, in turn, direct the cell to undergo cell cycle arrest, DNA repair or apoptosis. The p38 MAPK pathways play roles in skin inflammation and UV-induced skin tanning responses (reviewed in [15]). UV light has also been implicated in initiating the activation of RNA binding proteins (RBPs) that affect the stability of specific mRNAs [16-18].

2.1.3c Transcriptional responses

While the regulatory mechanisms responsible for deciding cellular fate following UV irradiation have not been fully elucidated, it appears that varying UV doses result in distinct transcriptional responses. For example, it has been shown in human skin fibroblasts that the transcriptional upregulation and repression events are highly divergent between UVC-induced cell cycle arrest and apoptosis. Not surprisingly, low-dose UVC treatment induces transient responses that result in cell cycle arrest, repair and recovery. Cells exposed to high dose UVC show a dramatic shift towards the repression of many genes and the induction of pro-apoptotic genes [19].

Consistent with dose-dependent changes in the outcome of UV exposure, a similar dose-dependent shift in the expression of UV-induced genes has been reported using a conditional p53 induction system [20]. Because the induction of UV lesions is a stochastic event throughout the genome, the probability that a gene sustains damage is proportional to its length [21]. This has led to the concept of UV light-induced gene size regulation first postulated by McKay *et. al.* [20]. This study found that smaller p53 target-genes tend to be induced following increasing doses of UV light. The UV-mediated induction of longer

genes has been selected against, presumably due to an increased tendency for longer genes to sustain more DNA damaging lesions [21].

There is also a growing awareness of the role that UV light plays in modulating mRNA stability [22-24]. As will be discussed later, UV light often triggers increased mRNA stabilization by, for example, increasing the affinity of stabilizing proteins to AU-rich element (ARE) stability determinant containing mRNAs [25-28]. Other groups have found evidence that suggests non-ARE containing transcripts, including the poly(A) tail lacking histone mRNA, are stabilized by UV light in a p38 MAPK independent manner [22]. It has been hypothesized that UV light inhibits mRNA deadenylation and subsequent degradation, meaning that transcripts with normally very short half-lives can be stabilized following UV exposure [24]. This effect however, must be under the control of currently unidentified regulatory elements.

2.2 DNA Repair

The ability for an organism to repair its DNA is a constant requirement across all biological kingdoms. From the most primitive of bacteria to man, the essence of life remains the same; DNA. All life forms replicate, produce protein and transmit genetic information using this relatively simple molecule. After considering the already discussed environmental toxins and susceptibility of DNA to be damaged or mutated, it becomes obvious that if genetic fidelity, surveillance and repair systems had not evolved shortly after the origin of DNA (or RNA), life as we know it would cease to exist. In addition to

the DNA base damage discussed above (i.e. CPDs and 6-4PPs), DNA strand breaks (single and double-stranded) and interstrand cross-links are generated by a variety of damaging agents and must also be repaired. A multitude of mechanisms exist to identify and repair these diverse families of DNA damage [29]. This section will briefly overview the most prominent repair pathways, while devoting special attention to NER.

Because of the wide variety of exogenous and endogenous DNA damage and mutations faced by organisms, multiple processes have evolved. DNA repair can be grouped into three categories; direct reversion of DNA base damage, strand-break repair, and excision repair. Elements of these processes are highly conserved throughout animal kingdoms.

2.2.1 Direct repair

Direct repair mechanisms are the simplest of all as they utilize a single factor to recognize DNA damage and repair it. The two mediators of direct DNA repair are photolyases and methylguanine DNA methyltransferases. Photolyases are present in all three kingdoms, but not universally. For example, they are found in *E. coli* but not *B. subtilis*. They are absent in placental mammals or some yeast species such as *Schizosaccharomyces*, but they are present in opossums and *S. cerevisae* [30]. There are two distinct photolyase types. One is responsible for the repair of CPDs and the other for 6-4PPs [29]. Methylguanine DNA methyltransferases are ubiquitous in nature and are responsible for removing O^6MeGua lesions using a mechanism similar to the photolyases. Mice lacking these methyltransferases are highly susceptible to alkylating agent-induced tumourigenesis [31].

2.2.2 Homologous recombination and nonhomologous end-joining

Double DNA strand breaks can result from reactive oxygen species, ionizing radiation or exposure to certain chemical toxins. They are repaired by homologous recombination (HR) or nonhomologous end-joining (NHEJ). HR relies on the availability of a complimentary stretch of DNA on the sister chromosome opposite to where the break occurred. Following a double strand break, a protein complex known as the MRN complex (in humans) binds to the breaks on both strands. A section of DNA is then removed from the 5' end of each cut, creating 3' overhangs. These overhangs are then able to bind to corresponding sequences from the other paired chromosome, causing *strand invasion.* DNA polymerases can now extend the 3' end of the invading strand and generate properly encoded complimentary sequence. Specific endonucleases can then separate the two double stranded DNA molecules. A very similar process occurs during meiosis and is responsible for "cross-over" of sections of genetic information situated on chromosomes near the sites of recombination (reviewed in [32]).

NHEJ repairs double strand breaks without using a complimentary template. Instead, this process directly joins the broken ends together using small overhangs on each strand known as microhomologies. The process is initiated by the binding of the Ku70 and Ku80 proteins to the exposed ends, which then recruit the DNA-PKcs and the XRCC4-DNA ligase IV complexes to join the two ends together [29, 33]. NHEJ is evolutionarily conserved across all kingdoms of life and is the main repair mechanism of double strand breaks in mammalian cells [34]. Dysfunctional NHEJ has been linked to genetic instability, cancer, and neurological abnormalities [35].

2.2.3 Excision repair

When only one strand of the DNA has been damaged, repair mechanisms can use the other strand as a template for repairing any damage or deletions on the complimentary strand. Depending on the type of damage, one of three different excision repair pathways are activated; base excision repair (BER), mismatch repair (MMR), or nucleotide excision repair (NER). There are overlapping features and players associated with these three repair mechanisms.

2.2.3a Base excision repair

BER is employed to remove damage inflicted on a single base that is not helix-distorting. The altered bases removed by BER are oxidized, alkylated, deaminated or uracil [36]. Each of these types of damage are recognized by a separate DNA glycosylase which removes the damaged base. This forms an AP (apurinic/apyrimidinic or abasic) site that is cleaved by AP endonuclease [37]. The resulting single-strand break is then repaired through short patch (the single nucleotide is replaced) or long patch (a larger stretch of 2-10 nucleotides is removed and resynthesized) BER. The choice of the short or long patch repair depends on the type of damage, cell cycle stage, cellular differentiation state and species. Specialized DNA polymerases are required for each pathway [38].

2.2.3b Mismatch repair

Mismatch repair is a highly conserved mechanism used for correcting deletions, insertions or nucleotide base-pairing errors in DNA replication, recombination or repair. The rates of replication fidelity and base misincorporation vary among polymerases.

Translesion polymerases (those required to bypass certain DNA lesions) for example, are much more error-prone than replicative DNA polymerases. MMR acts as a proofreading mechanism to ensure genomic integrity is maintained following nascent DNA synthesis. MMR machinery is able to discriminate between the template strand and daughter strand (possibly due to the hemimethylation of nascent DNA or the presence of nicks in the unligated daughter strand). Any base anomaly or mismatch will alter the DNA structure, signaling for repair. Often large sections of DNA (up to thousands of nucleotides) surrounding the lesion are removed during MMR, and are resynthesized by DNA polymerases. MMR also plays roles in DNA damage signaling and suppression of homologous recombination [39, 40].

2.2.3c Nucleotide excision repair

Nucleotide excision repair (NER) is the most versatile and well studied DNA repair pathway in humans. It is responsible for repairing a wide range of lesions, but its role in repairing UV-induced CPDs and 6-4pps is especially well-characterized. As alluded to above, NER is split into two sub-pathways, transcription coupled (TC) and global genomic (GG). TC-NER is responsible for repairing lesions on an actively transcribing strand of DNA, while GG-NER repairs helix distorting lesions anywhere on the genome (including the non transcribed-strand of a gene) in a passive manner [41]. Mechanistically, the only difference between the two processes is how they identify sites of DNA damage. An overview of these process is presented in Figure 3.

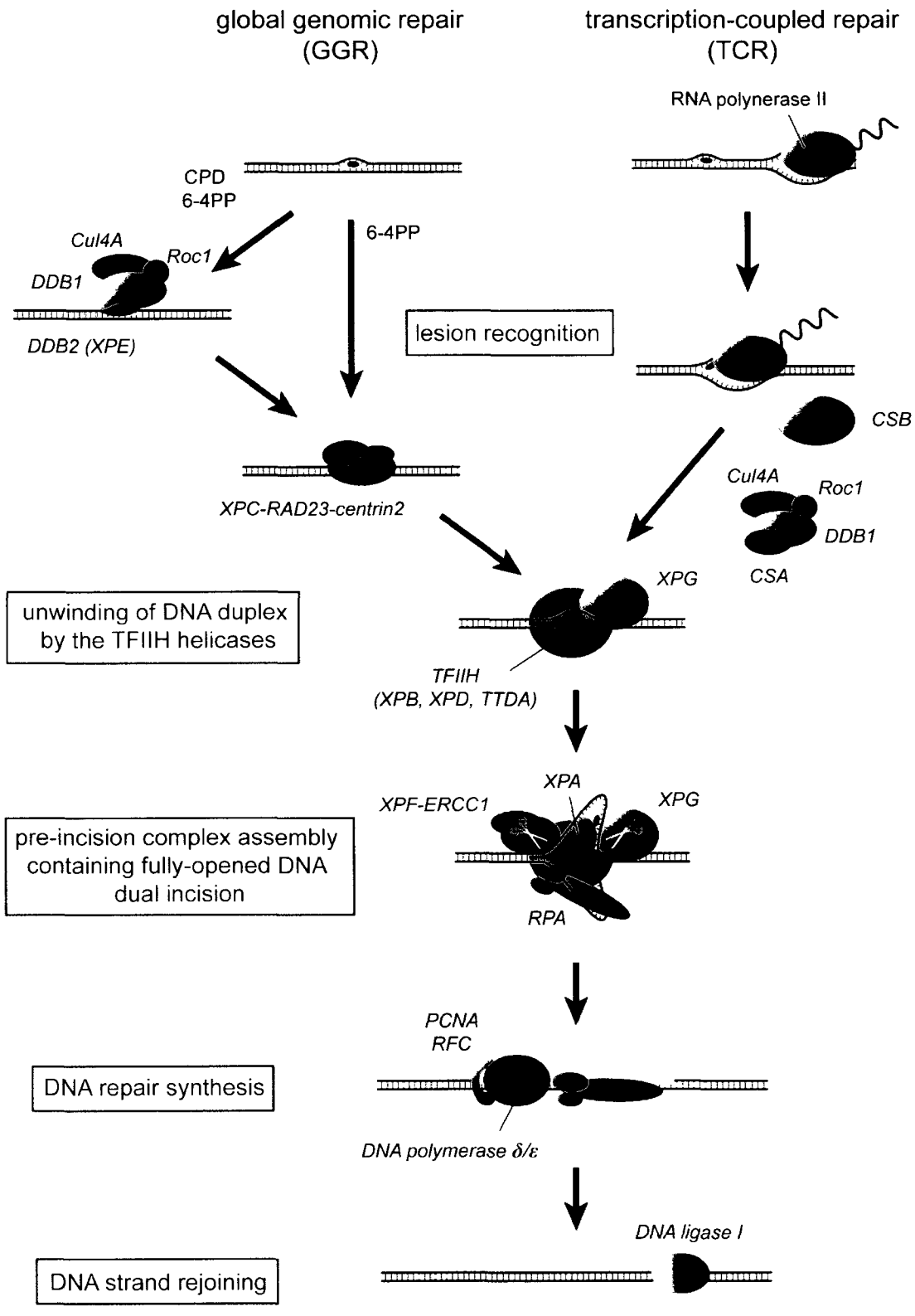

Figure 3. Human nucleotide excision repair (NER) pathways. GGR and TCR NER branches differ only in the recognition of DNA lesions. See text for details. Adapted from [53].

Global genomic NER

The main recognition factors in GG-NER are the p53 inducible XPC and DDB2/p48 (DNA damage binding protein 2) [10]. Both proteins form complexes following UV irradiation. XPC complexes with hHR23A or B, the human orthologs of the yeast Rad23p proteins, as well as centrin 2. hHR23B is more prevalent and is thought to stabilize XPC, while centrin 2 is thought to increase the complex's affinity for damaged DNA [42]. DDB2 binds tightly with the 127 kDa DDB1 and forms the UV-DDB complex (UV Damaged DNA Binding protein) [43]. Both UV-DDB and XPC complexes bind readily to 6-4PPs, but only UV-DDB is able to bind to CPDs [44, 45]. The binding of the XPC complex to DNA lesions is required to recruit the core repair factors needed in subsequent steps of NER. DDB2 is thought to be especially sensitive to the subtle distortions induced by CPDs, and its ability to bind to these lesions is necessary for XPC to recognize them [10, 46]. Complicating matters further is the fact that both DDB2 and XPC are polyubiquitinylated following UV exposure and DNA binding. This leads to the rapid proteasome-mediated degradation of DDB2, but not XPC [47, 48]. It has been shown that the degradation of DDB2 is required for GG-NER to continue [49]. It has been suggested that this remodels local chromatin structure and enables access of XPC to the site of DNA damage [50].

Transcription-coupled NER

As mentioned in previous sections, TC-NER is initiated by stalled RNA polymerase II when it encounters a helix distorting lesion during transcription elongation. Neither XPC or UV-DDB is required for TC-NER. Instead, two proteins, CSA and CSB

(Cockayne Syndrome proteins A and B) appear to play a role in transmitting information about the stalled polymerase and initiating subsequent steps of NER [14]. While the exact mechanism is unknown, it has been proposed that these factors aid in the temporary removal of RNA polymerase II [51]. They may also be required to recruit the multifunctional TFIIH (transcription factor IIH) complex [52]. TFIIH is also thought to directly interact with the XPC complex following GG-NER lesion recognition [53].

The recruitment of TFIIH is where the two sub-pathways of NER converge. Among other factors, this complex contains the XPB and XPD helicase proteins which are responsible for unwinding the damage-containing region of DNA. Following this, other factors are required to form and stabilize the *pre-incision complex* which fully opens the DNA and facilitates repair. The XPA and XPG proteins are responsible for forming this complex, while replication protein A (RPA) binds to XPA and stabilizes the pre-incision complex. All these factors have affinity for damaged DNA. The next step involves the structure-specific NER endonucleases XPG and ERCC1-XPF (XPG plays dual roles in the process). These induce single-strand breaks at the 3'(XPG) and 5'(ERCC1-XPF) junctions between single and double-stranded DNA at either side of the pre-incision complex. This results in the removal of a 24-32bp oligonucleotide containing the damaged base(s). This gap is then filled in with DNA polymerase aided by PCNA and replication factor C. Lastly, DNA ligase connects the newly synthesized DNA, completing the process. (Reviewed in [10] and [53])

2.2.4 Loss of NER capacity and human disease

The loss of any one of the above mentioned factors contributes to deficiencies in GG-NER, TC-NER or both. The loss of these repair pathways leads to hereditary human diseases. The three most common are xeroderma pigmentosum (XP), Cockayne syndrome (CS) and trichothiodystrophy (TTD) (Table 1). Studying these rare diseases can illuminate unsolved questions surrounding DNA repair pathways in normal individuals and can also aid in our understanding of the etiology of skin cancer, offering novel therapeutic targets.

2.2.4a Xeroderma pigmentosum

XP is a rare hereditary disease characterized by deficiencies in factors required for both GG and TC-NER. Less than 1000 cases have been described worldwide since its first documented discovery in 1863. These individuals are concentrated in the USA, Europe, northern Africa and Japan. Cell fusion studies have identified eight subgroups of XP, each of which are defined by mutations in genes encoding XP-A through XP-G proteins [14] as well as XP-V(variant) in which the polymerase responsible for translesion synthesis (TLS), pol η is defective [54]. XPE and XPC cells are deficient for GG-NER but not TC-NER, while the rest of the XP variants are deficient in both sub-pathways [55].

Clinically, XP manifests itself in patients as a severe sun sensitivity and high incidence of UV light-induced early onset skin cancers [56]. It causes severe damage to the sun exposed portions of the eye and in 20% of cases, neurological deterioration occurs. In addition to sun sensitivity, XP patients are highly susceptible to internal cancers caused by other mutagens such as tobacco smoke [57]. Not surprisingly, XP patients have a life expectancy some 30 years shorter than the general population [56]. The severity of

Table 1. Inheritable human syndromes associated with loss of NER

Primary Disease	Implicated gene	Alternate nomenclature	Overlap with other diseases*	TCR	GGR	Cancer prone
XP	*XPA*	*XPA*	DSC	-	-	+
	XPB	*ERCC3*	CS and TTD	-	-	+
	XPC	*XPC*	Unknown	+	-	+
	XPD	*ERCC2*	CS, TTD and COFS	-	-	+
	XPE	*DDB2*	Unknown	+	-	+
	XPF	*ERCC4*	Unknown	-	-	+
	XPG	*ERCC5*	CS and COFS	-	-	+
CS	*CSA*	*ERCC8*	Unknown	-	+	-
	CSB	*ERCC6*	UV^SS, COFS and DSC	-	+	-
	XPB	*ERCC3*	XP and TTD	-	-	+
	XPD	*ERCC2*	XP and TTD	-	-	+
	XPG	*ERCC5*	XP	-	-	+
	ERCC1	*ERCC1*	COFS	-	-	Unknown
TTD	*XPB*	*ERCC3*	XP and CS	-	-	-
	XPD	*ERCC2*	XP and CS	-	-	-
	TTDA	*GTF2H5*	Unknown	-	-	-
	TTDN1	*C7orf11*	Unknown	+	+	Unknown
	Others	Unknown	Unknown	+	+	Unknown

*Mutations in the gene implicated in the primary disease, listed in the first column, can also cause other diseases with defective DNA repair. COFS, cerebro-oculo-facio-skeletal syndrome; CS, Cockayne syndrome; DSC, De Sanctis–Cacchione syndrome; TTD, trichothiodystrophy; UV^SS, ultraviolet-sensitive syndrome; XP, xeroderma pigmentosum. Adapted from [55].

symptoms varies considerably between and within subgroups, but generally the symptoms associated with the XP-E subgroup are the least severe. XP-E cell lines (lacking functional DDB2) are also less sensitive to UV than are the other complementation groups [58].

2.2.4b Cockayne Syndrome

CS is another rare autosomal recessive inherited disorder linked to TC-NER deficiency (but not GG-NER), and is defined molecularly by mutations in the CSA and CSB genes. Symptoms are usually severe and include dwarfism, neurological impairment, opthalmologic disorders, microencephaly, and characteristic facial deformations [59]. Like XP, CS patients show increased sun sensitivity, but unlike XP, CS does not confer an increased risk of skin cancer. This discrepancy may highlight the role that global genomic integrity plays in suppressing cancer. Instead, CS individuals may be protected from cancer as they are especially sensitive to solar-induced apoptosis, and they are still able to conduct GG-NER [55]. The wide range of symptoms associated with CS has led some to speculate that it has roles distinct from TC-NER such as transcription [60].

2.2.4c Trichothiodystrophy

TTD is the last NER-related disorder to be discussed here. In most cases of TTD mutations in XPB, XPD or TTD-A (all subunits of TFIIH) are the causative agents. TTD cells are defective at both branches of NER. Some TTD individuals exhibit sun sensitivity, but have no increased susceptibility to skin cancer. Neurological symptoms similar to those observed in CS are common. The most common and characteristic phenotype of TTD, however, is the presence of dystrophic, short brittle hair with reduced sulphur [61].

2.3 p53 and Cellular Stress Response

Of all the cellular responses to UV light exposure described above, perhaps the most important player in mediating a cell's response to such environmental cues is the p53 tumour suppressor and transcription factor. Responses to a wide array of environmental stimuli all converge in some way with p53. It is responsible for directing cellular defences in response to bulky DNA lesions, DNA strand breaks, hypoxia, viral infection, oncogene activation, spindle damage, heat shock, cold shock, media depletion, proteasome inhibition, and blockage of RNA polymerase II (RNA polII) (Figure 4a). Depending on the type, duration and dose of environmental stress and the physiological conditions by which it finds itself surrounded, p53 can mediate responses involved in cell cycle arrest or progression, DNA repair, antiangiogenesis or apoptosis [1, 62, 63].

2.3.1 p53: form and function

p53 is one of the most studied of all proteins. Since its discovery as the first tumour-suppressor gene in 1979 [64], over 53,000 articles have been published about p53 at the time of writing. Its importance in human biology is highlighted by the fact that it is mutated in approximately 50% of all cancers, and it is postulated that in the other half, p53 function is disrupted in some way [8]. Because p53 is a major node of highly interconnected pathways regulating cellular metabolism, growth, and stress response, its absence or mutation always results in deleterious consequences. Patients with Li-Fraumeni syndrome for example, which is characterized by germ-line p53 mutations, show a great propensity to develop many types of cancers, and at a very young age [65].

A

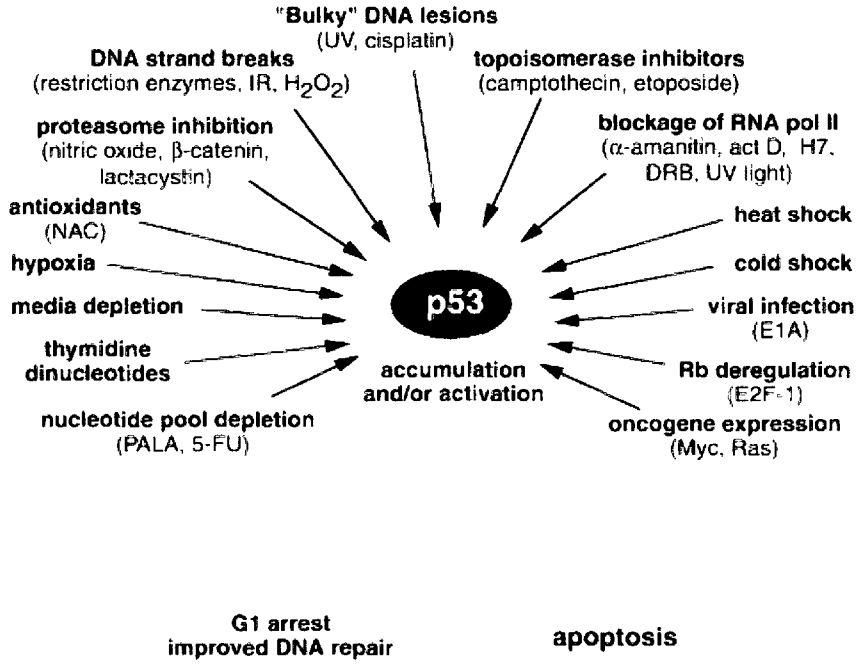

B

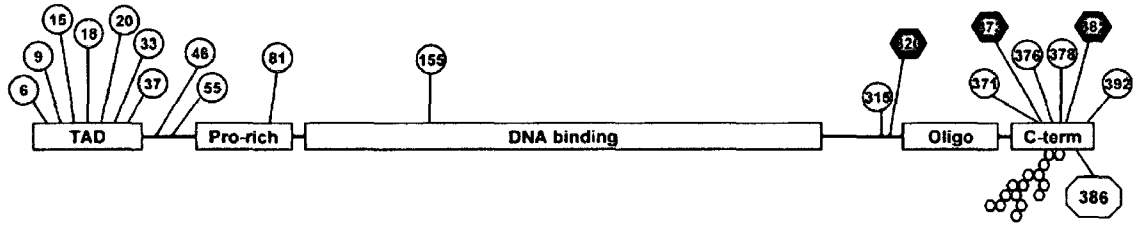

Figure 4. The p53 tumour suppressor, form and function. (A) The p53 response is triggered by many different stresses involving both DNA-damaging and non-DNA-damaging agents. The outcome it promotes varies depending on the type and quantity of stress event. Reproduced from [62]. (B) Structure and post-translational modification of the p53 protein. TAD, transactivation domain; Oligo, oligomerization domain; circles, Ser/Thr phosphorylation sites; hexagons, acetylation sites; octagon, sumoylation site. Reproduced from [1].

Structurally, the p53 protein is 393 amino acids long and contains a transactivation domain at its N-terminal, a proline rich area, a sequence-specific DNA binding domain, an oligomerization domain, and a regulatory C-terminal domain [8]. Either constitutively or upon cellular stress, p53 is extensively post-translationally modified at several amino acid residues through methylation, phosphorylation, acetylation, sumoylation and glycosylation (Figure 4b). This wide range of potential modifications allows p53 to differentially interact with proteins or transactivate specific subsets of genes as cellular conditions dictate. They also control the stability and cellular localization of p53 [66]. Oligonucleotide array experiments have identified hundreds of genes regulated by p53, most of which are upregulated through transactivation [67]. Bioinformatics analyses have revealed thousands of putative p53 target sequences in the human genome [68, 69]. Other genes are also repressed either directly or indirectly through the sequestration of transcription factors (reviewed in [62]).

Following cellular stress, p53 suppresses tumourigenesis by directing cells to undergo cell cycle arrest, allowing for an assessment of cellular damage. p53 can then initiate DNA repair of bulky lesions or strand breaks. If the damage is too severe to be repaired, p53 can orchestrate a cascade of events that leads to apoptosis, thus ensuring unrepaired harmful mutations or genomic instability are not transmitted to daughter cells, thereby limiting cellular transformation and tumour formation [63] (Figure 5a).

Because p53 is responsible for inducing cell cycle arrest or apoptosis, its constitutive expression and activation would be highly toxic to cells. While it is constantly expressed, it has a short half-life due to ubiquitin-mediated proteasomal degradation. The E3 ubiquitin ligase responsible for this destruction is MDM2, which is itself a p53

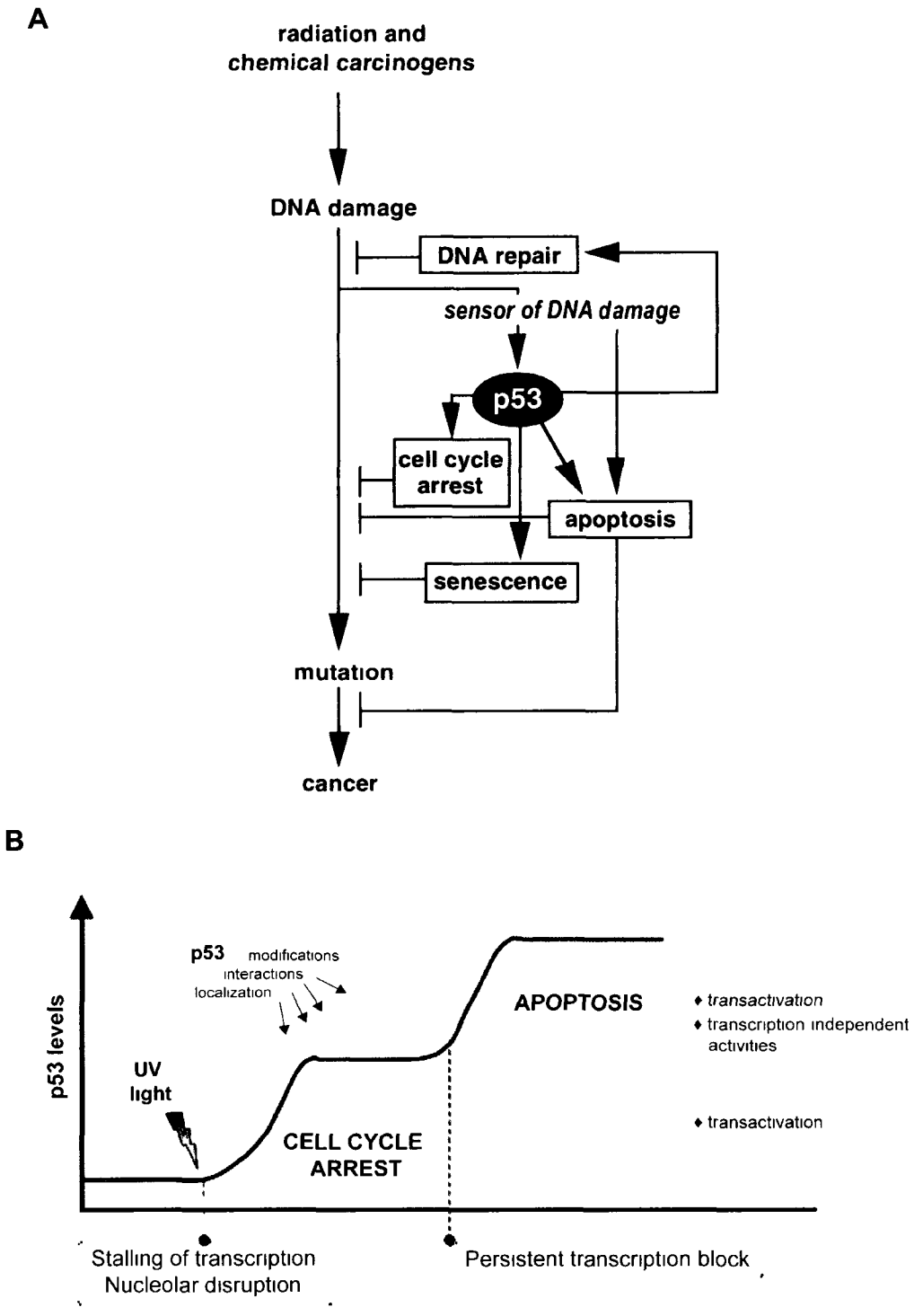

Figure 5. p53 mediates cellular responses by sensing stress (A) p53 acts as a damage sensor and mediates DNA repair, cell cycle arrest, apoptosis, and senescence by transactivating specific subsets of target-genes Adapted from [62] (B) p53 UV response Following UV radiation, p53 accumulates due to the stalling of transcription machinery and/or nucleolar disruption p53 target-genes are transactivated, commencing cell cycle arrest If the transcription block persists, p53 levels are increased further and apoptosis is induced See text for more detail Adapted from [1]

transactivated gene. MDM2 can also inhibit the transcriptional activity of p53 through interacting with its transactivation domain. This autoregulatory loop is broken following a DNA damage-inducing event, when p53 and MDM2 dissociate from each other via the post-translational modification of p53 and/or MDM2. This negative feedback loop allows for rapid adjustments following cellular stress that ensure an appropriate amount of p53 is available to mount a response without becoming toxic to cells under normal conditions [70]. Evidence for the importance of this MDM2-mediated suppression of p53 under normal conditions comes from the finding that the embryonic lethality of MDM2-null mice is rescued by the ablation of p53 as well [71, 72]. Many studies and reviews have been dedicated to the p53-mediated response to each of the above mentioned endogenous and exogenous stresses. Here, only UV light mediated p53 activation will be considered.

2.3.2 p53-mediated responses to UV light

UV light induces transcription-blocking DNA lesions and it appears that the blockage of RNA polII elongation by DNA lesions is the primary signal to accumulate p53 protein. Cells that are defective in the repair of such adducts on the transcribed strand of active genes induce p53 at much lower levels than wild-type cells [73]. Further evidence for this comes from work in which RNA synthesis inhibitors actinomycin D, DRB, H7 and α-amanitin, which block the elongation of RNA polII, were able to induce p53 protein levels in the absence of DNA damage [74].

Much work has been done to elucidate the factors that are involved in sensing RNA polymerase blockage and transducing signals to p53. There are many candidate proteins associated with the transcriptional machinery that may play this role. They include Cdk-

Activating kinase, $TAF_{II}250$ acetyl transferase, and kinase and the p300 and PCAF transcription activators. All these factors play roles in post-translational modification of p53 protein or p53 interacting proteins. In total there are over a dozen kinases, phosphatases and acetyl transferases that modify p53 directly or indirectly following UV light exposure. p53 may also be activated through the specific inhibition of its degradation through the 26S proteasome pathway or by nuclear structural changes that disrupt its nuclear export (reviewed in [62]).

In addition to post-translational modifications and cellular localization, there is evidence that stress-responsive transcription factors such as AP-1 and NF-κB drive p53 expression under certain genotoxic conditions [75]. However, since the blockage of RNA polymerase also induces p53 accumulation, this must be a secondary response that is only useful in inducing p53 under specific cellular stresses that do not impair transcription.

One final way that UV light may induce p53-mediated transactivation is through the RNA binding protein HuR. Work by Mazan-Mamczarz and colleagues in human RKO colorectal carcinoma cells showed that following exposure to UVC, p53 expression is elevated. This increase was not attributed to increased mRNA synthesis or stability, nor could it be accounted for solely by increased protein stability. Instead, they linked it to increased translation. They further showed that direct interactions between the 3'UTR of p53 and HuR were modulated by UVC exposure, and when HuR was depleted, p53 expression also dropped [76].

It is through these protein-protein interactions and post-translational modifications that p53 is able to mediate cell cycle arrest, DNA repair, and apoptosis following UV light radiation.

2.3.2a Cell cycle arrest

The most important p53 target-gene for inducing cell cycle arrest is the cyclin-dependent kinase (CDK) inhibitor $p21^{WAF1/CIP1}$. p21 can cause G1 and G2 arrest through the inhibition of several CDK complexes [63, 77]. It may also block the elongation of DNA replication during S phase by interfering with PCNA (proliferating cell nuclear antigen) [78]. In addition to inducing p21, p53 can also inhibit cell growth by inducing the anti-proliferative BTG2 protein [79]. p53 also appears to mediate S phase progression following UV light by preventing sustained cyclin E expression [80].

2.3.2b Apoptosis

The familiar effects of sunburn are caused in part by p53-mediated apoptosis as an adaptive response to UV-induced DNA damage. p53 can activate a multi-pronged program of cell death in response to overwhelming DNA damage. Its ability to induce apoptosis is considered its most important method of tumour suppression [1]. p53 induces apoptosis in both transcription dependent and independent manners. It is able to upregulate genes involved in both death receptor and mitochondrial apoptotic pathways [81]. PUMA and Noxa are thought to be of particular importance as p53-induced apoptosis is inhibited in mice when PUMA or Noxa are disrupted [82, 83]. These studies did not however assess PUMA and Noxa's role in p53-mediated apoptosis in response to UV light exposure. p53 target-genes such as IGF-BP3 suppress survival signalling pathways, while other genes that play roles in survival or apoptosis inhibition such as Bcl-2 or survivin are downregulated by p53 [81, 84].

p53 can also induce apoptosis by shuttling death receptors to the cell surface, activating caspases or localizing to the mitochondria where it induces the permeabilization of the outer mitochondrial membrane causing the release of cytochrome c [85, 86]. The mitochondrial localization of p53 has been observed for IR, it is currently unknown if UV light elicits the same response.

2.3.2c DNA repair

The role of p53 in DNA repair is complicated and remains controversial. Through studies on p53-deficient Li-Fraumeni cells or viral p53 suppression, it has been shown that p53 is necessary for GG-NER of CPDs and to a lesser extent, 6-4PPs, while it is dispensable for TC-NER following UVC radiation [87]. Other investigations have further shown that loss of p53 does not increase rates of UV-induced apoptosis [88, 89]. These studies were among the first to suggest that loss of p53 impairs genome-wide repair of UV-induced DNA lesions which could lead to genomic instability. Since these early studies, the role for p53 in GG-NER was validated in a number of human and mouse models using different UV wavelengths and other diverse DNA adduct-forming toxins (reviewed in [46]).

The most likely explanation for a requirement for p53 in inducing GG-NER is in its role as a transcription factor. In response to UV light, p53 transactivates several genes involved in DNA repair. In the context of GG-NER, the DDB2 and XPC genes appear to be the most important. Both genes encode proteins involved in the early recognition of genome wide CPDs and 6-4PPs and the loss of either results in a condition known as xeroderma pigmentosum E or C, respectively. Due to a lack of DDB2 induction, $p53^{-/-}$

cells are deficient in GGR [90, 91]. However, overexpression of DDB2 in p53-deficient cells does rescue GGR of CPDs in irradiated cells [92]. Basal levels of both DDB2 and XPC proteins are higher in p53 proficient cells prior to UV exposure [91, 93]. This suggests that the damage recognition factors are required immediately following insult and the p53-mediated induction is a secondary effect, possibly meant to replenish DDB2 and XPC levels so they can continue their task in repairing remaining lesions. A third p53-inducible gene, gadd45 (growth arrest and DNA damage inducible 45) also plays a role in GG-NER (but not TC-NER) through interactions with PCNA [94].

There are conflicting reports that p53 may contribute to TC-NER under certain circumstances. For example, work from Elliot Drobetsky's lab has found that TC-NER was enhanced in a p53-dependent manner in response to UVB, but not UVC exposure [95, 96]. This contradictory evidence of p53's role in TC-NER highlights the potential differences in cellular responses to the more physiologically relevant UVB when compared to UVC studies. According to Latonen and colleagues, UVB requires 100-fold more energy to induce the same amount of DNA damage as UVC, and when this difference is taken into account, p53 accumulation, target-gene activation, and cellular responses are very similar between the two sources of UV light [97]. These caveats should be kept in mind when evaluating studies of photobiology. Other groups have suggested that p53 can directly bind to single-stranded or damaged DNA through its C-terminal domain, which initiates transactivation of p53 target-genes [98, 99]. Wang and colleagues have proposed that p53 may affect NER by directly binding to TFIIH-associated factors that are involved in TC-NER [100]. Lastly, there is evidence that, following UV radiation, p53 is required for global chromatin relaxation, a crucial step in DNA lesion recognition and GG-NER [101].

2.3.3 To arrest, repair or die; how p53 determines cell fate

The outcome of UV exposure depends on a host of factors such as cell type, wavelength of UV light, dose, cellular location, and differentiation. Exactly how p53 decides which cellular fate to promote is not yet clear. The levels of cellular p53 appear to play a role in the response, as cells expressing low levels generally undergo cell cycle arrest, while those expressing higher levels undergo apoptosis [102]. This suggests a dose-dependent response with different outcomes once certain thresholds of damage and/or p53 levels have been reached (Figure 5b). The induction of these different p53 levels appears to be mediated by stalled transcription and persistent unrepaired DNA damage, which correlate with UV dose [62]. Low doses of UV light tend to induce transient cell cycle arrest and DNA repair processes through the induction of p53 targets such as p21 and Gadd45. High UV doses, on the other hand, induce higher levels of p53 and pro-apoptotic genes like Bax and Noxa while pro-survival or DNA repair genes are repressed [97, 103, 104].

The fact that high doses of UV light preferentially induce apoptosis, while lower doses induce cell cycle arrest and DNA repair agrees with the gene-size theory of UV-mediated p53 target-gene induction [20]. Because p53 is a transcription factor and is post-translationally modified following cellular stress, it does not require *de novo* transcription to activate downstream expression. The genes it upregulates however do need to undergo rapid RNA polymerase II-mediated transcription. Smaller genes tend to be preferentially upregulated by higher UV doses due to the fact that they contain fewer DNA lesions (which block transcription), while larger p53-responsive genes are upregulated at lower

doses of UV. Not only are shorter p53 target-genes selected for expression following increasing doses of UV light, target-genes that would be deleterious to cells coping with cellular stress are actively excluded from induction [20]. Importantly, this study also found a correlation between smaller and pro-apoptotic genes. Conversely, pro-survival genes were found to be longer than average-size genes. For example, the feedback inhibition of p53 by the 37kbp MDM2 E3 ubiquitin ligase, is blocked at high UV doses, while the much shorter gene encoding the pro-apoptotic 6.6kbp PUMA is still upregulated at high doses of UV light [20].

Lastly, NER capacity plays a role in determining the p53-mediated fate of a cell. Cells deficient in TC-NER are more sensitive to UV-induced apoptosis compared with wild type cells as they induce high levels of p53 [105, 106] .

2.4 mRNA Stability

2.4.1 Importance of mRNA stability

The tight control of gene expression affects all aspects of cellular biology and developmental pathways. Protein levels are regulated through myriads of intersecting processes such as chromatin structural modification, transcription initiation, elongation and efficiency, mRNA processing, nuclear export, mRNA stability, translation rates, and protein stability. mRNA stability is perhaps the most dynamic regulator of gene expression. Eukaryotic transcript half-lives range from 20 minutes to over 24 hours. This may represent up to a 1,000-fold difference in mRNA levels [107]. Adding to the importance of post-transcriptional regulation, are the findings from studies in yeast and

mammalian cells that there appear to be less correlation than previously believed between levels of steady-state mRNA and the proteins they encode [108, 109]. Clearly, this is a powerful form of regulation that would allow for rapid induction and suppression of gene products as conditions dictate (discussed in [110]). If this regulation was inhibited in only a small subset of genes, the effect could be disastrous for the cell. The ability for mRNA to be translated into functional protein underpins almost every biological function an organism undertakes throughout its life. Whether or not a particular transcript is used as a blueprint for protein synthesis depends on many factors. The sheer amount or location of mRNA available plays a role, as does its affinity for the translation machinery. Once initiated, the efficiency and speed of translation plays a role in the abundance of protein produced. The mechanisms that dictate mRNA turnover rates and the players that regulate them can affect all of the factors listed above. Not only do they dictate whether or not a protein will be made, but also under what conditions it should be synthesised, for how long, and in what quantities. Many genes encoding potentially oncogenic products have extremely unstable transcripts with very short half-lives. Increased stability of these mRNAs can contribute to carcinogenesis [111, 112].

mRNA stability plays very important roles in many aspects of genetic expression programs. For example, it has been shown that the stability of specific genes changes during developmental and cellular differentiation processes. There is also a growing body of evidence that suggests transcriptionally inducible genes are unstable (have short half-lives) and presumably are under tight transcriptional control [113, 114]. One recent study identified the half-lives of nearly 20,000 genes in mouse embryonic stem cells using microarray analysis. They found a positive correlation between unstable mRNAs and genes

involved in the regulation of transcription, cell cycle, apoptosis, signal transduction, and developmental pathways. Conversely, they found that genes encoding structural, metabolic, and protein synthesis related proteins (i.e. "house-keeping" genes) were more likely to be synthesized from stable mRNAs. Furthermore, they were able to show that genome wide, overall decay rates decreased following differentiation [115]. It has generally been observed that early response gene mRNAs, such as those involved in inflammatory or immune responses, are short lived. This means their expression patterns can be dramatically altered simply by regulating their transcript half-lives. This also means that when they are no longer needed, protein synthesis can be abruptly terminated through the destruction of mRNA [116].

Along with other methods of post-transcriptional regulation such as cellular localization or enhanced translation efficiency, differential mRNA stability has evolved as a mechanism to allow for rapid and efficient induction or suppression of stress response genes without having to rely on *de novo* transcription [28, 117]. This is especially important, as mRNA synthesis is often impaired following external stress events such as UV light exposure [104, 118, 119]. The importance of mRNA stability in overcoming external insults is highlighted by a cDNA array study by Fan and colleagues [120]. They found that in response to various insults, such as heat shock or UV light exposure, approximately 50% of the stress-regulated genes showed altered mRNA stability (they were either more or less stable following the stimuli). As the significance of mRNA stability becomes more apparent, many groups are turning to genome-wide approaches to study the global effects mRNA stability has on gene expression [115, 116, 121-124].

Given the importance mRNA stability plays in gene expression, it is not surprising that stability deregulation has been implicated in many disease states such as myotonic dystrophy [125], inflammatory bowel disease [126], and various cancers [111, 112]. The implications of deregulated mRNA stability in human disease has been extensively reviewed in [127]. Similarly, the inability of cells to rapidly degrade error-filled or prematurely terminated transcripts through the use of the nonsense-mediated decay pathway (which will be discussed soon) has deleterious consequences for human health [128].

2.4.2 Regulation of mRNA stability

The regulation of mRNA stability (or rate of decay) is mediated by specific *cis*-acting elements found in the untranslated regions (UTRs) and coding regions of many mRNAs and *trans*-acting factors that interact with these stability determinants. This section will summarize the ways in which mRNA stability is regulated through this paradigm of interacting sequence elements and RNA-binding proteins (RBPs) and/or micro RNAs (miRNA). For an overview, see Table 2.

2.4.2a Cis-acting elements

Sequence elements have been shown to act as stability determinants in a variety of mRNAs. These elements are either sequence-specific as in the case of AU-rich elements found in many short-lived transcripts [129] or form secondary stem-loop structures that act as protein-binding platforms. Two prominent examples of the latter type of stability determinant are iron-responsive elements (IREs), which have been found in the 3'UTR of

Table 2. *Cis*-acting mRNA stability determinants.

Determinant	Location	Description	Example
AU-rich element (ARE) [136]	3'UTR		
Class I (dispersed AUUUA)		AUUUA-$(N)_{89}$-AUUUA$(N)_{17}$-AUUUUAAGAUUUA	c-myc
Class II (tandem AUUUA)		AAUAUUUAUUUAUUUAUUUAUUUAA	GM-CSF
Class III (U-rich, non AUUUA)		AUCCUGCCCAGUGUGUUGUUUGUAAAUAA	c-jun
Iron response element (IRE) [130]	3'UTR	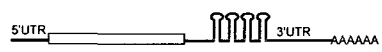	Transferrin receptor
Histone stem-loop [131]	3'UTR	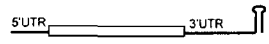	Histone
Coding region determinant (CRD) [133]	coding region	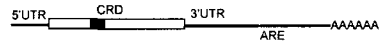	c-fos, c-myc
Jun kinase response element (JRE) [132]	5'UTR	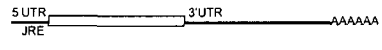	IL-2
Stem-loop destabilizing element (SLDE) [172]	3'UTR	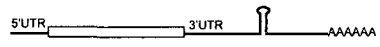	GM-CSF
miRNA target site [156]	3'UTR (usually)	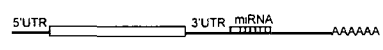	miR-1,124
Premature termination codon (PTC) [153]	coding region	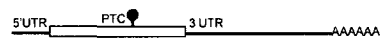	NMD*
Intron content/length [158]	coding region	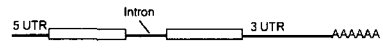	CXCL1
Alternate polyadenylation [159]	3'UTR	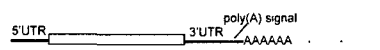	FGF2

* The presence of a PTC induces mRNA degradation through nonsense-mediated decay (NMD). GM-CSF, granulocyte macrophage-colony stimulating factor; IL-2, interleukin 2; CXCL1, chemokine ligand 1; FGF2, fibroblast growth factor 2. Adapted from [121].

the transferrin receptor [130] and the histone-stem-loop that replaces the usual poly(A) tail in histone mRNAs [131]. Depending on cellular iron concentrations or cell cycle status, these elements either stabilize or destabilize their respective transcripts. Examples of stability determinants residing in the 5'UTR or coding region include the Jun kinase response element in the IL-2 5'UTR [132] and the coding region determinant in the *c-fos* mRNA (which also contains an ARE in its 3'UTR) [133]. The vast majority of these elements, however, reside in the 3'UTR. Some authors have suggested that this is because sequences in this region are less constrained than in the translation initiation regions of the 5'UTR or the protein coding regions, and have therefore been allowed to evolve with greater variation [134].

Of the 3'UTR stability determinants discovered to date, the most prominent and well-studied are the AU rich elements (AREs) which were first identified as destabilizing elements by Shaw and Kamen [135]. Structurally, AREs are a stretch of adenine and uracil residues that are often, but not always arranged in characteristic AUUUA motifs of varying length. They have been grouped into 3 main classes depending on the arrangement of this AUUUA motif. Class I ARE-containing mRNAs contain dispersed single motifs and a separate U-rich region. Class II AREs are found as tandem $AUUU_n(A)$ repeats, while class III AREs are defined as having no canonical motif other than U-rich regions [136]. While much work has been done to elucidate the exact appearance of these elements, the identification of a canonical ARE has remained elusive [137-140]. They have been functionally defined as having the capacity to induce deadenylation-dependent degradation of host mRNAs [138]. Essentially, AREs function in controlling mRNA metabolism by

recruiting factors that either enhance or inhibit deadenylation-dependent decay [141]. AREs also play roles in nucleocytoplasmic transport of mRNA and translation [116].

Since the discovery of AREs in 1986 [135], their role in promoting and/or regulating mRNA decay has been extensively documented [17, 25, 26, 115, 129, 137, 138, 142-152]. These destabilizing elements have been found in many transiently expressed transcripts such as growth factors, lymphokines, and cytokines [reviewed in 129, 141, 150]. According to the most recent version of the ARE database, approximately 8% of human genes contain AREs [140]. The large number of genes potentially regulated by AREs highlights the importance of these elements. Their role in inducing rapid decay in many genes containing them has been validated by microarray experiments in mouse embryonic stem cells as well as human lymphocytes [115, 121]. These studies also noted however, that many ARE-containing transcripts were not rapidly degraded, highlighting the complex regulatory mechanisms that have evolved to coordinate the expression of ARE-containing genes in response to varying physiological, developmental, and tissue-specific conditions.

Two additional ways that the sequence within a particular mRNA can affect its stability are nonsense-mediated decay (NMD) and miRNA-mediated gene silencing. NMD is a highly conserved process that functions as a quality control mechanism for RNA. It is responsible for identifying and destroying mRNAs that contain premature stop codons, thus ensuring that mutated transcripts are not translated into protein [153]. miRNAs are ~22nt non-coding RNAs that interact with mRNAs through imperfect complimentary sequences, typically within 3'UTRs, in order to interfere with their expression (a general process known as RNA interference, RNAi). miRNAs are incorporated into the RNA-

induced silencing complex (RISC), which guides the RNAi machinery to the target sequence by forming a double-stranded RNA complex with it. miRNAs function in two ways; they inhibit target-gene translation and they induce rapid deadenylation-mediated decay of bound mRNAs. Both function to limit protein production [Reviewed in 153, 154]. In vertebrates, it is estimated that 1% of all genes encode miRNAs [155, 156], and computational studies have predicted that 20-30% of all protein coding mRNAs are subject to this method of gene silencing [157].

There is further evidence that intron content may encode mRNA decay rates. Zhao and Hamilton have shown that the inclusion of an intron in a CXCL1 mRNA expression construct drastically increased its half-life compared to an intron-free cDNA construct [158]. Finally, it has been shown that alternate polyadenylation occurs in a subset of eukaryotic genes, leading to alternate-length 3'UTRs [159]. One recent EST and cDNA mapping analysis on the human and mouse genome has predicted that over 5,000 genes might contain previously unreported 3' extensions after the discovery of polyadenylation sites lying in the 5-10kb region following currently annotated transcript ends [160]. Given the abundance of regulatory signals contained within 3'UTRs, the decision to use a truncated or full-length transcript via alternate poly(A) signals represents yet another layer of complexity imposed on the regulation of mRNA stability.

When one considers all the ways in which an mRNA can control its own fate through nucleotide sequence alone: AU-rich elements, iron-response elements, jun kinase response elements, histone stem-loops, premature stop codons, miRNA target-sites, intron content and alternate length 3'UTRs, it becomes evident that in nature there exists an incredibly fine-tuned system of post-transcriptional regulation that relies simply on the

variable half-life of an mRNA. When one further imagines these various stability determinants and their various binding partners working in tandem within the same gene, an almost infinite array of regulatory paradigms presents itself.

2.4.2b Trans-acting factors

As alluded to above, mRNA stability determinants are regulated though an abundant number of RBPs that convert an mRNA sequence into a meaningful code of transcript destruction or salvation. Only through association with these factors, and competitive and cooperative interactions between the various RBPs, can transcripts that contain these elements have their rates of decay tightly regulated.

The mRNA stability of genes involved in eukaryotic iron metabolism is regulated through IREs and 2 IRE-binding proteins (IRP1 and IRP2). The 3'UTR of the transferrin receptor contains five IRE stem-loops that target it for rapid decay. The ferritin mRNA, whose product acts as an iron sequestration molecule, contains a single IRE in its 5'UTR that affects translation initiation. During conditions of low intracellular iron concentrations, the IRPs are upregulated and bind to both sets of IREs. They block decay by binding to the receptor 3'UTR IREs and block translation initiation of ferritin through interactions with its 5'UTR IRE. In this way cells can maximize iron uptake and prevent sequestration. The process is reversed when iron levels are high, leading to the endonucleolytic cleavage of the transferrin receptor protein and the upregulation of ferritin [161].

The mRNA of metazoan histones contain a conserved 3' terminal 25-26 nucleotide stem-loop motif in place of a poly(A) tail. This element regulates histone mRNA translation and decay in a cell cycle-dependent manner through interactions with the stem-

loop binding protein. This protein in turn recruits factors required to initiate the rapid decay of histone mRNAs in a process similar to that of polyadenylated transcripts [162].

AU-rich elements are under constant and dynamic regulation through interactions with *trans*-acting ARE binding proteins (ARE-BPs). To date, approximately a dozen such ARE-BPs have been discovered [150]. The vast majority of these proteins aid in the rapid destruction of ARE-containing mRNAs by either blocking translation of nascent mRNAs, decoupling poly(A) binding protein from the poly(A) region, or by actively transporting and targeting the transcript for destruction by the exoribonuclease-containing exosome complex [163]. The best characterized of the ARE-associated destabilizing proteins are AUF1 (or heterogeneous nuclear ribonucleoprotein D, hnRNP D) and tristetraprolin (TTP). The only well-characterized ARE-BPs shown to stabilize ARE-containing transcripts are the ELAV (embryonic lethal, abnormal vision, drosophila) family of proteins consisting of HuR, HuB, HuC and HuD [107]. HuR is ubiquitously expressed, while other members of this family show neuronal specific expression. The Hu family of proteins were first identified as specific tumour antigens in neurological cancers [164, 165].

Because of its ubiquity and interactions with so many genes, HuR is the most important stabilizing ARE-BP and as such, has been extensively studied. Through gel-shift assays and UV-crosslinking experiments, HuR has been shown to bind ARE-containing mRNAs [25, 26, 107, 143, 146, 166]. Many of the targets that HuR stabilizes play roles in cell signaling, stress response, cell cycle progression and proliferation. Given this repertoire of genes, it is perhaps not surprising that the overexpression of HuR has been linked with neoplastic transformation and tumour progression [167-169]. The specific mechanism HuR might employ to convey this increased stability remains enigmatic. It was

first postulated that HuR blocks deadenylation-mediated ribonuclease decay by enhancing the binding of poly(A) binding proteins with the poly(A) tail and 5'cap of ARE containing transcripts, thereby rendering the transcript inaccessible to poly(A) ribonucleases. Conversely, destabilizing ARE-binding proteins are thought to uncouple the poly(A) tail complex, thereby leaving the transcript susceptible to deadenylation and 3' to 5' exonuclease attack [141].

Non-ARE-binding proteins have also been shown to bind to specific stability determinants and modify deadenylation-dependent decay, but less is known about them. One example is CUG-binding protein 1 (CUG-BP1), which seems to bind with high affinity to UGU-rich regions as well as CUG repeats [170, 171]. A novel stem-loop destabilizing element (termed SLDE by the authors) found in the 3'UTR of granulocyte colony-stimulating factor (G-CSF) mRNA also appears to enhance mRNA decay through unidentified specific RNA-protein interactions [172].

2.4.3 Pathways to destruction: mechanisms of mRNA decay

RNA decay is a very prominent process in all kingdoms of life. Not only must protein coding mRNAs be degraded once they are no longer useful, but introns, spacer fragments, small non-coding RNAs (ncRNA), and mutant mRNAs must also be degraded in an efficient manner. Adding to these endogenous RNA products, cells must also have methods for detecting and destroying viral RNA. Considering the wide array of RNA that must be destroyed, the efficiency of the various degradation pathways is incredibly high. It has been proposed that this efficiency has evolved for several reasons. Firstly, many types of small, ncRNA can exert dramatic effects on gene expression. Secondly, by rapidly

degrading RNA, potential DNA-RNA hybrids that may interfere with transcription or DNA replication can be avoided. A third possible explanation for the evolution of rapid RNA degradation is that the accumulation of large amounts of random RNA fragments might lead to the sequestration of RNA binding proteins, which would make the availability of such proteins limiting. This would have deleterious effects for pre-mRNA processing, translation, alternative splicing, and properly regulated mRNA decay [173]. To deal with the variation in mRNA species they encounter, all life forms have evolved highly sophisticated methods of detection and destruction of unwanted or unneeded RNAs. For the sake of brevity, this review will focus only on the eukaryotic degradation of protein coding mRNAs, again, with the realization that many other RNA decay processes have evolved to deal with the accumulation of ncRNA.

The majority of eukaryotic mRNA decay occurs via a deadenylation-dependent pathway (Figure 6). Following the dissociation between the poly(A) tail and poly(A)-binding protein and the removal of the poly(A) tail by specific exoribonucleases (deadenylases), mRNA is degraded in one of two main pathways. After the removal of the 5' cap by the decapping proteins, Dcp1 and Dcp2, mRNA is degraded in a 5'-3' manner by the Xrn1 exonuclease. Alternatively, the body of the transcript is degraded in a 3'-5' fashion through interactions with a large complex of exonucleases known as the exosome. These processes are highly conserved from yeast to higher mammals; however, it appears that the exosome-mediated 3'-5' decay pathway is much more prevalent in mammalian cells [174]. While deadenylases, decappers, and exonucleases of the exosome are all involved in various pathways of mRNA decay, the mechanisms of ARE-mediated decay are the best understood and will be described here.

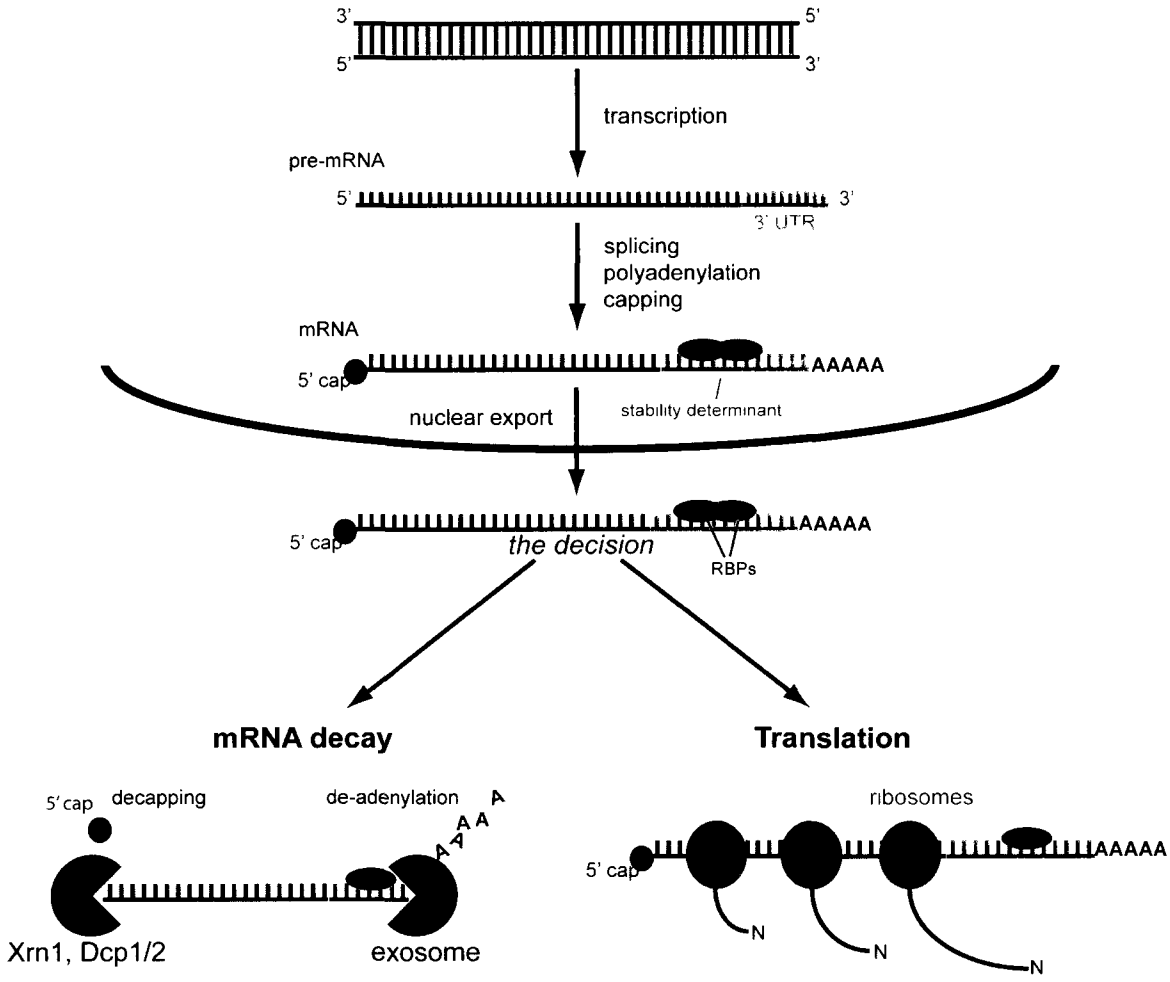

Figure 6. Eukaryotic mRNA decay. Following transcription and pre-mRNA processing, RNA binding proteins that either promote (red oval) or impair (green oval) mRNA degradation associate with stability determinants usually found in the 3'UTR (i.e. AU-rich elements). These proteins are often nucleocytoplasmic shuttling factors. Depending on cellular conditions and/or the relative abundance or affinity of these various binding factors, a particular mRNA will either be localized to ribosomal assemblies to be translated or to exoribonuclease containing exosomes to undergo decapping and deadenylation-dependent degradation. RBP, RNA binding protein; Xrn1, cytoplasmic 5' endonuclease; Dcp1/2, decapping complexes 1 and 2.

2.4.3a ARE-mediated decay (AMD)

Is has been shown that the exosome is essential for the degradation of ARE-containing mRNAs [145, 175]. However, work by Stoecklin and colleagues found that, in addition to components of the exosome, inhibition of Xrn1 by RNA interference strongly inhibited the decay of ARE-containing reporter constructs in mammalian cells, suggesting that the 5'-3' decay pathway is also used in AMD [176]. In support of these findings, Murray and Schoenberg found that AREs can differentially activate either 3'-5' or 5'-3' decay or both simultaneously [177]. Importantly for all mRNA decay, but especially in AMD, the substrates for these exonucleases are never naked RNA; rather, they are always highly processed or "tagged" RNAs containing a specific compliment of RNA-binding proteins (including ARE-BPs). These complexes of RNA and protein are known as ribonuclear protein complexes (RNPs). It has been proposed that this *allosteric model* for the activation of the exosome exists as a way of targeting specific RNAs for degradation at specific times and locations [178]. Chen and colleagues [145] first proposed that ARE-BPs mediate interactions between the exosome and ARE-containing mRNAs. They were able to show that the ARE-BPs KSRP (KH-type splicing regulatory protein) and TTP interact directly with components of the exosome, and were able to enhance decay of an mRNA containing the *c-fos* ARE. Destabilizing ARE-BPs recruit the exosome components to the target mRNA, while stabilizing proteins may hinder these interactions, sequester mRNAs away from sites of decay, or transport them to the translation apparatus [163]. For example, it has been shown that the translation of p53 is enhanced through interactions with HuR [76]. ARE-BPs are also able to influence decapping and deadenylation steps of mRNA turnover [179, 180].

2.4.3b Nonsense-mediated decay (NMD)

The last mechanism of RNA decay to be considered here is NMD. NMD is responsible for locating and eliminating mRNAs that contain premature termination codons (PTC) upstream of the normal stop codon. PTCs are often created following frameshift mutations. In this way, NMD removes error-containing mRNAs from the pool of translating transcripts [141, 181]. The importance of NMDs is highlighted by the fact that an estimated 30% of human disease alleles engage the NMD machinery and often NMD contributes to pathology [128, 182]. There are two main competing theories as to how the NMD machinery recognizes PTCs (reviewed in [153]) .

The first is the *downstream marker model.* This model posits that there are "marker" proteins associated with mRNAs downstream of any PTC and upstream of the proper termination codon. Normally, the translating ribosome and associated factors would encounter these marker proteins prior to the proper termination codon and dislodge them. When a PTC is present, the translational machinery stops before it reaches the marker protein. It is hypothesized that interactions between factors associated with translation termination can interact with the marker proteins and this interaction recruits components of NMD. Potential markers have been identified in yeast [183] and in mammalian cells. The exon junction protein complex deposited upstream of exon-exon junctions following RNA splicing events is widely thought to act as a marker for NMD [184]. The fact that mammalian stop codons are usually located within the last exon also supports this model [185].

The second model for PTC detection and initiation of NMD is the *aberrant termination model.* This idea predicts that there is a difference in translation termination

events between normal mRNAs and mRNAs containing a PTC. Essentially, following normal translation termination a specific RNP arrangement and structure protects mRNAs from decay. PTCs may induce alternate conformations or binding events which can trigger NMD [153]. The close proximity of the normal stop codon to the poly(A) tail might play a role in the proper termination of translation and/or stable conformation of an mRNA. The inclusion of the poly(A) tail and its associated binding partners also contributes to overall stability. The space between a stop codon and proteins associated with the 3'UTR may be important as it has been shown that the addition of extra sequence within the 3'UTR can induce NMD [186]. While neither of these two models can account for all evidence or be applied to all instances of NMD, it appears aspects of each of them are at play under different conditions. It has also been postulated that both models may be working in conjunction to induce aberrant translation termination, which induces NMD [153]. In addition to its role in RNA surveillance and quality control, NMD also appears to have roles in the post-transcriptional regulation of wild type mRNAs. For example, pre-mRNA splicing factors can regulate their own expression by targeting their own mRNAs for NMD, thereby affecting splicing patterns of their target pre-mRNAs [187].

2.4.4 Compartmentalized decision making: stress granules and P-bodies

It appears that following the inhibition of translation or the induction of a stress event, the decision to degrade a particular mRNA is made in discreet cytoplasmic foci known as stress granules, while the destruction of mRNAs targeted for decay occurs in processing or P-bodies

2.4.4a Stress granules

Stress granules are dynamic structures that form in cells exposed to environmental stress (i.e. heat, hypoxia, UV light irradiation). They contain aggregates of untranslated or stalled translationally initiated mRNAs, translation initiation factors, as well RNA binding proteins involved in regulating translation and stability. It is thought that stress granules are used by cells to reprogram their expression pattern by minimizing the translation of housekeeping genes and inducing the synthesis of proteins involved in stress response and repair. This selective recruitment of specific mRNAs is thought to regulate their translation and stability [188]. Stress granules have been referred to as "triage centers" of RNA metabolism because they sort specific mRNAs for reinitiation of translation, decay, or storage as intracellular conditions dictate [189].

2.4.4b Processing bodies

P-bodies on the other hand, lack ribosomal subunits or translation initiation factors and appear to be the location of mRNA decay. Instead, they contain deadenylases, the 5'-3' exonuclease XRN1, decapping proteins, components of nonsense-mediated decay and components of the RISC complex. Not surprisingly, P-bodies also house mRNAs subject to general, nonsense, and ARE-mediated decay, as well as those mRNAs targeted by miRNA or siRNA pathways [188]. P-bodies are sometimes referred to as GW bodies in the literature, on account of the inclusion of GW182 proteins required for RNA interference [190]. These two RNA granules are dynamic and interact with each other (Figure 7). For example mRNAs bound to destabilizing proteins such as TTP and BRF1 can be delivered

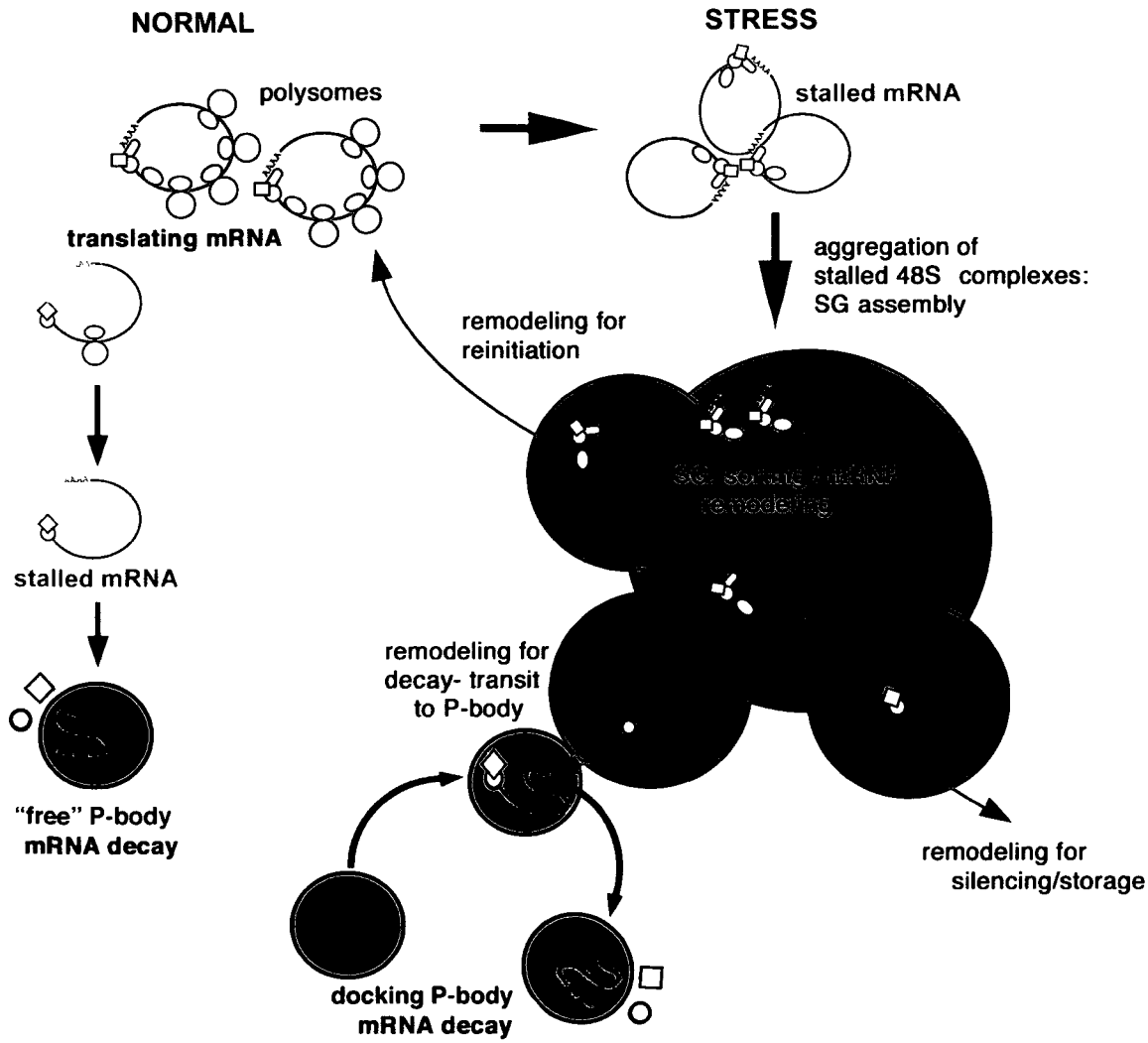

Figure 7. Interaction between processing bodies and stress granules. Following stress, mRNAs containing stalled ribosomal subunits (grey ovals) aggregate within newly assembled stress granules (green, SG). Here, they are sorted for storage, decay, or remodelling and reinitiation of translation. Processing bodies (blue, P-body) contain *trans*-acting RNA binding proteins and decay factors. They can associate with stress granules or decay stalled mRNA independently. Adapted from [192].

from stress granules to P-bodies for decay. Stress granules can also deliver their cargo to polysomes for translation [191, 192].

2.4.5 External stimuli: orchestrating rates of decay

In order for mRNA decay to play a meaningful role in regulating gene expression, external cues must affect the processes that determine RNA turnover. mRNA stability has been shown to be regulated by such environmental stimuli as developmental and differentiation cues, hormonal regulation, diurnal variation, hypoxia, UV light, polyamine depletion, ionizing radiation, heat shock, and proinflammatory stimuli [16, 22, 193-197]. While the exact mechanisms controlling the regulation of mRNA stability have not all been worked out, it is becoming clear that changes in cellular localization of RNA binding proteins and/or their affinity for specific mRNAs or subsets of mRNAs following cellular perturbation, are responsible. As in most areas of RNA stability research, current understanding of the coordinate regulation of stability is best understood in ARE biology. The basic paradigm of AMD regulation, however, provides clues and mechanisms that are likely at play for regulating the stability of non ARE-containing mRNAs as well. There is evidence that a large number of non ARE-containing mRNAs are stabilized following UV light, including histone mRNAs that lack a 3'UTR [22].

2.4.5a Regulation of ARE-mediated decay

ARE-dependent decay functions as a sensor for changing physiological conditions and allows cells to mount an appropriate cellular response. ARE-BPs are also nucleo-cytoplasmic shuttling proteins, and it is thought that they affect target mRNA stability in

part by transporting them from the nucleus to cytoplasm and on to sites of decay, translation, or storage. Therefore, cellular localization of RNA binding proteins in response to external stimuli is one way in which cells can modify the stability of mRNA. A good example of this comes from work on the cationic amino acid transporter, Cat-1, which is involved in transporting the essential amino acids arginine and lysine [198]. Expression of Cat-1 increases during nutritional stress, and it has been shown that amino acid limitation induces ARE-dependent mRNA stabilization through interactions with HuR, which itself shows increased cytoplasmic localization during starvation. The authors have termed this ARE a nutrient sensor. This represents an adaptive response to amino acid depletion that relies on a rapid induction of specific mRNA stabilization. In general, stabilization of target mRNAs by HuR is enhanced following treatment or exposure to such stimuli, which causes the redistribution of HuR from the nucleus to the cytoplasm [143, 166].

There is accumulating evidence that ARE-BPs work in antagonistic fashions, often competing for the same AREs in the same 3'UTRs, or binding simultaneously to multiple regions of specific transcripts [163, 199]. The implications for this competitive regulation are not fully elucidated, but it is likely that the ratio of stabilizing to destabilizing ARE-BPs associated with a given mRNA under specific physiological conditions dictate its fate. Such antagonizing roles for HuR and TTP have been postulated for COX-2 gene regulation and this interaction appears to be disrupted in colon tumourigenesis [200]. Many studies have functionally linked AUF1 and HuR and many mRNAs have been shown to be regulated by both proteins [201-203]. One study using RNA immunoprecipitation followed by cDNA microarray analysis revealed that HuR and AUF1 may have over 250 target mRNAs in common [163]. Complicating matters further, fluorescence resonance energy

transfer (FRET) analysis has shown that HuR and AUF1 proteins form homodimers and heterodimers with each other [204].

It is interesting to note that most ARE-BPs contain AREs in their own mRNA, and it is tempting to speculate that these elements are under the control of multiple ARE-BPs or their own protein products, implying self-regulation. In fact, ARE-BPs have been shown to bind to their own transcript. TTP, a destabilizing ARE-BP, was shown to interact with its own 3'UTR and destabilize it [205]. Pullmann and colleagues [206] have shown through immunoprecipitation experiments that HuR mRNA is capable of binding to its own protein in untreated cells. Furthermore, they showed that several other ARE-BP mRNAs are found bound to HuR as well as their own proteins in a 3'UTR-dependent manner. Alternate splicing of ARE-BPs may also play a role in selective stabilization of target mRNAs. Different isoforms of AUF1 have varying affinities for AREs and not all isoforms target mRNAs for destruction. It appears that the relative concentrations of each isoform dictate the effect of AUF1 on target stability more so than the absolute amount of cellular AUF1 [199].

2.4.5b Post-transcriptional RNA regulons

Situations exist in which it may be desirable to coordinate induction or repression of a subset of genes involved in particular responsive pathway. One relatively simple way a cell can rapidly modify the expression of a subset of genes is to modify the stability of specific transcription factors. Through the phosphorylation of the *Schizosaccharomyces pombe* (Fission yeast) RNA-BP Csx1 in response to oxidative stress, Csx1 binds to and stabilizes the mRNA of the Atf1 transcription factor. Therefore, during oxidative stress, all

the genes dependent on Atf1 can be upregulated [207]. Considering the rapidity with which differential mRNA stability can regulate expression patterns and the fact that many cellular stress events transiently block nascent transcription, the ability for cells to regulate complete pathways to mount an adaptive response is paramount to their survival. This has led to the concept of "post-transcriptional operons or regulons", first proposed by Keene and Tenenbaum [117, 208]. Essentially, this theory posits that *trans*-acting factors (primarily RBPs or miRNAs) cooperatively modify the post-transcriptional regulation of multiple, functionally-related mRNAs in response to environmental cues through interactions with untranslated regions within the mRNAs being regulated.

The idea is in some ways homologous with bacterial operons in which related pathway genes are physically transcribed together into polycistronic transcripts. These are then processed into individual genes [209]. RNA operons or groups of similarly regulated mRNAs contain the same response elements that theoretically will interact with the same RBPs under specific conditions to create highly specific RNP complexes (Figure 8). mRNAs often contain more than one stability determinant which would mean they could be members of multiple regulons (*RNA operon* and *regulon* are used interchangeably), each one requiring a different combination of binding partners and/or environmental signals [210]. Experimental evidence for the RNA operon model comes from studies that demonstrate distinct classes of mRNA have similar and simultaneously alterable half-lives [113]. Evidence also comes from work that shows ARE-BPs regulate many related genes in the same manner, especially those involved in mediating immune response [211].

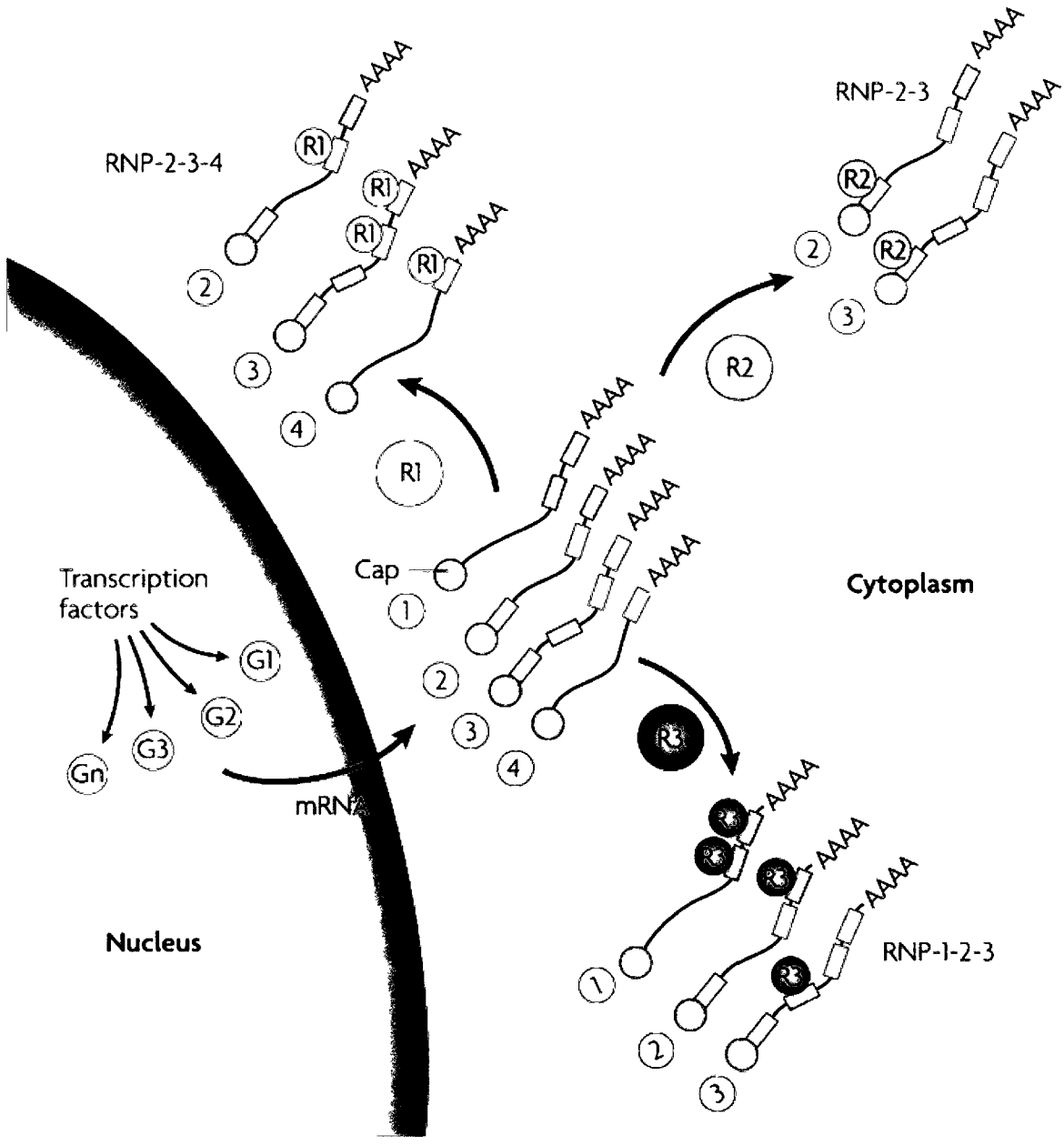

Figure 8. Post-transcriptional RNA regulons coordinate the decay of subsets of mRNAs. The four mRNAs (labelled with numbered white circles) form three different RNA operons, labelled as ribonucleoprotein (RNP)-2-3-4, RNP-2-3 and RNP-1-2-3. The make-up of each regulon is determined by the binding of RBPs (labelled R1, R2 and R3) to specific sequence elements. The four transcripts contain different combinations of RBP-binding elements. Therefore, mRNAs that contain more than one binding element can be members of more than one RNP complex. Adapted from [210].

2.4.6 The 3'UTR, mRNA stability and disease

Not surprisingly, aberrant stability regulation has been implicated in many disease states [reviewed in 134] and cancer [111]. For example, myotonic dystrophy results from a hyperamplification of a 3'UTR CTG repeat in the cAMP-dependent protein kinase DMPK gene. Essentially, these repeats sequester the RNA binding CUG-BP away from its other targets, leading to the observed disease phenotype [125]. ARE function has been lost in genes with truncated or rearranged 3'UTRs, often leading to over-stabilized mRNAs. Mutating the regulatory AREs in the 3'UTR of TNF increases its stability, which has been linked to chronic inflammatory arthritis and inflammatory bowel disease [126]. Finally, a polymorphism found in the 3'UTR of TNF-α disrupts HuR binding, leading to a decrease in protein expression in NZW mice [212].

Recently, much attention has been given to the idea that 3'UTR-mediated differential mRNA stability plays a role in the deregulation of gene expression observed in the cancer phenotype [111, 112]. There are numerous examples of aberrant 3'UTR biology in cancer. The 3'UTR of cyclin D1 is truncated in two lymphocytic leukaemia cell lines [213] and was found to be rearranged in patients with mantle cell lymphomas or t(11q13)-associated leukemia [214]. An ARE-missing cyclin D1 3'UTR has also been observed in the breast cancer cell line MDA MB-453 [215]. Human papilloma virus type 16 (HPV-16) genomes are frequently found integrated into host chromosomes in human cervical cancers. The 3'UTR of the viral oncogenes E6 and E7 contains a destabilizing ARE, but the 3'UTR region is often disrupted during integration causing a loss of instability and an overexpression of E6 and E7 oncogenes in the host tissue due to increased mRNA stability [216].

2.4.6a Targeting mRNA stability as a therapeutic approach

Because of the emerging understanding of how deregulated mRNA turnover can cause disease, there is a growing interest in developing therapeutic approaches to target mRNA stability. The majority of the current approaches rely on targeting upstream signalling cascades such as p38-MAPK or PKC pathways that induce post-translational modifications of RNA binding proteins [217]. Because these pathways affect many genes unrelated to mRNA stability or disease, more RNA-stability specific approaches have also been investigated. Three of these are summarized briefly below.

Stoecklin and colleagues [147] overexpressed TTP in a mast cell tumour model to destabilize abnormally stable IL-3 mRNA. They were able to decrease proliferation *in vitro*, delay tumor progression in mice and showed for the first time that tumor suppression can be achieved by interfering with mRNA turnover. Work has also focused on blocking the anti-apoptotic bcl-2 mRNA from being stabilized by the ARE-BP nucleolin. This may offer a novel approach to inducing apoptosis in tumour cells [218]. Lastly, by tethering the decay promoting ARE-BP KSRP to non ARE-containing mRNAs, Chou and colleagues [219] were able to increase these mRNA decay rates by targeting them for exosome mediated decay. Using the same approach, they were able to suppress HIV-1 Rev expression and dramatically decrease HIV replication.

More generally, technological advances in targeting specific mRNAs involved in disease phenotypes through the use of antisense oligonucleotides, RNA interference, rybozymes and other specialized endoribonucleases have demonstrated the therapeutic potential of targeting aberrant mRNA expression [220].

2.5 Summary, Hypothesis and Objectives

2.5.1 Summary

UV light is a powerful environmental mutagen. It induces a number of cellular responses that ultimately dictate whether a cell will succumb to UV-mediated DNA damage or if it will repair it and survive. These responses are multifaceted and are mediated by many players. One of the most important players is the p53 tumour suppressor. Depending on environmental cues and the amount of UV exposure, p53 will direct cells to arrest their cell cycle progression, initiate DNA repair, or induce apoptosis. However, due to its ability to promote apoptosis, constitutive exposure to p53 is harmful to cells and in the absence of stress, it is kept in check through rapid ubiquitin-mediated degradation [71, 72, 221].

While much work has been done to elucidate the p53-mediated transcriptional response to UV damage, little has been done to investigate the role post-transcriptional regulation has on dictating the expression of these p53 target-genes. Following UV light exposure, mRNA synthesis is dramatically impaired due to RNA polymerase blocking lesions [119]. This is especially problematic for longer genes as UV lesions are induced in a stochastic manner [21]. Therefore, the ability for an mRNA to increase its stability following UV insult would dramatically increase its chances of being expressed in sufficient quantities despite its limited transcription.

p53 itself bypasses the need for *de novo* transcription through a vast array of post-transcriptional modifications. Our group has previously found that it circumvents transcriptional blockage of its target-genes, by preferentially inducing shorter genes

following high UV doses, while suppressing longer ones [20]. Several genes, however, did not follow this pattern. One of them was the gene encoding the GG-NER lesion recognition DDB2 protein [20]. This gene is approximately 24kb long and would therefore be predicted to sustain multiple lesions with a moderate dose of UV light ($10J/m^2$) [104]. Despite this, we have found that DDB2 mRNA levels remain elevated following UV irradiation.

DDB2 has been shown to bind damaged DNA within minutes of UV irradiation [222], with the repair of most CDPs occurring within 6 hours [91]. Paradoxically, both mRNA and protein levels of DDB2 do not spike until 24 and 48 hours respectively, after UV treatment. It has subsequently been shown that the DDB2 protein is rapidly degraded by the ubiquitin-proteosome pathway following UV irradiation [47, 223, 224].

2.5.2 Hypothesis and objectives

The benefits of a model that predicts the widespread post-transcriptional regulation of p53 target-genes at the level of mRNA stability would be two-fold. First, if p53 target-gene transcripts are short-lived before or immediately after exposure to UV light, this would provide an efficient means of keeping the expression of potentially apoptotic genes in check. Secondly, a rapid increase in the stability of a select group of mRNAs following UV light would allow for the prolonged expression of genes required to mount a stress response without the requirement for nascent mRNA synthesis.

A. We hypothesize that p53 target-genes are relatively short-lived and a subset of them are post-transcriptionally regulated following UV light at the level of mRNA stability.

The transcriptional regulation of DDB2 following UV light exposure is paradoxical in that its upregulation occurs long after most CPDs have been repaired. Despite its longer gene size, we have found that the p53-dependent induction of DDB2 is sustained following UV light exposure. If DDB2 mRNA was stabilized following UV insult, this may provide sufficient template for continued protein synthesis and lesion recognition in the absence of nascent DDB2 transcription. As an example of a p53 target-gene that is post-transcriptionally regulated following UV light:

B. We hypothesize that post-transcriptional regulation of DDB2 mRNA contributes to UV-induced DDB2 expression (Figure 9).

Through the use of a conditional p53-inducible cell line, we have determined that p53 target-mRNAs in general, and DDB2 specifically, are short-lived under normal conditions and if their stabilities are increased by UV light. We further isolated and characterized a DDB2 mRNA stability determinant using a destabilized EGFP reporter system that allowed for a multifaceted analysis of how this determinant affects DDB2 mRNA and protein expression.

The inability to repair lesions throughout the genome during GG-NER is the defining feature of the genetically heritable XP-E syndrome, a condition caused by deficient DDB2 [58, 225]. Understanding the post-transcriptional regulation of DDB2 may shed light on DNA repair in general and the etiology of XP-E specifically. Furthermore, this work will add to the knowledge of regulatory paradigms that dictate p53 target-gene induction following UV exposure. Lastly, it offers new methods to study and visualize mRNA decay that do not rely on cytotoxic chemical transcription inhibitors.

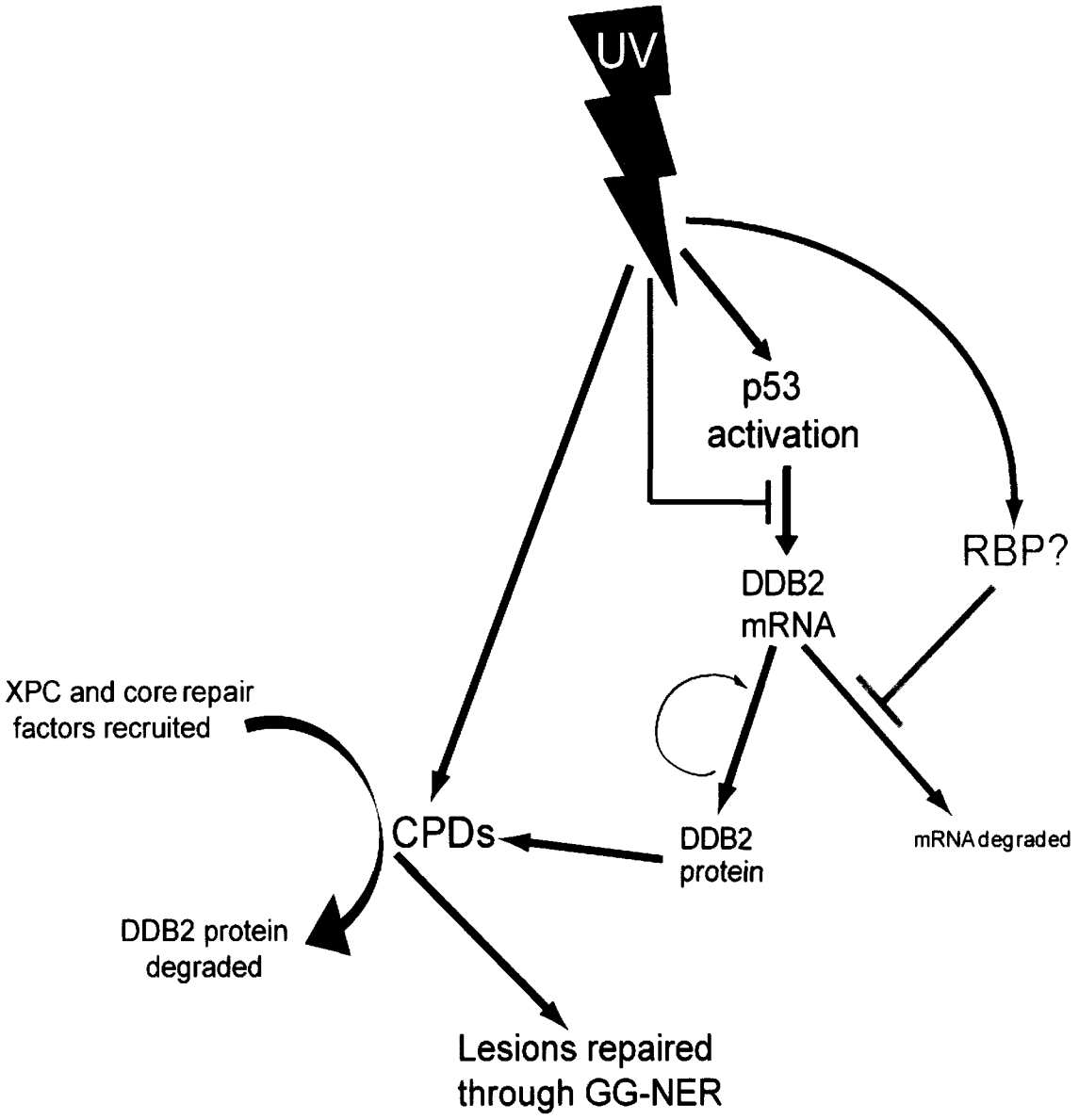

Figure 9. DDB2 is regulated at multiple levels following UV light exposure. UV light induces DNA helix-distorting lesions throughout the genome and induces p53 activation, which in turn upregulates DDB2 expression. DDB2 protein binds to CPDs, recruits core repair factors, and is rapidly degraded. CPDs are then removed by the GG-NER pathway. The transcriptional upregulation of DDB2 by p53 occurs well after the majority of repair is complete. UV-induced lesions impair transcription by blocking RNA polymerase II elongation. UV-mediated post-transcriptional regulation (grey lines) may increase the pool of available DDB2 mRNA to the translation machinery by blocking mRNA decay without relying on *de novo* mRNA synthesis. RBP, RNA binding protein; CPD, cyclobutane pyrimidine dimer; GG-NER, global genomic nucleotide excision repair.

Chapter 3 Materials and Methods

3.1 Cell culture and UV treatment

HT29-tsp53 human colon cancer cells express a temperature sensitive p53 variant that has a substitution of valine to alanine at position 135 (V135A) [226]. Cells were maintained at 38°C in a humidified atmosphere with 5% CO_2. Where indicated, HT29-tsp53 cells were incubated at 32°C to induce functional p53 for the indicated period of time (Figure 10). HeLa Tet-Off (TO) cells (Clontech Laboratories, Mountainview, CA) and all cell lines derived from them were maintained at 37°C in a humidified atmosphere with 5% CO_2, and were supplemented with 200μg/ml G418 antibiotic (Sigma-Aldrich, St. Louis, MO). All cell lines were grown in Dulbecco's modified Eagle's medium (DMEM) supplemented with 10% fetal calf serum (FCS) (Thermo Fisher Scientific, Waltham, MA).

Where indicated, growth medium was removed and cells were exposed to the indicated fluence of UV light at 1 $J/m^2/s$ from a germicidal bulb (Philips, Markham, ON) emitting predominately at 254 nm (UVC). Following UV exposure, fresh medium was replaced and cells recovered for the indicated period of time. To inhibit expression of the Tet Response Element (TRE) and downstream reporter constructs in the HeLa TO cells, growth medium was removed and replaced with fresh media containing doxycycline (Dox) at a final concentration of 1μg/ml where indicated. To inhibit nascent RNA synthesis, actinomycin D (Act D, Sigma-Aldrich) was added to antibiotic-free media to a final concentration of 5μg/ml or 1μg/ml in HT29-tsp53 or HeLa TO cells, respectively. To

A

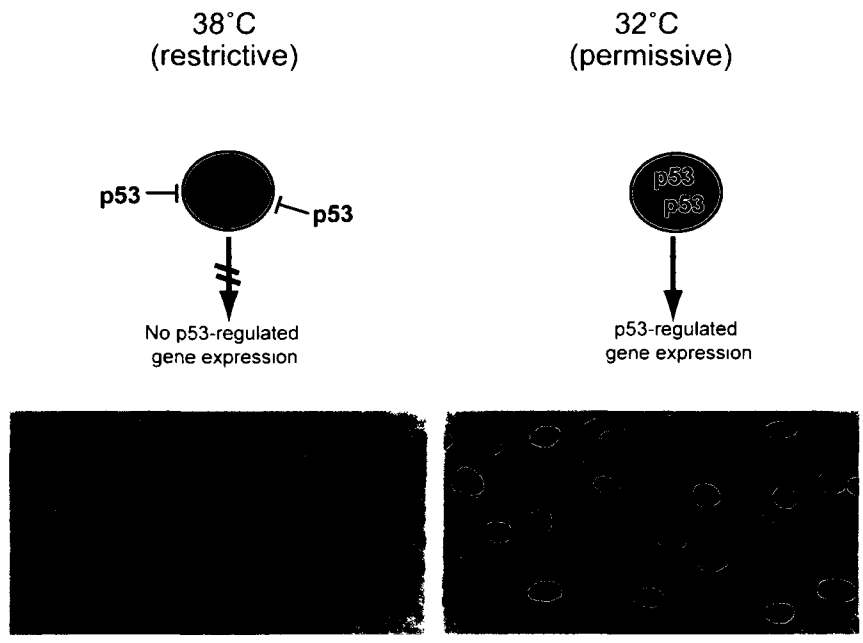

B

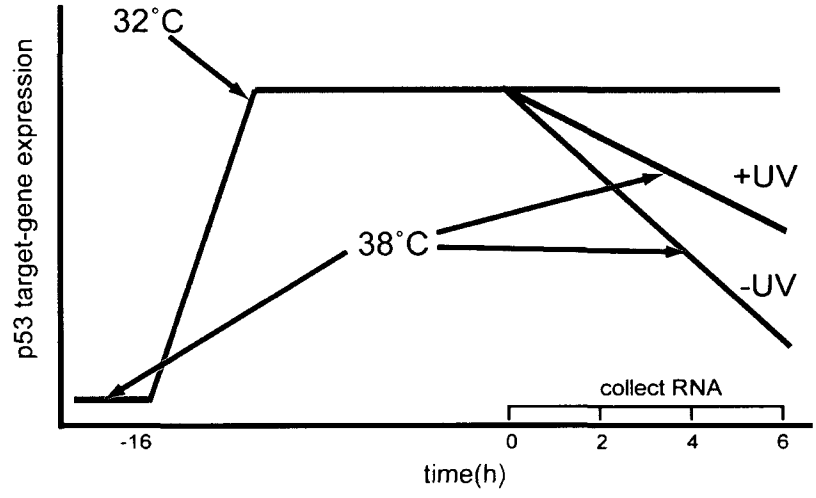

Figure 10. HT29-tsp53 cell line and experimental scheme. (A) At 38°C, tsp53 is cytoplasmic and cannot drive target-gene expression, while at 32°C, it is nuclear and behaves as wild-type. Image reproduced from [226]. (B) p53 target-gene expression can be activated at permissive conditions and rapidly inhibited under restrictive conditions. When transcription is inhibited, mRNAs that are stabilized by UV light should decrease more slowly following UV treatment. Therefore, mRNA decay rates can be inferred from collecting samples at various times with and without UV exposure following the inhibition of p53 target-gene transactivation.

inhibit protein synthesis, cycloheximide (CHX, Sigma-Aldrich) was added to antibiotic-free media to a final concentration of 50μg/ml in HT29-tsp53 cells.

3.2 Quantitative RT-PCR

Cells were trypsinized, harvested and washed with PBS. Total RNA was isolated using the RNeasy RNA isolation kit (Qiagen, Valencia, CA) according to manufacturer's specifications. Five micrograms of total RNA was reverse-transcribed by using the First Strand cDNA Synthesis Kit (MBI Fermentas, Burlington, ON). Quantitative reverse transcriptase polymerase chain reaction (RT-PCR) analysis was performed using the Sybr green fluorescent DNA stain (Invitrogen, Carlsbad, CA) and the LightCycler 2 thermo cycler machine with Light-Cycler software version 3 (Roche Diagnostics, Switzerland).

When possible, intron-spanning primers were used to measure the expression of: DDB2 (CCACCTTCATCAAAGGGATTGG and CTCGGATCTCGCTCTTCTGGTC), DDB2 3'UTR (GAGAGACACTAAAGAAGG and TATCAAAAGAGCACAAATC), p21 (CTCAAATCGTCCAGCGACCTT and CATTGTGGGAGGAGCTGTGAA), FAS (CCCAGAATACCAAGTGCAGATG and TCCTTTCTGTGCTTTCTGCATG), MDM2 (AGGTGATTGGTTGGATCAGG and GAAGCCAATTCTCACGAAGG), PIG3 (TCTCTATGGTCTGATGGG and TTGCCTATGTTCTTGTTG), BTG2 (GTGAGCGAGCAGAGGCTTAAGG and TGCGGTAGGACACCTCATAGGG), Maspin (CTTTTCTGTGGATGCCGATT and CCTGCCAGGGCTTAACATAA), XP-C (AAGTTCACTCGCCTCGGTTGC and TTCTTTCCTGATTTTAGCCTTTTT) and EGFP (CGACGGCAACTACAAGACC and CCATCATCCTGCTCCTCCAC). Expression of each transcript was normalized to the expression of β-actin

(GGGCATGGGTCAGAAGGAT and GTGGCCATCTCTTGCTCGA) or GAPDH (AACAGCGACACCCACTCCTC and GGAGGGGAGATTCAGTGTGGT) mRNA levels. RT-PCR was also performed using primers for GFP, β-actin, DDB2, DDB2 3'UTR, ACP2 (ACCGGCAAGAGGTTTATGTG and AGCAGCCTGTCCTCAGTGAT) and ACP2 3'UTR (ACACGGTCTTGCCTCTCAGT and ACAGACAACCTTCCGTCCTG). To ensure the antisense area of the ACP2 3'UTR was in fact expressed, three additional ACP2 3'UTR primers were designed that amplified a region that: partly overlaps with the DDB2 3'UTR (ACACGGTCTTGCCTCTCAGT and GGGAATGTGGGTTTCCTTCT), overlaps the DDB2 3'UTR and a DDB2 intron (TTTGGCCCTTTAACAAATCG and TCCCAAAGTGCTGGGATTTAC), or is completely within a DDB2 intron (CTGGGGAAGGATTCTTGACA and GTCCTTTGATGCCTTTTTGC). For all genes, elongation time and salt concentrations were optimized to ensure high replication efficiency. Melting point analysis and gel electrophoresis confirmed the identify and singularity of amplicon. Lastly, a dilution series was used to generate standard curves for each primer set to ensure sample expression fell within the linear range of detection.

3.3 cDNA microarrays

HT29-tsp cells were switched from restrictive conditions to permissive for 16h, then returned to restrictive with or without UV treatment at time of temperature shift. Six hours later, they were harvested and total RNA was collected. Human Gene 1.0 ST oligonucleotide arrays (Affymetrix, Santa Clara, CA) were used for expression analysis. cDNA synthesis and experimental procedures were performed according to the manufacturer specifications at the Ottawa Genomics Innovation Centre Affymetrix Gene-

Chip Facility (Ottawa, ON). GeneSpring GX 11 analysis software (Agilent Technologies, Santa Clara, CA) was used to analyse microarray data. Genes were considered to be p53-induced if they were previously known p53 targets (as found in the p53FamTaG target-gene database, www2.ba.itb.cnr.it/p53FamTaG/) to rule out effects of temperature shift, *and* were induced at least 2-fold in all experiments after 16h under permissive conditions.

3.4 Immunoblotting

Cells were trypsinized, harvested, rinsed with PBS, lysed with RIPA buffer and sonicated for 20s using a microtip (Branson Sonifier, VWR International Ltd., Mississauga, ON). Protein concentrations were determined using the BioRad Protein Assay (BioRad, Mississauga, ON). Whole cell lysates were prepared using LDS NuPAGE sample buffer (Invitrogen Canada Inc., Burlington, ON). Proteins were separated in 4–12% Bis-Tris NuPAGE precast gels, transferred to nitrocellulose membranes (Hybond-C Extra, Amersham, Baie d'Urfe, QC) and stained with Ponceau S Red (5 mg/ml in 2% glacial acetic acid) to confirm transfer of proteins. Membranes were blocked in PBSMT-A (PBS, 5% nonfat dry milk powder, 0.05% Tween 20) for 1 hr at room temperature. They were incubated with primary antibody against β-actin clone AC-74 (Sigma-Aldrich Canada Ltd. Oakville, ON), CUG-BP1 (3B1) or GFP (B-2) HRP (Santa Cruz Biotechnology, Santa Cruz, CA) for 1hr at room temperature or with XPE/DDB2 AF3297 primary antibody (R&D Systems, Minneapolis, MN) overnight at 4°C. Secondary antibodies (for β-actin and CUG-BP1: Goat anti-mouse IgG Peroxidase Conjugate from Calbiochem, [Darmstadt, Germany] and for DDB2: Rabbit anti-goat IgG-HR Peroxidase from R&D Systems) were applied for 45 minutes. All antibodies were diluted in PBSMT-B (PBS, 0.5% nonfat dry

milk powder, 0.05% Tween 20). Protein bands were visualized using SuperSignal West Pico Chemiluminescent Substrate (Pierce, Rockford, IL) and Kodak X-ray film (Rochester, NY). Membranes were stripped with Restore Western Blot Stripping Buffer (Pierce, Rockford, IL) in order to visualize additional proteins on the same blot.

3.5 EGFP reporter plasmid construction

Fragments spanning various regions of the DDB2 3'UTR were PCR amplified using primer pairs listed in Figure 11. Primers used to generate the IL-1β 3'UTR fragment were CGGAATTCGAGAGCTGTACCCAGAGAGTC (including an EcoR1 linker) and CGGGATCCCTTCAGTGAAGTTTATTTCAG (including a BamH1 linker). Mutant C-3 fragment oligonucleotides and their complimentary sequences (see Table 4, Results section for sequences) were synthesized and annealed together using Oligo Annealing Buffer (Promega, Madison, WI) according to manufacturer's instructions. For final insertion into the pTRE-d2EGFP reporter plasmid, all fragments contained an EcoR1 linker on their 5' end and an Xba1 linker on their 3' end. All fragments were cloned into pCR2.1-TOPO cloning vector using the TOPO TA cloning kit (Invitrogen, Burlington, ON) according to manufacturer's instructions. Fragments were excised with EcoRI and Xba1 restriction enzymes (New England Biolabs, Ipswich, MA) and ligated into pTRE-d2EGFP reporter plasmid (Clonetech Laboratories, Mountainview, CA). Once cloning was completed, all fragments were sequenced and compared to DDB2 mRNA NCBI Reference Sequence: NM_000107.2.

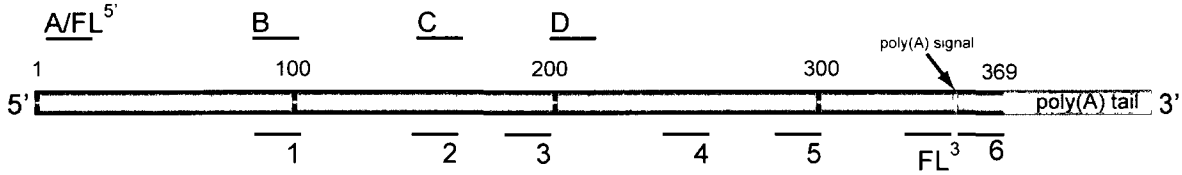

5' Primer(location)	Sequence (with EcoR1 linkers)
A/FL^5 (1)	GGAATTCGAGAGACACTAAAGAAGG
B (91)	GGAATTCGGGCCAAAAGTATCCAAGGT
C (150)	GGAATTCGGACTGGGACACTTTTATGTTAATG
D (200)	GGAATTCTCCAGAGTTGGTGACACAGC
3' Primer(location)	**Sequence (with Xba1 linkers)**
1 (100)	CGTCTAGACTTTTGGCCCTTTAACAAATCA
2 (164)	CGTCTAGAAAAGTGTCCCAGTCCCACAG
3 (198)	CGTCTAGACAGTCTCTGGAGGCAAGTCC
4 (250)	CGTCTAGACCAGGCTAGATACAGAGGGG
5 (300)	CGTCTAGAACCACCCACTGAGAGGAGAA
6 (363)	CGTCTAGACGGTATGGTTTTATTGGCCA
FL^3 (343)	CGTCTAGATATCAAAAGAGCACAAATC

Figure 11. Diagram of the DDB2 3'UTR and location and sequence of cloning primers. Fragments of the DDB2 3'UTR were cloned into reporter constructs using primers situated at the locations indicated by letters or numbers. Letters (above the diagram) represent 5' primers, while numbers (below diagram) represent 3' primers. See text for details on vector cloning strategies. Small numbers above diagram represent nucleotide position. FL; full-length primers.

3.6 d2EGFP transfections and fluorescence-activated cell sorting (FACS)

HeLa TO cells were seeded at 50% confluence and 24 hours later were transfected with empty pTRE-d2EGFP constructs or constructs containing various 3'UTR fragments using GeneJuice Transfection Reagent (EMD Chemicals, Gibbstown, NJ) according to manufacturer's instructions. Cells were passaged for approximately one week. EGFP-positive cells were then separated from the main population through high-speed cell sorting using a DakoCytomation MoFlo flow cytometer (Dako, Denmark). Experimental procedures were performed according to manufacturer's instructions at the Flow Cytometry Facility at the Ottawa Genomics Innovation Center (Ottawa, ON). This small EGFP-enriched population of cells was further passaged for 1 to 2 weeks and the process was repeated until over 80% of cells were EGFP-expressing.

Single-cell derived clones were generated by plating FACS-generated cells at an extremely low confluency on 6cm tissue culture dishes so that each colony formed was from a single cell. These colonies were then isolated from one another using small plastic rings adhered to the plate using vacuum grease. Colonies within each ring were trypsinized, collected and transferred to individual 30mm tissue culture dishes.

3.7 Flow cytometry

Following indicated times of Dox exposure, d2EGFP-expressing HeLa cells were trypsinized, washed and collected in PBS. One parameter flow cytometry was carried out using a Beckman Coulter Epics XL flow cytometer (Beckman Coulter, Mississauga, ON). EGFP fluorescence was excited at 488 nm and emission was measured at 510 nm. Data was analysed using FCS Express 3.0 software (De Nova Software, Los Angeles, CA).

Total fluorescence was calculated by subtracting the background fluorescence of EGFP-negative cells (% GFP-negative cells * mean fluorescence) from fluorescence of EGFP-positive cells (% GFP-positive cells * mean fluorescence) from each sample. All samples were then expressed as a percentage of total fluorescence compared to the no Dox samples.

3.8 Live cell imaging

Live cell imaging was performed on an automated Zeiss Axiovert 200 Inverted Fluorescent microscope fitted with a Colibri LED illumination system (Carl Zeiss International, Germany) and Bioptechs environmental chamber (Bioptechs, Butler, PA). d2EGFP-expressing HeLa cells were seeded at 40-60% confluence in antibiotic-free complete media for at least 16 hours on Delta T live cell imaging open tissue culture dishes (Bioptechs). Time lapse images were collected every half-hour following Dox treatment and fluorescence was calculated by averaging the total pixel intensity of at least 3 individual cells/cell line.

3.9 RNA interference

HeLa cell lines were maintained in antibiotic-free media at least 48 h prior to transfection. Cells at 50–80% confluence in 10cm culture dishes were transfected with ON-TARGETplus SmartPool siRNA duplexes targeting CUG-binding protein 1 (CUGBP1) or a control non-targeting (NT) duplex (Dharmacon Inc., Lafayette, CO) at 50 nM final concentration using Oligofectamine Reagent and Opti-MEM I (Invitrogen, Burlington, ON) according to manufacturer's instructions. Cells were split 1:3, 24h following transfection and treated with Dox 48h following transfection.

Chapter 4 Results

4.1 UV light differentially affects the p53-dependent expression of DDB2, MDM2 and FAS

HT29-tsp53 cells are a human colorectal carcinoma-derived cell line that expresses a transgene encoding a temperature sensitive murine variant of p53 (V135A) [226]. At the restrictive temperature (38°C), this variant is in a mutant conformation and remains cytoplasmic [227, 228]. At the permissive temperature (32°C), p53 is in wild-type conformation and localizes to the nucleus where it rapidly induces target-gene expression [20, 227-229] (Figure 10, Materials and Methods). This cell line permits the tight temporal regulation of p53 function without a requirement for *de novo* transcription or translation and it does not require DNA damage to induce target-gene expression [20, 229, 230]. HT29-tsp53 cells were switched to the permissive temperature at the time of UV exposure (between 0 and 30 J/m^2), and 6 hours later RNA was extracted for real-time RT-PCR analysis. Three similarly-sized genes, DDB2, MDM2 and FAS were induced to a similar extent in the absence of DNA damage (Figure 12A). However, there was a significant difference in the pattern of DDB2 expression compared to MDM2 and FAS when cells were UV-irradiated (Figure 12B). Specifically, UV light prevented the full p53-dependent induction of MDM2 and FAS in a dose-dependent manner with 50% inhibition at 20 J/m^2. In contrast, the induction of DDB2 was not significantly inhibited at doses of 20 J/m^2 or less (Figure 12B). Therefore, UV light differentially affected the expression of these three genes.

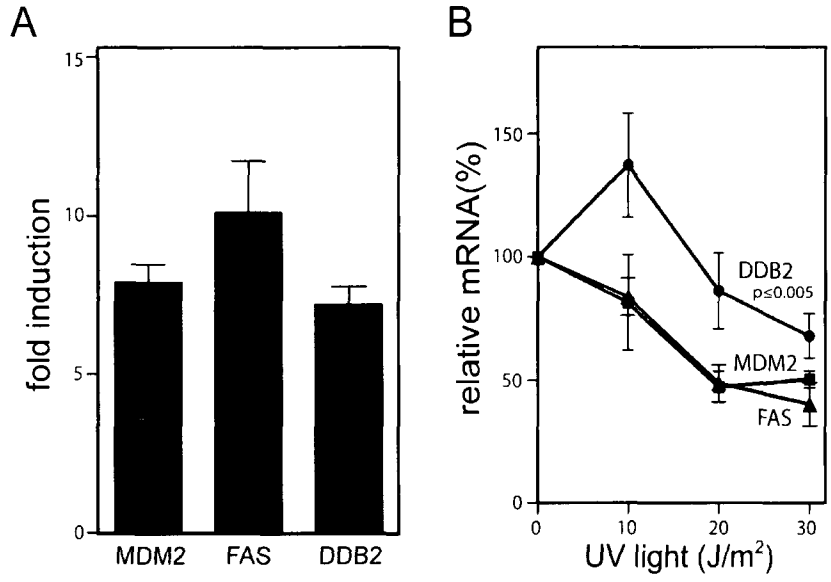

Figure 12. HT29-tsp53 cells induce p53 target-genes at the permissive temperature and their induction is differentially affected by UV light. (A) Cells were grown at the restrictive temperature (38°C) then switched to the permissive temperature (32°C) for 6h. The expression of MDM2, FAS, and DDB2 mRNA were analysed by real-time RT-PCR and expressed as fold increase in expression. (B) Transcript-specific effect of UV light on p53 target-gene expression. Cells were grown at the restrictive temperature, then treated with indicated doses of UV light and switched to permissive temperature for 6 hours. Expression presented as % of relative mRNA compared to levels 6h after induction with no UV (100%). P value for DDB2 in B determined by 2-way ANOVA. Measured by real-time RT-PCR. All values represent the mean ± standard error of 3 independent experiments.

Under identical conditions, we previously reported that UV light led to a decrease in the number and fold induction of p53 target-genes [20]. We found that the median size of p53-regulated genes identified through our previous work was 14 kbp, about 50% smaller than the median size of known genes [20, 231]. The median size of UV-inhibited p53 target-genes was 23 kbp while the median size of genes induced at the highest dose of UV light was only 8 kbp [20]. Thus, the inhibitory effect of UV-induced DNA damage on p53 target-gene expression was more pronounced on large genes while compact genes escaped this inhibition [20].

The DDB2 gene (GeneID: 1643) is 24 kbp long, which is similar to MDM2 and FAS gene lengths. Therefore, the differences in expression are not related to gene size. Because the pattern of DDB2 expression is consistent with a smaller target-gene, we first considered the possibility that the use of an alternate cryptic downstream promoter could produce a DDB2 transcript from a smaller locus. Although the RT-PCR product was only 501 nucleotides, the PCR primers spanned the majority of the genomic locus: 18.3 of the 24.2 kbp. The differential response to UV light cannot be explained by the expression of a compact variant of DDB2 initiating from an internal cryptic promoter. Instead, we considered the possibility that, in addition to transcriptional upregulation, DDB2 is also post-transcriptionally regulated following UV exposure.

4.2 p53 target-transcripts are short lived and some are stabilized by UV light

The rapid reversibility of p53 activity in HT29-tsp53 cells provided us a unique model system to study mRNA stability of p53-regulated transcripts [229]. To validate this approach, HT29-tsp53 cells were grown in permissive conditions for 16 hours, then

switched back to the restrictive temperature for 6h (Figure 13A). It has been accepted for some time that UV light is able to increase gene expression through the post-transcriptional stabilization of specific mRNAs [22, 24-26, 232]. To assess the role of UV light in the stability of p53 target-transcripts, we also exposed cells to UV light (20 J/m^2) at the time of the temperature shift back to restrictive conditions. Cells treated with and without UV were collected 6 hours after temperature shift. All samples were analysed using an Affymetrix oligonucleotide microarray platform (Table 3). To generate a list of target-genes, we used the p53FamTaG database for validated p53 targets (www2.ba.itb.cnr.it/ p53FamTaG). We found that most p53-inducible gene (those induced at least 2-fold after 16h at permissive temperature) had a very short half-life. 82% of genes (27/33) had 20% or less expression remaining after 6 hours compared to the induced levels. On average, only 11% of the induced expression level remained after 6h. Of those short-lived transcripts, UV light caused nearly 50% of them (13/27) to exhibit an increase in expression compared with the non-UV treated sample (Table 3). This suggested to us that post-transcriptional regulation may play a significant role in the p53 stress response to UV light.

To further validate the finding that p53 target-genes are short-lived, the above experiment was repeated without the UV light component and panel of p53 targets were analysed by quantitative RT-PCR (Figure 13B). These results were in agreement with the microarray findings. Our results indicated that p53 target-genes are relatively short-lived (less than 2h half-lives) compared to previous estimates of an average mammalian mRNA half-life of 7-10 hours [113, 115, 121]. These previous studies of global mRNA turnover rates found strong correlations between gene function and mRNA half-lives, with

Table 3 Microarray analysis of p53 target-mRNA expression

Gene	Fold induction at 32°C for 16h	remaining expression (%)*	UV, remaining expression (%)*
GDF15	7.22	0.17	8.78
MDM2	7.86	0.27	22.68
TP53INP1	11.64	0.85	22.25
WWP1	2.09	0.92	18.35
POLH	4.19	0.93	25.94
C12orf5	4.13	1.12	25.20
BTG2	6.03	1.20	8.97
DDIT4	3.66	1.50	3.01
EFNB1	2.25	1.60	40.00
CDKN1A	9.61	2.11	11.85
GADD45A	5.94	2.56	20.96
FAS	6.23	3.00	8.30
SESN1	4.27	3.09	11.15
TNFSF10	3.30	3.48	1.74
SerpinB5	3.16	5.09	48.15
LIF	2.50	5.33	4.00
ZMAT3	6.29	6.14	43.73
LDB1	2.15	6.96	79.13
DUSP5	2.14	8.77	18.42
RRM2B	6.78	9.63	54.27
XPC	2.30	10.77	24.62
DDB2	4.43	11.49	43.63
CCNG1	3.14	13.55	46.73
TDG	2.09	15.60	2.75
RPS27L	2.45	16.55	55.17
BAX	2.23	20.33	30.08
BLCAP	2.18	20.34	37.29
CES2	5.03	22.69	55.93
FDXR	2.40	28.57	57.14
SEMA3B	2.90	31.58	73.68
EI24	2.04	32.69	66.35
TP53I3	5.81	38.08	65.33
TAP1	2.17	40.17	75.21

* Expression remaining after 6h at restrictive conditions (following 16h at permissive temperature). UV, 20J/m^2. Values represent the mean of 2 independent experiments.

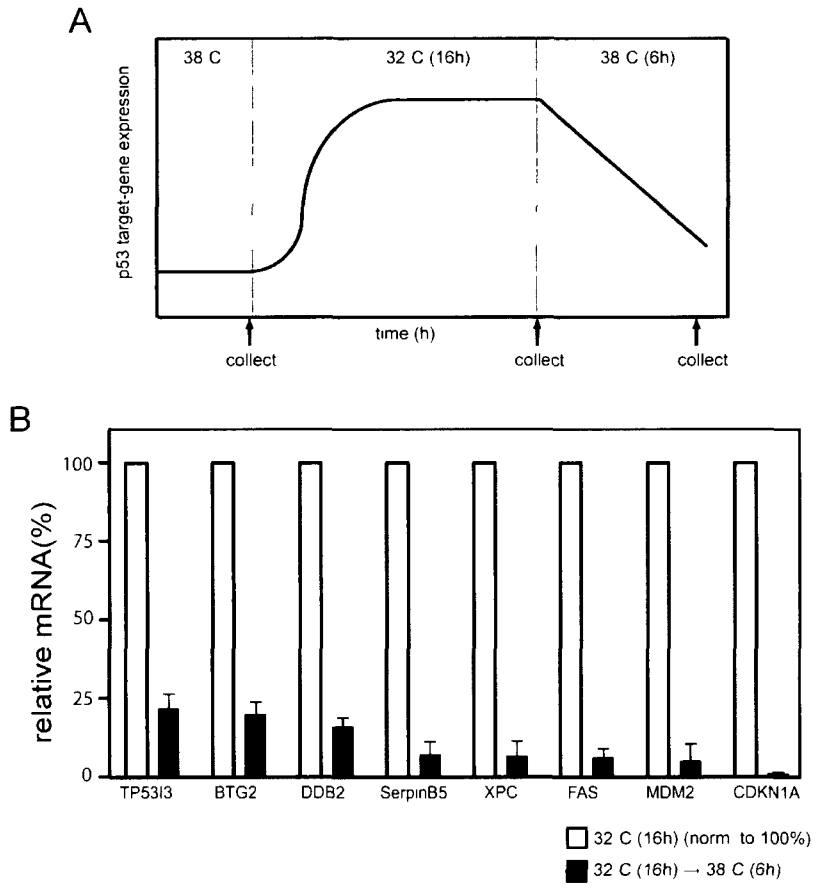

Figure 13. The mRNAs of p53 target-genes are short-lived. (A) Experimental scheme. HT29-tsp53 cells were grown at the permissive temperature for 16h and were switched to restrictive conditions for 6h. Samples were collected at all 3 time points and analysed by real-time RT-PCR for expression of indicated genes (B). All genes were induced at least 5-fold following 16h growth at permissive conditions, open bars (normalized to 100%). Closed bars, % mRNA expression remaining 6h after shift back to the restrictive temperature. Values represent the mean ± standard error of 3 independent experiments.

transcriptionally inducible genes having considerably shorter-lived transcripts. Our results, then, are in accordance with this. Together these findings indicate that p53 target-genes are short-lived and that a subset of them are post-transcriptionally regulated by UV light.

4.3 UV light increases the stability of the DDB2 transcript

Following these experiments, we looked more closely at the expression patterns of a smaller group of p53 targets and how UV light affects their stability. As a positive control, we examined the expression of the $p21^{WAF1}$ mRNA because it is a UV-stabilized p53 induced transcript [25, 232]. HT29-tsp53 cells were incubated at the permissive temperature for 16 hours to strongly induce p53 target-gene expression. These cells were then exposed to either 0 or 20 J/m^2 of UV light and returned to the restrictive temperature. At indicated times, total RNA was collected for real-time RT-PCR analysis. Under these conditions, $p21^{WAF1}$ expression increased approximately 30-fold at the permissive temperature (Figure 14A). The $p21^{WAF1}$ mRNA decayed rapidly, such that only 20% of the induced $p21^{WAF1}$ mRNA remained following 2 hours at the restrictive temperature (Figure 14B). The $p21^{WAF1}$ mRNA decayed far more slowly following UV exposure (Figure 14B), as previously reported [25, 232]. Therefore, this cell line affords a novel and powerful means of examining the decay of transcripts regulated by p53.

The expression of FAS, MDM2 and DDB2 were again induced to a similar extent at the permissive temperature (Figure 14A). The expression of these transcripts decreased four-fold within 4 to 6 hours at the restrictive temperature, in the absence of UV light (Figure 14C-E). Therefore, these transcripts are also relatively unstable. While UV

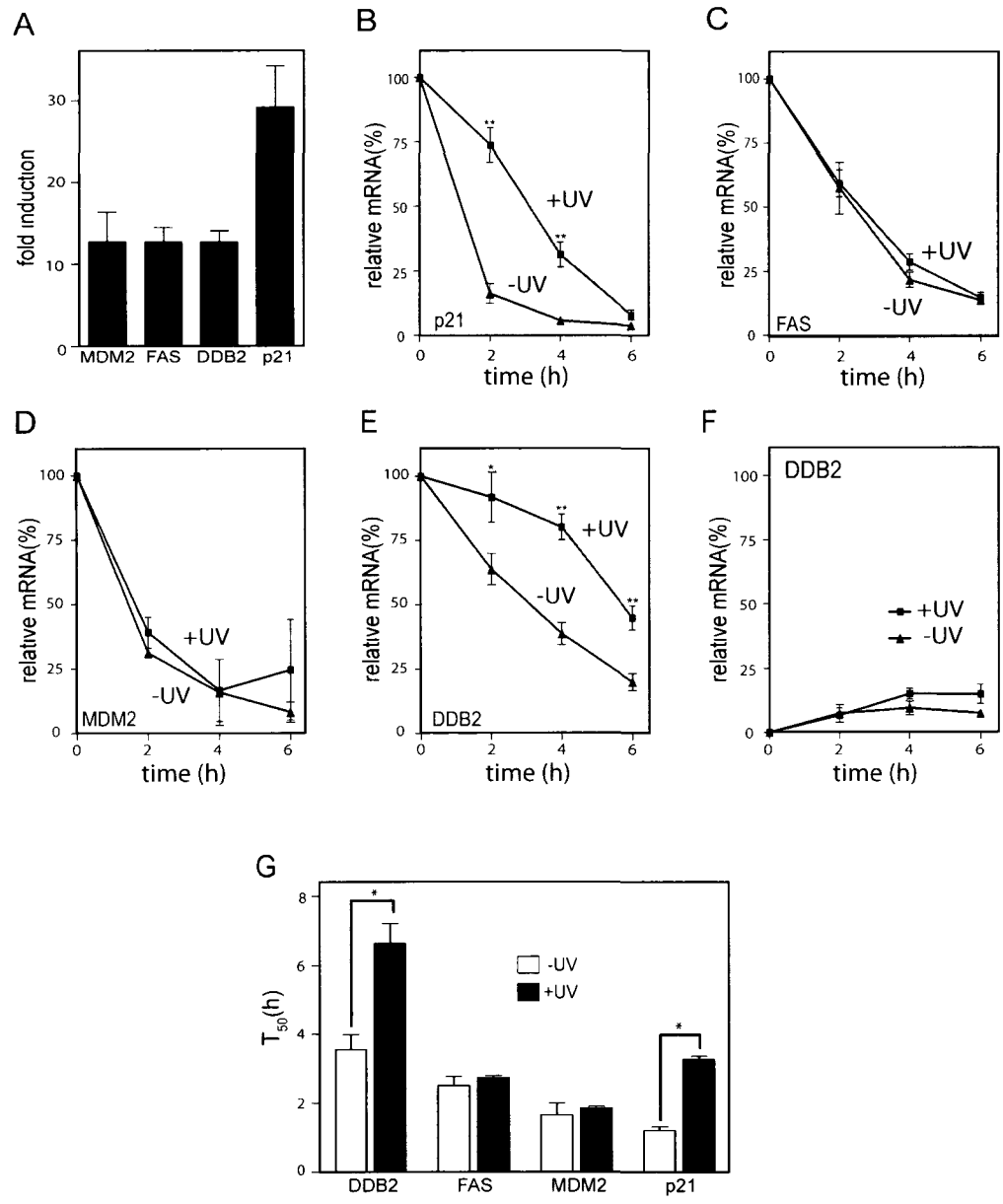

Figure 14. DDB2 and p21 ^{WAF1}, but not FAS or MDM2 mRNA are stabilized by UV light. (A) HT29-tsp53 cells grown at the restrictive temperature were switched to the permissive temperature for 16h. The expression of FAS, DDB2, MDM2, and p21 ^{WAF1} mRNA were analysed by real-time RT-PCR and expressed as fold increase in expression. (B-E) Following this, they were treated with or without UV light (20J/m^2) at time 0h, and were switched back to the restrictive temperature. Samples were collected at indicated times and analysed by real-time RT-PCR for expression of the gene indicated. Expression presented as % of relative mRNA compared to time of temperature shift/UV treatment. (F) The effect of UV light on the expression of DDB2 transcript following p53 induction is not due to UV-mediated transcription. Experiment from panels B-E was repeated with cells maintained entirely at the restrictive temperature (38°C) and treated with or without UV light (20J/m^2). (G) The effect of UV light on the half-life (T_{50}) of each transcript in parts B-E was measured by linear regression; open bars (-UV), closed bars (+UV). UV light significantly increased the T_{50} for DDB2 ($p=0.0015$) and p21 ^{WAF1} ($p<0.0001$). All values represent the mean ± standard error of 3 independent experiments. Significant differences in B and E (*$p<0.05$, **$p<0.001$) were determined using Student *t* test.

exposure did not affect FAS or MDM2 expression (Figure 14C and D), it did significantly increase the amount of residual DDB2 mRNA in cells switched to the restrictive temperature (Figure 14E). To ensure that the relative increase in DDB2 mRNA levels following UV exposure was not due to p53-independent UV-mediated transcription, cells were maintained at the restrictive temperature and treated with either 0 or 20 J/m^2 of UV light (Figure 14F). No significant increase in DDB2 mRNA was detected following UV treatment when cells were maintained at the restrictive temperature. The half-lives of these 4 transcripts in the presence and absence of UV light were estimated. There was no significant increase in the half-lives of either the MDM2 or FAS mRNA following UV exposure, while the half-lives of DDB2 and $p21^{WAF1}$ mRNA increased significantly following UV exposure ($p = .0015$ and $p < .0001$, respectively) (Figure 14G).

4.3.1 $p21^{WAF1}$ and DDB2 mRNA are stabilized in a UV dose-dependent manner

To determine how UV dose affects the expression of these p53-induced transcripts, cells were again incubated for 16 hours at the permissive temperature to drive p53-dependent gene expression. Cells were then irradiated with the indicated dose of UV light, returned to the restrictive temperature and RNA was collected 0, 3 or 6 hours later. As expected, expression of our positive control ($p21^{WAF1}$ mRNA) increased in a dose-dependent manner at 3 hours. Due to its rapid turnover, this was less apparent at 6 hours (Figure 15A, left panels) [25, 232]. UV light led to a dose-dependent increase in DDB2 expression at both time points (Figure 15A and B, middle panels), while expression of FAS, its size matched control (25 kpb, GeneID: 355), was not greatly increased by UV light at either time point (Figure 15 A and B, right panels).

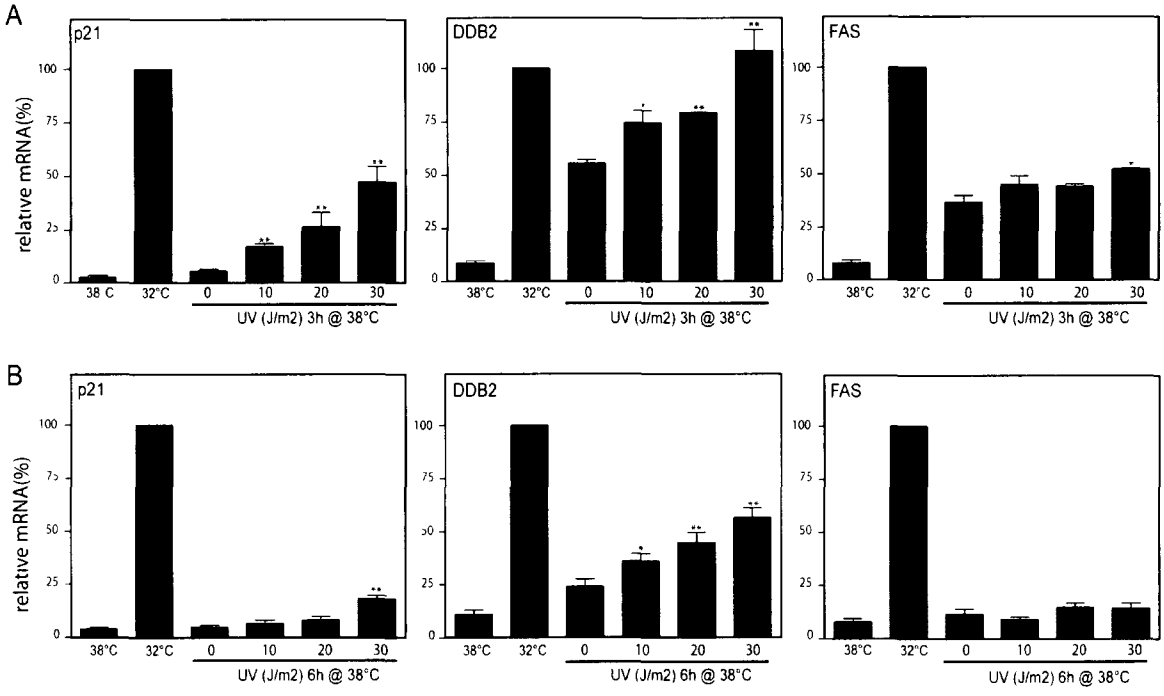

Figure 15. mRNA stabilization of p21 ^{WAF1} and DDB2 are UV-dose dependent. HT29-tsp53 cells grown at the restrictive temperature were switched to the permissive temperature for 16h. Following this, they were treated with indicated dose of UV light at time 0h, and were switched back to the restrictive temperature. They were collected 3h (A) or 6h (B) later. Relative expression of p21 ^{WAF1} (left panels), DDB2 (middle panels) and FAS (right panels) were analysed by real-time RT-PCR. All values represent the mean ± standard error of 3 independent experiments. Significant differences (*$p<0.05$, **$p<0.001$) were determined using Student *t* test.

4.3.2 Actinomycin D and UV light stabilize DDB2 and p21^{WAF1} mRNA

The decay of specific mRNAs is commonly assessed under conditions in which nascent RNA synthesis is blocked with transcriptional inhibitors such as actinomycin D (Act D) [25, 233]. HT29-tsp53 cells were incubated at the permissive temperature for 16 hours to drive p53 target-gene expression. Cells were then exposed to either 0 or 20 J/m^2 of UV light and Act D was added to block nascent RNA synthesis while cells remained at the permissive temperature (Figure 16A). The expression of DDB2 was monitored over a 6 hour period and p21^{WAF1} again served as a positive control. Consistent with increased stability of the DDB2 and p21^{WAF1} transcripts following UV exposure in our previous experiments, UV light led to an increase in DDB2 and p21^{WAF1} expression in the presence of Act D (Figure 16A). This independent method further indicates that DDB2 mRNA decay is inhibited following exposure to UV light.

Curiously, the apparent half-lives of p21^{WAF1} and DDB2 transcripts under these conditions were far higher than the half-lives observed in Figure 14. Therefore, we sought to determine if the half-lives of these transcripts were affected by temperature change. Again HT29-tsp53 cells were incubated at the permissive temperature for 16 hours to increase the expression of DDB2 and p21^{WAF1} mRNA. Cells were returned to the restrictive temperature in the presence or absence of Act D and RNA was collected to monitor the decay of these transcripts by real-time RT-PCR (Figure 16B). At the restrictive temperature, Act D treatment resulted in decreased decay of both transcripts (Figure 16B). The decay of the DDB2 and p21^{WAF1} transcripts was not significantly affected by changes in temperature (compare lower lines in Figure 16A with the upper line in Figure 16B). Instead, Act D appears to inhibit the decay of the DDB2 and p21^{WAF1}

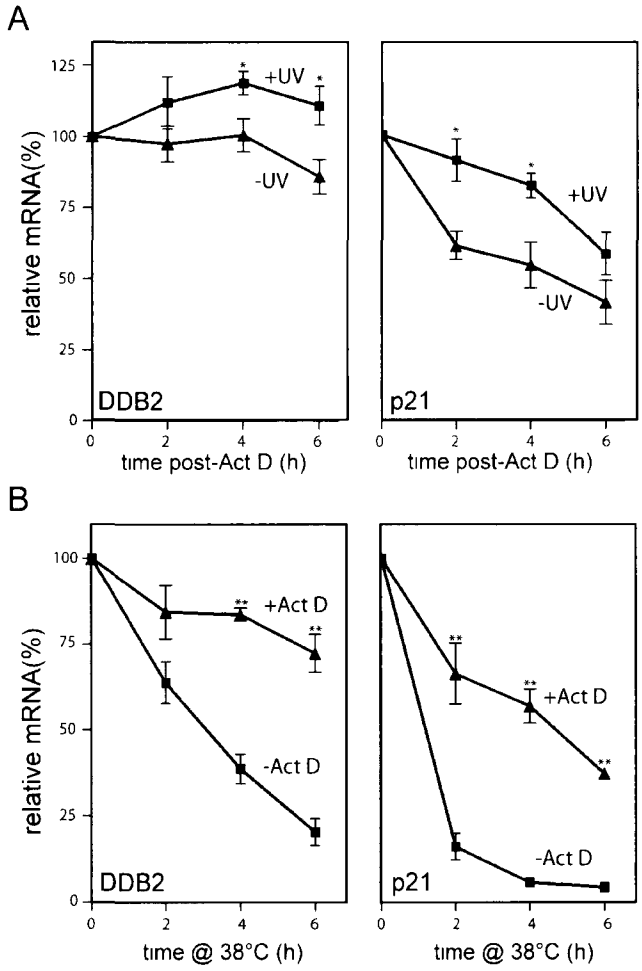

Figure 16. UV light stabilizes DDB2 and p21 ^{WAF1} mRNA following treatment with Act D. For all parts HT29-tsp53 cells were incubated at the permissive temperature for 16h. (A) At time 0h, cells were treated with Act D, with or without UV light (20J/m^2) and maintained at the permissive temperature. (B) Act D itself is able to stabilize DDB2 and p21 mRNAs. At time 0h cells were switched back to the restrictive temperature and treated with or without Act D. All samples were analysed by real-time RT-PCR. All Act D treatments were 5µg/ml. All values represent the mean ± standard error of at least 3 independent experiments. Significant differences (*$p<0.05$, **$p<0.001$) were determined using Student *t* test.

transcripts Similar mRNA stabilizing effects of Act D have been reported previously for a variety of other transcripts [138, 234] Transcription inhibitors such as Act D, DRB, H7 and α-amanitin can induce p53 in the absence of DNA damage [74] The induction of the p53 response and in turn p53 target-genes, could offer a partial explanation for these observations

4.4 DDB2 protein levels are affected by mRNA stability

It has been shown previously that DDB2 protein is degraded immediately following UV exposure [47] In the absence of UV light, we found that DDB2 protein begins to decay between 4 and 6 hours following the removal of p53 mediated gene-transactivation Following exposure to UV light, the protein is rapidly degraded within 2 hours (Figure 17A, compare lanes 2 and 7) However, in contrast to unirradiated cells, UV treated cells appear to recover DDB2 expression (Figure 17A, lanes 7-10) Increased mRNA stability and consequent translation could help maintain a pool of DDB2 protein available for GG-NER Treatment of HT29-tsp53 cells with the translation inhibitor, cycloheximide (CHX), led to the virtual ablation of DDB2 following UV exposure (Figure 17B, lanes 7-10) with only a modest effect in unirradiated cells (lanes 3-6) Therefore, DDB2 protein expression following UV exposure is highly dependent on ongoing protein synthesis and this requires available mRNA template

4.5 The 3'UTR of DDB2 decreases the stability of a reporter transcript

Our work described above indicates that DDB2 is subject to post-transcriptional regulation at the level of mRNA stability It is well established that transcript stability is

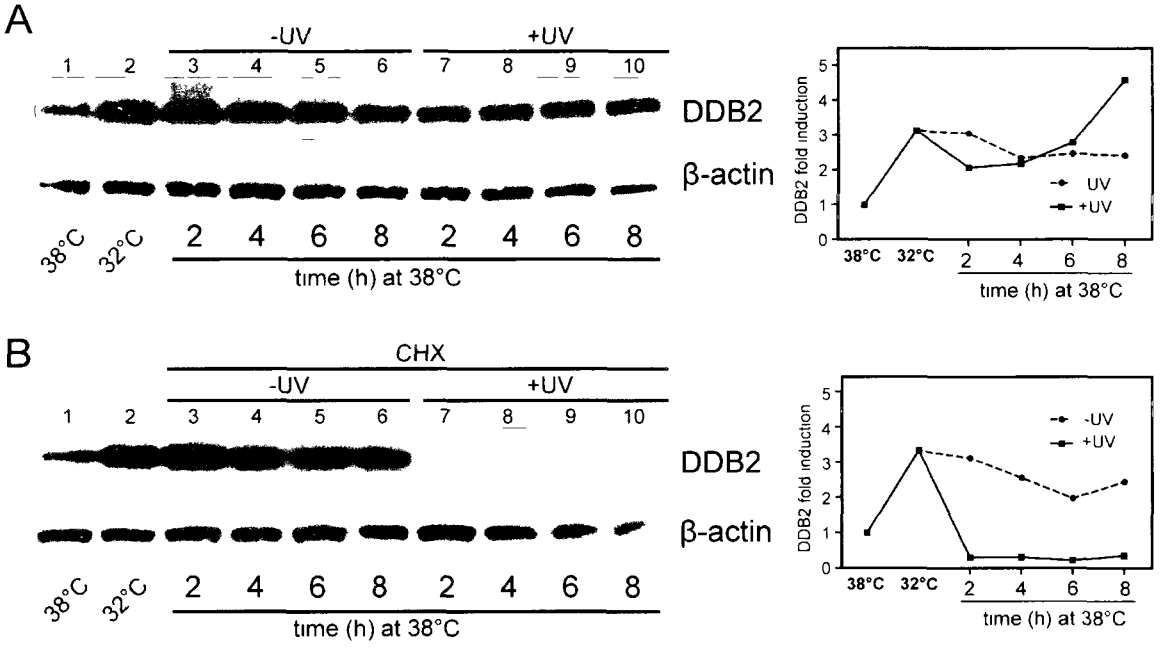

Figure 17. mRNA stability affects DDB2 protein levels.(A) Whole-cell lysates from HT29-tsp53 cells were collected from experiment in Figure 14A-E and subjected to immunoblot analysis. (B) Experiment repeated as in A, except cycloheximide (CHX) was added (50μg/ml) at the time of temperature shift and UV treatment (20J/m^2). For both parts, 50μg protein/lane was used. Left panels, normalized protein quantification by densitometry.

often regulated through elements found in 3' untranslated regions (3'UTRs). The most common of these are the destabilizing AU-rich elements (AREs) [135, 141]. The DDB2 3'UTR does not contain any canonical AREs. We therefore aimed to assess whether or not the short half-life of the DDB2 transcript was due to a previously unrecognized regulatory element in its 3'UTR.

4.5.1 EGFP reporter gene system (pTRE-d2EGFP)

The DDB2 3'UTR (343 bps) was fused into a tet-responsive construct (pTRE-d2EGFP) expressing a destabilized version of EGFP (d2EGFP). d2EGFP has a short half-life (2 hours) due to the presence of mouse ornithine decarboxylase (MODC)-derived PEST amino acid sequence that targets it for protein degradation [235]. Initially, the full length DDB2 3'UTR was cloned into the reporter construct between the d2EGFP cDNA and an SV40 poly(A) signal. Hence, the 3'UTR of DDB2 is expressed as a 3'UTR of d2EGFP (Figure 18A). We reasoned that the expression of the d2EGFP protein would be proportional to the stability of its mRNA.

The tetracycline-controlled transactivator regulatory plasmid has been stably integrated into commercially available HeLa TO (tet-off) cells. Upon addition of doxycycline (Dox), transcription of the d2EGFP cDNA is rapidly inhibited allowing for the measurement of remaining d2EGFP mRNA and protein as a function of time. Any destabilizing element contained within the DDB2 3'UTR should decrease the stability of d2EGFP mRNA and expression of EGFP protein.

4.5.2 Transient EGFP reporter construct experiments

pTRE-d2EGFP plasmids with and without the cloned full length DDB2 3'UTR insert (FL Ins or -Ins, respectively) were transiently transfected in HeLa TO cells and 24h later, doxycycline was added to the cell culture medium. Total RNA was extracted at 0, 2, 4 and 6 hours post-Dox treatment. Primers recognizing the coding region of EGFP were used to detect d2EGFP mRNA by real-time RT-PCR. Consistent with the presence of a destabilizing element in the 3'UTR of DDB2, the expression of the d2EGFP transcript was reduced in the FL Ins construct compared to the -Ins reporter. The calculated half-lives of these transcripts were 4 and 15 hours, respectively (Figure 18B). Whole cell extracts were collected from similarly treated cells 6 and 24 hours following the addition of Dox. Western blot analysis shows the expression of d2EGFP decreased more in the FL Ins construct (Figure 18C). These results indicated that the 3'UTR of DDB2 decreased the stability of the d2EGFP mRNA and this could be similarly detected at the protein level.

Even without the addition of Dox to terminate transcription of the reporter construct, the FL Ins containing cells show less d2EGFP protein, suggesting that steady-state levels of DDB2 protein may be affected by the short half-life of its transcript. Indeed, DDB2 protein levels in unirradiated or p53-deficient cells are very low to the point of being undetectable [91].

4.5.3 Fluorescence activated cell sorting to generate stable d2EGFP-expressing cell lines

Because of difficulties controlling for transfection efficiencies, stable cell lines constitutively expressing the d2EGFP reporters were generated using fluorescence activated cell sorting (FACS). HeLa TO cells were transfected with either –Ins or FL Ins

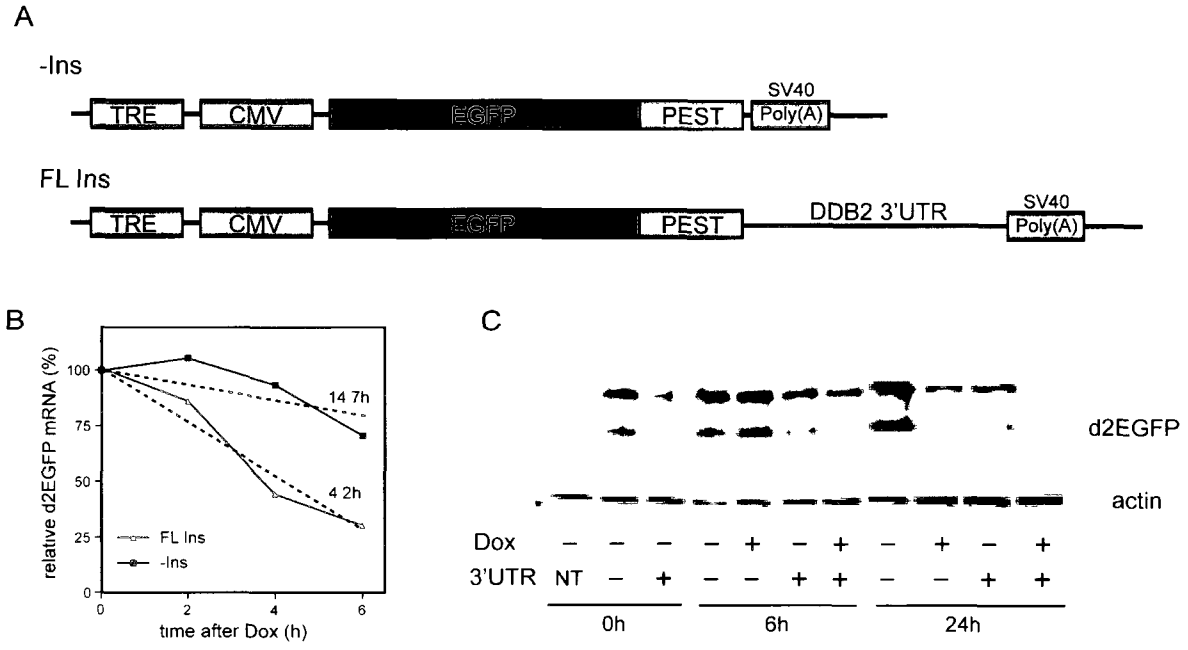

Figure 18. The DDB2 3'UTR alters the mRNA stability and protein expression of the pTRE-d2EGFP vector. (A) Diagram of the tet-off regulated d2EGFP vector on its own or fused with the DDB2 3'UTR (-Ins or FL Ins, respectively). TRE, Tet Response Element; CMV, Cytomegalovirus promoter; EGFP, Enhanced Green Fluorescence Protein; PEST, mouse ornithine decarboxylase (MODC)-derived protein degradation element. (B) HeLa TO cells were transfected with the -Ins or FL Ins pTRE-d2EGFP and doxycycline (Dox) was added 24 hours after transfection. Total RNA was collected at indicated times and quantified by real-time RT-PCR. mRNA half-lives are indicated and were calculated by linear regression. (C) Western blot analysis of d2EGFP protein collected at 0h, 6h, or 24h after Dox addition. (20μg of total protein/well). Transfections were performed 24h before any Dox treatment. NT, no transfection.

reporter plasmid. Then they were propagated and sorted sequentially to enrich the population for d2EGFP-positive cells. Through this selective process, we obtained populations with greater than 80% d2EGFP-positive cells. The stable population expressed the expected d2EGFP protein and mRNA as validated through flow cytometry and RT-PCR (Figure 19). Importantly, the expression of d2EGFP remained doxycycline-responsive as assessed by flow cytometry because these cells completely lose d2EGFP expression upon extended culture in Dox. After exposure to Dox for 48 hours, their fluorescence profile was nearly identical to that of control non-d2EGFP expressing parental HeLa TO cells (Figure 20).

The validity of using these pooled populations of FACS generated cells for future experiments was examined by growing single cell-derived colonies from both the -Ins and FL Ins EGFP-enriched cell lines. In all clones isolated and analysed, there did not appear to be significant differences in percent d2EGFP-positive cells compared to the respective parental stable cell lines. Furthermore, the Dox-induced decrease in d2EGFP expression from basal levels does not significantly differ between the pooled populations and clones (Figure 21). Because these single-cell derived clones behaved in a similar fashion to both the stable pools generated through FACS and the transiently transfected HeLa TO cells, all subsequent analyses were performed using the stable pools of d2EGFP-enriched cells, unless otherwise stated.

To examine the kinetics of d2EGFP mRNA decay in the FACS generated d2EGFP expressing cells, Dox was added to both cell lines and total RNA was collected 0, 2, 4 and 6 hours later. In accordance with the transient transfection experiments, the d2EGFP

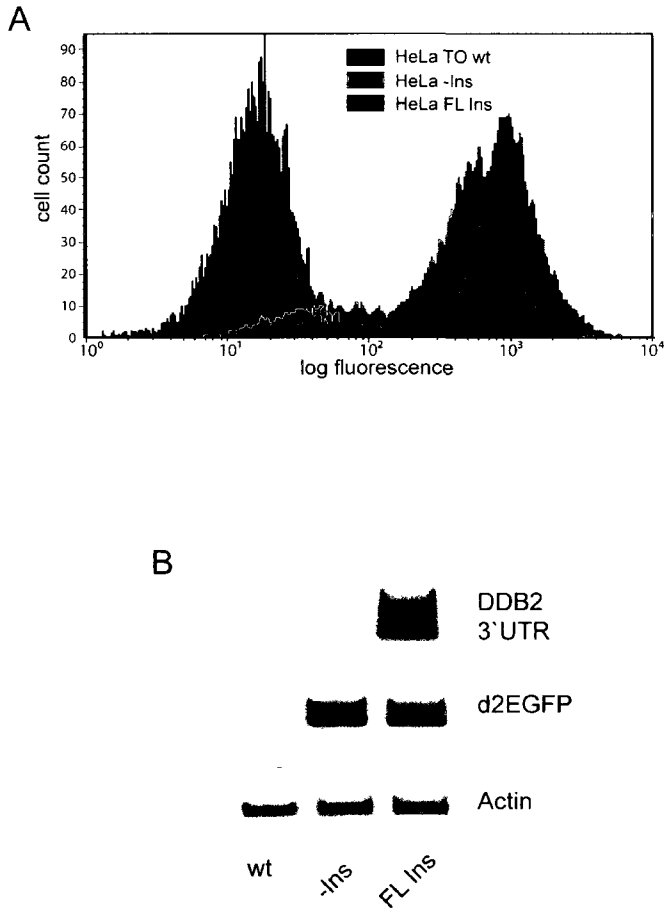

Figure 19. FACS-generated HeLa TO cells stably express -Ins or FL Ins d2EGFP constructs. (A) Representative one parameter flow cytometry histogram comparing the d2EGFP fluorescence of HeLa TO wt parental cells with cells stably expressing -Ins or FL Ins d2EGFP reporter constructs. (B) RT-PCR showing stable d2EGFP and DDB2 3'UTR mRNA expression. Run on 1% agarose gel by electrophoresis.

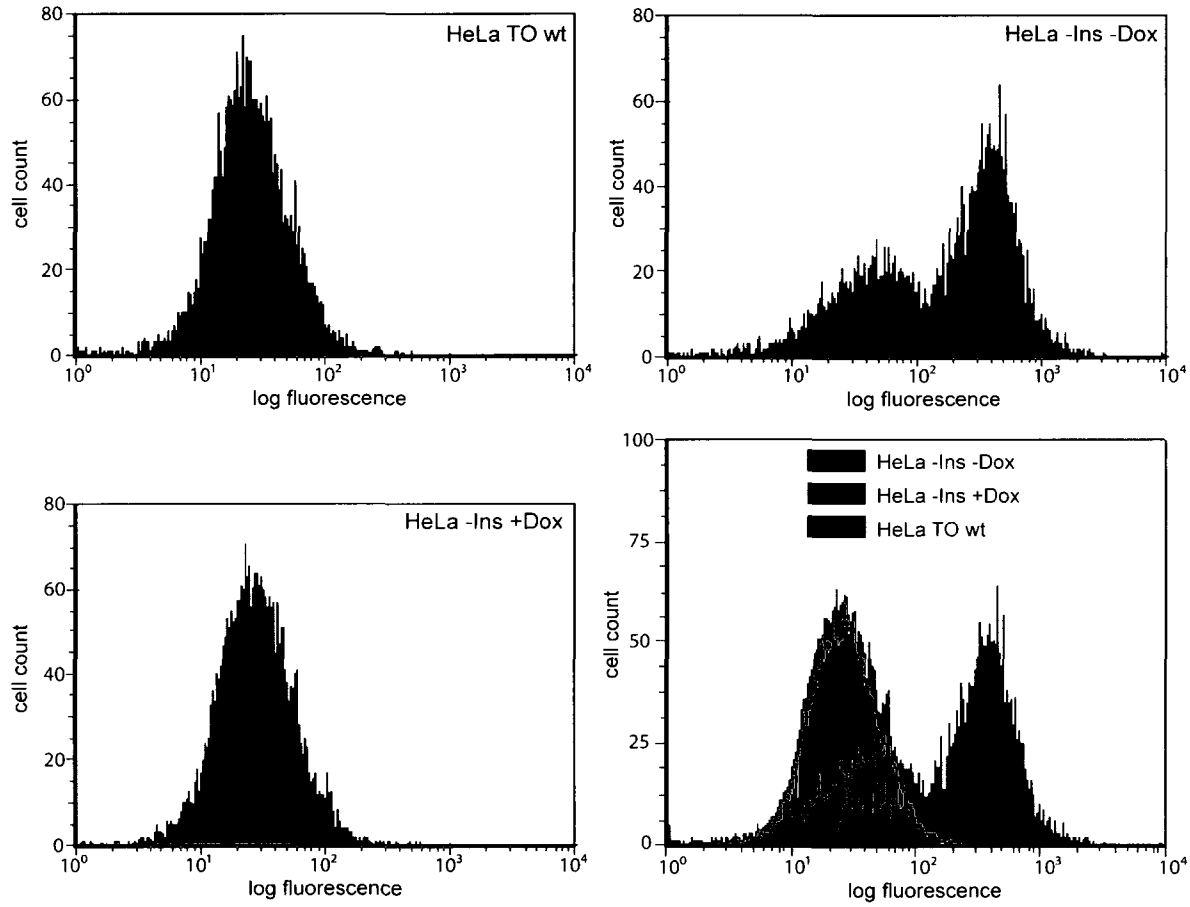

Figure 20. Tet-off expression system in HeLa -Ins cells validated by flow cytometry. One parameter flow cytometry histograms showing that the addition of Dox to stable HeLa -Ins cells completely inhibits the detection of d2EGFP fluorescence. Top panels, parental HeLa TO wt (left) and -Ins (right) cells before Dox addition. Bottom left panel, HeLa -Ins cells treated with Dox for 48 hours. Bottom right panel, merged histogram of the other 3 panels shows a virtual overlap of d2EGFP fluorescence between HeLa parental and stable -Ins cells.

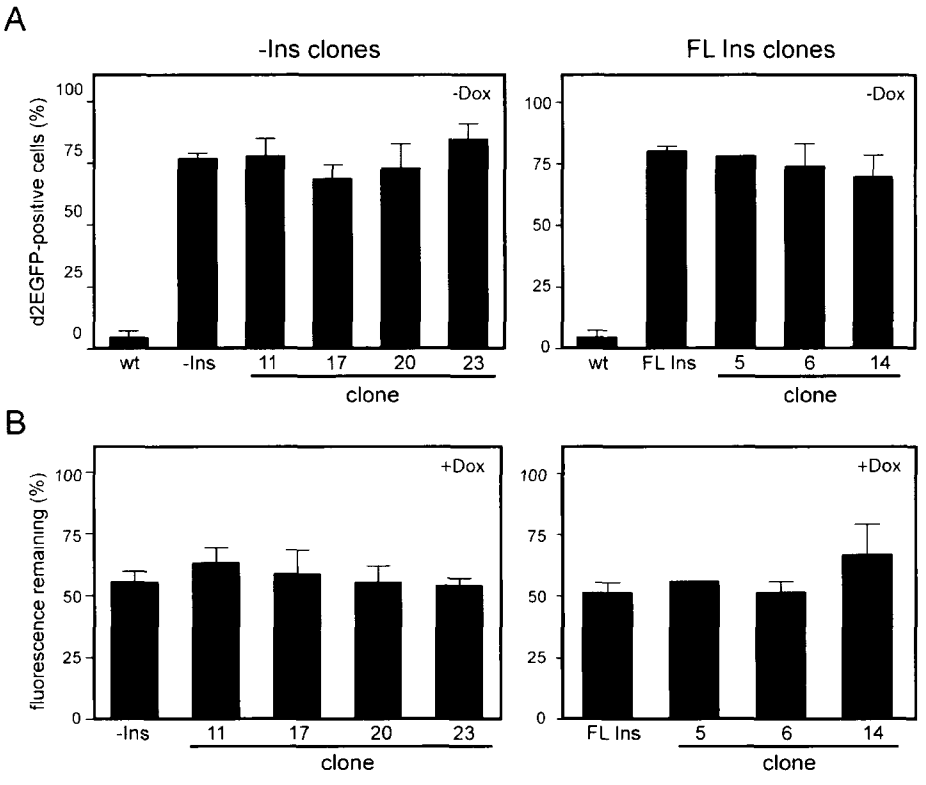

Figure 21. Single cell-derived clones are indistinguishable from pooled cell lines. (A) Percentage of cells determined to be positive for d2EGFP expression in a panel of HeLa -Ins and FL Ins-derived clones (left and right panels, respectively). (B) Relative d2EGFP fluorescence remaining in the pooled and single cell-derived clone cell populations following 6h Dox treatment. Fluorescence was calculated by subtracting the background fluorescence of the GPF-negative population of each cell line. All results were obtained by one parameter flow cytometry. Values represent the mean ± standard error of 2 independent experiments.

mRNA in the stable HeLa FL Ins cells decayed at a greater rate than the -Ins cells (Figure 22A, left panel). Remarkably, the half-life of the FL Ins d2EGFP mRNA (3.5 hours) was almost identical to that of endogenous DDB2 in HT29-tsp53 cells (3.8 hours) (Figure 14G). Primers specific for the 3'UTR of DDB2 yielded similar results in the FL Ins cells, while virtually no expression was detected in -Ins cells (Figure 22A, right panel).

To further validate these effects, we used the transcription inhibitor actinomycin D (Act D) in the absence of Dox to measure the decay of d2EGFP mRNA in both cell lines. Once again, there was a more rapid decrease in the expression of d2EGFP mRNA in the presence of the DDB2 3'UTR (Figure 22B). Together, these findings strongly suggest that the 3'UTR of DDB2 directs the d2EGFP mRNA for accelerated decay and that this is consistent with the decay rate of endogenous DDB2.

Interestingly, we also observed an approximately 30% increase in DDB2 mRNA stability in the cells harbouring the DDB2 3'UTR compared to the –Ins or parental HeLa TO cell lines, following Act D treatment (Figure 22C). This may suggest that the vast overexpression of the DDB2 3'UTR sequesters destabilizing binding factor(s) away from endogenous DDB2 3'UTR, thereby stabilizing endogenous DDB2.

4.5.4 The 3'UTR of DDB2 decreases the expression of d2EGFP protein

To visualize the impact of d2EGFP mRNA stability on protein expression, live-cell imaging was used to monitor green fluorescence of individual cells after the addition of Dox. Figure 23A shows representative images of an equal time following Dox addition to both HeLa -Ins and FL Ins cell lines. Quantitative time course data of EGFP fluorescence was accumulated by randomly selecting individual cells of each population and

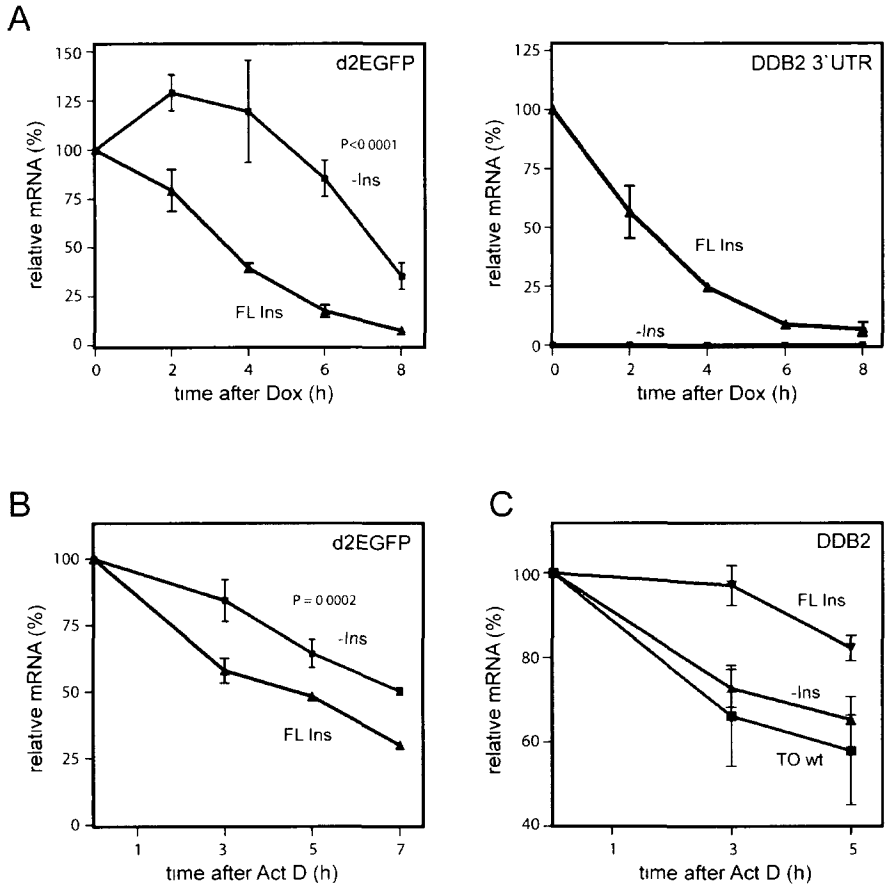

Figure 22. The DDB2 3'UTR destabilizes d2EFGP mRNA in HeLa FL Ins cells. (A) d2EGFP (left panel) and DDB2 3'UTR (right panel) mRNA expression in HeLa -Ins and FL Ins cells following Dox treatment at times indicated. d2EGFP (B) and DDB2 (C) mRNA expression in indicated cell lines following actinomycin (Act D) treatment (1µg/ml) at times indicated. FL Ins significance compared to: -Ins, p=0.0006; TO wt, p=0.048 as determined by 2-way ANOVA. All samples were analysed by real-time RT-PCR and expressed as % of initial (before Dox) mRNA levels for each cell line. Values represent the mean ± standard error of at least 2 independent experiments. P values in A and B determined by 2-way ANOVA.

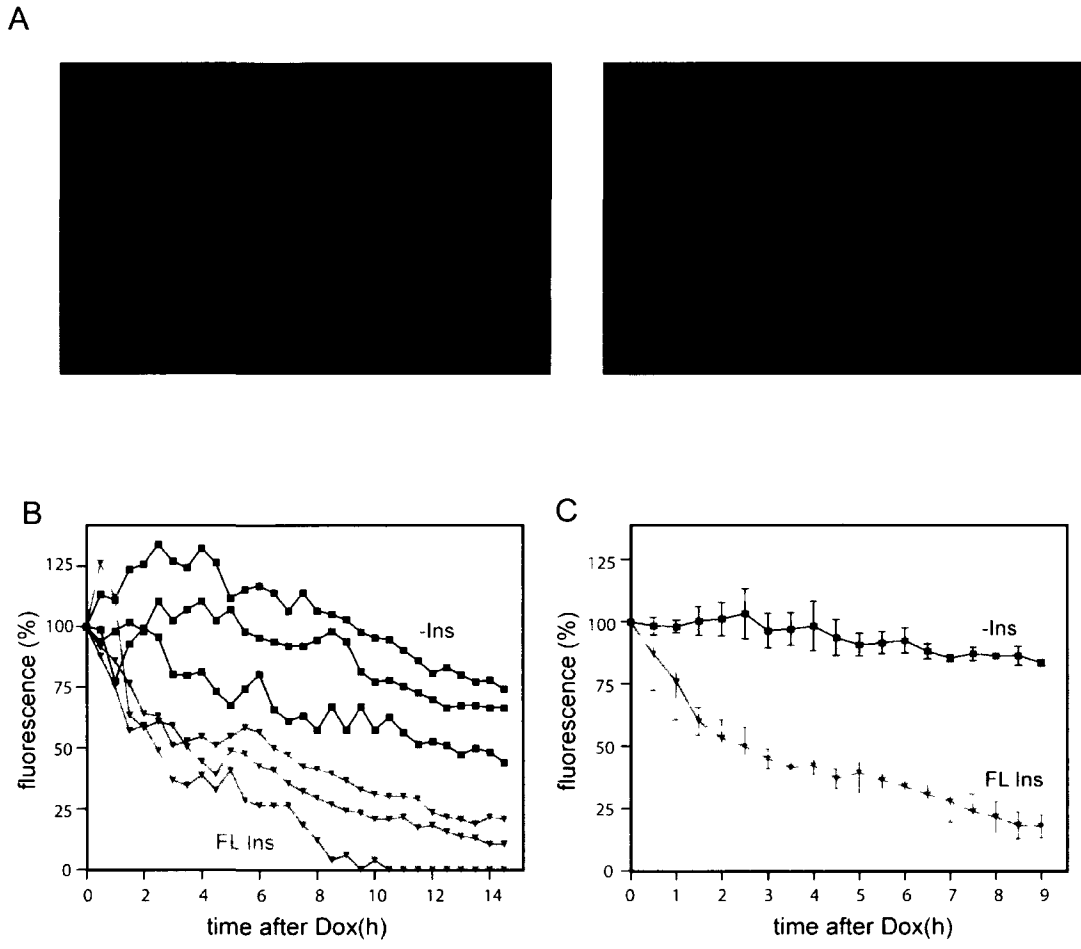

Figure 23. Live-cell d2EGFP imaging of stable HeLa cell lines shows protein levels are affected by differential mRNA stability. (A) Still-frame images of live HeLa -Ins (left panel) and HeLa FL Ins (right panel) cells at equal time following Dox treatment. (B) Quantitative results of representative experiment comparing cells of both lines following Dox treatment at indicated times. Each line represents green fluorescence as measured by mean pixel intensity for 1 individual cell. (C) Values represent the mean ± standard error of at least 2 independent experiments, each quantifying at least 2 cells/cell line. Expressed as % of initial (before Dox) fluorescence levels for each cell line. $P<0.0001$, as determined by 2-way ANOVA.

determining mean pixel intensity as a function of time following Dox treatment (Figure 23B). The mean intensity of several cells over multiple experiments (Figure 23C) showed a clear trend in agreement with our real-time RT-PCR data. These results further argue that the decreased mRNA stability resulting from the inclusion of the DDB2 3'UTR has a measurable effect on d2EGFP protein expression and therefore most likely plays a physiological role in its native endogenous context.

4.6 Localization of a destabilizing element in the DDB2 3'UTR

In order to localize putative *cis*-acting determinants of mRNA stability in the 3'UTR of the DDB2 transcript, similar d2EGFP reporter constructs were generated with fragments of various locations and lengths of the DDB2 3'UTR. Primers were designed to amplify the 360bp 3'UTR into sequential regions. Forward primers are designated A through D, depending on their distance from the 5' end. Reverse primers are designated 1 through 6. Refer to Figure 11 for a schematic diagram of the location and nomenclature of these primers. We created various length fragments spanning the entire 3'UTR. The nomenclature for the various fragments consists first of a letter and then a number separated by a hyphen. The letter corresponds to the location of the forward primer (5' end of the fragment) while the number signifies the reverse primer (or 3' end).

4.6.1 Proximal 3'UTR fragment analysis

In the first attempt to localize stability determinants, d2EGFP reporter constructs containing proximal fragments of increasing sizes (A-1 through A-5) were created and stably integrated into HeLa TO cell through FACS (Figure 24A). Highly enriched

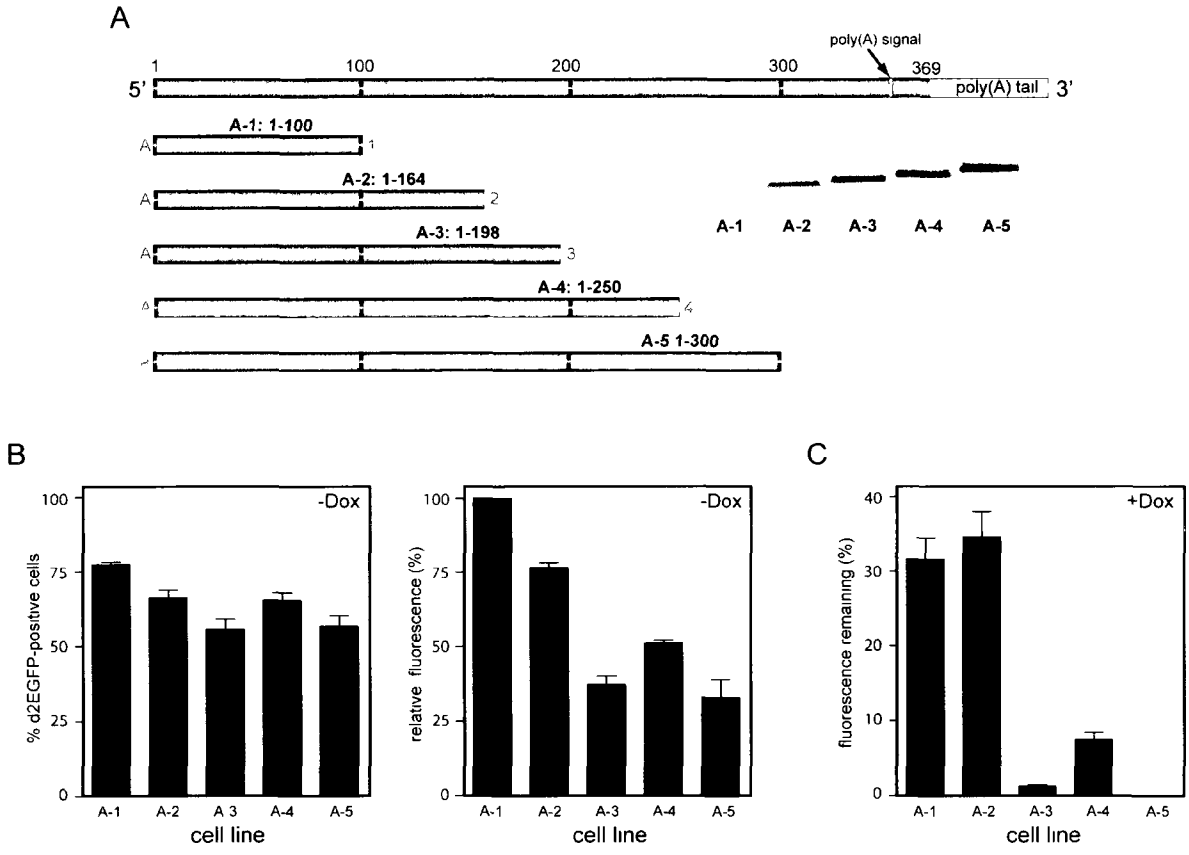

Figure 24. Flow cytometric analysis of cells containing proximal DDB2 3'UTR fragments. (A) Schematic diagram of the size and location of A-fragments of the DDB2 3'UTR cloned into the pTRE-d2EGFP vector and stably transfected into HeLa TO cells. Inset: restriction digested fragments run on 1% agarose DNA gel. (B) Percentage of d2EGFP-positive cells (left panel) and the relative fluorescence (right panel) of each cell line prior to Dox treatment. (C) Percentage of fluorescence remaining in each cell line following 12h of Dox treatment. Values represent the mean ± standard error of at least 2 independent experiments. Statistical analysis of part C is displayed in Table 4.

d2EGFP-positive populations were obtained for all cell lines (Figure 24B, left panel), but those containing A-3, A-4 and A-5 fragments had significantly lower baseline d2EGFP expression (Figure 24B, right panel). After 12h with Dox, fragment A-1 (1-100bp) and A-2 (1-164bp)-containing cells still expressed over 30% of their basal d2EGFP fluorescence, while the rest showed less than 10%. A-3 (1-198bp) and A-5 (1-300bp) fragment containing cells expressed essentially no EGFP (Figure 24C). These results argue that there is a destabilizing region located somewhere between the end of the A-2 region (164bp) and the end of the A-3 region (198bp). To ensure that differences observed in d2EGFP protein expression were due to differential mRNA stability, we performed real-time RT-PCR analysis on the A-2 and A-3 fragment-containing cell lines (Figure 25). Both Dox time course (Figure 25B) and Act D transcription inhibition assays (Figure 25C) confirmed that the d2EGFP mRNA in cells containing the A-3 fragment is indeed targeted for rapid decay at a rate consistent with FL Ins-containing cells.

4.6.2 Distal 3'UTR fragment analyses

To further localize the stability determinant, new constructs containing distal fragments starting from the 3' end of the DDB2 3'UTR were made that included or excluded the region between the 3' ends of the A-2 and A-3 fragments (C-6,150-363bp and D-6, 200-363bp, respectively) and are illustrated in Figure 26A. As before, stable cell lines containing these constructs were generated using FACS. Dox time course (Figure 26B) and live cell imaging experiments (Figure 26C) showed that the d2EGFP mRNA and protein in the cells containing fragment C-6 were both highly unstable compared with the D-6

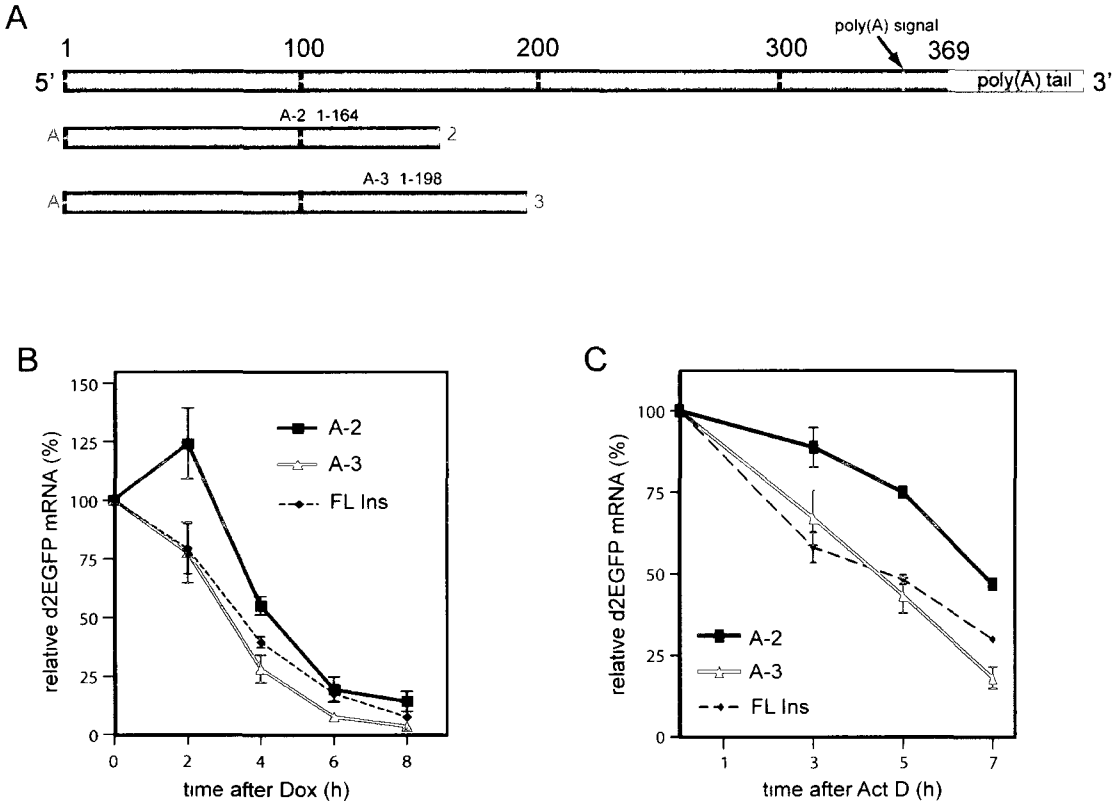

Figure 25. A destabilizing element is located within the A-3, but not the A-2 fragment. (A) Schematic diagram of the size and location of the proximal DDB2 3'UTR fragments cloned into the pTRE-d2EGFP vector and stably transfected into HeLa TO cells. (B) d2EGFP mRNA expression in indicated cell lines following Dox treatment. d2EGFP mRNA expression in A-2-containing cells was significantly different from either A-3 or FL Ins-containing cells, $P<0.005$ as determined by 2-way ANOVA. (C) d2EGFP mRNA expression in indicated cell lines following actinomycin (Act D) treatment (1μg/ml). All data measured by real-time RT-PCR and expressed as % of initial (before Dox) mRNA levels for each cell line. Values represent the mean ± standard error of at least 3 independent experiments.

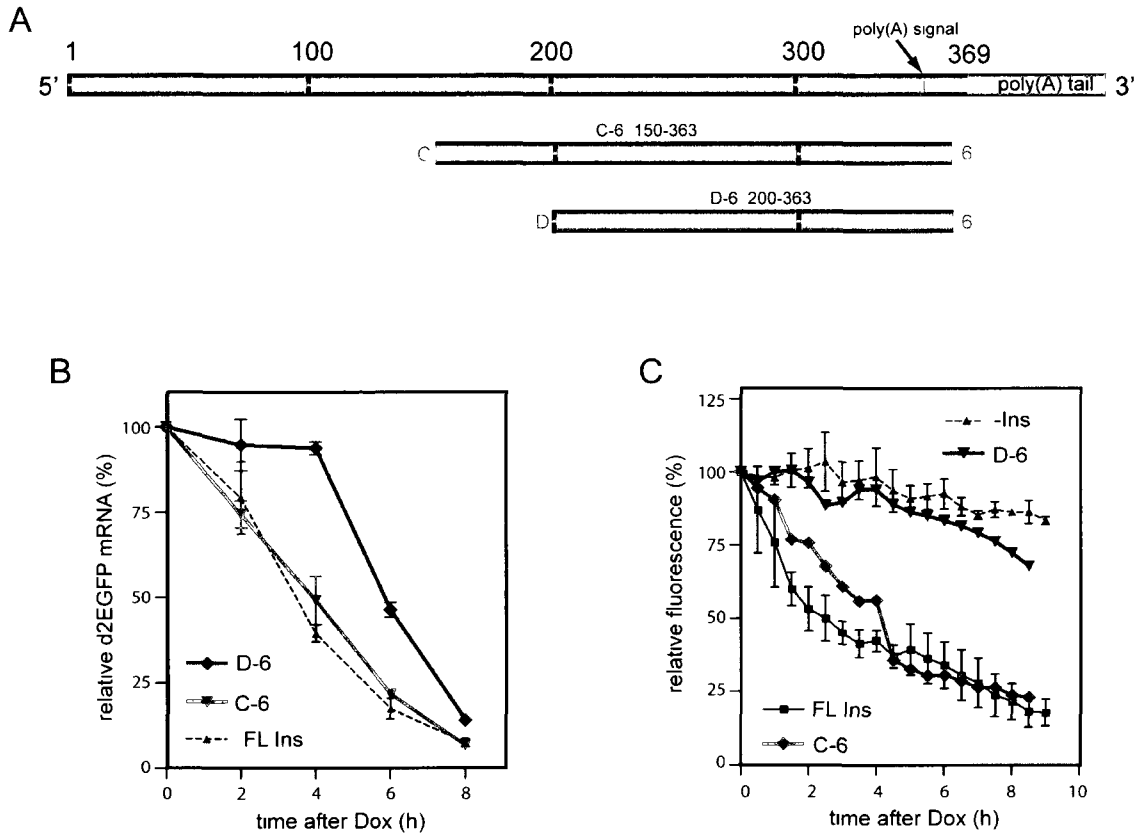

Figure 26. A destabilizing element is located within the C-6, but not the D-6 fragment. (A) Schematic diagram of the size and location of the distal 3'UTR fragments cloned into the pTRE-d2EGFP vector and stably transfected into HeLa TO cells. (B) d2EGFP mRNA expression in indicated cell lines following Dox treatment as measured by real-time RT-PCR. Values represent the mean ± standard error of at least 2 independent experiments. d2EGFP mRNA expression in D-6-containing cells was significantly different from either C-6 or FL Ins-containing cells, $P<0.0001$ as determined by 2-way ANOVA. (C) Representative live cell d2EGFP imaging analysis following Dox treatment in indicated cell lines. All results expressed as % of initial (before Dox) expression levels for each cell line.

fragment-containing cells. Again, this was consistent with the proximal fragment analyses and pointed to a stability determinant located between nucleotides 150 and 198.

Finally, a short fragment containing only the overlapping portion of A-3 and C-6 was created (C-3, 150-198bp). This is illustrated in Figure 27A. Real-time RT-PCR analysis of Dox time point experiments confirmed that this region did contain the destabilizing element. The d2EGFP mRNA in cells harbouring the C-3 fragment decayed at precisely the same rate as it did in FL Ins-containing cells (Figure 27B).

The 3'UTR of interleukin-1β (IL-1β) has been previously shown to contain AREs and is rapidly targeted for degradation [236]. The cell-lines whose fragments caused short d2EGFP half-lives (i.e. those that contain the region of the C-3 fragment) were compared with cells expressing a construct containing the full-length 3'UTR of IL-1β. The d2EGFP mRNA stability of all these cell lines was almost identical to that of the IL-1β 3'UTR-containing cells, indicating that these fragments are in fact similarly unstable when compared with a previously characterized labile 3'UTR (Figure 27C).

Together, these results point to the presence of a destabilizing element located within a 49bp region between nucleotides 150 and 198 (C-3 fragment). We have termed this element the 3'DDE (3'UTR DDB2 destabilizing element). The results of the various fragment analyses are summarized in Table 4. When classifying the fragments as stable or unstable in Table 4, we have deemed the A-2 fragment to be intermediate based on d2EGFP mRNA expression at 6h following Dox, despite the fact that it is lower than the expression observed in FL Ins cells. We made this designation based on the fact that in the 12h flow cytometry experiment as well as the Act D transcription inhibition assay, A-2 fragment-containing cells showed significantly increased d2EGFP expression compared

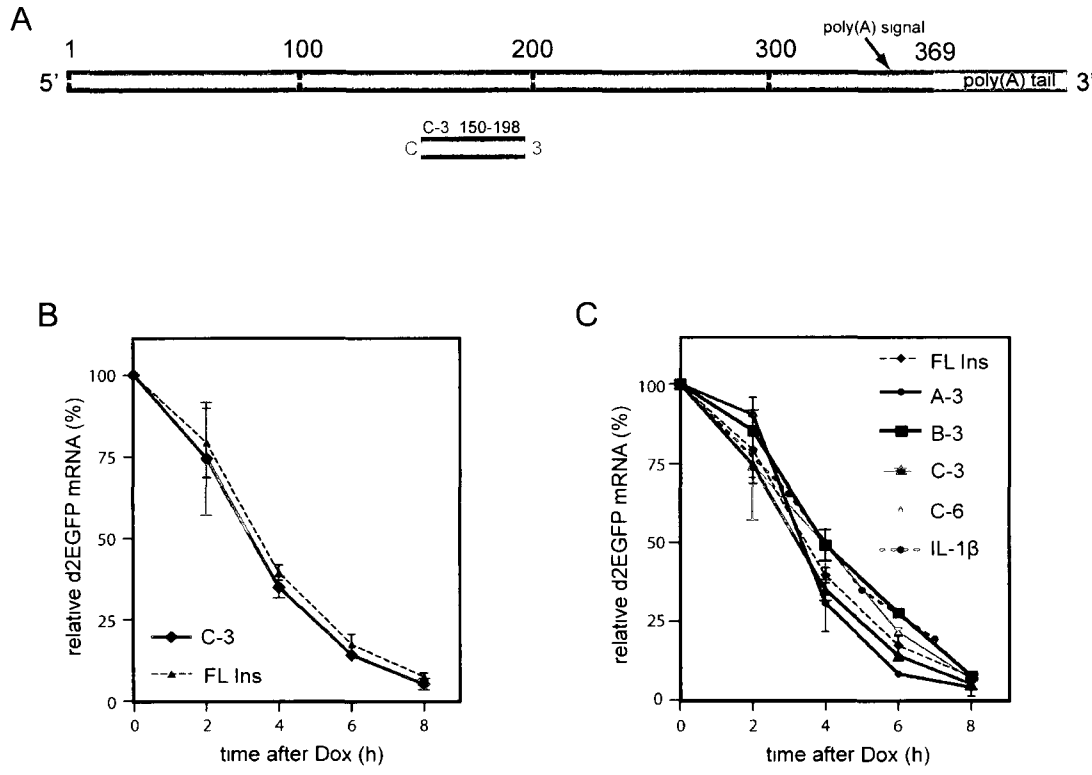

Figure 27. The minimal C-3 fragment contains the destabilizing element. (A) Schematic diagram of the size and location of the C-3 3'UTR fragment cloned into the pTRE-d2EGFP vector and stably transfected into HeLa TO cells. (B) d2EGFP mRNA expression in indicated cell lines following Dox treatment. Values represent the mean ± standard error of at least 3 independent experiments (C) d2EGFP mRNA expression in unstable fragment-containing cell lines following Dox treatment. IL-1β, full-length 3'UTR of interleukin 1β was fused into pTRE-d2EGFP plasmid. All data measured by real-time RT-PCR and expressed as % of initial (before Dox) mRNA levels for each cell line.

Table 4. Summary of DDB2 3'UTR fragment analyses

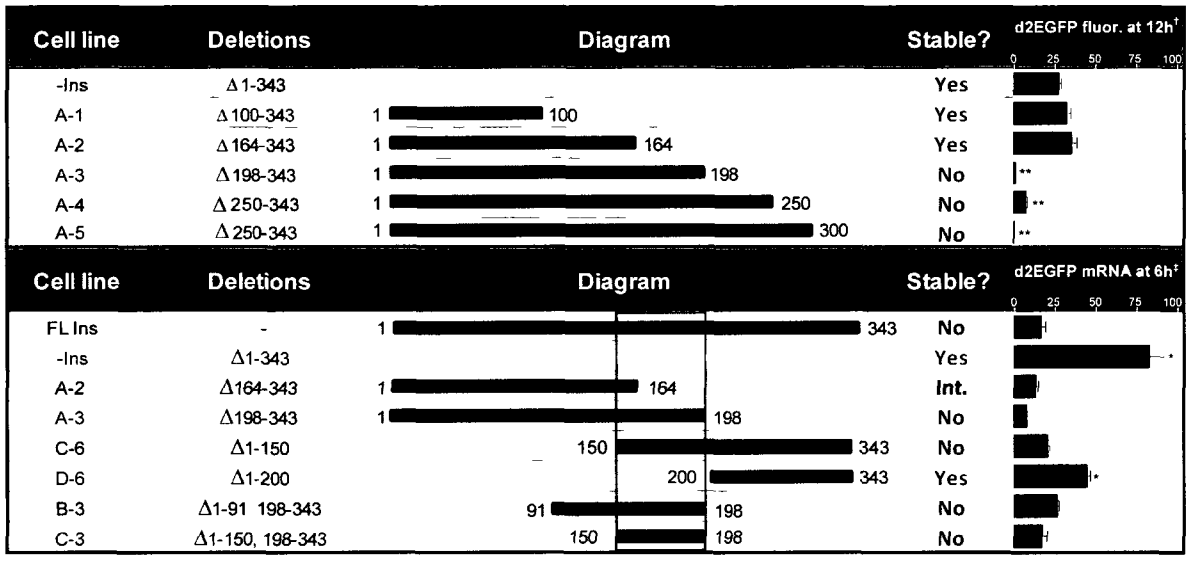

Significant differences (*p<0.05, **p<0.001) were determined using Student *t* test. Statistical significance compared to d2EGFP stability of -Ins cell line in top half of table (significantly unstable) and compared to FL Ins cell line in bottom half of table (significantly stable).

† Fluorescence measured by flow cytometry from experiment in figure 24.

‡ mRNA levels measured by real-time RT-PCR from Dox time course experiments in figure 25.

Red box indicates putative location of stability determinant.

with FL Ins or A-3 fragment-containing cells. A possible explanation for these findings may have to do with our cloning strategy. The A-2 fragment overlaps with the C-3 and A-3 fragments by 14nt. Unfortunately, for thermodynamic considerations of the primer sets, this overlap was unavoidable. This short region contains 2 sequences that may determine stability as will be discussed below. Consequently, this region may show partial instability.

4.7 Further characterization of the 3'DDE

Regulatory regions found in the 3' and 5' UTRs of mRNAs function through interactions with RNA binding proteins that have affinity for specific *cis*-acting regulatory sequences, structures or a combination of both [237]. mRNA secondary structures are extremely complex and varied. We used RNAstructure Version 4.5 RNA folding software [238, 239] to predict the secondary structure of the DDB2 3'UTR. Figure 28A displays several representative structures predicted to form. While there was some variation within the 16 predicted structures, nearly all contained an identical approximately 100bp elongated stem-loop region (Figure 28B). This region contains a 20 nt inverted repeat that is predicted to form a stable hairpin loop (blue shaded area), as well as a 13nt region that is nearly universally predicted to remain single-stranded (green shaded area). Just upstream of the single-stranded region is a putative CUG motif (shaded yellow). These have been shown to act as targets for RBP interactions [125, 240]. One of these proteins, CUG binding protein 1 (CUG-BP1), has been implicated in mRNA deadenylation and degradation [170].

Importantly, these structures are predicted to form regardless of whether the 3'UTR is analysed alone or in the context of the DDB2 or d2EGFP mRNA. When we compared

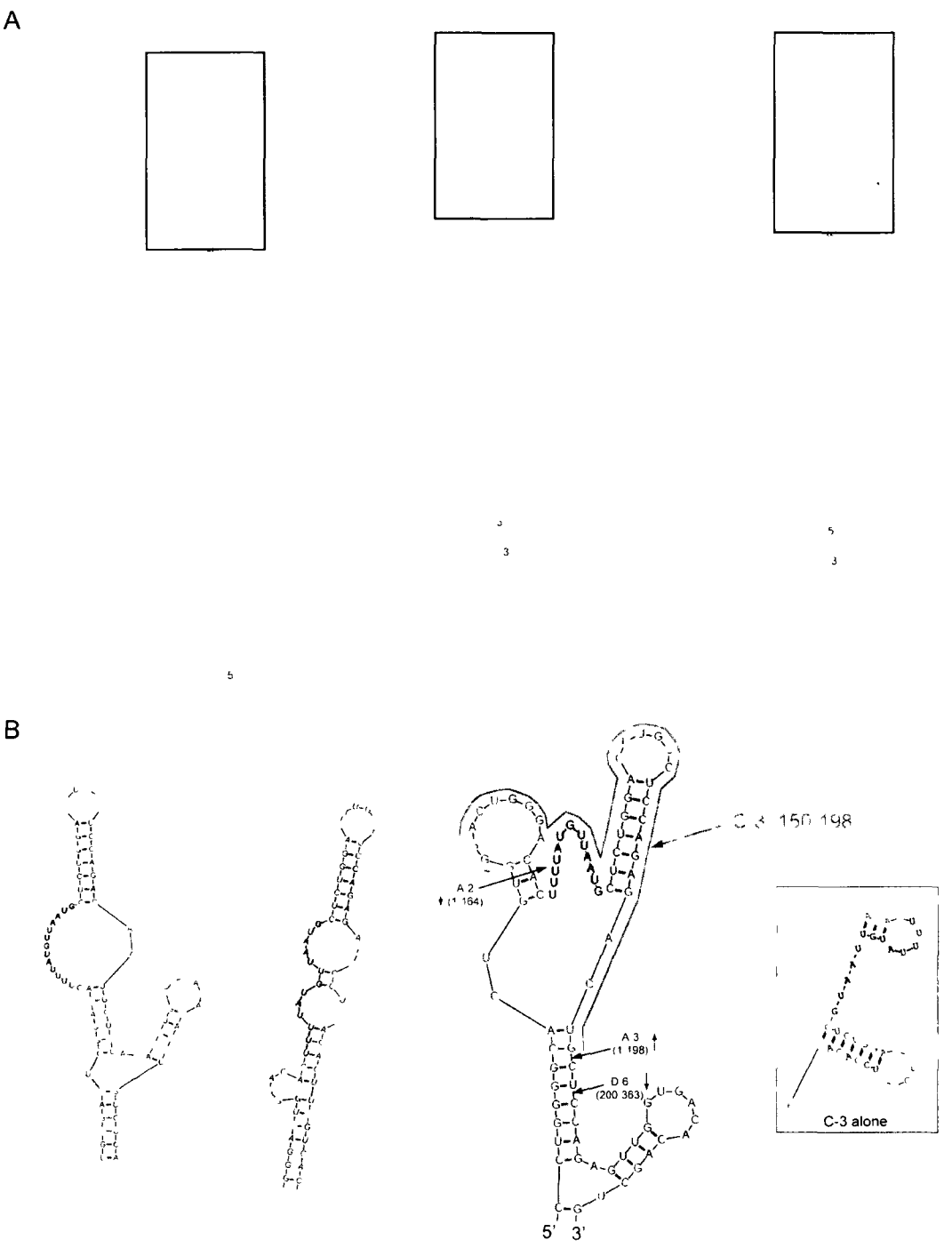

Figure 28. Predicted mRNA secondary structures of the DDB2 3'UTR. (A) Three representative structures of the full-length 3'UTR as predicted by RNAstructure version 4.5. (B) Blown up images of boxed areas from (A) contain the 3'DDE (fragment C-3, red line). In all predicted structures, this region folds similarly and consists of a putative CUG binding motif (yellow), a single-stranded region (green), and an inverted repeat that forms a stable hairpin loop structure (blue). Also indicated is location of other fragment ends. Vertical arrows indicate the direction in which the fragment continues away from its end. Inset: predicted folding of C-3 fragment alone when present within the d2EGFP construct.

our 3'UTR fragment analysis data with these structures, we found that all unstable fragment constructs contain this region of secondary structure, whereas the stable transcripts do not. The smallest unstable fragment (C-3 150-198bp), the putative site of the 3'DDE, corresponds exactly with this 20nt hairpin loop, 13nt single-stranded region and CUGGG motif as is indicated with a red line in Figure 28B. When the structure of only the 49nt C-3 fragment within the d2EGFP reporter plasmid is considered, there is a small amount of base-pairing in the single stranded region and the hairpin loop is still predicted to form (Figure 28B, boxed area on right).

4.7.1 Effects of the stem-loop structure of the 3'DDE

While the DDB2 3'UTR does not appear to contain an ARE, there is evidence in the literature for stem-loop structures that are structurally and functionally distinct from AREs but act to destabilize mRNA. Brown and colleagues [241] found just such an element in granulocyte colony-stimulating factor mRNA and have called it a stem-loop destabilizing element (SLDE). It has more recently been shown that the structure of this loop, and not its sequence, is essential for its destabilizing effects [172].

To investigate the possibility that this DDB2 stem-loop was responsible for the destabilizing effect of the C-3 fragment, we first created two alternate C-3 fragments containing mutations in the inverted repeat sequences (SLmut1 and SLmut2). These stem-loop mutants are diagrammed in Figure 29A. SLmut1 has been modified by converting two guanine residues to cytosines on the 5' side of the stem of the loop such that the hairpin is not predicted to form. In SLmut2, the mismatched cytosines in SLmut1 on the 3' side of the stem were changed to guanines to restore a perfect inverted sequence that is predicted to

form a similar stem-loop structure. All mutant structure predictions were verified as discussed above with RNAstructure folding software. As before, these stem-loop mutant fragments were cloned into the d2EGFP vector and transfected into HeLa TO cells where they were enriched for d2EGFP expression by FACS. Real-time RT-PCR analysis of Dox time course experiments comparing these mutant C-3 fragment-containing cells with the wild type C-3 cells showed no statistical difference in d2EGFP mRNA stability with either SLmut cell line (Figure 29B).

Following this, we generated two additional stem-loop mutant C-3 fragments (SLmut3 and SLmut4). Rather than targeting the inverted repeat sequences, in SLmut3 we changed two uracils to adenines at the top of the loop formation. These modifications do not affect the formation of the stem-loop but might alter any potential protein binding site at the top of the loop. Lastly, SLmut4 has the entire stem-loop region deleted (Figure 29A). These fragments were again cloned into the d2EGFP reporter, but were transiently transfected into HeLa TO cells along with C-3 wt fragment-containing 2EGFP plasmid. The basal d2EGFP mRNA expression and stability of C-3 fragment-containing cells was similar, regardless of the method used to introduce the reporter plasmid. Again, the modifications introduced into the SLmut3 and SLmut4 C-3 fragments had no effect on d2EGFP mRNA stability (Figure 29C).

Taken together, the results of the stem-loop mutant fragment analyses suggested that the 20 nt hairpin structure predicted to form in the C-3 fragment was not responsible for its destabilizing effects. Therefore, the 3'DDE must reside within the 30 nucleotide region upstream of the hairpin loop.

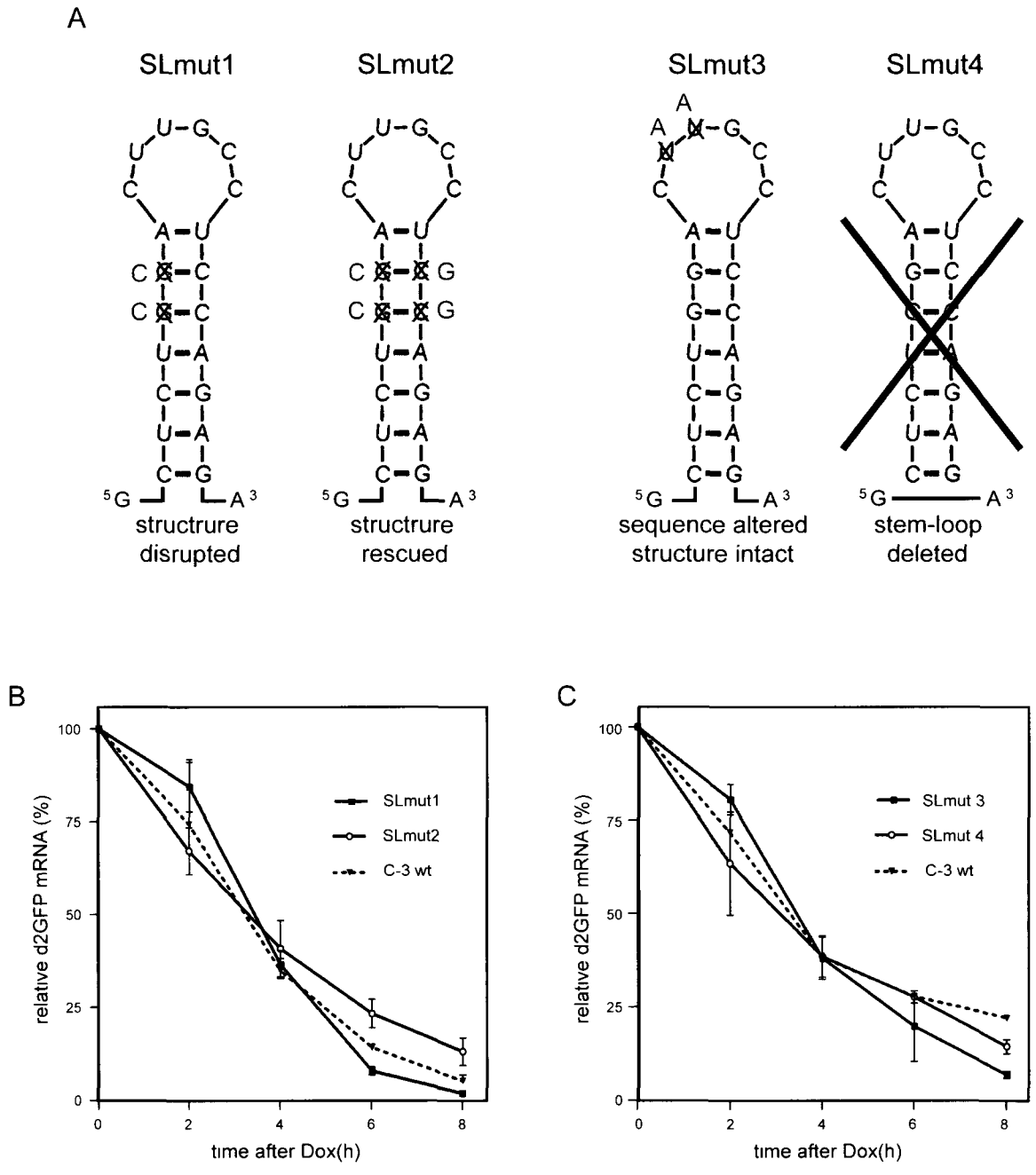

Figure 29. The stem-loop structure of the 3'DDE does not confer instability to d2EGFP mRNA. (A) Schematic diagram of 4 stem-loop modifications made to the C-3 fragment. Predicted structural changes are described below diagram. (B) d2EGFP mRNA expression in SLmut1 and 2 and C-3 wt-containing cell lines following Dox treatment. (C) d2EGFP mRNA expression following Dox treatment in HeLa TO cells transiently transfected with SLmut3, SLmut4, or C-3 wt-containing d2EGFP reporter plasmids. All samples were analysed by real-time RT-PCR. Values represent the mean ± standard error of at least 2 independent experiments.

4.7.2 Effects of the single-stranded region of the 3'DDE

Following our analysis of the 3'DDE hairpin loop, we turned our attention to the single-stranded (SS) region of the 3'DDE. As mentioned earlier, the DDB2 3'UTR does not contain a canonical ARE (tandem or dispersed AUUUA motifs). There is evidence in the literature, however, for U-rich regions acting as stability determinants [136]. The SS region of the 3'DDE is U-rich. Eight of thirteen residues are uracils, including a poly-U region at its 5' end. To investigate whether or not the predicted single-stranded (SS) region might confer instability on the d2EGFP reporter construct, we again created a series of variants of the DDB2 3'UTR C-3 fragment containing mutants and deletions within the SS region. These constructs were again tested in our HeLa TO d2EGFP reporter system via transient transfections. The various fragments used in this analysis are shown in Figure 30A.

The first modification forced the SS region into a hairpin loop by mutating the 5' end from UUUU to GGGG and the 3' end from AAUG to CCCC (SSmut1). This created a short inverted repeat that was predicted to form a small stem-loop. Next, we mutated the U-rich region at the 5' end of the SS region to adenines (SSmut 2). Both of these alterations (especially SSmut2) appeared to destabilize the d2EGFP reporter even further compared to the transiently transfected C-3 wt containing reporter (Figure 30B, left panel). Deleting the entire SS region (ΔSS) greatly increased the stability of the encoded mRNA such that almost 50% of d2EGFP mRNA remained at 8h following Dox addition (Figure 30B, left panel, blue line). These experiments suggest that the SS region of the C-3 fragment is critical in determining the stability of this reporter construct, but that it may not be simply its single-strandedness that is important (compare the structure of C-3 wt with SSmut1,

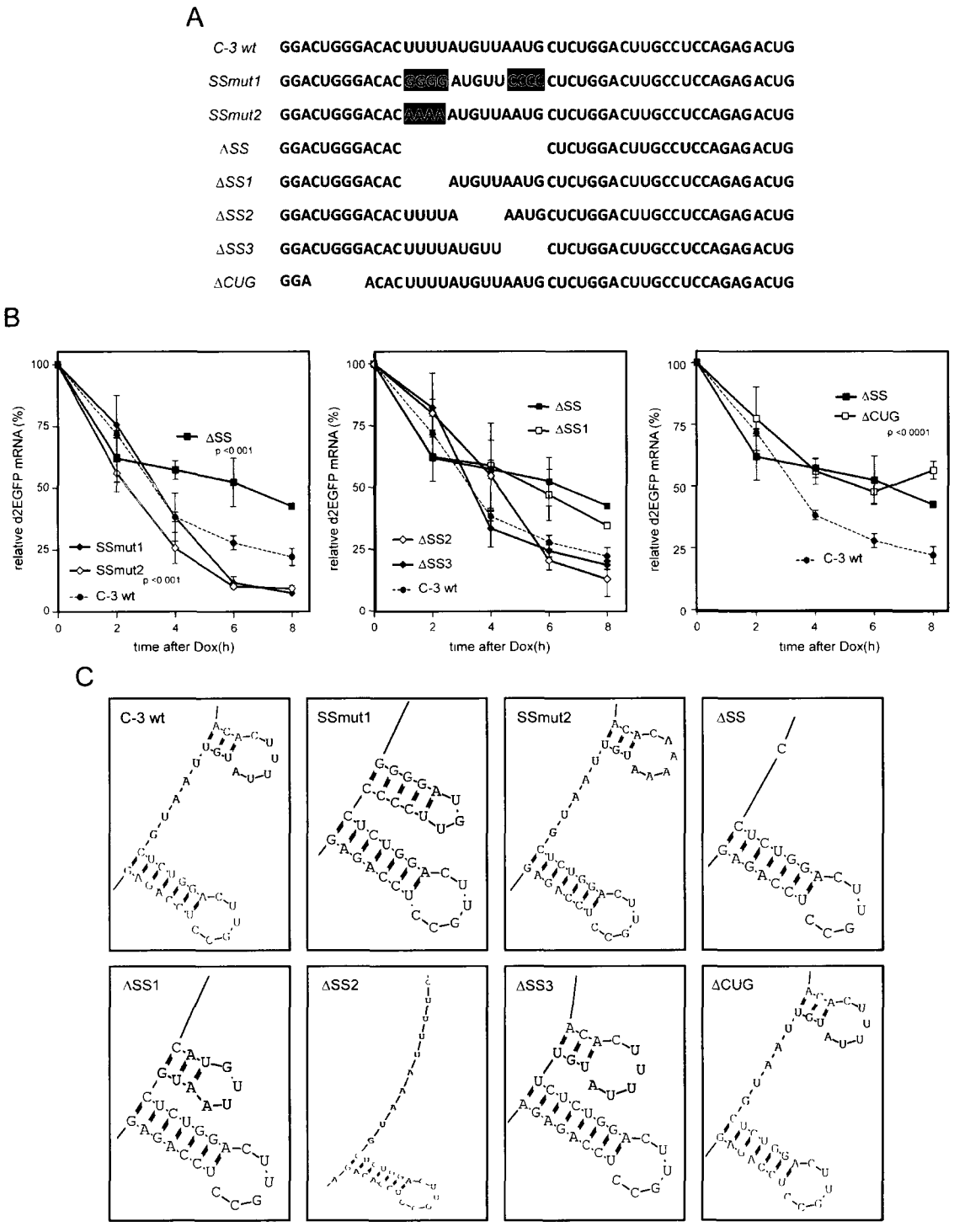

Figure 30. The single-stranded region of the 3'DDE confers instability to d2EGFP mRNA. (A) Sequence of modified C-3 fragments. Green, single-stranded region; blue, inverted repeats of stem-loop; red, mutated nucleotides. (B) Dox time course analyses as described in figure 28B with indicated constructs. Values represent the mean ± standard error of at least 2 independent experiments. P values are in relation to C-3 wt data as determined by 2-way ANOVA. (C) Predicted secondary structures of C-3 fragments within the pTRE-d2EGFP construct using RNAstructure version 4.5 [238].

Figure 30C). They also suggest that modifications of this SS region may increase the efficiency with which the C-3 fragment targets d2EGFP mRNA for decay.

The ΔSS fragment analysis suggested that the SS region of the C-3 fragment was important for its mRNA destabilizing properties. A series of smaller deletions of the SS region (ΔSS1, 2 and 3) were created to refine the region required for enhanced mRNA turnover (Figure 30A). Using the same d2EGFP reporter system, we found that the ΔSS1 fragment (in which the 5' poly-U region was deleted), did not target d2EGFP mRNA as efficiently for degradation as the ΔSS2, ΔSS3, or C-3 wt fragments did. Instead, d2EGFP mRNA stability increased to the same level as when the entire SS region was deleted. The deletions in the ΔSS2 and ΔSS3 fragments had no effect on stability (Figure 30B, middle panel).

Lastly, we looked at the CUGGG motif at the 5' end of the SS region. When this sequence was deleted from the C-3 fragment (ΔCUG), mRNA stability was increased to the same degree as deleting the entire SS region (ΔSS) or the four uracil residues at the beginning of the SS region (ΔSS1) (Figure 30B, right panel).

Taken together, these results indicate that the hairpin loop predicted to form in the C-3 (nt150-198) region of the DDB2 3'UTR has no effect on the mRNA stability of this fragment. On the other hand, the SS region and specifically the poly-U region at its 5' end (nucleotides 13-16), does appear to play a role. There may also be a stability determinant just upstream of this containing a CUGGG motif (nucleotides 4-8). Between these two sequences, we have therefore isolated a 13 nucleotide region of the DDB2 3'UTR that defines the 3'DDE and affects the stability of the 3'UTR. How the various SS region

modifications are predicted to affect the structure of this region are shown in Figure 30C. The C-3 fragment stability analysis is summarized in Table 5.

4.8 CUG-binding protein 1 does not mediate the stability of the 3'DDE

Our investigation of the SS region indicated that a CUGGG motif may play a role in stability. As a preliminary investigation into potential RNA binding proteins that may associate with the 3'DDE, we used short interfering RNA (siRNA) to knockdown the expression of CUG-BP1 protein in a panel of stable (-Ins and D-6) and unstable (FL Ins and C-3) d2EGFP-expressing cell lines (Figure 31). 48 hours after siRNA transfection, we collected cells before and after exposure to Dox for 4 hours. As expected, the amount of d2EGFP mRNA remaining after Dox treatment was significantly lower in the 3'DDE containing cell lines (FL Ins and C-3) compared with the cell lines lacking this region. In all cell lines tested, depleting CUG-BP1 levels did not affect the stability of the d2EGFP reporter genes. This argues against a role for CUG-BP1 in mediating the destabilizing effects of the 3'DDE.

Together, the data presented here indicate that p53 target-gene transcripts are short-lived with a subset being stabilized by UV light. One such UV-stabilized p53 target gene, DDB2, contains a previously unknown destabilizing element within its 3'UTR. This element (termed the 3'DDE) is 13 nt long, contains UUUU and CUGGG regions and is predicted to remain single stranded. Furthermore, it does not appear to interact with CUGBP1.

Table 5. Summary of modified C-3 fragment analyses

C-3 fragment	Sequence	Stable?	d2EGFP mRNA @ 6h (0 25 50 75 100)
C-3 wt	GGACUGGGACACUUUUAUGUUAAUG CUCUGGACUUGCCUCCAGAGACUG	No	
SLmut1	GGACUGGGACACUUUUAUGUUAAUG CUCU[GC]ACUUGCCUCCAGAGACUG	No	
SLmut2	GGACUGGGACACUUUUAUGUUAAUG CUCU[GC]ACUUGCCU[GC]AGAGACUG	No	
SLmut3	GGACUGGGACACUUUUAUGUUAAUG CUCUGGAC[AA]GCC UCCAGAGACUG	No	
SLmut4	GGACUGGGACACUUUUAUGUUAAUG ACUG	No	
SSmut1	GGACUGGGACAC[GGGG]AUGUU[CCCC]CUCUGGACUUGCCUCCAGAGACUG	No	
SSmut2	GGACUGGGACAC[AAAA]AUGUUAAUG CUCUGGACUUGCCUCCAGAGACUG	No	
ΔSS	GGACUGGGACAC CUCUGGACUUGCCUCCAGAGACUG	Yes	*
ΔSS1	GGACUGGGACAC AUGUUAAUG CUCUGGACUUGCCUCCAGAGACUG	Yes	*
ΔSS2	GGACUGGGACACUUUUA AAUGCUCUGGACUUGCCUCCAGAGACUG	No	
ΔSS3	GGACUGGGACACUUUUAUGUU CUCUGGACUUGCCUCCAGAGACUG	No	
ΔCUG	GGA ACACUUUUAUGUUAAUG CUCUGGACUUGCCUCCAGAGACUG	Yes	*

Significant differences (*p<0.05) are compared to d2EGFP stability of C-3 wt fragment (significantly stable) and were determined using Student *t* test.
Yellow shading, CUGGG motif; green shading, single-stranded region; blue, inverted repeats of stem-loop; red, mutated nucleotides.

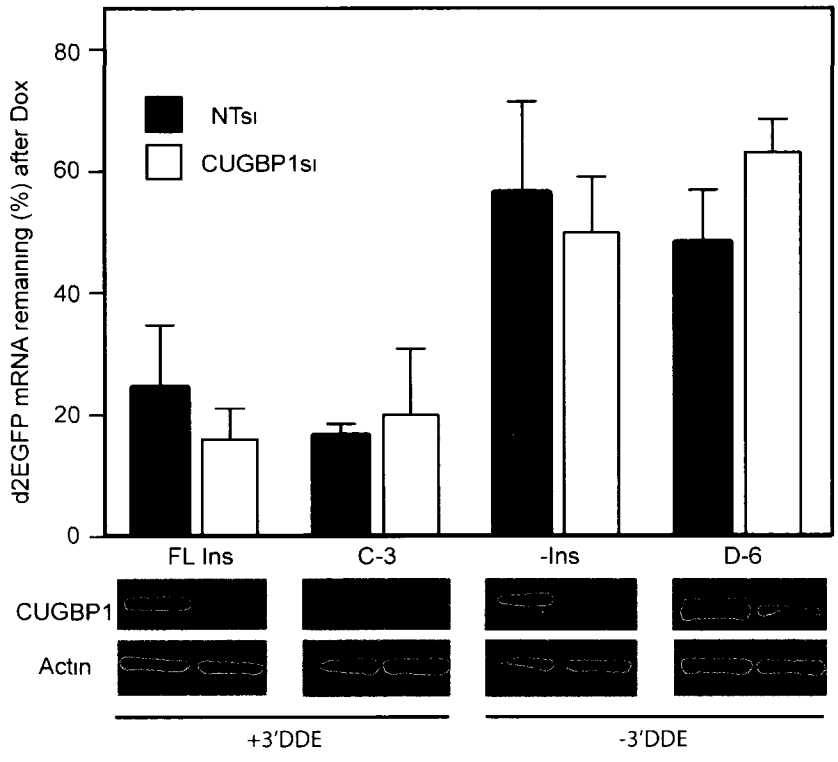

Figure 31. CUG-binding protein 1 does not mediate mRNA stability of the DDB2 3'UTR. The indicated stably expressing d2EGFP HeLa cell lines were transfected with either CUG-binding protein 1-targeting siRNA (CUGBP1si) or a non-targeting siRNA control (NTsi). 48h later they were treated with Dox. Total mRNA was collected before and 4h after Dox and measured by real time RT-PCR. Data presented as percentage of d2EGFP mRNA remaining after 4h Dox treatment compared to -Dox sample for each cell line and siRNA transfection (top). To monitor CUG-BP1 knockdown efficiency, cell lysates (25µg protein/lane) from same experiment were also collected and subjected to immunoblot analysis (bottom). Values represent the mean ± standard error of at least 2 independent experiments.

Chapter 5 Discussion

5.1 Summary of major findings

Throughout the course of the work presented here, we have found evidence that the mRNA of DDB2 is regulated post-transcriptionally at the level of mRNA stability. We have previously shown that p53 target-gene expression is inversely proportional to gene length following increasing doses of UV light [20]. Larger genes are more likely to sustain DNA damage following UV light [21], and so their expression was shown to be preferentially inhibited following moderate to high doses of UV light. Using the same temperature-sensitive p53-expressing cell line HT29-tsp53, we show here that following UV light exposure, DDB2 message remains significantly elevated compared to p53-regulated transcripts of similar size. This suggests that the expression of DDB2 mRNA following UV light is consistent with a smaller target. We attribute this discrepancy to the fact that the DDB2 mRNA is stabilized by UV light in a dose-dependent manner, while the transcripts of some other similar-sized p53 target-genes are not.

We also show that the post-transcriptional regulation of DDB2 mRNA impacts DDB2 protein expression. This is particularly relevant given DDB2's role in recognizing and thus initiating the repair of UV-induced DNA lesions [58]. Its inability to be transcribed following damaging events within its own locus would presumably become a limiting factor in its ability to be translated following prolonged exposure to DNA damaging agents.

mRNA stability determinants are located within the 3'UTR of many labile and dynamically-regulated transcripts [111, 134, 137, 242, 243]. Using a destabilized EGFP-variant reporter gene under the control of a tet-responsive promoter and a variety of analysis techniques, we have discovered the presence of a previously uncharacterized destabilizing element within the 3'UTR of DDB2. We have termed this the 3'UTR DDB2 destabilizing element (3'DDE).

In silico structural analysis of this region revealed the presence of a hairpin loop and a single-stranded region. Through mutational analysis, we have demonstrated that the single-stranded region confers instability to the fused EGFP transgene. Lastly, we show that the RNA binding protein CUG-BP1 does not appear to regulate the stability of a 3'DDE-containing reporter gene.

5.2 Many p53-regulated transcripts are short-lived

HT29-tsp53 cells express a temperature sensitive variant of p53 that allows for the rapid and reversible manipulation of p53 activity [20, 226, 229]. Incubation of these cells at the permissive temperature leads to the accumulation of $p21^{WAF1}$ within 2 hours and the rapid onset of a G_1 cell cycle arrest [229]. Returning these cells to the restrictive temperature leads to the rapid loss of p53 activity, as evidenced by the loss of $p21^{WAF1}$ protein and cell cycle re-entry [229]. The decline in $p21^{WAF1}$ protein levels is the result of a combination of the rapid loss of p53 activity coupled with the short half-life of both the $p21^{WAF1}$ mRNA and protein.

In the present work, we used this well-characterized cell line to monitor the decay of specific p53-regulated mRNAs (Figures 13 and 14). All of the highly p53-responsive

transcripts examined here decayed rapidly at the restrictive temperature (half-lives between 1.5 and 4 hours) compared to genome-wide estimates of rates of mRNA decay that range from 7 to 10 hours [113, 115, 116, 244]. The present results suggest that many p53-responsive transcripts are subject to negative regulation at the level of mRNA stability.

5.2.1 p53 expression and transactivational activity is tightly controlled

Under normal conditions, p53 expression and its ability to transactivate target-genes is inhibited largely though its interaction with the E3 ubiquitin ligase, MDM2, itself a p53 target-gene [245, 246]. Because p53 can induce cell cycle arrest and apoptosis, its overexpression is incompatible with cell viability. Dramatic evidence for this comes from the finding, nearly 15 years ago, that loss of MDM2 was embryonic lethal in mice, unless it was against a p53-null background [71, 72]. It was also found that there was no difference in cell viability or growth rates between p53-null or p53/MDM2-null fibroblasts [247].

These studies demonstrated how important MDM2 was in suppressing the pro-apototic p53-mediated expression program. On the other hand, studies have, not surprisingly, linked overexpression of MDM2 with the inactivation of p53 and subsequent tumourigenesis [248-251]. Therefore, the tight regulation of this negative feedback loop is crucial for maintaining a correct balance between cellular viability and effective p53-mediated stress responses [221, 252].

5.2.2 Rapid decay of p53 target-mRNAs keeps p53 stress responses in check

Several groups have assessed mRNA decay on a genome-wide scale using oligonucleotide microarrays [115, 116, 124]. Gene ontology analysis of these data sets

indicates that specific functional classes of transcripts are far more likely to be subject to negative regulation by mRNA decay [113, 115, 116, 124]. Salient to the p53 response, regulators of apoptosis and cell cycle are over represented among the short-lived transcripts [113, 115, 116, 124]. Conversely, transcripts encoding metabolic enzymes and structural proteins tend to have longer half-lives [113, 116]. Our results showing that p53-inducible transcripts are short-lived are consistent with these global assessments of mRNA turnover.

If MDM2-mediated downregulation of p53 protein levels and activity has been strongly selected for by evolution, then it follows that tight regulation on the expression of p53 target-genes, has also been selected for. The benefit of producing labile transcripts is that it allows for the dynamic control of induction and termination of protein expression as conditions dictate [28]. We propose then, that the rapid mRNA decay of p53-induced genes is another way that cells keep their p53 response in check. This allows for continued cell cycle progression and cell survival before and after a p53-induced stress response is mounted.

5.3 UV-induced DNA lesions pose a challenge for coordinating gene expression

UV light can induce intrastrand adducts in the template strand of active genes and these result in the arrest of RNA polII [119]. UV lesions are induced in a stochastic manner so the probability that a gene sustains damage is proportional to its size. Moderate doses of UV light are sufficient to decrease the synthesis of nascent RNA measurably [253]. Previously, we hypothesized that UV-induced DNA lesions would pose a challenge to p53- and UV-induced gene expression [20, 104].

Using HT29-tsp53 cells, we previously identified over 80 transcripts that were significantly upregulated at the permissive temperature [20]. Exposure of these cells to either 10 or 30 J/m^2 of UV light led to a decrease in the number of genes induced at the permissive temperature. Strikingly, there was a switch in the spectrum of p53-induced genes to compact genes with fewer and smaller introns. Compact genes were similarly induced following UV exposure at the restrictive temperature and in other cell systems [20, 254, 255]. Therefore, the coordinated regulation of UV-responsive transcripts requires that their regulation is insensitive to the inhibitory effects of UV photoproducts. One way to circumvent this problem is through the evolution of compact UV-responsive genes.

5.3.1 Post-transcriptional regulation of DDB2

The DDB2 gene is approximately 24 kbp in size. In response to 10 J/m^2, one predicts that the DDB2 gene should sustain approximately 2.5 intrastrand DNA adducts in the template strand of DNA (discussed in [20, 104]). Here we show that, despite this fact, DDB2 was induced more efficiently than similar sized p53 target-genes (Figure 12). This effect could not be accounted for by the activation of a cryptic downstream promoter. Instead, the stability of the DDB2 message was increased in a UV dose-dependent manner (Figure 15) to an extent comparable to the well-characterized p53-responsive UV-stabilized p21^{WAF1} mRNA [25, 232]. These findings suggest that differential mRNA stability plays a role in the expression of a subset of p53 target-genes, including DDB2 and p21^{WAF1}.

5.3.2 UV light increases the stability of a subset of p53 target-gene mRNAs

It has been estimated that over 50% of all stress-related genes are regulated at the level of mRNA decay [120]. Importantly, many UV-induced transcripts are stabilized by UV light [22, 24, 25, 150, 232, 234]. This implies that many UV- and stress-regulated transcripts are short-lived under normal conditions but that specific RNA binding proteins protect these messages under appropriate conditions. For example, the $p21^{WAF1}$ mRNA contains an ARE sequence that makes it unstable under most conditions [232, 256]. In response to UV light, the HuR protein binds this ARE and blocks degradation of the transcript [25]. Our findings in Figure 14B are consistent with this.

Work by Myriam Gorospe's group has led her to speculate that post-transcriptional regulation such as increased mRNA stability, nuclear export, and translation of specific mRNAs following DNA damage may be a widely-used method by cells to permit the efficient expression of stress-response genes despite transcriptional blockages imposed by DNA damage [28]. In this way, organisms have evolved yet another technique to bypass the deleterious effects of DNA damage residing within genes required to mount a suitable stress response. Here, we show that, while the majority of p53 target-genes are short lived, a subset of p53 target-gene transcripts are stabilized by UV light (Table 3, Figure 14).

5.3.3 The coordinated regulation of p53 target-genes may constitute an RNA regulon

Many inherently unstable transcripts encoding dynamically regulated products contain *cis*-acting elements that promote their degradation [150]. The best-characterized *cis*-acting determinant of mRNA decay is the AU-rich element (ARE) that targets specific mRNAs for rapid decay [124, 150, 257]. These elements are most often located within the

3'UTRs of labile mRNAs [140, 258]. The $p21^{WAF1}$ mRNA has a well-characterized ARE in its 3'UTR [232, 256]. According to the AU-rich element-containing mRNA database (ARED 3.0, http://brp.kfshrc.edu.sa/ARED/), the FAS mRNA also contains ARE sequences in its 3'UTR [140]. Therefore, the rapid decrease in the expression of $p21^{WAF1}$ and FAS (Figure 14B,C) is consistent with the presence of known destabilizing elements in their 3'UTRs. In contrast, there are no identifiable ARE sequences in the DDB2 and MDM2 transcripts.

Keene and Tenenbaum first proposed the notion that subsets of functionally related eukaryotic mRNAs may be grouped into tightly regulated post-transcriptional operons or regulons whose expression are jointly coordinated through interactions with specific RBPs [208]. Examples of these specific clusters of co-regulated RNPs have since been identified and the concept has grown to include regulation by non-coding RNAs and changing physiological conditions [117, 210, 259]. We propose that p53 target-genes may also fall into this expression paradigm. As mentioned, p53-regulated genes are indirectly regulated based on their size following UV light. Furthermore, functionally related genes were found to be of similar length [20].

In the present study, we have shown that p53 target-genes are relatively unstable (Figure 13, Table 3). The expression of short-lived messages allows for the tight regulation of expression following rapidly changing cellular conditions [28]. Often, these mRNAs are encoded by genes involved with regulatory functions such as transcription factors or stress-response proteins [115]. The short half-lives of p53 target-genes may be the result of common post-transcriptional regulatory events that serve to limit the pro-apoptotic and anti-survival effects of many p53 target-genes. Consistent with the RNA regulon theory,

we have found that a subset of these genes are stabilized by UV light. Future work might uncover common interacting *trans*-acting factors or stability determinants among these genes that regulate their expression, similar to the 3'DDE we have identified in DDB2.

5.4 DDB2 expression is regulated at a variety of levels

DDB2 is involved in the early recognition of DNA helix-distorting lesions caused by UV light. It is able to bind with high affinity to both 6-4pps as well as CPDs, but is especially essential for the detection of CPDs [10, 50, 91]. The DDB2 protein and mRNA are extensively regulated prior to, and following UV irradiation. Its basal expression and eventual upregulation following exposure to UV light is dependent on p53 [90, 91]. The DDB2 protein is rapidly degraded following UV insult [47] and here, we show that its transcript is simultaneously stabilized in response to UV light.

5.4.1 DDB2 protein is rapidly degraded following exposure to UV light

Immediately following UV irradiation, DDB2 protein colocalizes with sites of DNA damage [50, 260, 261]. DDB2 forms part of a larger E3 ubiquitin ligase complex consisting primarily of DDB2, DDB1 and CUL4A [262] that leads to the mono-ubiquitination of histone H2A and polyubiquitination of DDB2 and XPC and the degradation of DDB2 [48, 49, 263-267]. The degradation of DDB2 is thought to be required to allow XPC, a crucial DNA damage-recognition protein, to gain access to sites of damage and initiate assembly of the repair complex [50]. This degradation leads to the rapid depletion in DDB2 levels. Here, we show that in the absence of protein synthesis, DDB2 protein is completely degraded within 2h of UV radiation (Figure 17B). Without

sufficient transcript from which to replenish protein levels, this rapid loss of DDB2 could become limiting and impair further repair in the face of prolonged DNA damage [47, 92]

5.4.2 p53-dependent induction of DDB2

It has been known now for several years that p53 transcriptionally upregulates DDB2 following UV irradiation and $p53^{-/-}$ cells are deficient in GGR [91] We have found that in our conditional p53 induction system, DDB2 mRNA is upregulated over 10-fold following 16 hours of p53 activation (Figure 14A) Overexpression of DDB2 in p53-deficient cells restores NER capacity [92] Therefore, the p53-dependent regulation of DDB2 is clearly critical to its function in DNA repair [91, 225] However, both mRNA and protein levels of DDB2 do not spike until 24 and 48 hours, respectively, following UV exposure [47, 223] Therefore, the p53-mediated transcriptional induction of DDB2 appears to be too slow to contribute significantly to GG-NER following acute exposure, but likely plays a critical role in the response to chronic daily exposure [268]

5.4.3 DDB2 mRNA is stabilized by UV light

Here, we present evidence that DDB2 mRNA is stabilized following UV irradiation As mentioned above, DDB2 protein is rapidly depleted by UV exposure before transcriptional regulation is possible, and its p53-mediated induction is much too slow to facilitate repair in an appropriate timeframe This paradoxical regulation of DDB2 has not escaped notice [10]

Post-transcriptional regulation of DDB2 following UV exposure offers a mechanism that allows maintenance of DDB2 mRNA levels under conditions in which

mRNA synthesis is inhibited. This would allow translation of DDB2 that, in turn, can aid in the surveillance and detection of lesions within the normal timeframe of repair. It should be noted that the mRNA stabilization presented here lasts for 6 hours (Figure 14E), which is approximately the amount of time required for the repair of UV light induced CPDs [91]. We also show that UV stabilization of DDB2 mRNA is UV dose-dependent (Figure 15). This suggests to us a model whereby increasing exposure to UV light (concomitant with more DNA lesions) leads to an increase in DDB2 mRNA stability to allow for efficient lesion detection under conditions of increased transcription blockage. A model of DDB2 transcriptional and post-transcriptional regulation following UV light exposure is presented in Figure 32.

DDB2 has been shown to bind with varying affinities to a variety of DNA lesions, not all of which are induced by UV light. For example, it can bind to cisplatin or nitrogen mustard-induced adducts [44]. It is also induced following ionizing radiation [91, 269]. It would therefore be interesting to investigate whether the post-transcriptional regulation documented here, following UV light exposure, applies to these other mutagenic sources as well. If the mRNA of DDB2 or other p53 target-genes were stabilized by a wide variety of extracellular stimuli, these findings would add to a growing consensus that post-transcriptional regulation is in many ways the front line of defence against multiple cellular stresses.

5.5 UV light stabilizes DDB2 mRNA in HT29-tsp53, but not HeLa TO cells

Our results clearly show that UV light stabilizes DDB2 mRNA in HT29-tsp53 cells following p53 induction (Figures 14-16). We have also demonstrated that DDB2 mRNA is

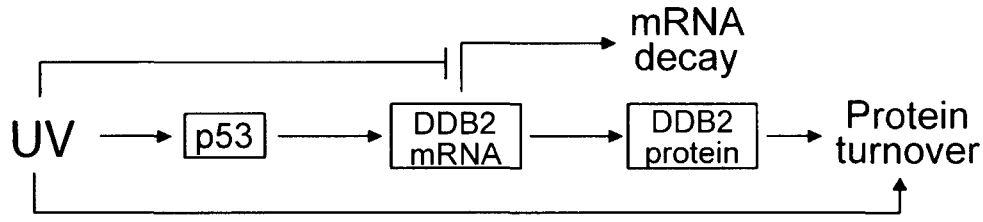

Figure 32. UV light-mediated post-transcriptional regulation of DDB2. UV irradiation induces p53, which in turn upregulates DDB2 transcription. DDB2 protein binds to DNA lesions and is subsequently degraded in a ubiquitin-dependent manner, while UV light impairs mRNA synthesis within the period of damage recovery. Together, these processes deplete the pool of available DDB2. To partially counter this, UV light also stabilizes already present DDB2 transcript, which presumably allows for translation to proceed during periods of prolonged genotoxic stress

relatively unstable in unstressed cells (Figure 13) and that its 3'UTR is able to destabilize an EGFP reporter transcript and protein (Figures 18, 22, 23). However, we did not observe UV-mediated alterations in the stability of DDB2 3'UTR fragment-tethered reporter transcripts whether or not they contained the 3'DDE (Figure S-1, supplemental data). We propose two possible reasons for this discrepancy.

5.5.1 UV-responsive element may be in the DDB2 5'UTR or coding region

Firstly, it is possible that our EGFP reporter system does not recapitulate certain aspects of DDB2 transcript regulation. We have used only the 3'UTR or portions of it to induce the rapid turnover of the d2EGFP transgene. It is possible that in an endogenous context, the DDB2 3'UTR interacts with specific binding factors that are recruited by elements contained within other regions of the gene. Due to the circularization of mature mRNAs through interactions with poly(A) binding proteins and the 5'cap structure, 3' and 5'UTRs (and proteins that may bind to them) can come into contact with each other [141]. It is also possible that the UV-mediated stabilization observed in HT29-tsp53 cells is dependent on separate sequences elsewhere in the mRNA, either in the coding region or 5'UTR. This potential non-3'UTR element, (or multiple elements) may not interact with the 3'DDE. In response to UV light though, it would have to overcome the destabilizing effect of the 3'UTR element.

The *c-fos* mRNA contains two such stability determinants. It contains a destabilizing ARE in its 3'UTR as well as a coding region stability determinant known as the mCRD that confers instability following translation [270]. A complex of proteins assembles on the mCRD and it has been hypothesized that the movement of ribosomes

through this coding region disrupts the complex, triggering deadenylation-mediated decay. Therefore the mCRD complex appears to protect untranslated *c-fos* mRNA from deadenylation induced through the 3'UTR ARE [271]. A situation similar to this could be envisioned for the regulation of the DDB2 mRNA as well. The 3'DDE confers instability, but following UV light, this effect is abrogated or overcome through altered interactions in the 5'UTR or coding region. Additionally, translation of the DDB2 mRNA may be coupled to its UV-mediated stabilization. These scenarios could not be replicated through the isolation and insertion of the 3'UTR or a single 3'UTR stability determinant into a reporter construct. Experiments utilizing similar HeLa TO cells, expressing the full DDB2 mRNA (including both UTRs) in place of the d2EGFP transgene, may rescue the UV-mediated stabilization observed in HT29-tsp cells and allow for the discovery of a secondary UV-responsive stability determinant.

5.5.2 HeLa cells do not mount a p53-mediated stress response

A second possibility for the lack of a UV response in HeLa cells is their p53 status. HeLa cells are cervical carcinoma-derived cells that express virtually no p53 due the activation of human papilloma virus (HPV)-derived E6 ubiquitin ligase that targets p53 for destruction [272, 273]. Without functional p53 levels, HeLa cells cannot mount a robust response to DNA damage [274]. DDB2 mRNA levels rely strongly on basal p53 expression [91], therefore HeLa cells express very low levels of DDB2. As our earlier results in HT29-tsp53 cells show, p53 induction is required to see differential mRNA stability following UV light (Figure 14F). We have also been unable to show that UV light significantly alters the stability of endogenous DDB2 mRNA in HeLa TO cells (Figure S-

2). Together, this suggests that UV light mediates a p53-induced stress response that culminates in the stabilization of DDB2 mRNA, and that this response is absent in the HeLa cells used in our reporter construct analysis. To test this hypothesis and circumvent these limitations, future work could utilize the tet-responsive reporter system in a p53-proficient cell line.

5.6 Differential mRNA stability is not dependent on insert size or GC content

When comparing full-length DDB2 3'UTR containing cell HeLa TO lines with those lacking any insert, we observed a dramatic decrease in reporter-gene stability. It occurred to us that the length of these fragments or their nucleotide content, as opposed to any specific sequence element within them, may play a role in determining the turnover rate of the d2EGFP mRNA.

5.6.1 The size of the 3'UTR fragment does not affect its stability

One study in yeast has suggested that shorter mRNAs form closed loop structures more easily and are therefore translated more efficiently. They are presumably also less susceptible to deadenylation and exonuclease attack [275]. Studies on nonsense mediated decay (NMD) have shown that the distance between termination codons and the poly(A) tail plays a role in eliciting decay [186]. Work in yeast and *C. elegans* has also found a correlation between long 3'UTRs and the induction of NMD [276, 277].

It has been shown that alternate polyadenylation signals are found in most 3'UTRs. EST data indicates that nearly half of all human genes are subject to alternate length 3'UTR expression because of these signals [278]. When alternate polyadenylation occurs, large

regions of the 3'UTR are often removed, taking with them regulatory elements that affect their nuclear export, translational efficiency, and mRNA stability [237]. Subsequently, studies have shown that shorter 3'UTRs often encode more stable mRNAs, often due to loss of miRNA target sites [279-281]. One recent study found that cancer cells express substantial amounts of mRNA isoforms with shorter, alternate 3'UTRs. The expression of these isoforms in several oncogenes led to increased mRNA stability, far greater protein production, and a greater rate of oncogenic transformation [281].

The various fragments we used to isolate the 3'DDE spanned proximal and distal regions of the 3'UTR. They were also variable in length (49 to 343 nt), such that they functioned as approximate size controls for one another. When fragment size was plotted against d2EGFP mRNA remaining at 6h following Dox addition, we found no correlation between insert length and mRNA decay ($r = -0.243$) (Figure 33A, left panel). Using this approach, we concluded that the length of the insert did not affect its stabilizing properties. In fact, the stability of the longest fragment (FL Ins, 343 nt) was nearly identical to the shortest (C-3, 49 nt). We also saw large differences in the stability conferred by our C-3 mutant and deletion constructs, and to ensure that these stabilities were also not fragment size-dependent, all 12 C-3 variant constructs' stability were plotted against their nucleotide length (Figure 33A, right panel). These fragments ranged in size from 29 to 49 nt, and again, there was no correlation between size and stability ($r = 0.515$). From this, we can conclude that shorter fragments do not, in general, protect the d2EGFP from degradation, nor do they enhance decay.

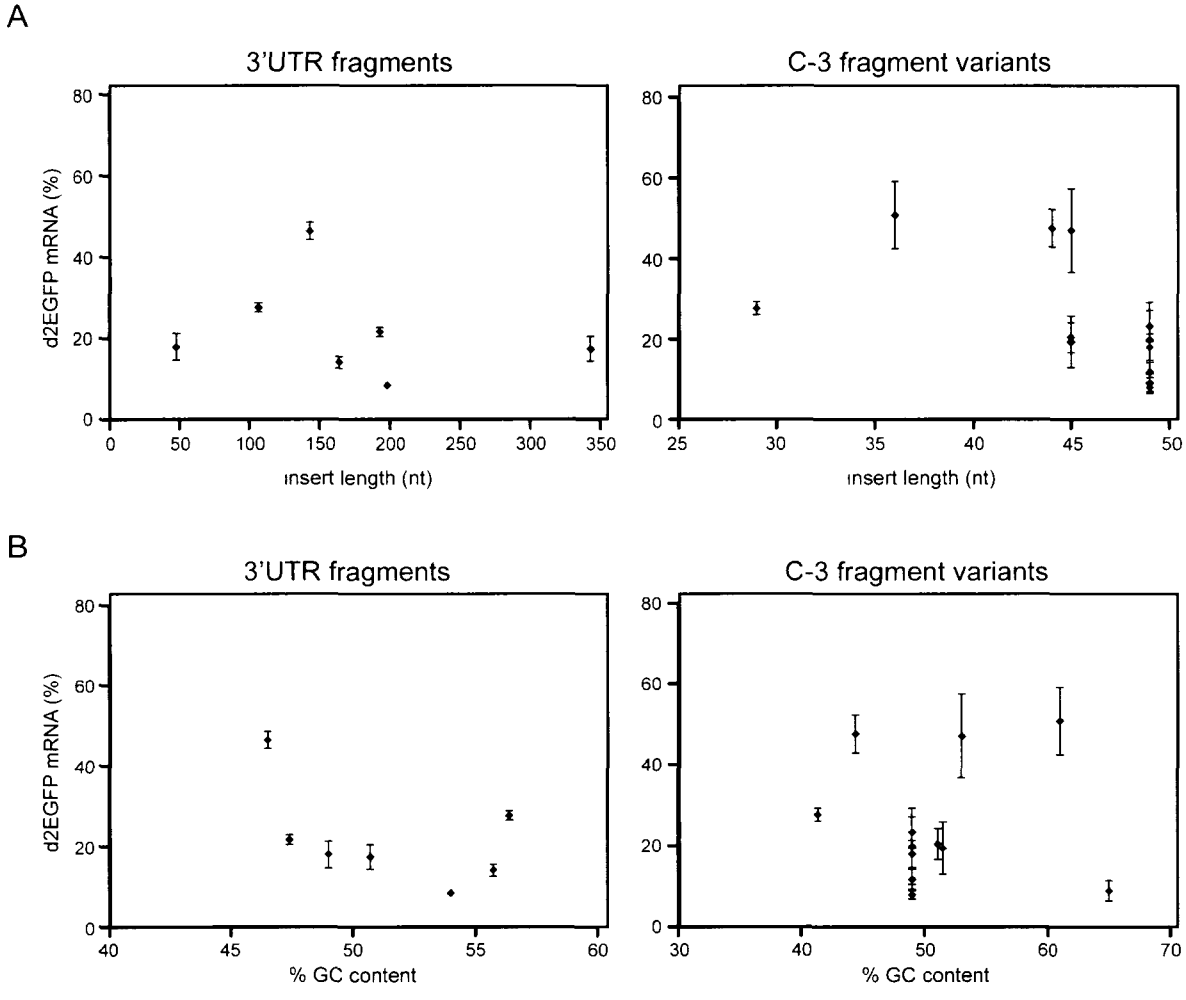

Figure 33. d2EGFP mRNA stability is not dependent on insert size or GC content. % d2EGFP mRNA remaining following 6h Dox treatment was plotted against (A) DDB2 3'UTR fragment or C-3 variant nucleotide length (left and right panels, respectively) or (B) % GC content in DDB2 3'UTR fragment or C-3 variants (left and right panels, respectively). Correlation coefficients: A, (3'UTR fragments) r = -0.243; (C-3 variants) r = -0.515. B, (3'UTR fragments) r = -0.492, (C-3 variants) r = -0.012. Values represent the mean ± standard error of at least 2 independent experiments.

5.6.2 The GC content of the 3'UTR fragment does not affect its stability

We also examined nucleotide content among all the fragments and C-3 variants to ensure there was no correlation between mRNA stability and %GC, and inversely, AU content. Nucleotide composition plays a large role in determining mRNA turnover rates. *Cis*-acting elements such as AREs, GU-rich elements, CU rich elements or tandem CUG repeats can extend dozens or hundreds of base pairs [136, 151, 240, 243, 282], making the elucidation of distinct stability determinants difficult. Secondly, high GC content has been correlated with highly stable secondary structure. This in turn has been shown to impede the RNAi machinery [283]. It is possible then, that genes containing high GC content in their regulatory regions may be less susceptible to miRNA-mediated degradation.

While there was a range in % GC content in the fragments used in the current study, from 41% (SLmut4) to 65% (SSmut2), this appears to have had no effect on the mRNA stability of either the DDB2 3'UTR fragments or the C-3 variants ($r = -0.492$ for fragments and -0.012, for C-3 variants) (Figure 33B). These results further support our claim that differences in stability among DDB2 3'UTR fragments are due to sequence elements within them rather than their percent composition by base.

5.7 The DDB2 3'UTR contains a novel stability determinant

Regulatory elements are often found in the 3'UTR of eukaryotic genes. Following our observation that the DDB2 mRNA was relatively short-lived, but could be stabilized by UV light, we surmised that its 3'UTR might contain a signal that targets the DDB2 transcript for rapid decay during unstressed conditions. When the 3'UTR was fused downstream of a EGFP reporter construct, transgene stability was greatly reduced. This

3'UTR does not contain any characterized ARE or other obvious stability determinant. There are, however, several U-rich areas which have been previously classified as ARE-like elements [136, 140, 141]. Through serial analysis of each region of the 3'UTR, we initially isolated a short 49 nt fragment (C-3) that retains the ability to destabilize a reporter gene. To the best of our knowledge, the 3'DDE represents a novel stability determinant.

5.7.1 Structural considerations of the 3'DDE

In silico analysis of predicted folding of the C-3 fragment of the DDB2 3'UTR predicted that it contains three distinct features. The most prominent was an inverted repeat that is predicted to form a hairpin structure with a 6 nt loop (Figure 28). We focused initially on this structure because other groups have found such non ARE-related stem-loops that modulate stability [172, 241]. Our mutational analysis of this region, however, indicated that point mutations in the inverted repeat and the loop had no effect on the mRNA stability of this fragment. In addition, the deletion of this structure did not affect reporter gene expression (Figure 29).

The second feature in the C-3 fragment was a short region that was predicted to remain unpaired in a variety of contexts. The single-stranded motif, specifically a poly-U region at its 5' end, does affect the stability of the d2EGFP transgene. Deleting the entire SS region or just the uracil residues increased d2EGFP mRNA expression equally (Figure 30B). U-rich regions have been functionally defined as a class of ARE (class III), despite their lacking the signature AUUUA motif [136, 140, 284]. Although, previously documented class III AREs are usually much longer than the short poly-U rich region identified here [284], it may be interesting to note that, in the context of the C-3 fragment

alone, this poly-U sequence is predicted to form the loop portion of a shorter hairpin to the 5' side of the previously mentioned hairpin loop. When this secondary loop was altered or the poly-U sequence was changed to poly-A (SSmut1 and SSMut2, Figure 30), the reporter gene's stability actually *decreased* further than was observed in the C-3 wt fragment-transfected cells.

A third feature of the C-3 fragment was a CUGGG motif that, in the full-length DDB2 3'UTR, was predicted to form the loop of a secondary shorter hairpin structure (Figure 28B). In the context of the C-3 fragment, it was not predicted to interact with other structural elements described above, nor was its removal predicted to alter their structure (ΔCUG, Figure 30C). CUG motifs have been shown to act as targets for RBP interactions [125, 240] and may affect transcript stability through interactions with CUG-BP1 [170]. While they generally exist as tandem CUG repeats [125, 240], our analysis shows that the CUGGG motif present in the C-3 fragment may act as a stability determinant. Deleting it resulted in an increase in d2EGFP expression similar to that seen in the SS (ΔSS) or poly-U (ΔSS1) -deleted fragments (Figure 30B). It is also possible that CUG alone, and not the entire CUGGG motif is responsible for this destabilizing effect.

Both the SS and CUG regions may facilitate interactions with destabilizing proteins, or perhaps the removal of them interferes with protein binding elsewhere. A third possibility is that the stabilizing alterations we have made actually enhance interactions with stabilizing proteins. It will be imperative in future studies to identify factors that interact with these putative stability determinants of the 3'DDE.

Because the nucleotide sequences of UTRs are not used to encode proteins, their secondary structure is often more important than their sequence in regulating their cognate

mRNAs. The discovery that vast amounts of an organism's genome does not encode protein and that much of this is still transcribed has led to the assumption that large amounts of non-coding RNA (ncRNA) must play other biological roles [285]. Closer inspection revealed that much of this ncRNA formed highly intricate secondary structures that were found to be conserved across species, more closely than the sequences themselves [286]. The bioinformatics approach to predicting mRNA secondary structures is a powerful tool for discovering conserved structural sequence elements and inferring their functions. However, it is an ongoing process and many computation and conceptual limitations still exist [287]. While the predicted secondary structures of the DDB2 3'UTR fragments and mutant variants described above are highly probable, two general caveats should be considered here.

First, mRNA folding predictions are based on thermodynamic calculations of low-energy base pairing that are invisible to physiological factors, including the availability and competition of binding proteins associated with a particular mRNA [287, 288]. Furthermore, they do not take into account how mRNA structure might be affected by close proximities to other RNA and DNA species in a cellular context. Secondly, even if mRNA folding algorithms were able to take all these factors into account, the system we have used in these studies is highly artificial in the sense that the folding is predicted based on the immediate presence of the expression vector and the EGFP transcript. The modifications introduced into the C-3 fragments used in these studies are asserting their effects within 50 nt fragments. They may not produce the same results as they would within the full length 3'UTR. We did however confirm that the predicted folding

characteristics of the various fragments are similar whether they are in the DDB2 gene context or within the d2EGFP expression vector.

5.7.2 The DDB2 3'UTR and 3'DDE is highly conserved among primates

The method of "phylogenic footprinting" is a useful tool for discovering functional elements in coding or non-coding regions of the genome through their preservation in divergent species via selective pressure over evolutionary time [289]. Various studies have attempted to estimate homology among eukaryotic 3'UTRs and it appears there is a wide range of conservation rates between species and within untranslated regions [290-293]. One study comparing 77 mouse and human orthologs found that, on average, among 5'UTRs, introns and 3'UTRs, there was a higher conservation in 3'UTR (56%) compared with the 5'UTRs (50%) and introns (23%). This study also identified highly conserved regions among the 3'UTRs studied [292]. Consequently, it does appear that functional elements within untranslated regions have been evolutionarily conserved [294].

The DDB2 gene is not highly conserved among eukaryotes. Unlike its binding partner, DDB1, there is no DDB2 homologue in *Drosophila, C. elegans,* or yeast [58]. While their genomes contain the DDB2 gene, rodents such as mice and hamsters express DDB2 at very low levels or not at all [90, 295]. In mice, DDB2 lacks a p53 response element and is not transactivated following exposure to UV light. Subsequently, rodent cells do not perform GGR of CPDs [90]. However, deletion of DDB2 in mice does lead to UV-induced skin cancer, consistent with XP-E in humans [296]. Therefore, DDB2 must play a protective role in rodents.

In order to assess the evolutionary conservation of the 3'DDE, we compared the DDB2 3'UTR sequences of several mammalian species using ClustalW sequence alignment program (http://www.ebi.ac.uk/Tools/clustalw2/index.html?). Between humans and mice, there is moderate homology throughout the entire DDB2 3'UTR (65%). Among primates, there is 94% conservation (Figure 34). When the inter-species alignment focuses on the C-3 region (highlighted yellow), the similarity among species appears to be similar to the entire 3'UTR. There is almost perfect sequence conservation among primates and humans in the C-3 region. Only small substitutions at the top of the hairpin loop and near the beginning of the single-stranded region have been made. Whether this striking similarity among primates is due to sequence conservation or a lack of evolutionary divergence is difficult to say.

The relatively low homology of the 3'UTR between humans and mice is not surprising considering many mammals lack functional DDB2 expression and it is completely absent in other eukaryotes. Therefore, conclusions reached through sequence homology analysis are limited. If more distantly related life forms do not express or contain homologues of DDB2, we might not expect the sequences of potential functional elements to be conserved throughout evolution. On the other hand, it is possible that new functions for elements within the DDB2 3'UTR could have evolved and been conserved since the divergence of these life forms.

The average mutation rate for a given neutral DNA sequence has been estimated at 0.5% per site per million years [297]. If the evolutionary divergence between humans and rodents occurred 80 million years ago (as is currently accepted), then according to the Jukes-Cantor equation [298], genetic sequences between these species that are under no

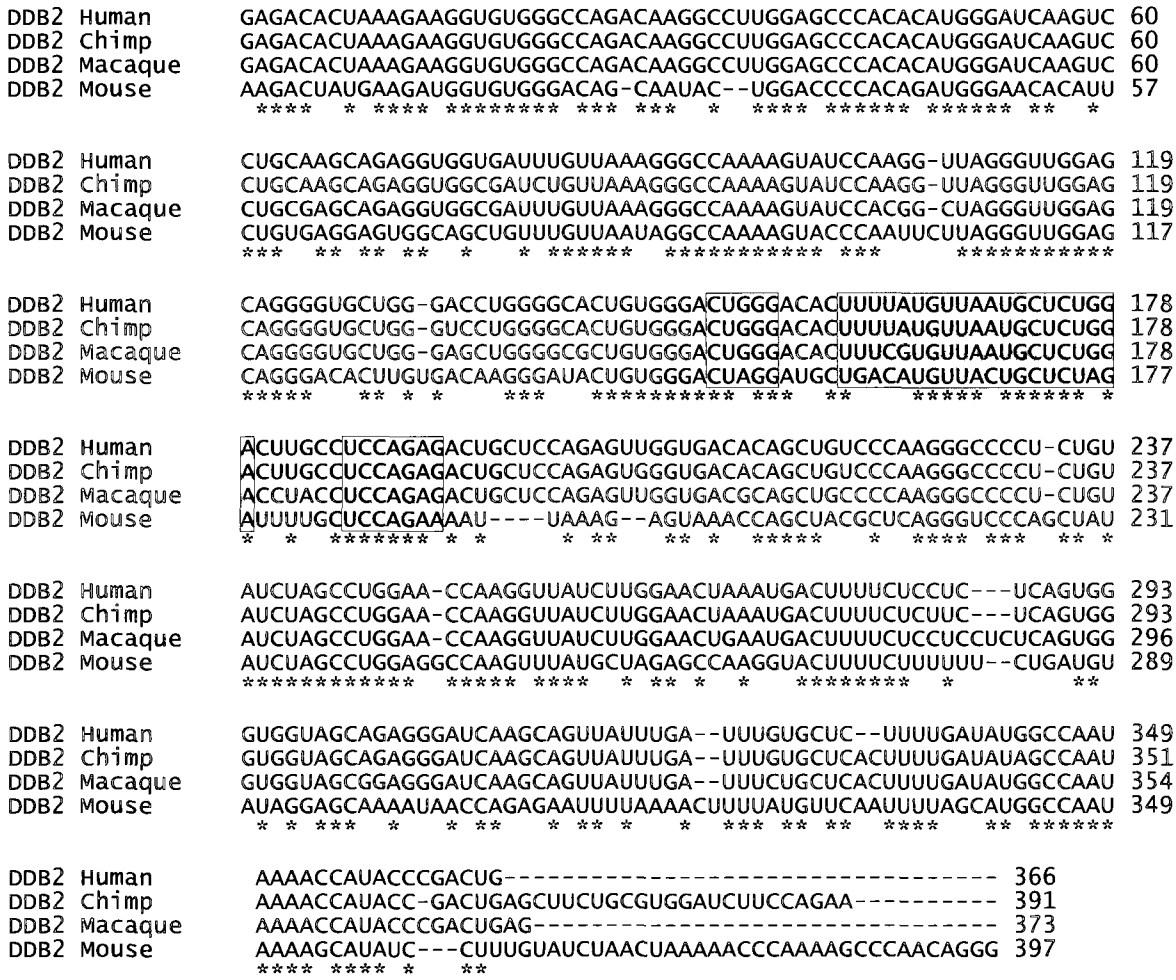

Figure 34. Mammalian sequence conservation of the DDB2 3'UTR. Sequences aligned using ClustalW alignment software. Yellow, location of the C-3 fragment; purple, CUG motif; green, SS region; blue, inverted repeats that form hairpin loop. * Indicates identical nucleotide among all 4 species

selective pressures should be 51% identical today [292]. Given this argument and the 65% sequence homology present between the mouse and human DDB2 3'UTR, perhaps there is moderate conservation among elements within the DDB2 3'UTR across mammalian species.

5.8 Yet another level of DDB2 regulation?

Through our analysis of the human DDB2 gene locus, we noticed that the ACP2 (acid phosphatase 2, lysosomal) gene is encoded on the opposite strand of human chromosome 11 such that the 2 genes' 3'UTRs completely overlap in opposite directions (see Figure S-3A in supplemental data for diagram). This chromosomal arrangement has been conserved in the genomes of chimpanzees, dogs, cows, mice and chickens, while homologs of the ACP2 gene are also present in zebrafish, fruit flies, mosquitoes, and *C.elegans*. This discovery led us to speculate on the possibility that these inverted overlapping 3'UTRs might function as natural antisense transcripts that regulate the expression of either or both genes. The 3'UTR of ACP2, is substantially longer than the average human 3'UTR [294] which may allow for extensive post-transcriptional regulation. There is precedence in the literature for such antisense regulation occurring in the human genome [299, 300]. One study has even suggested that over 20% of human transcripts might form antisense pairs [301]. To confirm that the antisense portion of the ACP2 3'UTR is in fact expressed, we designed three sets of primers that could not amplify a DDB2-derived transcript fragment, but would amplify various regions of the ACP2 3'UTR. The primers we designed: 1) amplified a region of the ACP2 3'UTR that overlapped completely within a DDB2 intron (green arrow pairs , Figure S-3A); 2) spanned a region from a DDB2

intron to the DDB2 3'UTR (blue arrow pairs, Figure S-3A); or 3) amplified a region from the non-overlapping portion of the ACP2 3'UTR to a DDB2 intron (far left and right red arrow pairs, Figure S-3A). All of these primer sets produced products (data not shown), indicating that the antisense transcript is expressed in human cells.

By RT-PCR, we found that when the DDB2 3'UTR was highly expressed (FL Ins HeLa TO cells), both ACP2 coding and 3'UTR levels were low compared to when reporter transcription was repressed with Dox for 48 hours (Figure S-3B). This indicates that overexpressing the DDB2 3'UTR may decrease expression of ACP2. Endogenous DDB2 is normally expressed at low levels, and the result seen here may be a result of grossly overexpressing its 3'UTR beyond physiological levels. Still, it would be interesting to perform the reciprocal experiment and overexpress ACP2 to see if this decreases DDB2 expression. Shorter Dox time course experiments did not show any decreases in ACP2 coding or 3'UTR expression levels in the FL Ins cell line (Fig S-3C). Taken together, these data suggest that while a DDB2 3'UTR antisense transcript is expressed, any interaction between these untranslated regions may be passive and is not dynamically regulated.

Whether this is a true biological phenomenon or an artifact of our DDB2 3'UTR-overexressing reporter construct remains to be elucidated. If the former is the case, this would add yet another layer of complexity on the already bewildering array of regulatory mechanisms imposed on DDB2 expression.

5.9 Proceed with caution: measuring mRNA decay

Throughout the course of these studies, we used several methods to monitor mRNA stability. The steady-state level of a given mRNA species at a given time is a reflection of

both mRNA synthesis and decay. Both of these variables can change dramatically depending on physiological conditions. Because of this, measuring the decay rate of an mRNA is more meaningful than knowing the absolute amount at a specific point in time [110, 302]. Rates of RNA decay are usually measured using kinetic labelling techniques, transcriptional inhibitors, or transcriptional-pulse experiments that utilize inducible reporter constructs. All these techniques, however, can introduce significant changes or stress responses in cell physiology and affect endogenous mRNA decay kinetics [110, 138, 234]. Because of these limitations, care must be exercised when comparing experimentally determined decay rates from one study to the next.

5.9.1 The use of chemical transcription inhibitors should be re-evaluated

In addition to UV light, our results show that the transcription inhibitor, Act D can stabilize both DDB2 and p21 ^{WAF1} mRNA (Figure 16). Similar mRNA stabilizing effects of transcription inhibitors, Act D or 6-dichloro-1-b-D-ribofuranosyl-benzimidazole (DRB), have been reported previously for a variety of transcripts [233]. There is a growing awareness that such transcription inhibitors can alter cellular physiology, result in severe cytotoxicity, and most importantly for the present study, affect the stability of many mRNAs [234]. For example, it has been reported that transcription inhibitors such as Act D, DRB, H7 and α-amanitin can induce p53 in the absence of DNA damage [74]. Indeed, Act D has even been used as a DNA damaging agent with the intention of inducing a p53 response [274]. The induction of the p53 response and, in turn, p53 target-genes could drastically affect numerous cellular functions. The issue is further compounded by the fact that most studies (including this one) that use such transcription inhibitors normalize their

data to the mRNA of a housekeeping gene such as β-actin. If the experimental variables being studied also affect the stability of this gene, the results may be difficult to interpret.

Therefore, these data suggest that caution should be exercised when using general transcription inhibitors to assess mRNA stability as they appear to induce cellular stress responses. Additionally, it is difficult to use them to definitively measure the half-life of a particular mRNA without taking into effect normalization caveats.

5.9.2 Alternate methods for measuring mRNA decay

Through the use of a temperature-sensitive p53-induction/repression system as well as a transgene-specific transcription inhibition approach, our work sidesteps many of the cytotoxic or secondary physiological effects seen with other methods used to study mRNA turnover rates. However, as with any artificial gene induction/repression system, care must be taken to minimize effects caused by the methodology employed. We have found little evidence that temperature had any effect on transcript stability during our temperature shift experiments described in HT29-tsp53 cells.

Doxycycline is primarily used as an antibacterial agent and is utilized clinically to treat conditions such as acne, Lyme disease and multi-resistant *Staphylococcus aureus* (MRSA) infections [303]. Very little work has been done with regards to its cellular toxicity with respect to its use in Tet-on/off expression systems. One limited study found a correlation between high Dox concentration and reduced colony formation and cell division in human lung fibroblasts and rat adrenal PC-12 cells [304]. However, the concentration used in the present studies was 2-10 times lower than that which caused cytotoxic effects. In addition to the low doses used in our study, we are looking directly at

the effects of stability on the specific gene that the TRE is driving. Therefore there is a small chance that secondary cytotoxic effects altered our results.

5.10 Perspectives and significance

The findings reported here could have wide-ranging applications and significance to many aspects of research surrounding p53, GG-NER, and post-transcriptional regulation.

Because the d2EGFP reporter construct used in these studies contains a destabilized EGFP variant, its protein expression levels can be correlated with its mRNA stability. It is this feature that allowed us to use live cell imaging and flow cytometry to monitor EGFP fluorescence as an alternate means of measuring mRNA stability. While other groups have used flow cytometry to assess mRNA stability [199], to the best of our knowledge, this is the first time that live cell imaging techniques have been used to study the effects mRNA decay has on protein expression in live cells.

Our approach for elucidating post-transcriptional regulation of subsets of p53 target-genes and our finding that many of them are short-lived prior to UV exposure suggests a novel regulatory paradigm that allows cells to orchestrate a rapid induction of stress related proteins. Simultaneously, it would allow cells to keep the anti-proliferative and pro-apoptotic p53-response in check. This system would also keep unrequired protein synthesis to a minimum, thereby streamlining resource allocation. As mentioned above, the temperature induction/repression system employed here in the study of p53 target activation is beneficial over traditional chemical and cytotoxic approaches used to study

p53 stress responses and mRNA stability. Its use herein measuring p53 target-gene mRNA decay represents a novel use for this well-characterized mutant p53 allele.

Our finding that DDB2 is post-transcriptionally modified following UV light may help fill in current gaps of understanding about how DDB2 is regulated and how its regulation may apply to GG-NER. The identification of a stability determinant in the DDB2 3'UTR opens the possibility that RBPs may modulate DDB2 stability following a DNA damaging event. The characterization of these factors and how they are regulated might offer new therapeutic options for the treatment of DNA repair disorders like XP-E that affect the GG-NER repair pathway. Their discovery might also be important in future studies that target cancer through the disruption or modulation of DNA repair.

Chapter 6 References

1. Latonen, L. and M. Laiho, *Cellular UV damage responses--functions of tumor suppressor p53.* Biochim Biophys Acta, 2005. **1755**(2): p. 71-89.
2. Tyrrell, R.M., *Activation of mammalian gene expression by the UV component of sunlight--from models to reality.* Bioessays, 1996. **18**(2): p. 139-48.
3. Clydesdale, G.J., G.W. Dandie, and H.K. Muller, *Ultraviolet light induced injury: immunological and inflammatory effects.* Immunol Cell Biol, 2001. **79**(6): p. 547-68.
4. Bockstahler, L.E., *Induction and enhanced reactivation of mammalian viruses by light.* Prog Nucleic Acid Res Mol Biol, 1981. **26**: p. 303-13.
5. Madan, V., J.T. Lear, and R.M. Szeimies, *Non-melanoma skin cancer.* Lancet. **375**(9715): p. 673-685.
6. Miller, D.L. and M.A. Weinstock, *Nonmelanoma skin cancer in the United States: incidence.* J Am Acad Dermatol, 1994. **30**(5 Pt 1): p. 774-8.
7. de Gruijl, F.R., H.J. van Kranen, and L.H. Mullenders, *UV-induced DNA damage, repair, mutations and oncogenic pathways in skin cancer.* J Photochem Photobiol B, 2001. **63**(1-3): p. 19-27.
8. Vousden, K.H. and X. Lu, *Live or let die: the cell's response to p53.* Nat Rev Cancer, 2002. **2**(8): p. 594-604.
9. Kielbassa, C., L. Roza, and B. Epe, *Wavelength dependence of oxidative DNA damage induced by UV and visible light.* Carcinogenesis, 1997. **18**(4): p. 811-6.
10. Sugasawa, K., *UV-induced ubiquitylation of XPC complex, the UV-DDB-ubiquitin ligase complex, and DNA repair.* J Mol Histol, 2006. **37**(5-7): p. 189-202.
11. Pfeifer, G.P., Y.H. You, and A. Besaratinia, *Mutations induced by ultraviolet light.* Mutat Res, 2005. **571**(1-2): p. 19-31.
12. Matsumura, Y. and H.N. Ananthaswamy, *Toxic effects of ultraviolet radiation on the skin.* Toxicol Appl Pharmacol, 2004. **195**(3): p. 298-308.
13. Bebenek, K., et al., *Proofreading of DNA polymerase eta-dependent replication errors.* J Biol Chem, 2001. **276**(4): p. 2317-20.
14. Leibeling, D., P. Laspe, and S. Emmert, *Nucleotide excision repair and cancer.* J Mol Histol, 2006. **37**(5-7): p. 225-38.
15. Jinlian, L., Z. Yingbin, and W. Chunbo, *p38 MAPK in regulating cellular responses to ultraviolet radiation.* J Biomed Sci, 2007. **14**(3): p. 303-12.
16. Lafarga, V., et al., *p38 Mitogen-activated protein kinase- and HuR-dependent stabilization of p21(Cip1) mRNA mediates the G(1)/S checkpoint.* Mol Cell Biol, 2009. **29**(16): p. 4341-51.
17. Dean, J.L., et al., *The involvement of AU-rich element-binding proteins in p38 mitogen-activated protein kinase pathway-mediated mRNA stabilisation.* Cell Signal, 2004. **16**(10): p. 1113-21.
18. Tchen, C.R., et al., *The stability of tristetraprolin mRNA is regulated by mitogen-activated protein kinase p38 and by tristetraprolin itself.* J Biol Chem, 2004. **279**(31): p. 32393-400.
19. Gentile, M., L. Latonen, and M. Laiho, *Cell cycle arrest and apoptosis provoked by UV radiation-induced DNA damage are transcriptionally highly divergent responses.* Nucleic Acids Res, 2003. **31**(16): p. 4779-90.
20. McKay, B.C., et al., *Regulation of ultraviolet light-induced gene expression by gene size.* Proc Natl Acad Sci U S A, 2004. **101**(17): p. 6582-6.
21. Sauerbier, W. and K. Hercules, *Gene and transcription unit mapping by radiation effects.* Annu Rev Genet, 1978. **12**: p. 329-63.

22. Bollig, F., et al., *Evidence for general stabilization of mRNAs in response to UV light.* Eur J Biochem, 2002. **269**(23): p. 5830-9.
23. Blattner, C., et al., *UV-Induced stabilization of c-fos and other short-lived mRNAs.* Mol Cell Biol, 2000. **20**(10): p. 3616-25.
24. Gowrishankar, G., et al., *Inhibition of mRNA deadenylation and degradation by ultraviolet light.* Biol Chem, 2005. **386**(12): p. 1287-93.
25. Wang, W., et al., *HuR regulates p21 mRNA stabilization by UV light.* Mol Cell Biol, 2000. **20**(3): p. 760-9.
26. Westmark, C.J., V.B. Bartleson, and J.S. Malter, *RhoB mRNA is stabilized by HuR after UV light.* Oncogene, 2005. **24**(3): p. 502-11.
27. Sureban, S.M., et al., *Functional antagonism between RNA binding proteins HuR and CUGBP2 determines the fate of COX-2 mRNA translation.* Gastroenterology, 2007. **132**(3): p. 1055-65.
28. Gorospe, M., *HuR in the mammalian genotoxic response: post-transcriptional multitasking.* Cell Cycle, 2003. **2**(5): p. 412-4.
29. Sancar, A., et al., *Molecular mechanisms of mammalian DNA repair and the DNA damage checkpoints.* Annu Rev Biochem, 2004. **73**: p. 39-85.
30. Sancar, A., *Structure and function of DNA photolyase.* Biochemistry, 1994. **33**(1): p. 2-9.
31. Kawate, H., et al., *Separation of killing and tumorigenic effects of an alkylating agent in mice defective in two of the DNA repair genes.* Proc Natl Acad Sci U S A, 1998. **95**(9): p. 5116-20.
32. Sung, P. and H. Klein, *Mechanism of homologous recombination: mediators and helicases take on regulatory functions.* Nat Rev Mol Cell Biol, 2006. **7**(10): p. 739-50.
33. Moore, J.K. and J.E. Haber, *Cell cycle and genetic requirements of two pathways of nonhomologous end-joining repair of double-strand breaks in Saccharomyces cerevisiae.* Mol Cell Biol, 1996. **16**(5): p. 2164-73.
34. Guirouilh-Barbat, J., et al., *Impact of the KU80 pathway on NHEJ-induced genome rearrangements in mammalian cells.* Mol Cell, 2004. **14**(5): p. 611-23.
35. Kerzendorfer, C. and M. O'Driscoll, *Human DNA damage response and repair deficiency syndromes: linking genomic instability and cell cycle checkpoint proficiency.* DNA Repair (Amst), 2009. **8**(9): p. 1139-52.
36. Liu, Y., et al., *Coordination of steps in single-nucleotide base excision repair mediated by apurinic/apyrimidinic endonuclease 1 and DNA polymerase beta.* J Biol Chem, 2007. **282**(18): p. 13532-41.
37. Boiteux, S. and M. Guillet, *Abasic sites in DNA: repair and biological consequences in Saccharomyces cerevisiae.* DNA Repair (Amst), 2004. **3**(1): p. 1-12.
38. Fortini, P. and E. Dogliotti, *Base damage and single-strand break repair: mechanisms and functional significance of short- and long-patch repair subpathways.* DNA Repair (Amst), 2007. **6**(4): p. 398-409.
39. Iyer, R.R., et al., *DNA mismatch repair: functions and mechanisms.* Chem Rev, 2006. **106**(2): p. 302-23.
40. Li, G.M., *Mechanisms and functions of DNA mismatch repair.* Cell Res, 2008. **18**(1): p. 85-98.
41. Nouspikel, T., *DNA repair in mammalian cells : Nucleotide excision repair: variations on versatility.* Cell Mol Life Sci, 2009. **66**(6): p. 994-1009.
42. Araki, M., et al., *Centrosome protein centrin 2/caltractin 1 is part of the xeroderma pigmentosum group C complex that initiates global genome nucleotide excision repair.* J Biol Chem, 2001. **276**(22): p. 18665-72.
43. Dualan, R., et al., *Chromosomal localization and cDNA cloning of the genes (DDB1 and DDB2) for the p127 and p48 subunits of a human damage-specific DNA binding protein.* Genomics, 1995. **29**(1): p. 62-9.

44. Payne, A. and G. Chu, *Xeroderma pigmentosum group E binding factor recognizes a broad spectrum of DNA damage.* Mutat Res, 1994. **310**(1): p. 89-102.
45. Batty, D., et al., *Stable binding of human XPC complex to irradiated DNA confers strong discrimination for damaged sites.* J Mol Biol, 2000. **300**(2): p. 275-90.
46. Ford, J.M., *Regulation of DNA damage recognition and nucleotide excision repair: another role for p53.* Mutat Res, 2005. **577**(1-2): p. 195-202.
47. Rapic-Otrin, V., et al., *Sequential binding of UV DNA damage binding factor and degradation of the p48 subunit as early events after UV irradiation.* Nucleic Acids Res, 2002. **30**(11): p. 2588-98.
48. Sugasawa, K., et al., *UV-induced ubiquitylation of XPC protein mediated by UV-DDB-ubiquitin ligase complex.* Cell, 2005. **121**(3): p. 387-400.
49. El-Mahdy, M.A., et al., *Cullin 4A-mediated proteolysis of DDB2 protein at DNA damage sites regulates in vivo lesion recognition by XPC.* J Biol Chem, 2006. **281**(19): p. 13404-11.
50. Fitch, M.E., et al., *In vivo recruitment of XPC to UV-induced cyclobutane pyrimidine dimers by the DDB2 gene product.* J Biol Chem, 2003. **278**(47): p. 46906-10.
51. Cooper, P.K., et al., *Defective transcription-coupled repair of oxidative base damage in Cockayne syndrome patients from XP group G.* Science, 1997. **275**(5302): p. 990-3.
52. Henning, K.A., et al., *The Cockayne syndrome group A gene encodes a WD repeat protein that interacts with CSB protein and a subunit of RNA polymerase II TFIIH.* Cell, 1995. **82**(4): p. 555-64.
53. Sugasawa, K., *Xeroderma pigmentosum genes: functions inside and outside DNA repair.* Carcinogenesis, 2008. **29**(3): p. 455-65.
54. Masutani, C., et al., *Xeroderma pigmentosum variant (XP-V) correcting protein from HeLa cells has a thymine dimer bypass DNA polymerase activity.* EMBO J, 1999. **18**(12): p. 3491-501.
55. Hanawalt, P.C. and G. Spivak, *Transcription-coupled DNA repair: two decades of progress and surprises.* Nat Rev Mol Cell Biol, 2008. **9**(12): p. 958-70.
56. Kraemer, K.H., M.M. Lee, and J. Scotto, *Xeroderma pigmentosum. Cutaneous, ocular, and neurologic abnormalities in 830 published cases.* Arch Dermatol, 1987. **123**(2): p. 241-50.
57. Kraemer, K.H., *Nucleotide excision repair genes involved in xeroderma pigmentosum.* Jpn J Cancer Res, 1994. **85**(2): p. inside front cover.
58. Tang, J. and G. Chu, *Xeroderma pigmentosum complementation group E and UV-damaged DNA-binding protein.* DNA Repair (Amst), 2002. **1**(8): p. 601-16.
59. de Boer, J. and J.H. Hoeijmakers, *Nucleotide excision repair and human syndromes.* Carcinogenesis, 2000. **21**(3): p. 453-60.
60. Bradsher, J., et al., *CSB is a component of RNA pol I transcription.* Mol Cell, 2002. **10**(4): p. 819-29.
61. Itin, P.H., A. Sarasin, and M.R. Pittelkow, *Trichothiodystrophy: update on the sulfur-deficient brittle hair syndromes.* J Am Acad Dermatol, 2001. **44**(6): p. 891-920; quiz 921-4.
62. Ljungman, M., *Dial 9-1-1 for p53: mechanisms of p53 activation by cellular stress.* Neoplasia, 2000. **2**(3): p. 208-25.
63. Vogelstein, B., D. Lane, and A.J. Levine, *Surfing the p53 network.* Nature, 2000. **408**(6810): p. 307-10.
64. DeLeo, A.B., et al., *Detection of a transformation-related antigen in chemically induced sarcomas and other transformed cells of the mouse.* Proc Natl Acad Sci U S A, 1979. **76**(5): p. 2420-4.
65. Chompret, A., *The Li-Fraumeni syndrome.* Biochimie, 2002. **84**(1): p. 75-82.
66. Xu, Y., *Regulation of p53 responses by post-translational modifications.* Cell Death Differ, 2003. **10**(4): p. 400-3.

67. Zhao, R., et al., *Analysis of p53-regulated gene expression patterns using oligonucleotide arrays.* Genes Dev, 2000. **14**(8): p. 981-93.
68. Wang, L., et al., *Analyses of p53 target genes in the human genome by bioinformatic and microarray approaches.* J Biol Chem, 2001. **276**(47): p. 43604-10.
69. Hoh, J., et al., *The p53MH algorithm and its application in detecting p53-responsive genes.* Proc Natl Acad Sci U S A, 2002. **99**(13): p. 8467-72.
70. Lahav, G., et al., *Dynamics of the p53-Mdm2 feedback loop in individual cells.* Nat Genet, 2004. **36**(2): p. 147-50.
71. Jones, S.N., et al., *Rescue of embryonic lethality in Mdm2-deficient mice by absence of p53.* Nature, 1995. **378**(6553): p. 206-8.
72. Montes de Oca Luna, R., D.S. Wagner, and G. Lozano, *Rescue of early embryonic lethality in mdm2-deficient mice by deletion of p53.* Nature, 1995. **378**(6553): p. 203-6.
73. Yamaizumi, M. and T. Sugano, *U.v.-induced nuclear accumulation of p53 is evoked through DNA damage of actively transcribed genes independent of the cell cycle.* Oncogene, 1994. **9**(10): p. 2775-84.
74. Ljungman, M., et al., *Inhibition of RNA polymerase II as a trigger for the p53 response.* Oncogene, 1999. **18**(3): p. 583-92.
75. Sun, X., H. Shimizu, and K. Yamamoto, *Identification of a novel p53 promoter element involved in genotoxic stress-inducible p53 gene expression.* Mol Cell Biol, 1995. **15**(8): p. 4489-96.
76. Mazan-Mamczarz, K., et al., *RNA-binding protein HuR enhances p53 translation in response to ultraviolet light irradiation.* Proc Natl Acad Sci U S A, 2003. **100**(14): p. 8354-9.
77. Li, Y., et al., *Cell cycle expression and p53 regulation of the cyclin-dependent kinase inhibitor p21.* Oncogene, 1994. **9**(8): p. 2261-8.
78. Waga, S., et al., *The p21 inhibitor of cyclin-dependent kinases controls DNA replication by interaction with PCNA.* Nature, 1994. **369**(6481): p. 574-8.
79. Rouault, J.P., et al., *Identification of BTG2, an antiproliferative p53-dependent component of the DNA damage cellular response pathway.* Nat Genet, 1996. **14**(4): p. 482-6.
80. Stubbert, L.J., et al., *The anti-apoptotic role for p53 following exposure to ultraviolet light does not involve DDB2.* Mutat Res, 2009. **663**(1-2): p. 69-76.
81. Benchimol, S., *p53-dependent pathways of apoptosis.* Cell Death Differ, 2001. **8**(11): p. 1049-51.
82. Villunger, A., et al., *p53- and drug-induced apoptotic responses mediated by BH3-only proteins puma and noxa.* Science, 2003. **302**(5647): p. 1036-8.
83. Shibue, T., et al., *Integral role of Noxa in p53-mediated apoptotic response.* Genes Dev, 2003. **17**(18): p. 2233-8.
84. Hoffman, W.H., et al., *Transcriptional repression of the anti-apoptotic survivin gene by wild type p53.* J Biol Chem, 2002. **277**(5): p. 3247-57.
85. Ding, H.F., et al., *Essential role for caspase-8 in transcription-independent apoptosis triggered by p53.* J Biol Chem, 2000. **275**(49): p. 38905-11.
86. Chipuk, J.E., et al., *Direct activation of Bax by p53 mediates mitochondrial membrane permeabilization and apoptosis.* Science, 2004. **303**(5660): p. 1010-4.
87. Adimoolam, S. and J.M. Ford, *p53 and regulation of DNA damage recognition during nucleotide excision repair.* DNA Repair (Amst), 2003. **2**(9): p. 947-54.
88. Ford, J.M., E.L. Baron, and P.C. Hanawalt, *Human fibroblasts expressing the human papillomavirus E6 gene are deficient in global genomic nucleotide excision repair and sensitive to ultraviolet irradiation.* Cancer Res, 1998. **58**(4): p. 599-603.
89. Ford, J.M. and P.C. Hanawalt, *Li-Fraumeni syndrome fibroblasts homozygous for p53 mutations are deficient in global DNA repair but exhibit normal transcription-coupled repair and enhanced UV resistance.* Proc Natl Acad Sci U S A, 1995. **92**(19): p. 8876-80.

90. Tan, T. and G. Chu, *p53 Binds and activates the xeroderma pigmentosum DDB2 gene in humans but not mice.* Mol Cell Biol, 2002. **22**(10): p. 3247-54.
91. Hwang, B.J., et al., *Expression of the p48 xeroderma pigmentosum gene is p53-dependent and is involved in global genomic repair.* Proc Natl Acad Sci U S A, 1999. **96**(2): p. 424-8.
92. Fitch, M.E., et al., *The DDB2 nucleotide excision repair gene product p48 enhances global genomic repair in p53 deficient human fibroblasts.* DNA Repair (Amst), 2003. **2**(7): p. 819-26.
93. Adimoolam, S. and J.M. Ford, *p53 and DNA damage-inducible expression of the xeroderma pigmentosum group C gene.* Proc Natl Acad Sci U S A, 2002. **99**(20): p. 12985-90.
94. Smith, M.L., et al., *Interaction of the p53-regulated protein Gadd45 with proliferating cell nuclear antigen.* Science, 1994. **266**(5189): p. 1376-80.
95. Mathonnet, G., et al., *UV wavelength-dependent regulation of transcription-coupled nucleotide excision repair in p53-deficient human cells.* Proc Natl Acad Sci U S A, 2003. **100**(12): p. 7219-24.
96. Therrien, J.P., et al., *Human cells compromised for p53 function exhibit defective global and transcription-coupled nucleotide excision repair, whereas cells compromised for pRb function are defective only in global repair.* Proc Natl Acad Sci U S A, 1999. **96**(26): p. 15038-43.
97. Latonen, L., Y. Taya, and M. Laiho, *UV-radiation induces dose-dependent regulation of p53 response and modulates p53-HDM2 interaction in human fibroblasts.* Oncogene, 2001. **20**(46): p. 6784-93.
98. Jayaraman, J. and C. Prives, *Activation of p53 sequence-specific DNA binding by short single strands of DNA requires the p53 C-terminus.* Cell, 1995. **81**(7): p. 1021-9.
99. Bakalkin, G., et al., *p53 binds single-stranded DNA ends through the C-terminal domain and internal DNA segments via the middle domain.* Nucleic Acids Res, 1995. **23**(3): p. 362-9.
100. Wang, X.W., et al., *p53 modulation of TFIIH-associated nucleotide excision repair activity.* Nat Genet, 1995. **10**(2): p. 188-95.
101. Rubbi, C.P. and J. Milner, *p53 is a chromatin accessibility factor for nucleotide excision repair of DNA damage.* EMBO J, 2003. **22**(4): p. 975-86.
102. Chen, X., et al., *p53 levels, functional domains, and DNA damage determine the extent of the apoptotic response of tumor cells.* Genes Dev, 1996. **10**(19): p. 2438-51.
103. Reinke, V. and G. Lozano, *Differential activation of p53 targets in cells treated with ultraviolet radiation that undergo both apoptosis and growth arrest.* Radiat Res, 1997. **148**(2): p. 115-22.
104. McKay, B.C., M. Ljungman, and A.J. Rainbow, *Persistent DNA damage induced by ultraviolet light inhibits p21waf1 and bax expression: implications for DNA repair, UV sensitivity and the induction of apoptosis.* Oncogene, 1998. **17**(5): p. 545-55.
105. Queille, S., et al., *Effects of XPD mutations on ultraviolet-induced apoptosis in relation to skin cancer-proneness in repair-deficient syndromes.* J Invest Dermatol, 2001. **117**(5): p. 1162-70.
106. Conforti, G., et al., *Proneness to UV-induced apoptosis in human fibroblasts defective in transcription coupled repair is associated with the lack of Mdm2 transactivation.* Oncogene, 2000. **19**(22): p. 2714-20.
107. Brennan, C.M. and J.A. Steitz, *HuR and mRNA stability.* Cell Mol Life Sci, 2001. **58**(2): p. 266-77.
108. Gygi, S.P., et al., *Correlation between protein and mRNA abundance in yeast.* Mol Cell Biol, 1999. **19**(3): p. 1720-30.
109. Ideker, T., et al., *Integrated genomic and proteomic analyses of a systematically perturbed metabolic network.* Science, 2001. **292**(5518): p. 929-34.

110. Ross, J., *mRNA stability in mammalian cells.* Microbiol Rev, 1995. **59**(3): p. 423-50.
111. Lopez de Silanes, I., M.P. Quesada, and M. Esteller, *Aberrant regulation of messenger RNA 3'-untranslated region in human cancer.* Cell Oncol, 2007. **29**(1): p. 1-17.
112. Audic, Y. and R.S. Hartley, *Post-transcriptional regulation in cancer.* Biol Cell, 2004. **96**(7): p. 479-98.
113. Yang, E., et al., *Decay rates of human mRNAs: correlation with functional characteristics and sequence attributes.* Genome Res, 2003. **13**(8): p. 1863-72.
114. Lam, L.T., et al., *Genomic-scale measurement of mRNA turnover and the mechanisms of action of the anti-cancer drug flavopiridol.* Genome Biol, 2001. **2**(10): p. RESEARCH0041.
115. Sharova, L.V., et al., *Database for mRNA half-life of 19 977 genes obtained by DNA microarray analysis of pluripotent and differentiating mouse embryonic stem cells.* DNA Res, 2009. **16**(1): p. 45-58.
116. Raghavan, A. and P.R. Bohjanen, *Microarray-based analyses of mRNA decay in the regulation of mammalian gene expression.* Brief Funct Genomic Proteomic, 2004. **3**(2): p. 112-24.
117. Keene, J.D. and P.J. Lager, *Post-transcriptional operons and regulons co-ordinating gene expression.* Chromosome Res, 2005. **13**(3): p. 327-37.
118. Epstein, J.H., K. Fukuyama, and K. Fye, *Effects of ultraviolet radiation on the mitotic cycle and DNA, RNA and protein synthesis in mammalian epidermis in vivo.* Photochem Photobiol, 1970. **12**(1): p. 57-65.
119. Tornaletti, S. and P.C. Hanawalt, *Effect of DNA lesions on transcription elongation.* Biochimie, 1999. **81**(1-2): p. 139-46.
120. Fan, J., et al., *Global analysis of stress-regulated mRNA turnover by using cDNA arrays.* Proc Natl Acad Sci U S A, 2002. **99**(16): p. 10611-6.
121. Raghavan, A., et al., *Genome-wide analysis of mRNA decay in resting and activated primary human T lymphocytes.* Nucleic Acids Res, 2002. **30**(24): p. 5529-38.
122. Melamed, D. and Y. Arava, *Genome-wide analysis of mRNA polysomal profiles with spotted DNA microarrays.* Methods Enzymol, 2007. **431**: p. 177-201.
123. Ohtsu, M., et al., *Novel DNA microarray system for analysis of nascent mRNAs.* DNA Res, 2008. **15**(4): p. 241-51.
124. Mata, J., S. Marguerat, and J. Bahler, *Post-transcriptional control of gene expression: a genome-wide perspective.* Trends Biochem Sci, 2005. **30**(9): p. 506-14.
125. Lu, X., N.A. Timchenko, and L.T. Timchenko, *Cardiac elav-type RNA-binding protein (ETR-3) binds to RNA CUG repeats expanded in myotonic dystrophy.* Hum Mol Genet, 1999. **8**(1): p. 53-60.
126. Kontoyiannis, D., et al., *Impaired on/off regulation of TNF biosynthesis in mice lacking TNF AU-rich elements: implications for joint and gut-associated immunopathologies.* Immunity, 1999. **10**(3): p. 387-98.
127. Hollams, E.M., et al., *MRNA stability and the control of gene expression: implications for human disease.* Neurochem Res, 2002. **27**(10): p. 957-80.
128. Frischmeyer, P.A. and H.C. Dietz, *Nonsense-mediated mRNA decay in health and disease.* Hum Mol Genet, 1999. **8**(10): p. 1893-900.
129. Gingerich, T.J., J.J. Feige, and J. LaMarre, *AU-rich elements and the control of gene expression through regulated mRNA stability.* Anim Health Res Rev, 2004. **5**(1): p. 49-63.
130. Klausner, R.D., T.A. Rouault, and J.B. Harford, *Regulating the fate of mRNA: the control of cellular iron metabolism.* Cell, 1993. **72**(1): p. 19-28.
131. Pandey, N.B. and W.F. Marzluff, *The stem-loop structure at the 3' end of histone mRNA is necessary and sufficient for regulation of histone mRNA stability.* Mol Cell Biol, 1987. **7**(12): p. 4557-9.

132. Chen, C.Y., et al., *Stabilization of interleukin-2 mRNA by the c-Jun NH2-terminal kinase pathway.* Science, 1998. **280**(5371): p. 1945-9.
133. Shyu, A.B., M.E. Greenberg, and J.G. Belasco, *The c-fos transcript is targeted for rapid decay by two distinct mRNA degradation pathways.* Genes Dev, 1989. **3**(1): p. 60-72.
134. Conne, B., A. Stutz, and J.D. Vassalli, *The 3' untranslated region of messenger RNA: A molecular 'hotspot' for pathology?* Nat Med, 2000. **6**(6): p. 637-41.
135. Shaw, G. and R. Kamen, *A conserved AU sequence from the 3' untranslated region of GM-CSF mRNA mediates selective mRNA degradation.* Cell, 1986. **46**(5): p. 659-67.
136. Xu, N., C.Y. Chen, and A.B. Shyu, *Modulation of the fate of cytoplasmic mRNA by AU-rich elements: key sequence features controlling mRNA deadenylation and decay.* Mol Cell Biol, 1997. **17**(8): p. 4611-21.
137. Akashi, M., et al., *Number and location of AUUUA motifs: role in regulating transiently expressed RNAs.* Blood, 1994. **83**(11): p. 3182-7.
138. Chen, C.Y. and A.B. Shyu, *AU-rich elements: characterization and importance in mRNA degradation.* Trends Biochem Sci, 1995. **20**(11): p. 465-70.
139. Lopez de Silanes, I., et al., *Identification of a target RNA motif for RNA-binding protein HuR.* Proc Natl Acad Sci U S A, 2004. **101**(9): p. 2987-92.
140. Bakheet, T., B.R. Williams, and K.S. Khabar, *ARED 3.0: the large and diverse AU-rich transcriptome.* Nucleic Acids Res, 2006. **34**(Database issue): p. D111-4.
141. Wilusz, C.J., M. Wormington, and S.W. Peltz, *The cap-to-tail guide to mRNA turnover.* Nat Rev Mol Cell Biol, 2001. **2**(4): p. 237-46.
142. Fan, X.C., V.E. Myer, and J.A. Steitz, *AU-rich elements target small nuclear RNAs as well as mRNAs for rapid degradation.* Genes Dev, 1997. **11**(19): p. 2557-68.
143. Peng, S.S., et al., *RNA stabilization by the AU-rich element binding protein, HuR, an ELAV protein.* EMBO J, 1998. **17**(12): p. 3461-70.
144. Blaxall, B.C., et al., *Differential expression and localization of the mRNA binding proteins, AU-rich element mRNA binding protein (AUF1) and Hu antigen R (HuR), in neoplastic lung tissue.* Mol Carcinog, 2000. **28**(2): p. 76-83.
145. Chen, C.Y., et al., *AU binding proteins recruit the exosome to degrade ARE-containing mRNAs.* Cell, 2001. **107**(4): p. 451-64.
146. Chen, C.Y., N. Xu, and A.B. Shyu, *Highly selective actions of HuR in antagonizing AU-rich element-mediated mRNA destabilization.* Mol Cell Biol, 2002. **22**(20): p. 7268-78.
147. Stoecklin, G., et al., *A novel mechanism of tumor suppression by destabilizing AU-rich growth factor mRNA.* Oncogene, 2003. **22**(23): p. 3554-61.
148. Winzen, R., et al., *Distinct domains of AU-rich elements exert different functions in mRNA destabilization and stabilization by p38 mitogen-activated protein kinase or HuR.* Mol Cell Biol, 2004. **24**(11): p. 4835-47.
149. Fialcowitz, E.J., et al., *A hairpin-like structure within an AU-rich mRNA-destabilizing element regulates trans-factor binding selectivity and mRNA decay kinetics.* J Biol Chem, 2005. **280**(23): p. 22406-17.
150. Barreau, C., L. Paillard, and H.B. Osborne, *AU-rich elements and associated factors: are there unifying principles?* Nucleic Acids Res, 2005. **33**(22): p. 7138-50.
151. Barreau, C., et al., *Protein expression is increased by a class III AU-rich element and tethered CUG-BP1.* Biochem Biophys Res Commun, 2006. **347**(3): p. 723-30.
152. Fialcowitz-White, E.J., et al., *Specific protein domains mediate cooperative assembly of HuR oligomers on AU-rich mRNA-destabilizing sequences.* J Biol Chem, 2007. **282**(29): p. 20948-59.
153. Shyu, A.B., M.F. Wilkinson, and A. van Hoof, *Messenger RNA regulation: to translate or to degrade.* EMBO J, 2008. **27**(3): p. 471-81.
154. Valencia-Sanchez, M.A., et al., *Control of translation and mRNA degradation by miRNAs and siRNAs.* Genes Dev, 2006. **20**(5): p. 515-24.

155. Bartel, D.P. and C.Z. Chen, *Micromanagers of gene expression: the potentially widespread influence of metazoan microRNAs.* Nat Rev Genet, 2004. **5**(5): p. 396-400.
156. Lim, L.P., et al., *Microarray analysis shows that some microRNAs downregulate large numbers of target mRNAs.* Nature, 2005. **433**(7027): p. 769-73.
157. Rajewsky, N., *microRNA target predictions in animals.* Nat Genet, 2006. **38 Suppl**: p. S8-13.
158. Zhao, C. and T. Hamilton, *Introns regulate the rate of unstable mRNA decay.* J Biol Chem, 2007. **282**(28): p. 20230-7.
159. Beaudoing, E. and D. Gautheret, *Identification of alternate polyadenylation sites and analysis of their tissue distribution using EST data.* Genome Res, 2001. **11**(9): p. 1520-6.
160. Lopez, F., et al., *The disparate nature of "intergenic" polyadenylation sites.* RNA, 2006. **12**(10): p. 1794-801.
161. Rouault, T. and R. Klausner, *Regulation of iron metabolism in eukaryotes.* Curr Top Cell Regul, 1997. **35**: p. 1-19.
162. Marzluff, W.F., E.J. Wagner, and R.J. Duronio, *Metabolism and regulation of canonical histone mRNAs: life without a poly(A) tail.* Nat Rev Genet, 2008. **9**(11): p. 843-54.
163. Lal, A., et al., *Concurrent versus individual binding of HuR and AUF1 to common labile target mRNAs.* EMBO J, 2004. **23**(15): p. 3092-102.
164. Manley, G.T., et al., *Hu antigens: reactivity with Hu antibodies, tumor expression, and major immunogenic sites.* Ann Neurol, 1995. **38**(1): p. 102-10.
165. Dalmau, J., et al., *Detection of the anti-Hu antibody in specific regions of the nervous system and tumor from patients with paraneoplastic encephalomyelitis/sensory neuronopathy.* Neurology, 1991. **41**(11): p. 1757-64.
166. Fan, X.C. and J.A. Steitz, *Overexpression of HuR, a nuclear-cytoplasmic shuttling protein, increases the in vivo stability of ARE-containing mRNAs.* EMBO J, 1998. **17**(12): p. 3448-60.
167. Lopez de Silanes, I., et al., *Role of the RNA-binding protein HuR in colon carcinogenesis.* Oncogene, 2003. **22**(46): p. 7146-54.
168. Lopez de Silanes, I., A. Lal, and M. Gorospe, *HuR: post-transcriptional paths to malignancy.* RNA Biol, 2005. **2**(1): p. 11-3.
169. Mazan-Mamczarz, K., et al., *Post-transcriptional gene regulation by HuR promotes a more tumorigenic phenotype.* Oncogene, 2008. **27**(47): p. 6151-63.
170. Marquis, J., et al., *CUG-BP1/CELF1 requires UGU-rich sequences for high-affinity binding.* Biochem J, 2006. **400**(2): p. 291-301.
171. Moraes, K.C., C.J. Wilusz, and J. Wilusz, *CUG-BP binds to RNA substrates and recruits PARN deadenylase.* RNA, 2006. **12**(6): p. 1084-91.
172. Putland, R.A., et al., *RNA destabilization by the granulocyte colony-stimulating factor stem-loop destabilizing element involves a single stem-loop that promotes deadenylation.* Mol Cell Biol, 2002. **22**(6): p. 1664-73.
173. Houseley, J. and D. Tollervey, *The many pathways of RNA degradation.* Cell, 2009. **136**(4): p. 763-76.
174. Wilusz, C.J. and J. Wilusz, *Bringing the role of mRNA decay in the control of gene expression into focus.* Trends Genet, 2004. **20**(10): p. 491-7.
175. Mukherjee, D., et al., *The mammalian exosome mediates the efficient degradation of mRNAs that contain AU-rich elements.* EMBO J, 2002. **21**(1-2): p. 165-74.
176. Stoecklin, G., T. Mayo, and P. Anderson, *ARE-mRNA degradation requires the 5'-3' decay pathway.* EMBO Rep, 2006. **7**(1): p. 72-7.
177. Murray, E.L. and D.R. Schoenberg, *A+U-rich instability elements differentially activate 5'-3' and 3'-5' mRNA decay.* Mol Cell Biol, 2007. **27**(8): p. 2791-9.
178. Mitchell, P. and D. Tollervey, *Musing on the structural organization of the exosome complex.* Nat Struct Biol, 2000. **7**(10): p. 843-6.

179. Lai, W.S., E.A. Kennington, and P.J. Blackshear, *Tristetraprolin and its family members can promote the cell-free deadenylation of AU-rich element-containing mRNAs by poly(A) ribonuclease.* Mol Cell Biol, 2003. **23**(11): p. 3798-812.
180. Gao, M., et al., *A novel mRNA-decapping activity in HeLa cytoplasmic extracts is regulated by AU-rich elements.* EMBO J, 2001. **20**(5): p. 1134-43.
181. Moore, M.J. and N.J. Proudfoot, *Pre-mRNA processing reaches back to transcription and ahead to translation.* Cell, 2009. **136**(4): p. 688-700.
182. Holbrook, J.A., et al., *Nonsense-mediated decay approaches the clinic.* Nat Genet, 2004. **36**(8): p. 801-8.
183. Gonzalez, C.I., et al., *The yeast hnRNP-like protein Hrp1/Nab4 marks a transcript for nonsense-mediated mRNA decay.* Mol Cell, 2000. **5**(3): p. 489-99.
184. Le Hir, H., M.J. Moore, and L.E. Maquat, *Pre-mRNA splicing alters mRNP composition: evidence for stable association of proteins at exon-exon junctions.* Genes Dev, 2000. **14**(9): p. 1098-108.
185. Nagy, E. and L.E. Maquat, *A rule for termination-codon position within intron-containing genes: when nonsense affects RNA abundance.* Trends Biochem Sci, 1998. **23**(6): p. 198-9.
186. Buhler, M., et al., *EJC-independent degradation of nonsense immunoglobulin-mu mRNA depends on 3' UTR length.* Nat Struct Mol Biol, 2006. **13**(5): p. 462-4.
187. Stalder, L. and O. Muhlemann, *The meaning of nonsense.* Trends Cell Biol, 2008. **18**(7): p. 315-21.
188. Anderson, P. and N. Kedersha, *RNA granules.* J Cell Biol, 2006. **172**(6): p. 803-8.
189. Kedersha, N. and P. Anderson, *Stress granules: sites of mRNA triage that regulate mRNA stability and translatability.* Biochem Soc Trans, 2002. **30**(Pt 6): p. 963-9.
190. Jakymiw, A., et al., *Disruption of GW bodies impairs mammalian RNA interference.* Nat Cell Biol, 2005. **7**(12): p. 1267-74.
191. Coller, J. and R. Parker, *General translational repression by activators of mRNA decapping.* Cell, 2005. **122**(6): p. 875-86.
192. Kedersha, N., et al., *Stress granules and processing bodies are dynamically linked sites of mRNP remodeling.* J Cell Biol, 2005. **169**(6): p. 871-84.
193. Guhaniyogi, J. and G. Brewer, *Regulation of mRNA stability in mammalian cells.* Gene, 2001. **265**(1-2): p. 11-23.
194. Levy, A.P., *Hypoxic regulation of VEGF mRNA stability by RNA-binding proteins.* Trends Cardiovasc Med, 1998. **8**(6): p. 246-50.
195. Xiao, L., et al., *Polyamines regulate the stability of activating transcription factor-2 mRNA through RNA-binding protein HuR in intestinal epithelial cells.* Mol Biol Cell, 2007. **18**(11): p. 4579-90.
196. Abdelmohsen, K., et al., *Ubiquitin-mediated proteolysis of HuR by heat shock.* EMBO J, 2009. **28**(9): p. 1271-82.
197. Seko, Y., et al., *The role of cytokine mRNA stability in the pathogenesis of autoimmune disease.* Autoimmun Rev, 2006. **5**(5): p. 299-305.
198. Yaman, I., et al., *Nutritional control of mRNA stability is mediated by a conserved AU-rich element that binds the cytoplasmic shuttling protein HuR.* J Biol Chem, 2002. **277**(44): p. 41539-46.
199. Raineri, I., et al., *Roles of AUF1 isoforms, HuR and BRF1 in ARE-dependent mRNA turnover studied by RNA interference.* Nucleic Acids Res, 2004. **32**(4): p. 1279-88.
200. Young, L.E., et al., *The mRNA Binding Proteins HuR and Tristetraprolin Regulate Cyclooxygenase 2 Expression During Colon Carcinogenesis.* Gastroenterology, 2009.
201. Pan, Y.X., H. Chen, and M.S. Kilberg, *Interaction of RNA-binding proteins HuR and AUF1 with the human ATF3 mRNA 3'-untranslated region regulates its amino acid limitation-induced stabilization.* J Biol Chem, 2005. **280**(41): p. 34609-16.

202. Sommer, S., et al., *The c-Yes 3'-UTR contains adenine/uridine-rich elements that bind AUF1 and HuR involved in mRNA decay in breast cancer cells.* J Steroid Biochem Mol Biol, 2005. **97**(3): p. 219-29.
203. Palanisamy, V., et al., *AUF1 and HuR proteins stabilize interleukin-8 mRNA in human saliva.* J Dent Res, 2008. **87**(8): p. 772-6.
204. David, P.S., R. Tanveer, and J.D. Port, *FRET-detectable interactions between the ARE binding proteins, HuR and p37AUF1.* RNA, 2007. **13**(9): p. 1453-68.
205. Brooks, S.A., J.E. Connolly, and W.F. Rigby, *The role of mRNA turnover in the regulation of tristetraprolin expression: evidence for an extracellular signal-regulated kinase-specific, AU-rich element-dependent, autoregulatory pathway.* J Immunol, 2004. **172**(12): p. 7263-71.
206. Pullmann, R., Jr., et al., *Analysis of turnover and translation regulatory RNA-binding protein expression through binding to cognate mRNAs.* Mol Cell Biol, 2007. **27**(18): p. 6265-78.
207. Rodriguez-Gabriel, M.A., et al., *RNA-binding protein Csx1 mediates global control of gene expression in response to oxidative stress.* EMBO J, 2003. **22**(23): p. 6256-66.
208. Keene, J.D. and S.A. Tenenbaum, *Eukaryotic mRNPs may represent posttranscriptional operons.* Mol Cell, 2002. **9**(6): p. 1161-7.
209. Osbourn, A.E. and B. Field, *Operons.* Cell Mol Life Sci, 2009. **66**(23): p. 3755-75.
210. Keene, J.D., *RNA regulons: coordination of post-transcriptional events.* Nat Rev Genet, 2007. **8**(7): p. 533-43.
211. Raghavan, A., et al., *HuA and tristetraprolin are induced following T cell activation and display distinct but overlapping RNA binding specificities.* J Biol Chem, 2001. **276**(51): p. 47958-65.
212. Di Marco, S., et al., *Polymorphism in the 3'-untranslated region of TNFalpha mRNA impairs binding of the post-transcriptional regulatory protein HuR to TNFalpha mRNA.* Nucleic Acids Res, 2001. **29**(4): p. 863-71.
213. Withers, D.A., et al., *Characterization of a candidate bcl-1 gene.* Mol Cell Biol, 1991. **11**(10): p. 4846-53.
214. Rimokh, R., et al., *Rearrangement of CCND1 (BCL1/PRAD1) 3' untranslated region in mantle-cell lymphomas and t(11q13)-associated leukemias.* Blood, 1994. **83**(12): p. 3689-96.
215. Lebwohl, D.E., et al., *A truncated cyclin D1 gene encodes a stable mRNA in a human breast cancer cell line.* Oncogene, 1994. **9**(7): p. 1925-9.
216. Jeon, S. and P.F. Lambert, *Integration of human papillomavirus type 16 DNA into the human genome leads to increased stability of E6 and E7 mRNAs: implications for cervical carcinogenesis.* Proc Natl Acad Sci U S A, 1995. **92**(5): p. 1654-8.
217. Eberhardt, W., et al., *Modulation of mRNA stability as a novel therapeutic approach.* Pharmacol Ther, 2007. **114**(1): p. 56-73.
218. Otake, Y., et al., *Drug-induced destabilization of bcl-2 mRNA: a new approach for inducing apoptosis in tumor cells.* Curr Opin Investig Drugs, 2004. **5**(6): p. 616-22.
219. Chou, C.F., et al., *Tethering KSRP, a decay-promoting AU-rich element-binding protein, to mRNAs elicits mRNA decay.* Mol Cell Biol, 2006. **26**(10): p. 3695-706.
220. Tafech, A., et al., *Destroying RNA as a therapeutic approach.* Curr Med Chem, 2006. **13**(8): p. 863-81.
221. Piette, J., H. Neel, and V. Marechal, *Mdm2: keeping p53 under control.* Oncogene, 1997. **15**(9): p. 1001-10.
222. Wakasugi, M., et al., *DDB accumulates at DNA damage sites immediately after UV irradiation and directly stimulates nucleotide excision repair.* J Biol Chem, 2002. **277**(3): p. 1637-40.

223. Nichols, A.F., et al., *Human damage-specific DNA-binding protein p48. Characterization of XPE mutations and regulation following UV irradiation.* J Biol Chem, 2000. **275**(28): p. 21422-8.
224. Nag, A., et al., *The xeroderma pigmentosum group E gene product DDB2 is a specific target of cullin 4A in mammalian cells.* Mol Cell Biol, 2001. **21**(20): p. 6738-47.
225. Tang, J.Y., et al., *Xeroderma pigmentosum p48 gene enhances global genomic repair and suppresses UV-induced mutagenesis.* Mol Cell, 2000. **5**(4): p. 737-44.
226. Merchant, A.K., T.L. Loney, and J. Maybaum, *Expression of wild-type p53 stimulates an increase in both Bax and Bcl-xL protein content in HT29 cells.* Oncogene, 1996. **13**(12): p. 2631-7.
227. Gannon, J.V. and D.P. Lane, *Protein synthesis required to anchor a mutant p53 protein which is temperature-sensitive for nuclear transport.* Nature, 1991. **349**(6312): p. 802-6.
228. Michalovitz, D., O. Halevy, and M. Oren, *Conditional inhibition of transformation and of cell proliferation by a temperature-sensitive mutant of p53.* Cell, 1990. **62**(4): p. 671-80.
229. McKay, B.C., et al., *The tumor suppressor p53 can both stimulate and inhibit ultraviolet light-induced apoptosis.* Mol Biol Cell, 2000. **11**(8): p. 2543-51.
230. Caelles, C., A. Helmberg, and M. Karin, *p53-dependent apoptosis in the absence of transcriptional activation of p53-target genes.* Nature, 1994. **370**(6486): p. 220-3.
231. Venter, J.C., et al., *The sequence of the human genome.* Science, 2001. **291**(5507): p. 1304-51.
232. Gorospe, M., X. Wang, and N.J. Holbrook, *p53-dependent elevation of p21Waf1 expression by UV light is mediated through mRNA stabilization and involves a vanadate-sensitive regulatory system.* Mol Cell Biol, 1998. **18**(3): p. 1400-7.
233. Chen, C.Y., N. Xu, and A.B. Shyu, *mRNA decay mediated by two distinct AU-rich elements from c-fos and granulocyte-macrophage colony-stimulating factor transcripts: different deadenylation kinetics and uncoupling from translation.* Mol Cell Biol, 1995. **15**(10): p. 5777-88.
234. Chen, C.Y., N. Ezzeddine, and A.B. Shyu, *Messenger RNA half-life measurements in mammalian cells.* Methods Enzymol, 2008. **448**: p. 335-57.
235. Li, X., et al., *Generation of destabilized green fluorescent protein as a transcription reporter.* J Biol Chem, 1998. **273**(52): p. 34970-5.
236. Kastelic, T., et al., *Induction of rapid IL-1 beta mRNA degradation in THP-1 cells mediated through the AU-rich region in the 3'UTR by a radicicol analogue.* Cytokine, 1996. **8**(10): p. 751-61.
237. Moore, M.J., *From birth to death: the complex lives of eukaryotic mRNAs.* Science, 2005. **309**(5740): p. 1514-8.
238. Mathews, D.H., et al., *Expanded sequence dependence of thermodynamic parameters improves prediction of RNA secondary structure.* J Mol Biol, 1999. **288**(5): p. 911-40.
239. Mathews, D.H., D.H. Turner, and M. Zuker, *RNA secondary structure prediction.* Curr Protoc Nucleic Acid Chem, 2007. **Chapter 11**: p. Unit 11 2.
240. Timchenko, L.T., et al., *Identification of a (CUG)n triplet repeat RNA-binding protein and its expression in myotonic dystrophy.* Nucleic Acids Res, 1996. **24**(22): p. 4407-14.
241. Brown, C.Y., C.A. Lagnado, and G.J. Goodall, *A cytokine mRNA-destabilizing element that is structurally and functionally distinct from A+U-rich elements.* Proc Natl Acad Sci U S A, 1996. **93**(24): p. 13721-5.
242. Grzybowska, E.A., A. Wilczynska, and J.A. Siedlecki, *Regulatory functions of 3'UTRs.* Biochem Biophys Res Commun, 2001. **288**(2): p. 291-5.
243. Vlasova, I.A., et al., *Conserved GU-rich elements mediate mRNA decay by binding to CUG-binding protein 1.* Mol Cell, 2008. **29**(2): p. 263-70.
244. Greenberg, J.R., *High stability of messenger RNA in growing cultured cells.* Nature, 1972. **240**(5376): p. 102-4.

245. Momand, J., et al., *The mdm-2 oncogene product forms a complex with the p53 protein and inhibits p53-mediated transactivation.* Cell, 1992. **69**(7): p. 1237-45.
246. Honda, R., H. Tanaka, and H. Yasuda, *Oncoprotein MDM2 is a ubiquitin ligase E3 for tumor suppressor p53.* FEBS Lett, 1997. **420**(1): p. 25-7.
247. McMasters, K.M., et al., *mdm2 deletion does not alter growth characteristics of p53-deficient embryo fibroblasts.* Oncogene, 1996. **13**(8): p. 1731-6.
248. Watanabe, T., et al., *Overexpression of the MDM2 oncogene in leukemia and lymphoma.* Leuk Lymphoma, 1996. **21**(5-6): p. 391-7, color plates XVI following 5.
249. Finlay, C.A., *The mdm-2 oncogene can overcome wild-type p53 suppression of transformed cell growth.* Mol Cell Biol, 1993. **13**(1): p. 301-6.
250. Eischen, C.M., et al., *Disruption of the ARF-Mdm2-p53 tumor suppressor pathway in Myc-induced lymphomagenesis.* Genes Dev, 1999. **13**(20): p. 2658-69.
251. Rayburn, E., et al., *MDM2 and human malignancies: expression, clinical pathology, prognostic markers, and implications for chemotherapy.* Curr Cancer Drug Targets, 2005. **5**(1): p. 27-41.
252. Marine, J.C., et al., *Keeping p53 in check: essential and synergistic functions of Mdm2 and Mdm4.* Cell Death Differ, 2006. **13**(6): p. 927-34.
253. Tornaletti, S., *DNA repair in mammalian cells: Transcription-coupled DNA repair: directing your effort where it's most needed.* Cell Mol Life Sci, 2009. **66**(6): p. 1010-20.
254. April, C.S. and G.S. Barsh, *Distinct pigmentary and melanocortin 1 receptor-dependent components of cutaneous defense against ultraviolet radiation.* PLoS Genet, 2007. **3**(1): p. e9.
255. Garinis, G.A., et al., *Transcriptome analysis reveals cyclobutane pyrimidine dimers as a major source of UV-induced DNA breaks.* EMBO J, 2005. **24**(22): p. 3952-62.
256. Joseph, B., M. Orlian, and H. Furneaux, *p21(waf1) mRNA contains a conserved element in its 3'-untranslated region that is bound by the Elav-like mRNA-stabilizing proteins.* J Biol Chem, 1998. **273**(32): p. 20511-6.
257. Hau, H.H., et al., *Tristetraprolin recruits functional mRNA decay complexes to ARE sequences.* J Cell Biochem, 2007. **100**(6): p. 1477-92.
258. Bakheet, T., et al., *ARED: human AU-rich element-containing mRNA database reveals an unexpectedly diverse functional repertoire of encoded proteins.* Nucleic Acids Res, 2001. **29**(1): p. 246-54.
259. Anderson, P., *Post-transcriptional regulons coordinate the initiation and resolution of inflammation.* Nat Rev Immunol. **10**(1): p. 24-35.
260. Moser, J., et al., *The UV-damaged DNA binding protein mediates efficient targeting of the nucleotide excision repair complex to UV-induced photo lesions.* DNA Repair (Amst), 2005. **4**(5): p. 571-82.
261. Fitch, M.E., I.V. Cross, and J.M. Ford, *p53 responsive nucleotide excision repair gene products p48 and XPC, but not p53, localize to sites of UV-irradiation-induced DNA damage, in vivo.* Carcinogenesis, 2003. **24**(5): p. 843-50.
262. Shiyanov, P., A. Nag, and P. Raychaudhuri, *Cullin 4A associates with the UV-damaged DNA-binding protein DDB.* J Biol Chem, 1999. **274**(50): p. 35309-12.
263. Li, J., et al., *DNA Damage Binding Protein Component DDB1 Participates in Nucleotide Excision Repair through DDB2 DNA-binding and Cullin 4A Ubiquitin Ligase Activity.* Cancer Res, 2006. **66**(17): p. 8590-8597.
264. Wang, Q.E., et al., *DNA repair factor XPC is modified by SUMO-1 and ubiquitin following UV irradiation.* Nucleic Acids Res, 2005. **33**(13): p. 4023-34.
265. Guerrero-Santoro, J., et al., *The cullin 4B-based UV-damaged DNA-binding protein ligase binds to UV-damaged chromatin and ubiquitinates histone H2A.* Cancer Res, 2008. **68**(13): p. 5014-22.

266. Kapetanaki, M.G., et al., *The DDB1-CUL4ADDB2 ubiquitin ligase is deficient in xeroderma pigmentosum group E and targets histone H2A at UV-damaged DNA sites.* Proc Natl Acad Sci U S A, 2006. **103**(8): p. 2588-93.
267. Fujiwara, Y., et al., *Characterization of DNA recognition by the human UV-damaged DNA-binding protein.* J Biol Chem, 1999. **274**(28): p. 20027-33.
268. McKay, B.C., M. Ljungman, and A.J. Rainbow, *Potential roles for p53 in nucleotide excision repair.* Carcinogenesis, 1999. **20**(8): p. 1389-96.
269. Tusher, V.G., R. Tibshirani, and G. Chu, *Significance analysis of microarrays applied to the ionizing radiation response.* Proc Natl Acad Sci U S A, 2001. **98**(9): p. 5116-21.
270. Veyrune, J.L., et al., *c-fos mRNA instability determinants present within both the coding and the 3' non coding region link the degradation of this mRNA to its translation.* Oncogene, 1995. **11**(10): p. 2127-34.
271. Grosset, C., et al., *A mechanism for translationally coupled mRNA turnover: interaction between the poly(A) tail and a c-fos RNA coding determinant via a protein complex.* Cell, 2000. **103**(1): p. 29-40.
272. May, E., J.R. Jenkins, and P. May, *Endogenous HeLa p53 proteins are easily detected in HeLa cells transfected with mouse deletion mutant p53 gene.* Oncogene, 1991. **6**(8): p. 1363-5.
273. Scheffner, M., et al., *The E6 oncoprotein encoded by human papillomavirus types 16 and 18 promotes the degradation of p53.* Cell, 1990. **63**(6): p. 1129-36.
274. Kessis, T.D., et al., *Human papillomavirus 16 E6 expression disrupts the p53-mediated cellular response to DNA damage.* Proc Natl Acad Sci U S A, 1993. **90**(9): p. 3988-92.
275. Amrani, N., et al., *Translation factors promote the formation of two states of the closed-loop mRNP.* Nature, 2008. **453**(7199): p. 1276-80.
276. Muhlrad, D. and R. Parker, *Aberrant mRNAs with extended 3' UTRs are substrates for rapid degradation by mRNA surveillance.* RNA, 1999. **5**(10): p. 1299-307.
277. Pulak, R. and P. Anderson, *mRNA surveillance by the Caenorhabditis elegans smg genes.* Genes Dev, 1993. **7**(10): p. 1885-97.
278. Tian, B., et al., *A large-scale analysis of mRNA polyadenylation of human and mouse genes.* Nucleic Acids Res, 2005. **33**(1): p. 201-12.
279. Wiestner, A., et al., *Point mutations and genomic deletions in CCND1 create stable truncated cyclin D1 mRNAs that are associated with increased proliferation rate and shorter survival.* Blood, 2007. **109**(11): p. 4599-606.
280. Sandberg, R., et al., *Proliferating cells express mRNAs with shortened 3' untranslated regions and fewer microRNA target sites.* Science, 2008. **320**(5883): p. 1643-7.
281. Mayr, C. and D.P. Bartel, *Widespread shortening of 3'UTRs by alternative cleavage and polyadenylation activates oncogenes in cancer cells.* Cell, 2009. **138**(4): p. 673-84.
282. Wein, G., et al., *The 3'-UTR of the mRNA coding for the major protein kinase C substrate MARCKS contains a novel CU-rich element interacting with the mRNA stabilizing factors HuD and HuR.* Eur J Biochem, 2003. **270**(2): p. 350-65.
283. Chan, C.Y., et al., *A structural interpretation of the effect of GC-content on efficiency of RNA interference.* BMC Bioinformatics, 2009. **10 Suppl 1**: p. S33.
284. Peng, S.S., C.Y. Chen, and A.B. Shyu, *Functional characterization of a non-AUUUA AU-rich element from the c-jun proto-oncogene mRNA: evidence for a novel class of AU-rich elements.* Mol Cell Biol, 1996. **16**(4): p. 1490-9.
285. Mattick, J.S., *The genetic signatures of noncoding RNAs.* PLoS Genet, 2009. **5**(4): p. e1000459.
286. Gorodkin, J., et al., *De novo prediction of structured RNAs from genomic sequences.* Trends Biotechnol, 2010. **28**(1): p. 9-19.
287. Eddy, S.R., *How do RNA folding algorithms work?* Nat Biotechnol, 2004. **22**(11): p. 1457-8.

288. Mathews, D.H. and D.H. Turner, *Prediction of RNA secondary structure by free energy minimization.* Curr Opin Struct Biol, 2006. **16**(3): p. 270-8.
289. Weitzman, J.B., *Tracking evolution's footprints in the genome.* J Biol, 2003. **2**(2): p. 9.
290. Larizza, A., et al., *Evolutionary dynamics of mammalian mRNA untranslated regions by comparative analysis of orthologous human, artiodactyl and rodent gene pairs.* Comput Chem, 2002. **26**(5): p. 479-90.
291. Miziara, M.N., P.K. Riggs, and M.E. Amaral, *Comparative analysis of noncoding sequences of orthologous bovine and human gene pairs.* Genet Mol Res, 2004. **3**(4): p. 465-73.
292. Jareborg, N., E. Birney, and R. Durbin, *Comparative analysis of noncoding regions of 77 orthologous mouse and human gene pairs.* Genome Res, 1999. **9**(9): p. 815-24.
293. Makalowski, W. and M.S. Boguski, *Evolutionary parameters of the transcribed mammalian genome: an analysis of 2,820 orthologous rodent and human sequences.* Proc Natl Acad Sci U S A, 1998. **95**(16): p. 9407-12.
294. Pesole, G., et al., *Structural and functional features of eukaryotic mRNA untranslated regions.* Gene, 2001. **276**(1-2): p. 73-81.
295. Hwang, B.J., et al., *p48 Activates a UV-damaged-DNA binding factor and is defective in xeroderma pigmentosum group E cells that lack binding activity.* Mol Cell Biol, 1998. **18**(7): p. 4391-9.
296. Yoon, T., et al., *Tumor-prone phenotype of the DDB2-deficient mice.* Oncogene, 2005. **24**(3): p. 469-78.
297. Li, W.-H., C. Luo, and C. Wu, *Evolution of DNA sequences*, in *Molecular evolutionary genetics*, R. Macintyre, Editor. 1985, Plenum Press: New York, NY. p. 1-94.
298. Jukes, T. and C. Cantor, *Evolution of protein molecules*, in *Mammalian protein metabolism*, H. Munro, Editor. 1969, Academic Press: New York, NY. p. 21-123.
299. Knee, R. and P.R. Murphy, *Regulation of gene expression by natural antisense RNA transcripts.* Neurochem Int, 1997. **31**(3): p. 379-92.
300. Yelin, R., et al., *Widespread occurrence of antisense transcription in the human genome.* Nat Biotechnol, 2003. **21**(4): p. 379-86.
301. Chen, J., et al., *Over 20% of human transcripts might form sense-antisense pairs.* Nucleic Acids Res, 2004. **32**(16): p. 4812-20.
302. Mitchell, P. and D. Tollervey, *mRNA turnover.* Curr Opin Cell Biol, 2001. **13**(3): p. 320-5.
303. Stieger, K., et al., *In vivo gene regulation using tetracycline-regulatable systems.* Adv Drug Deliv Rev, 2009. **61**(7-8): p. 527-41.
304. Ermak, G., V.J. Cancasci, and K.J. Davies, *Cytotoxic effect of doxycycline and its implications for tet-on gene expression systems.* Anal Biochem, 2003. **318**(1): p. 152-4.

Chapter 7 Appendices

7.1 Appendix 1: Supplemental Data

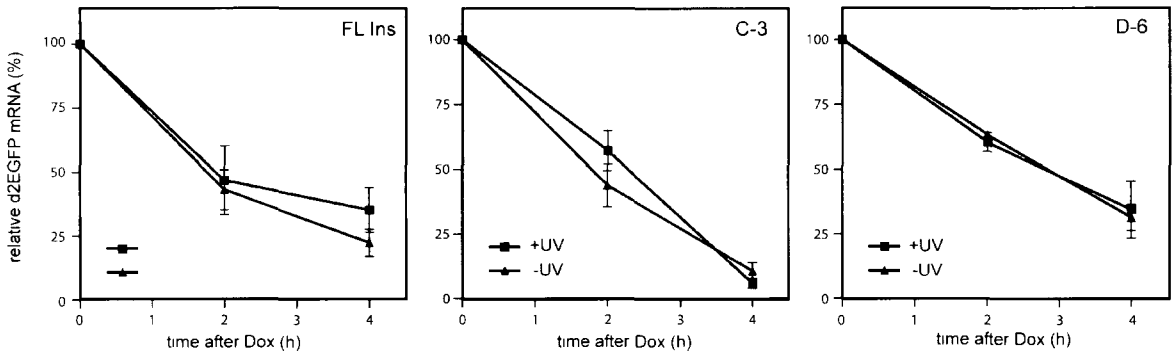

Figure S-1. UV light does not affect the mRNA stability of d2EGFP in the presence or absence of the 3'DDE. Indicated HeLa TO cell lines were treated with or without UV light (20 J/m^2) at the time of Dox addition. Total mRNA was collected at indicated times for real-time RT-PCR analysis of d2EGFP mRNA expression. FL Ins and C-3 cell lines contain the 3'DDE, while the D-6 cell line does not. Values represent the mean ± standard error of at least 2 independent experiments.

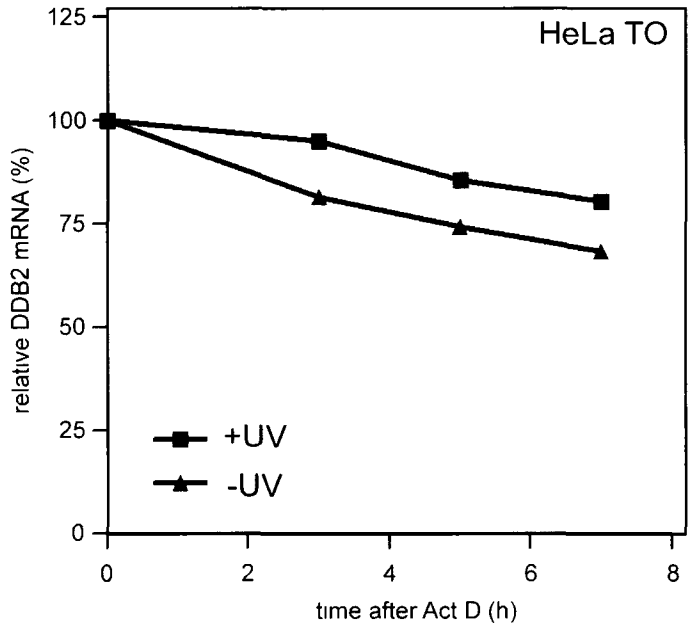

Figure S-2. DDB2 mRNA is not stabilized by UV light in HeLa TO cells. HeLa TO parental cells were treated with or without UV light (20 J/m^2) at the time of Act D addition. Total mRNA was collected at indicated times for real-time RT-PCR analysis of DDB2 mRNA expression. Representative experiment shown.

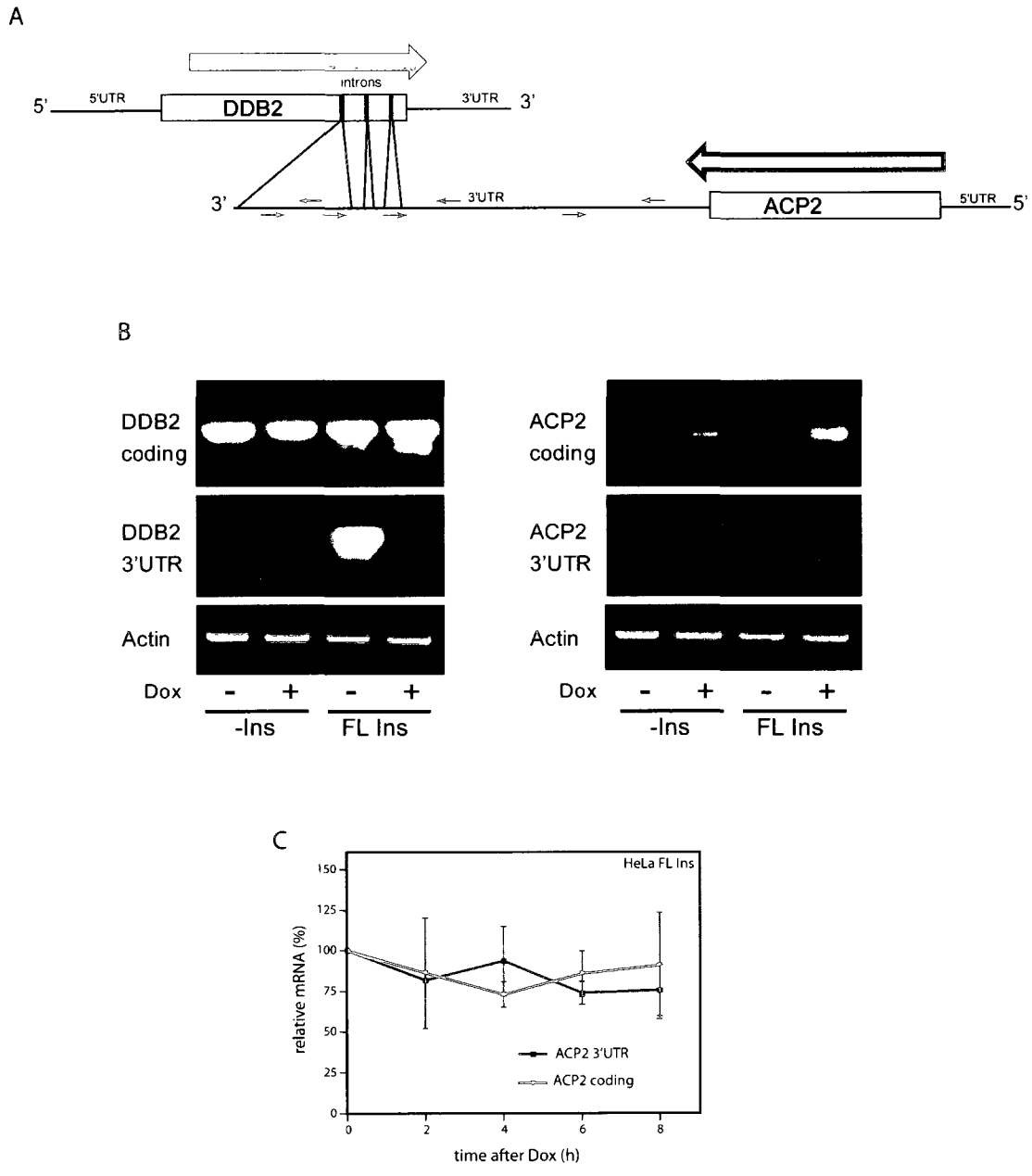

Figure S-3. The ACP2 3'UTR forms a perfect antisense with the DDB2 3'UTR. (A) Schematic diagram and genomic orientation of the two genes. Primer sets (coloured pairs of arrows) were designed to amplify different regions of the ACP2 3'UTR to ensure the antisense oligonucleotide was expressed. See text for detail. (B) –Ins and FL Ins HeLa cells were treated with or without Dox for 48h. Total mRNA was collected for RT-PCR. To ensure accuracy of product, ACP2 3'UTR primers amplified region not overlapping with DDB2 3'UTR (red arrows on the right in A). (C) ACP2 coding or 3'UTR mRNA expression FL Ins cells following Dox treatment as measured by real-time RT-PCR. Values represent the mean ± standard error of 2 independent experiments.

7.2 Appendix II: Publications

7.2.1 **DNA damage binding protein 2 mRNA is stabilized by UV light and contains a putative destabilizing element in its 3'UTR. pg 158.**
Conference: *DNA Damage, Mutation and Cancer*. Ventura, California. March 9-14, 2008. Brian Melanson, Bruce McKay. University of Ottawa, Department of Cellular and Molecular Medicine; Ottawa Hospital Research Institute

7.2.2 **Identification of a novel destabilizing element in the 3'UTR of DNA damage binding protein 2 (DDB2) mRNA. pg 160.**
Conference: *Eukaryotic mRNA Processing*. Cold Spring Harbor, New York. August 18-22, 2009. Brian Melanson, Bruce McKay. University of Ottawa, Department of Cellular and Molecular Medicine; Ottawa Hospital Research Institute.

7.2.3 Brian Melanson, Jeff Hamill, Reetesh Bose, Bruce McKay. **The p53-regulated transcript encoding DDB2 is post-transcriptionally regulated in response to UV Light,** 2010. Manuscript submitted for publication. pg 161.

7.2.4 Brian Melanson, Bruce McKay. **Identification of a novel destabilizing element in the 3'UTR of DDB2**, 2010. Manuscript in preparation.

7.2.1

DNA Damage, Mutation and Cancer. Ventura, California. March 9-14, 2008

DNA damage binding protein 2 mRNA is stabilized by UV light and contains a putative destabilizing element in its 3'UTR

Brian Melanson, Bruce McKay. University of Ottawa, Department of Cellular and Molecular Medicine; Ottawa Hospital Research Institute

The p53-induced DDB2 gene encodes the p48 subunit of the DNA damage binding complex (DDB) and is believed to be involved in DNA damage recognition during global genomic nucleotide excision repair (GG-NER) of UV-induced photolesions. Loss of DDB2 function results in xeroderma pigmentosum sub-group E (XP-E), a condition characterized by an increased sensitivity to UV induced skin cancer. DDB2's exact function remains somewhat elusive. DDB2 appears to be required for the recruitment of XPC and XPA to sites of UV-induced DNA damage and the subsequent repair of cyclobutane pyrimidine dimers. The expression of DDB2 is regulated at both transcriptional and post-transcriptional levels following UV exposure. First, immediately following UV exposure, protein levels decrease as DDB2 is targeted for proteasome-mediated degradation by a ubiquitin ligase complex containing Cullin-4A and DDB1. Degradation of DDB2 appears to be required for GG-NER. Second, transcription from the DDB2 gene is increased several hours following UV exposure in a p53-dependent manner. The timing of these opposing processes on DDB2 protein levels suggests that DDB2 levels could be limiting prior to the p53-dependent increase in DDB2 protein levels.

The present work identifies an additional level of regulation of DDB2 and GG-NER. We show that the half-life of the DDB2 transcript is increased during the first 6 hours following exposure to UV light, the time during which DDB2 may become limiting. Furthermore this UV stabilization is dose dependent, such that the amount of UV exposure correlates with the amount of mRNA stabilization. The regulation of mRNA stability has been shown to play an important role in regulating gene expression under a variety of stress conditions including UV exposure. The UV-induced stabilization of short-lived RNAs is frequently mediated by increased binding of RNA-binding proteins (RBPs) to *cis*-acting elements such as AU-rich elements (ARE) in the 3'UTR of stabilized transcripts. However, our analysis of the DDB2 mRNA suggests that it does not contain an ARE sequence.

To identify *cis*-acting elements in the DDB2, we have developed a DDB2 3'UTR fluorescent reporter system using a destabilized variant of enhanced green fluorescent protein (d2EGFP) expressed from a tetracycline regulated promoter (Tet-off). The 3'UTR of DDB2, and portions thereof, were inserted immediately downstream of the d2EGFP coding region. In this system, the addition of doxycycline leads to a rapid decrease in green fluorescence when the transcript is unstable whereas cells remain fluorescent if protein is continuously produced from stable mRNAs. We found that the presence of the 3'UTR of DDB2 lead to significant decreases in d2EGFP protein and mRNA expression compared control reporters. RNA interference was used to target a variety of components of known mRNA decay pathways. Targeting HuR with siRNA, for example, results in reduced expression from the DDB2 3'UTR construct.

We hypothesize that this observed UV stabilization of DDB2 mRNA allows UV-

irradiated cells to maintain adequate levels of this protein for initiation of repair while *de novo* transcription is impaired and DDB2 is depleted as part of the repair process. These findings help to highlight the complex regulatory mechanisms in place to ensure mammalian genomic surveillance and repair can occur efficiently following genotoxic insult and offer new avenues of inquiry for studying human DNA repair disorders.

7.2.2

Eukaryotic mRNA Processing. Cold Spring Harbor, New York. August 18-22, 2009.

Identification of a novel destabilizing element in the 3'UTR of DNA damage binding protein 2 (DDB2) mRNA

Brian Melanson, Bruce McKay. University of Ottawa, Department of Cellular and Molecular Medicine; Ottawa Hospital Research Institute

Differential mRNA stability plays an integral role in gene expression. Often, *cis*-acting elements within the 3'UTR of transiently expressed transcripts target labile mRNAs for rapid exosome-mediated degradation through interactions with various RNA binding proteins (RNA-BPs). DNA Damage Binding protein 2 (DDB2) is a p53-regulated gene whose protein product is involved in the early recognition of helix distorting lesions following UV-induced DNA damage and aids in global genomic nucleotide excision repair (GG-NER). Here we report that under unstressed conditions, its transcript is relatively unstable. The full-length DDB2 3'UTR was fused downstream of a Tetracycline regulated EGFP reporter construct was used to identify putative instability determinants in the 3'UTR of DDB2. This caused a decrease in GFP mRNA stability which was also observed at the protein level. Using this reporter system we have localized a destabilizing element within a 50 nucleotide region. We have termed this region the 3'UTR DDB2 destabilizing element (3'DDE). It does not contain any previously reported stability determinant such as an AU-rich element (ARE). *In silico* structural analysis of the 3'DDE has predicted the presence of two distinct features. There is an inverted repeat sequence that is predicted to form a stable 20 nucleotide stem-loop structure. There is also a pyrimidine-rich region to the 5' side of the stem-loop that is predicted to remain single stranded. Disrupting the stem-loop structure or sequence with point mutations did not abolish the instability. 3'DDE constructs with mutations and/or deletions that impose various structural and sequence alterations have been created to elucidate the precise destabilizing element. The 3'DDE represents a previously uncharacterized stability determinant that presumably regulates DDB2 gene expression.

7.2.3

The p53-regulated transcript encoding DDB2 is post-transcriptionally regulated in response to UV light

B.D. Melanson[a,b], J.D. Hamill[a], R. Bose[a,b]. and B.C. McKay[a,b,c,d]

[a] Cancer Therapeutics Program, Ottawa Hospital Research Institute, 501 Smyth Rd, Ottawa, ON, Canada K1H 8L6
[b] Department of Cellular and Molecular Medicine, University of Ottawa, 451 Smyth Rd, Ottawa, Ontario
Canada, K1H 8M5
[c] Department of Medicine, Ottawa Hospital, 501 Smyth Rd, Ottawa, ON, Canada K1H 8L6
[d] Department of Radiology, Ottawa Hospital, 501 Smyth Rd, Ottawa, ON, Canada K1H 8L6

Corresponding author:
Bruce C. McKay
Cancer Therapeutics Program
Ottawa Hospital Research Institute
501 Smyth Rd, Box 926
Ottawa, ON K1H 8L6
Canada
Phone: 613-737-7700 x70338
Fax: 613-247-3524
bmckay@ohri.ca

Keywords: DDB2, DNA repair, mRNA stability, p53, ultraviolet light

Abstract

The p53 tumour suppressor functions in large part as a sequence-specific transcriptional activator. Ultraviolet light (UV light) can activate p53 leading to widespread changes in the expression of genes containing p53 response elements. UV light also affects the stability of some UV responsive transcripts but the contribution of mRNA stability to p53-induced gene expression is unclear. Here we used a colorectal cancer cell line (HT29-tsp53) expressing a temperature sensitive variant of p53 to determine how mRNA stability affects p53-regulated gene expression. Incubation of HT29-tsp53 cells at the permissive temperature led to an increase in the expression of 53 transcripts, 21 of which are known p53-responsive genes. Returning these cells to the restrictive temperature led to a rapid loss of p53-dependent gene expression. These results indicate that p53-regulated transcripts are, in general, short-lived. This is likely to protect cells from precocious cell cycle arrest and/or apoptosis. Exposure of HT29-tsp53 cells to UV light as they were returned to the restrictive temperature led to heterogeneous responses. The transcript encoding the damage-specific DNA binding protein 2 (DDB2), involved in the repair of UV-induced DNA damage, was among the more UV-responsive transcripts. Detailed analysis of DDB2 expression indicated that UV exposure led to a significant dose-dependent increase in the half-life of the DDB2 transcript that contributed to post-UV expression of the protein. We propose that post-transcriptional regulation of DDB2 contributes to nucleotide excision repair and further suggest that DDB2 represents one of many p53-regulated mRNAs that are subject to post-transcriptional regulation under appropriate physiological conditions.

1.0. Introduction

Ultraviolet (UV) light is a prevalent environmental carcinogen [1]. UV light induces predominantly two DNA lesions: cyclobutane pyrimidine dimers (CPDs) and 6-4 photoproducts (6-4PPs). Cells respond to UV exposure by altering patterns of gene expression in a variety of ways. Notably, the p53 tumour suppressor is post-translationally stabilized following UV exposure [2] and this protein is best characterized as a sequence-specific transcriptional activator of genes containing a p53-response element [2,3]. Thus UV exposure leads to widespread p53-dependent changes in gene expression [3]. However, a single CPD or 6-4PP is sufficient to block progression of RNA polymerase II [4-6] so even modest doses of UV light significantly inhibit RNA synthesis [7-10]. UV light may also affect gene expression through *trans*- acting mechanisms [11,12]. These inhibitory effects of UV light on mRNA synthesis pose a challenge to the coordinated regulation of gene expression in UV-exposed cells [13]. Therefore, cells must have evolved ways to deal with reduced transcription in order to mount efficient transcription responses to this environmental carcinogen.

It has been estimated that over 50% of all stress-related genes are regulated at level of mRNA decay [14]. Importantly, many UV-induced transcripts are stabilized in response to this DNA damaging agent [15-20]. This implies that many UV- and stress-regulated transcripts are short-lived under normal conditions but that specific RNA binding proteins protect these messages under appropriate conditions. Notably, the p53-regulated CDKN1A mRNA encoding $p21^{WAF1}$ (hereafter referred to as $p21^{WAF1}$ for clarity) contains an adenylate uridylate (AU)-rich element (ARE) in its 3'UTR that makes it unstable under most conditions [20,21]. In response to UV light, the HuR RNA binding protein binds the

ARE and blocks degradation of the transcript [19]. Regulating mRNA decay is a very attractive post-transcriptional step to control gene expression under conditions of transcriptional stress [22] like that faced following UV exposure. However, the contribution of mRNA stability to the p53 response remains unclear.

Here, we used a colon carcinoma cell line expressing a temperature sensitive variant of p53 (HT29-tsp53 cells) and oligonucleotide microarrays to identify p53-regulated genes induced at the permissive temperature in HT29-tsp53 cells. In this model, the activity of p53 is tightly and reversibly regulated by temperature shift alone [23]. At the permissive temperature, this variant of p53 is nuclear [24], activates p53 target genes like $p21^{WAF1}$ without a requirement for an additional activating signal [13,23,25]. The cells arrest predominantly in the G_1 phase of the cell cycle at the permissive temperature but returning these cells to the restrictive temperature leads to the rapid loss of p53-target gene expression and cell cycle re-entry [13,23,25]. Thus, this model system provides a unique opportunity to rapidly eliminate p53 activity to study the decay of p53-induced transcripts. We found that most of the known p53 target genes induced at the permissive temperature decayed to basal levels within 2 to 6 hours at the restrictive temperature indicating that p53-regulated transcripts tend to be short-lived. A subset of p53-regulated transcripts was expressed preferentially when returned to the restrictive temperature following UV exposure. The DDB2 transcript was identified among this group and detailed expression analysis of DDB2 mRNA indicated that it was subject to post transcriptional regulation following UV exposure. Our results further indicate that the availability of DDB2 mRNA for translation is limiting for DDB2 expression following UV exposure. We suggest that

transcriptional and post-transcriptional regulation of DDB2 expression play an important role in the regulation of NER following UV exposure.

2.0. Materials and Methods

2.1. Cell Culture and UV treatment

HT29-tsp53 human colon cancer cells express a temperature sensitive variant of p53 that has a substitution of valine to alanine at position 135 (V135A) [23]. These cells were grown in Dulbecco's modified Eagle's medium (DMEM) supplemented with 10% fetal calf serum (FCS) (Thermo Fisher Scientific, Waltham, MA). Cells were maintained at the restrictive temperature (38°C) in a humidified atmosphere with 5% CO_2. Where indicated, HT29-tsp53 cells were incubated at the permissive temperature (32°C) to induce functional p53 for the indicated period of time.

Where indicated, growth medium was removed and cells were exposed to the indicated fluence of UV light at 1 $J/m^2/s$ from a germicidal bulb (Philips, Markham, ON) emitting predominately at 254 nm. Following UV exposure, fresh medium was replaced and cells recovered for the indicated period of time. To inhibit nascent RNA synthesis, actinomycin D (Act D, Sigma-Aldrich, St. Louis, MO) was added to antibiotic-free media to a final concentration of 5μg/ml.

2.2. Microarray analysis

Total RNA was isolated using the RNeasy RNA isolation kit (Qiagen, Valencia, CA) according to manufacturer's specifications and submitted for analysis at the Ottawa Genomics Innovation Centre Affymetrix Gene-Chip Facility (Ottawa, ON) using the

Human Gene 1.0 ST oligonucleotide arrays (Affymetrix, Santa Clara, CA). Data analysis was performed using GeneSpring GX 11 analysis software (Agilent Technologies, Santa Clara, CA). Genes exhibiting greater than a 3-fold increase in expression were identified. Known p53 target genes were identified from this list of transcripts. Transcripts were considered to be direct targets of p53 if they had been reported in the literature as direct targets (for recent compilation see [2]) or if both potential p53-response elements and supporting expression data were collated in the p53 family database (p53FamTaG available at http://www2.ba.itb.cnr.it/P53TAG/) [26].

2.3. Quantitative reverse transcriptase polymerase chain reaction

Cells were trypsinized, harvested and washed with PBS. Total RNA was isolated using the RNeasy RNA isolation kit (Qiagen, Valencia, CA) according to manufacturer's specifications Five micrograms of total RNA was reverse-transcribed by using first-strand cDNA synthesis kit (MBI Fermentas, Burlington, ON). Quantitative reverse transcriptase polymerase chain reaction (RT-PCR) was performed using the Sybr green fluorescent DNA stain (Invitrogen, Carlsbad, CA) and the LightCycler 2 quantitative PCR machine with Light-Cycler software version 3 (Roche Diagnostics, Switzerland).

Intron-spanning primers were used to measure the relative expression of DDB2 (CCACCTTCATCAAAGGGATTGG and CTCGGATCTCGCTCTTCTGGTC), p21 (CTCAAATCGTCCAGCGACCTT and CATTGTGGGAGGAGCTGTGAA), FAS (CCCAGAATACCAAGTGCAGATG and TCCTTTCTGTGCTTTCTGCATG), MDM2 (AGGTGATTGGTTGGATCAGG and GAAGCCAATTCTCACGAAGG), PIG3 (TCTCTATGGTCTGATGGG and TTGCCTATGTTCTTGTTG), BTG2

(GTGAGCGAGCAGAGGCTTAAGG and TGCGGTAGGACACCTCATAGGG), SERPINB2 (CTTTTCTGTGGATGCCGATT and CCTGCCAGGGCTTAACATAA) and XPC (AAGTTCACTCGCCTCGGTTGC and TTCTTTCCTGATTTTAGCCTTTTT). Expression of each transcript was normalized to the expression of ACTB (GGGCATGGGTCAGAAGGAT and GTGGCCATCTCTTGCTCGA).

2.4. Immunoblotting

Cells were harvested, rinsed with PBS, lysed with RIPA buffer, sonicated for 20 seconds using a microtip (Branson Sonifier, VWR International Ltd., Mississauga, ON) and protein concentrations determined using the BioRad Protein Assay (BioRad, Mississauga, ON). Whole cell lysates were prepared using LDS NuPAGE sample buffer (Invitrogen Canada Inc., Burlington, ON). Proteins were separated in 4–12% Bis-Tris NuPAGE precast gels, transferred to nitrocellulose membranes (Hybond-C Extra, Amersham, Baie d'Urfe, QC) and stained with Ponceau S Red (5 mg/ml in 2% glacial acetic acid) to confirm transfer of proteins. Membranes were blocked in PBSMT-A (PBS, 5% nonfat dry milk powder, 0.05% Tween 20) for 1 hr at room temperature. They were incubated with primary antibody against β-actin clone AC-74 (Sigma-Aldrich Canada Ltd.) for 1hr at room temperature or with XPE/DDB2 AF3297 primary antibody from R&D Systems (Minneapolis, MN) overnight at 4°C. Secondary antibodies, horseradish peroxidase-conjugated goat anti-mouse and rabbit anti-goat IgG were obtained from Calbiochem and R&D Systems, respectively. All antibodies were diluted in PBSMT-B (PBS, 0.5% nonfat dry milk powder, 0.05% Tween 20). Protein bands were visualized using SuperSignal West Pico Chemiluminescent Substrate (Pierce, Rockford, IL) and Kodak film. Membranes were

stripped with Restore Western Blot Stripping Buffer (Pierce, Rockford, IL) in order to visualize additional proteins on the same blot.

3.0. Results

3.1. p53-regulated transcripts are short-lived

HT29-tsp53 cells were derived from the HT29 colorectal carcinoma cell line. This subline expresses a temperature sensitive variant of murine p53 (V135A) [23]. At the restrictive temperature (38°C), this variant of p53 is in a mutant conformation and remains cytoplasmic while p53 rapidly switches to wild-type conformation and localizes to the nucleus at the permissive temperature where it acts as a transcriptional activator [13,24,25,27]. We have found that this cell line permits the tight temporal and reversible regulation of p53 function without a requirement for *de novo* transcription or translation [13,25]. Furthermore, there is no requirement for exogenous DNA damage to induce p53-dependent target gene expression [13,25].

As schematically represented in Figure 1A, HT29-tsp53 cells were incubated at the permissive temperature for 16 hours to strongly induce p53-target gene expression, at which time cells were returned to the restrictive temperature to eliminate p53 activity and total RNA was collected 6 hours later for microarray analysis. The expression of 53 separate transcripts increased at least 3 fold at the permissive temperature in two independent experiments (Supplementary Table 1). Twenty one of these putative p53 regulated transcripts are reportedly p53-responsive, as defined in the materials and methods (Table 1). Strikingly, the expression of almost all of these transcripts decreased close to basal levels within 6 hours at the restrictive temperature, regardless of fold

induction at the permissive temperature alone (Figure 1B). The rapid decrease in the expression of p53-induced transcripts at the restrictive temperature was confirmed by quantitative RT-PCR using primers specific for 8 of the 21 transcripts. Only two of these p53-induced genes (TP53I3 and CES2) appeared to retain significant expression, falling outside the 95% confidence interval (Figure 1B). TP53I3 retained the highest level of expression by RT-PCR, as well (Figure 1C). These results confirm that p53 activity is rapidly reversible in HT29-tsp53 cells and further indicates that p53-responsive transcripts are highly unstable.

3.2. The effect of UV light on p53-dependent gene expression

To determine the effect of UV light on p53-induced gene expression, similar microarray analysis was performed with UV-treated (20 J/m^2) samples. Returning UV-irradiated cells to the restrictive temperature also led a dramatic decrease in target gene expression (Figure 2A). There was more variation in the expression of p53-regulated transcripts following UV exposure compared to unirradiated controls (Figure 2A). Intriguingly, there appeared to be 2 distinct populations of transcripts (referred to as UV_{high} and UV_{low} populations) that each exhibited a statistically significant positive association between residual expression at the restrictive temperature 6 hours following UV exposure and fold induction at the permissive temperature (Figure 2B, right panel). Both populations exhibited a very tight linear correlation between residual expression at the restrictive temperature 6 hours following UV exposure and fold induction at the permissive temperature (r^2 values were 0.77 and 0.77). The slopes of the regression lines (0.60 and 0.25) in the right panel (+UV) were significantly non-zero (P=0.0009 and P=0.0004, F-

test) and the slopes were significantly different (P=0.002, F test). In the absence of UV light, there was essentially no residual induction in the UV_{low} group indicating that these p53-responsive mRNAs are very labile (Figure 2B left panel). There was more heterogeneity in the residual expression among the UV_{high} group, in the absence of UV light, but there was still no significant correlation between residual expression and fold induction at the restrictive temperature (P = 0.13, F test). These results indicate that fold induction at the permissive temperature does not predict the residual expression remaining at the restrictive temperature in the absence of UV light.

Gene ontology analysis was performed using GoStat software (http://gostat.wehi.edu.au/ [28]). Transcripts associated with the gene ontology terms apoptosis (GO: 0006915), response to DNA damage (GO: 0006974) and cell cycle arrest (GO: 0007050) were over represented ($P = 1 \times 10^{-6}$, 7.5×10^{5} and 4.8×10^{-5}, respectively) among the UV_{low} transcripts (Table 1). Response to DNA damage (GO: 0006974), apoptosis (GO: 0006915) and DNA repair (GO: 0006281) were overrepresented ($P = 1.6 \times 10^{-3}$, 0.03 and 0.01, respectively), in the UV_{high} group. The importance of global genomic NER (GG-NER) in the repair of UV-induced DNA damage and protection against skin carcinogenesis [29-33] led us to focus on DDB2 in detail as a biologically important UV-responsive transcript.

3.3. UV light increases the stability of the DDB2 transcript

UV light is able to increase gene expression through the post transcriptional stabilization of specific mRNAs [15,17,19,20,34]. Importantly, the p53-regulated $p21^{WAF1}$ transcript is labile but the stability of this transcript increases in response to a variety of

stresses including UV light [19,20]. Therefore, increased expression of $p21^{WAF1}$ mRNA following UV exposure is dependent on transcriptional and post-transcriptional regulation. Here, the expression of $p21^{WAF1}$ was used as a positive control to determine whether this model could be used to examine the effect of UV light on the stability of the DDB2 mRNA. HT29-tsp53 cells were incubated at the permissive temperature for 16 hours to strongly induce $p21^{WAF1}$, at which time cells were exposed to either 0 or 20 J/m^2 of UV light and immediately returned to the restrictive temperature to allow the decay of p53-induced transcripts. At the indicated times, RNA was collected for quantitative RT-PCR analysis. The amount of $p21^{WAF1}$ mRNA decreased rapidly at the restrictive temperature, consistent with its short half-life (Figure 3A) [19,20]. UV light led to a significant increase in the stability of the $p21^{WAF1}$ transcript (Figure 3A), as expected [19,20].

FAS was selected for comparison in detailed time course studies because it was induced to a similar extent to DDB2 and its expression was relatively unaffected by UV exposure (Table 1). Quantitative RT-PCR analysis confirmed that FAS mRNA was induced approximately 12 fold at the permissive temperature, the mRNA was short-lived and the stability of the accumulated transcripts at the restrictive temperature was unaffected by UV exposure (Figure 3B). Therefore, FAS mRNA is not subject to post-transcriptional regulation at the level of mRNA stability following UV-irradiation. Taken together, HT29-tsp53 cells represent a unique model to study the consequences of UV exposure on the decay of p53-responsive transcripts.

The expression of DDB2 transcript was assessed using the same experimental design. Incubation of HT29-tsp53 cells for 16 hours at the permissive temperature led to a 12 fold increase in DDB2 mRNA (comparable to FAS expression). These levels decreased

rapidly when HT29-tsp53 cells were switched back to the restrictive temperature (Figure 3C). Exposure of these cells to UV light, delayed the decay of the DDB2 transcript significantly (Figure 3C). To ensure that the relative increase in DDB2 mRNA levels following UV exposure was not due to p53-independent UV-mediated transcription, cells were maintained at the restrictive temperature and treated with either 0 or 20 J/m^2 of UV light. The small changes detected in DDB2 expression were negligible compared to the p53-dependent induction of DDB2 at the permissive temperature (Figure 3D). Taken together, the half-lives of DDB2 and $p21^{WAF1}$ mRNA increased significantly following UV exposure ($p = .0015$ and $p < .0001$, respectively) while the half-life of FAS mRNA was unaffected by UV light (Figure 3E).

To determine how UV dose affects the expression of these p53-induced transcripts, cells were again incubated for 16 hours at the permissive temperature to drive p53-dependent gene expression. Cells were then irradiated with the indicated dose of UV light, returned to the restrictive temperature and RNA was collected 0, 3 or 6 hours later for quantitative RT-PCR analysis. As expected, expression of our positive control ($p21^{WAF1}$ mRNA) increased in a dose-dependent manner at 3 hours while expression of FAS was not significantly increased at either time point (Figure 4A and B) [19,20]. Consistent with the results presented in Figure 3, UV light led to a dose-dependent increase in DDB2 expression at both time points (Figure 4A and B). Therefore, the stability of the DDB2 and $p21^{WAF1}$ but not the FAS mRNAs appears to be increased in a UV dose-dependent manner. To determine whether this apparent increase in stability could affect the induction of DDB2, HT29-tsp53 cells were switched to the permissive temperature at the time of UV exposure (between 0 and 30 J/m^2 of UV light) and 6 hours later RNA was extracted for

quantitative RT-PCR analysis. Using this experimental design, we previously reported that gene size had a dramatic impact on the efficiency with which p53 target genes could be induced in response to UV exposure [13]. Therefore, care was taken to compare the expression of transcripts expressed from similar size loci. The DDB2 gene (GeneID: 1643) is 24 kbp, the FAS locus GeneID: 355 is 25 kbp while the MDM2 gene (GeneID: 4193) is 33 kbp. DDB2, MDM2 and FAS were induced to a similar extent in the absence of DNA damage (Figure 5A) but there was a significant difference in the pattern of DDB2 expression compared to MDM2 and FAS when cells were UV-irradiated (Figure 5B). Specifically, UV light prevented the full p53-dependent induction of MDM2 and FAS in a dose-dependent manner with 50% inhibition by 20 J/m^2. In contrast, the induction of DDB2 was increased in response to lower doses of UV light and was not yet inhibited by 50% in response to 30 J/m^2 (Figure 5B). Therefore, UV light differentially affected the expression of these three similarly sized genes, consistent with the differentially effect of UV light on the stability of the DDB2 transcript.

The decay of specific mRNAs is commonly assessed under conditions in which nascent RNA synthesis is blocked with transcriptional inhibitors such as Act D [19,35]. HT29-tsp53 cells were incubated at the permissive temperature for 16 hours to drive p53 target gene expression. Cells were then exposed to either 0 or 20 J/m^2 of UV light and Act D was added to block nascent RNA synthesis while cells remained at the permissive temperature (Figure 6A). The expression of DDB2 was monitored by quantitative RT-PCR over a 6 hour period while $p21^{WAF1}$ again served as a positive control. Consistent with increased stability of the DDB2 and $p21^{WAF1}$ transcripts following UV exposure, more DDB2 and $p21^{WAF1}$ mRNA was detected in UV treated compared to un-irradiated samples

(Figure 6A). This independent method further indicates that DDB2 mRNA decay is inhibited following exposure UV light.

Curiously, the apparent half-lives of $p21^{WAF1}$ and DDB2 transcripts under these conditions were far higher than that the half-lives observed in Figure 3. Therefore, we sought to determine if Act D affected the half-lives of these transcripts or alternatively if the half-lives of these transcripts were affected by temperature shift alone. Again HT29-tsp53 cells were incubated at the permissive temperature for 16 hours to increase the expression of DDB2 and $p21^{WAF1}$ mRNA and then cells were returned to the restrictive temperature in the presence or absence of Act D. RNA was collected at various times to monitor the decay of these transcripts by quantitative RT-PCR (Figure 6B). At the restrictive temperature, Act D treatment resulted in greater expression of both transcripts (Figure 6B). The rate of decay of the DDB2 and $p21^{WAF1}$ mRNAs was not significantly affected by changes in temperature. It should also be noted that mRNA expression determined by quantitative RT-PCR is normalized to the expression of a control mRNA (ACTB) so a horizontal line indicates that the half-life of the indicated transcript is similar to that of ACTB. Therefore, differences in the apparent half-life of DDB2 and $p21^{WAF1}$ mRNAs detected by these two methods likely reflect the combined effect of this normalization process in the presence Act D as well as the potential stabilizing effect of this drug on the turnover of specific mRNAs [16,35]. Despite these apparent quantification differences, both methods indicate that UV light leads to increased stability of DDB2 mRNA.

3.4. DDB2 expression is dependent on ongoing translation following UV exposure

The present work indicates that DDB2 mRNA is post-transcriptionally regulated. Under normal culture conditions, the DDB2 transcript is relatively short-lived but the degradation of this specific mRNA is delayed in response to UV light, in an UV dose-dependent manner. To determine whether the availability of DDB2 mRNA is limiting for protein expression following UV exposure, DDB2 protein levels were assessed by immunoblot. HT29-tsp53 cells were again switched to the permissive temperature for 16 hours to drive p53-dependent gene expression, treated with 0 or 20 J/m^2 of UV light and whole cell extracts were collected for immunoblot analysis at 2 hour intervals. As expected, DDB2 protein levels increased significantly at the permissive temperature and decreased gradually at the restrictive temperature (Figure 7A, lanes 1-6). The induction of DDB2 protein is consistent with the p53-dependent transcription of the DDB2 gene at the permissive temperature while the gradual loss of DDB2 at the restrictive temperature is consistent with the short half-life of the DDB2 mRNA at the restrictive temperature.

Following UV exposure, DDB2 levels decreased abruptly following UV light (Figure 7B, lanes 2, 3 and 7) presumably because DDB2 is degraded in a proteasome-dependent manner following UV exposure [36]. Degradation of DDB2 appears to be required for the assembly of the NER complex at sites of UV-induced DNA damage and this, in turn, affects the repair of this damage [37]. Remarkably, DDB2 protein levels were stable and even recovered somewhat after this initial decrease in expression (Figure 7A) despite the fact that the abundance of DDB2 mRNA decreases slowly over this period of time (Figure 3). Blocking translation by the addition of cycloheximide led to the depletion of DDB2 in UV-treated samples (Figure 7B). We interpret these results to indicate that UV light leads to a dramatic decrease in DDB2 protein levels and that the sustained

expression of DDB2 is highly dependent on *de novo* translation following UV exposure. Therefore, the availability of DDB2 transcript for translation is critical for post-UV expression of DDB2.

4.0. Discussion

4.1. Most p53-regulated transcripts are short-lived

HT29-tsp53 cells express a temperature sensitive variant of p53 that allows for the rapid and reversible manipulation of p53 activity [13,23,25]. Incubation of these cells at the permissive temperature leads to the accumulation of $p21^{WAF1}$ within 2 hours and the rapid onset of a G_1 cell cycle arrest [25]. Returning these cells to the restrictive temperature leads to the rapid loss of p53 activity, as evidenced by the loss of $p21^{WAF1}$ protein and cell cycle re-entry [25]. The decline in $p21^{WAF1}$ protein levels is the result of a combination of the rapid loss of p53 activity coupled with the short half-life of both the $p21^{WAF1}$ mRNA and protein.

In the present work, we used this well-characterized cell line to monitor the decay of p53-regulated mRNAs. HT29-tsp53 cells were incubated at the permissive temperature to drive p53-dependent gene expression and the expression of many p53-regulated transcripts was determined at various times after cells were returned to the restrictive temperature using a combination of oligonucleotide microarrays and quantitative RT-PCR. Almost all of the highly p53-responsive transcripts monitored here decayed rapidly at the restrictive temperature [38,39]. The present results suggest that many p53-responsive transcripts are subject to negative regulation at the level of mRNA stability.

Under normal conditions, p53 expression and its ability to transactivate target genes is inhibited largely though its interaction with the E3 ubiquitin ligase, MDM2, itself a p53 target-gene [40,41]. Because p53 can induce cell cycle arrest and apoptosis, its overexpression is incompatible with cell growth and viability. Dramatic evidence for this comes from the finding that deletion of Mdm2 is embryonic lethal in mice [42,43]. This results from constitutively elevated p53 expression and activity because this phenotype is rescued by crossing Mdm2 null mice into a p53-null background [42,43]. On the other hand, overexpression of MDM2 and the concomitant decrease in p53 expression can be associated with tumorigenesis [44-47]. Therefore, the tight regulation of this negative feedback loop is crucial for maintaining the correct balance between cellular viability and effective p53-mediated stress responses.

Several groups have assessed mRNA decay on a genome-wide scale using oligonucleotide microarrays [39,48,49]. Gene ontology analysis of these data sets indicates that specific functional classes of transcripts are far more likely to be subject to negative regulation by mRNA decay [39,48-50]. Regulators of apoptosis and cell cycle are over represented among the short-lived transcripts [39,48-50], while transcripts encoding metabolic enzymes and structural proteins tend to have longer half-lives [39,50]. The short-lived classes of transcripts were highly represented in the UV_{low} group of p53-responsive transcripts (Table 1). The p53-responsive transcripts in this group were all highly unstable (Table 1). We propose that mRNA decay of this class of p53 target genes cooperates with proteasome-mediated regulation of p53 to keep the p53 transcriptional response in check to allow cell cycle progression and cell survival under appropriate conditions.

The UV_{high} group included both of the relatively stable p53-induced transcripts (CES2 and TP53I3) identified based on our microarray analysis (recall figure 1B) but not all of the transcripts in this group were inherently stable (DDB2, POLH and RRM2B, for example). It is likely that this group includes both inherently stable and UV-stabilized transcripts. The prominence of transcripts encoding DNA repair proteins raises the possibility that post-transcriptional regulation of transcripts encoding DNA repair proteins like DDB2 could permit their expression under conditions in which mRNA synthesis is inhibited by UV light [7-10]. This would aid in recovery from UV exposure prior to commitment to cell death.

Many inherently unstable transcripts encoding dynamically regulated products contain *cis*-acting elements that promote their degradation [18]. The best-characterized *cis*-acting determinant of mRNA decay is the ARE that targets specific mRNAs for rapid decay [49,51]. These elements are most often located within the 3'UTRs of labile mRNAs [52,53]. There is significant heterogeneity in the primary sequence of AREs but they typically contain 1 or more copies of an AUUUA sequence [52,53]. The $p21^{WAF1}$ mRNA has a well-characterized ARE in its 3'UTR [20,21]. According to the ARE database (ARED 3.0, http://brp.kfshrc.edu.sa/ARED/), the FAS mRNA also contains ARE sequences in its 3'UTR [52]. In contrast, there is no identifiable ARE sequence in the DDB2 and MDM2 transcripts, despite their short half-life. Therefore, the rapid decrease in the expression of p53 target genes like $p21^{WAF1}$ and FAS can be explained by ARE-mediated decay while there must be other mechanisms promoting the rapid turnover of other p53-responsive transcripts. We are currently undertaking studies to identify *cis*-acting elements in the DDB2 transcript that promote its rapid turnover in un-irradiated cells.

4.2. DDB2 protein expression is regulated at multiple levels

Xeroderma pigmentosum (XP) is a rare hereditary disease characterized by deficiencies in factors required for nucleotide excision repair (NER). Clinically, it manifests itself in patients as a high incidence of UV light-induced skin cancers and in some cases severe neurological degeneration [54,55]. Cell fusion studies have identified eight subgroups of XP, each of which is defined by mutations in different DNA repair genes. It is the XP-E subgroup that is characterized by defects in DDB2 protein [56]. This leads to a specific deficiency in the GG-NER subpathway of NER. GG-NER is responsible for detecting and repairing lesions throughout the genome without preference for transcribed regions [57]. XP-E patients typically do not show neurological abnormalities and have less severe sun sensitivity than other groups [56,58].

DDB2 is a 48kDa protein found in a complex with the 127kDa DDB1 protein [59]. Together, these subunits form what is known as the UV-damaged damaged DNA binding protein (UV-DDB) [59]. UV-DDB has been shown to bind with high affinity to 6-4PPs and to a lesser extent to CPDs both of which are helix distorting lesions formed in DNA following UV light exposure [56,59]. While its precise role in DNA repair remains enigmatic, it is thought that DDB2 facilitates repair through early damage recognition [60-63]. Immediately following UV irradiation, DDB2 protein colocalizes with sites of DNA damage [60,61,63]. DDB2 forms part of a larger ubiquitin ligase complex that leads to the mono-ubiquitination of histone H2A and polyubiquitination and degradation of DDB2 [37,59,64-68]. The degradation of DDB2 is thought to be required to allow XPC, a crucial DNA damage-recognition protein, to gain access to sites of damage and initiate assembly

of the repair complex [61]. This degradation leads to the depletion in DDB2 levels (recall Figure 7A) such that this protein could become limiting in the face of extensive DNA damage.

It has been known now for several years that p53 transcriptionally upregulates DDB2 following UV irradiation and $p53^{-/-}$ cells are deficient in GGR [69]. Overexpression of DDB2 in p53-deficient cells restores NER capacity [33]. Therefore, the p53-dependent regulation of DDB2 is clearly critical to its function in DNA repair [69,70]. However, the p53-dependent induction of DDB2 mRNA and protein is not maximal until repair is mostly complete [36,71]. The p53- mediated transcriptional induction of DDB2 is too slow to contribute significantly to the initial GG-NER response [72]. Furthermore, the rapid degradation of DDB2 and depletion of the protein at sites of DNA damage could pose a challenge for the repair of extensive DNA damage [36,37,73,74]. Increased stability of DDB2 mRNA observed here coupled with the efficient translation of the stabilized transcripts could provide a mechanism to circumvent the short term loss of DDB2 until transcription of the gene is induced.

5.0. Conclusions

The present work indicates that many p53-induced genes encode unstable RNAs. It is likely that this negatively regulation of p53 target genes decreases the likelihood that spurious activation of the p53 response prevents cell division. It is also clear from the present work that, at least some, p53-induced transcripts can be stabilized to augment the p53-dependent transcriptional response under appropriate conditions. Notably, the DDB2 transcript encodes a DNA repair protein that plays an important role in the repair of UV-

induced DNA damage by NER. Therefore, increased stability of the DDB2 mRNA following UV exposure represents an obvious example of a physiologically relevant response to a DNA damaging agent. We propose that increased stability of DDB2 mRNA represents a previously unrecognized level of DDB2 regulation that plays a role in sustaining adequate *DDB2* levels for NER. These results have important implications for the regulation of NER and prevention of skin carcinogenesis. Our findings also have broader implications for the p53-response. We envisage changes in mRNA stability as a mechanism to fine-tune the p53 response under specific cellular conditions.

6.0 Acknowledgements

This work was supported by the Canadian Institutes of Health Research. The authors would also like to thank the Ottawa Regional Cancer Foundation for seed funding. B.D.M. held an Ontario Graduate Scholarship in Science and Technology. B.C.M. was supported with a Research Scientist Award from the National Cancer Institute of Canada supported with funds provided by the Canadian Cancer Society.

7.0. References

[1] H. van Steeg and K.H. Kraemer Xeroderma pigmentosum and the role of UV-induced DNA damage in skin cancer, Mol Med Today 5 (1999) 86-94.

[2] T. Riley, E. Sontag, P. Chen and A. Levine Transcriptional control of human p53-regulated genes, Nat Rev Mol Cell Biol 9 (2008) 402-412.

[3] L. Latonen and M. Laiho Cellular UV damage responses--functions of tumor suppressor p53, Biochim Biophys Acta 1755 (2005) 71-89.

[4] S. Tornaletti and P.C. Hanawalt Effect of DNA lesions on transcription elongation, Biochimie 81 (1999) 139-146.

[5] M. Protic-Sabljic and K.H. Kraemer One pyrimidine dimer inactivates expression of a transfected gene in xeroderma pigmentosum cells, Proc Natl Acad Sci U S A 82 (1985) 6622-6626.

[6] W. Sauerbier and K. Hercules Gene and transcription unit mapping by radiation effects, Annu Rev Genet 12 (1978) 329-363.

[7] J.H. Epstein, K. Fukuyama and K. Fye Effects of ultraviolet radiation on the mitotic cycle and DNA, RNA and protein synthesis in mammalian epidermis in vivo, Photochem Photobiol 12 (1970) 57-65.

[8] L.V. Mayne and A.R. Lehmann Failure of RNA synthesis to recover after UV irradiation: an early defect in cells from individuals with Cockayne's syndrome and xeroderma pigmentosum, Cancer Res 42 (1982) 1473-1478.

[9] M. Ljungman and F. Zhang Blockage of RNA polymerase as a possible trigger for u.v. light-induced apoptosis, Oncogene 13 (1996) 823-831.

[10] B.C. McKay, F. Chen, S.T. Clarke, H.E. Wiggin, L.M. Harley and M. Ljungman UV light-induced degradation of RNA polymerase II is dependent on the Cockayne's syndrome A and B proteins but not p53 or MLH1, Mutat Res 485 (2001) 93-105.

[11] M.J. Mone, M. Volker, O. Nikaido, L.H. Mullenders, A.A. van Zeeland, P.J. Verschure, E.M. Manders and R. van Driel Local UV-induced DNA damage in cell nuclei results in local transcription inhibition, EMBO Rep 2 (2001) 1013-1017.

[12] D.A. Rockx, R. Mason, A. van Hoffen, M.C. Barton, E. Citterio, D.B. Bregman, A.A. van Zeeland, H. Vrieling and L.H. Mullenders UV-induced inhibition of transcription involves repression of transcription initiation and phosphorylation of RNA polymerase II, Proc Natl Acad Sci U S A 97 (2000) 10503-10508.

[13] B.C. McKay, L.J. Stubbert, C.C. Fowler, J.M. Smith, R.A. Cardamore and J.C. Spronck Regulation of ultraviolet light-induced gene expression by gene size, Proc Natl Acad Sci U S A 101 (2004) 6582-6586.

[14] J. Fan, X. Yang, W. Wang, W.H. Wood, 3rd, K.G. Becker and M. Gorospe Global analysis of stress-regulated mRNA turnover by using cDNA arrays, Proc Natl Acad Sci U S A 99 (2002) 10611-10616.

[15] F. Bollig, R. Winzen, M. Kracht, B. Ghebremedhin, B. Ritter, A. Wilhelm, K. Resch and H. Holtmann Evidence for general stabilization of mRNAs in response to UV light, Eur J Biochem 269 (2002) 5830-5839.

[16] C.Y. Chen, N. Ezzeddine and A.B. Shyu Messenger RNA half-life measurements in mammalian cells, Methods Enzymol 448 (2008) 335-357.

[17] G. Gowrishankar, R. Winzen, F. Bollig, B. Ghebremedhin, N. Redich, B. Ritter, K. Resch, M. Kracht and H. Holtmann Inhibition of mRNA deadenylation and degradation by ultraviolet light, Biol Chem 386 (2005) 1287-1293.

[18] C. Barreau, L. Paillard and H.B. Osborne AU-rich elements and associated factors: are there unifying principles?, Nucleic Acids Res 33 (2005) 7138-7150.
[19] W. Wang, H. Furneaux, H. Cheng, M.C. Caldwell, D. Hutter, Y. Liu, N. Holbrook and M. Gorospe HuR regulates p21 mRNA stabilization by UV light, Mol Cell Biol 20 (2000) 760-769.
[20] M. Gorospe, X. Wang and N.J. Holbrook p53-dependent elevation of p21Waf1 expression by UV light is mediated through mRNA stabilization and involves a vanadate-sensitive regulatory system, Mol Cell Biol 18 (1998) 1400-1407.
[21] B. Joseph, M. Orlian and H. Furneaux p21(waf1) mRNA contains a conserved element in its 3'-untranslated region that is bound by the Elav-like mRNA-stabilizing proteins, J Biol Chem 273 (1998) 20511-20516.
[22] M. Gorospe HuR in the mammalian genotoxic response: post-transcriptional multitasking, Cell Cycle 2 (2003) 412-414.
[23] A.K. Merchant, T.L. Loney and J. Maybaum Expression of wild-type p53 stimulates an increase in both Bax and Bcl-xL protein content in HT29 cells, Oncogene 13 (1996) 2631-2637.
[24] J.V. Gannon and D.P. Lane Protein synthesis required to anchor a mutant p53 protein which is temperature-sensitive for nuclear transport, Nature 349 (1991) 802-806.
[25] B.C. McKay, F. Chen, C.R. Perumalswami, F. Zhang and M. Ljungman The tumor suppressor p53 can both stimulate and inhibit ultraviolet light-induced apoptosis, Mol Biol Cell 11 (2000) 2543-2551.
[26] E. Sbisa, D. Catalano, G. Grillo, F. Licciulli, A. Turi, S. Liuni, G. Pesole, A. De Grassi, M.F. Caratozzolo, A.M. D'Erchia, B. Navarro, A. Tullo, C. Saccone and A. Gisel p53FamTaG: a database resource of human p53, p63 and p73 direct target genes combining in silico prediction and microarray data, BMC Bioinformatics 8 Suppl 1 (2007) S20.
[27] D. Michalovitz, O. Halevy and M. Oren Conditional inhibition of transformation and of cell proliferation by a temperature-sensitive mutant of p53, Cell 62 (1990) 671-680.
[28] T. Beissbarth and T.P. Speed GOstat: find statistically overrepresented Gene Ontologies within a group of genes, Bioinformatics 20 (2004) 1464-1465.
[29] A. Pines, C. Backendorf, S. Alekseev, J.G. Jansen, F.R. de Gruijl, H. Vrieling and L.H. Mullenders Differential activity of UV-DDB in mouse keratinocytes and fibroblasts: impact on DNA repair and UV-induced skin cancer, DNA Repair (Amst) 8 (2009) 153-161.
[30] T. Itoh Xeroderma pigmentosum group E and DDB2, a smaller subunit of damage-specific DNA binding protein: proposed classification of xeroderma pigmentosum, Cockayne syndrome, and ultraviolet-sensitive syndrome, J Dermatol Sci 41 (2006) 87-96.
[31] G. Kulaksiz, J.T. Reardon and A. Sancar Xeroderma pigmentosum complementation group E protein (XPE/DDB2): purification of various complexes of XPE and analyses of their damaged DNA binding and putative DNA repair properties, Mol Cell Biol 25 (2005) 9784-9792.
[32] T. Yoon, A. Chakrabortty, R. Franks, T. Valli, H. Kiyokawa and P. Raychaudhuri Tumor-prone phenotype of the DDB2-deficient mice, Oncogene 24 (2005) 469-478.
[33] M.E. Fitch, I.V. Cross, S.J. Turner, S. Adimoolam, C.X. Lin, K.G. Williams and J.M. Ford The DDB2 nucleotide excision repair gene product p48 enhances global genomic repair in p53 deficient human fibroblasts, DNA Repair (Amst) 2 (2003) 819-826.

[34] C.J. Westmark, V.B. Bartleson and J.S. Malter RhoB mRNA is stabilized by HuR after UV light, Oncogene 24 (2005) 502-511.
[35] C.Y. Chen, N. Xu and A.B. Shyu mRNA decay mediated by two distinct AU-rich elements from c-fos and granulocyte-macrophage colony-stimulating factor transcripts: different deadenylation kinetics and uncoupling from translation, Mol Cell Biol 15 (1995) 5777-5788.
[36] V. Rapic-Otrin, M.P. McLenigan, D.C. Bisi, M. Gonzalez and A.S. Levine Sequential binding of UV DNA damage binding factor and degradation of the p48 subunit as early events after UV irradiation, Nucleic Acids Res 30 (2002) 2588-2598.
[37] M.A. El-Mahdy, Q. Zhu, Q.E. Wang, G. Wani, M. Praetorius-Ibba and A.A. Wani Cullin 4A-mediated proteolysis of DDB2 protein at DNA damage sites regulates in vivo lesion recognition by XPC, J Biol Chem 281 (2006) 13404-13411.
[38] J.R. Greenberg High stability of messenger RNA in growing cultured cells, Nature 240 (1972) 102-104.
[39] A. Raghavan and P.R. Bohjanen Microarray-based analyses of mRNA decay in the regulation of mammalian gene expression, Brief Funct Genomic Proteomic 3 (2004) 112-124.
[40] J. Momand, G.P. Zambetti, D.C. Olson, D. George and A.J. Levine The mdm-2 oncogene product forms a complex with the p53 protein and inhibits p53-mediated transactivation, Cell 69 (1992) 1237-1245.
[41] R. Honda, H. Tanaka and H. Yasuda Oncoprotein MDM2 is a ubiquitin ligase E3 for tumor suppressor p53, FEBS Lett 420 (1997) 25-27.
[42] S.N. Jones, A.E. Roe, L.A. Donehower and A. Bradley Rescue of embryonic lethality in Mdm2-deficient mice by absence of p53, Nature 378 (1995) 206-208.
[43] R. Montes de Oca Luna, D.S. Wagner and G. Lozano Rescue of early embryonic lethality in mdm2-deficient mice by deletion of p53, Nature 378 (1995) 203-206.
[44] T. Watanabe, A. Ichikawa, H. Saito and T. Hotta Overexpression of the MDM2 oncogene in leukemia and lymphoma, Leuk Lymphoma 21 (1996) 391-397, color plates XVI following 395.
[45] C.A. Finlay The mdm-2 oncogene can overcome wild-type p53 suppression of transformed cell growth, Mol Cell Biol 13 (1993) 301-306.
[46] C.M. Eischen, J.D. Weber, M.F. Roussel, C.J. Sherr and J.L. Cleveland Disruption of the ARF-Mdm2-p53 tumor suppressor pathway in Myc-induced lymphomagenesis, Genes Dev 13 (1999) 2658-2669.
[47] E. Rayburn, R. Zhang, J. He and H. Wang MDM2 and human malignancies: expression, clinical pathology, prognostic markers, and implications for chemotherapy, Curr Cancer Drug Targets 5 (2005) 27-41.
[48] L.V. Sharova, A.A. Sharov, T. Nedorezov, Y. Piao, N. Shaik and M.S. Ko Database for mRNA half-life of 19 977 genes obtained by DNA microarray analysis of pluripotent and differentiating mouse embryonic stem cells, DNA Res 16 (2009) 45-58.
[49] J. Mata, S. Marguerat and J. Bahler Post-transcriptional control of gene expression: a genome-wide perspective, Trends Biochem Sci 30 (2005) 506-514.
[50] E. Yang, E. van Nimwegen, M. Zavolan, N. Rajewsky, M. Schroeder, M. Magnasco and J.E. Darnell, Jr. Decay rates of human mRNAs: correlation with functional characteristics and sequence attributes, Genome Res 13 (2003) 1863-1872.

[51] H.H. Hau, R.J. Walsh, R.L. Ogilvie, D.A. Williams, C.S. Reilly and P.R. Bohjanen Tristetraprolin recruits functional mRNA decay complexes to ARE sequences, J Cell Biochem 100 (2007) 1477-1492.
[52] T. Bakheet, B.R. Williams and K.S. Khabar ARED 3.0: the large and diverse AU-rich transcriptome, Nucleic Acids Res 34 (2006) D111-114.
[53] T. Bakheet, M. Frevel, B.R. Williams, W. Greer and K.S. Khabar ARED: human AU-rich element-containing mRNA database reveals an unexpectedly diverse functional repertoire of encoded proteins, Nucleic Acids Res 29 (2001) 246-254.
[54] K.H. Kraemer, N.J. Patronas, R. Schiffmann, B.P. Brooks, D. Tamura and J.J. DiGiovanna Xeroderma pigmentosum, trichothiodystrophy and Cockayne syndrome: a complex genotype-phenotype relationship, Neuroscience 145 (2007) 1388-1396.
[55] I. Rapin, Y. Lindenbaum, D.W. Dickson, K.H. Kraemer and J.H. Robbins Cockayne syndrome and xeroderma pigmentosum, Neurology 55 (2000) 1442-1449.
[56] J. Tang and G. Chu Xeroderma pigmentosum complementation group E and UV-damaged DNA-binding protein, DNA Repair (Amst) 1 (2002) 601-616.
[57] S. Tornaletti DNA repair in mammalian cells: Transcription-coupled DNA repair: directing your effort where it's most needed, Cell Mol Life Sci 66 (2009) 1010-1020.
[58] T. Itoh, D. Cado, R. Kamide and S. Linn DDB2 gene disruption leads to skin tumors and resistance to apoptosis after exposure to ultraviolet light but not a chemical carcinogen, Proc Natl Acad Sci U S A 101 (2004) 2052-2057.
[59] Y. Fujiwara, C. Masutani, T. Mizukoshi, J. Kondo, F. Hanaoka and S. Iwai Characterization of DNA recognition by the human UV-damaged DNA-binding protein, J Biol Chem 274 (1999) 20027-20033.
[60] M.E. Fitch, I.V. Cross and J.M. Ford p53 responsive nucleotide excision repair gene products p48 and XPC, but not p53, localize to sites of UV-irradiation-induced DNA damage, in vivo, Carcinogenesis 24 (2003) 843-850.
[61] M.E. Fitch, S. Nakajima, A. Yasui and J.M. Ford In vivo recruitment of XPC to UV-induced cyclobutane pyrimidine dimers by the DDB2 gene product, J Biol Chem 278 (2003) 46906-46910.
[62] Q.E. Wang, Q. Zhu, G. Wani, J. Chen and A.A. Wani UV radiation-induced XPC translocation within chromatin is mediated by damaged-DNA binding protein, DDB2, Carcinogenesis 25 (2004) 1033-1043.
[63] J. Moser, M. Volker, H. Kool, S. Alekseev, H. Vrieling, A. Yasui, A.A. van Zeeland and L.H. Mullenders The UV-damaged DNA binding protein mediates efficient targeting of the nucleotide excision repair complex to UV-induced photo lesions, DNA Repair (Amst) 4 (2005) 571-582.
[64] J. Li, Q.E. Wang, Q. Zhu, M.A. El-Mahdy, G. Wani, M. Praetorius-Ibba and A.A. Wani DNA Damage Binding Protein Component DDB1 Participates in Nucleotide Excision Repair through DDB2 DNA-binding and Cullin 4A Ubiquitin Ligase Activity, Cancer Res 66 (2006) 8590-8597.
[65] Q.E. Wang, Q. Zhu, G. Wani, M.A. El-Mahdy, J. Li and A.A. Wani DNA repair factor XPC is modified by SUMO-1 and ubiquitin following UV irradiation, Nucleic Acids Res 33 (2005) 4023-4034.
[66] J. Guerrero-Santoro, M.G. Kapetanaki, C.L. Hsieh, I. Gorbachinsky, A.S. Levine and V. Rapic-Otrin The cullin 4B-based UV-damaged DNA-binding protein ligase binds to UV-damaged chromatin and ubiquitinates histone H2A, Cancer Res 68 (2008) 5014-5022.

[67] M.G. Kapetanaki, J. Guerrero-Santoro, D.C. Bisi, C.L. Hsieh, V. Rapic-Otrin and A.S. Levine The DDB1-CUL4ADDB2 ubiquitin ligase is deficient in xeroderma pigmentosum group E and targets histone H2A at UV-damaged DNA sites, Proc Natl Acad Sci U S A 103 (2006) 2588-2593.
[68] K. Sugasawa, Y. Okuda, M. Saijo, R. Nishi, N. Matsuda, G. Chu, T. Mori, S. Iwai, K. Tanaka, K. Tanaka and F. Hanaoka UV-induced ubiquitylation of XPC protein mediated by UV-DDB-ubiquitin ligase complex, Cell 121 (2005) 387-400.
[69] B.J. Hwang, J.M. Ford, P.C. Hanawalt and G. Chu Expression of the p48 xeroderma pigmentosum gene is p53-dependent and is involved in global genomic repair, Proc Natl Acad Sci U S A 96 (1999) 424-428.
[70] J.Y. Tang, B.J. Hwang, J.M. Ford, P.C. Hanawalt and G. Chu Xeroderma pigmentosum p48 gene enhances global genomic repair and suppresses UV-induced mutagenesis, Mol Cell 5 (2000) 737-744.
[71] A.F. Nichols, T. Itoh, J.A. Graham, W. Liu, M. Yamaizumi and S. Linn Human damage-specific DNA-binding protein p48. Characterization of XPE mutations and regulation following UV irradiation, J Biol Chem 275 (2000) 21422-21428.
[72] B.C. McKay, M. Ljungman and A.J. Rainbow Potential roles for p53 in nucleotide excision repair, Carcinogenesis 20 (1999) 1389-1396.
[73] X. Chen, Y. Zhang, L. Douglas and P. Zhou UV-damaged DNA-binding proteins are targets of CUL-4A-mediated ubiquitination and degradation, J Biol Chem 276 (2001) 48175-48182.
[74] A. Nag, T. Bondar, S. Shiv and P. Raychaudhuri The xeroderma pigmentosum group E gene product DDB2 is a specific target of cullin 4A in mammalian cells, Mol Cell Biol 21 (2001) 6738-6747.

Figure legends

Figure 1. p53-induced transcripts are short-lived. (A) HT29-tsp53 cells were grown at the restrictive temperature (38°C) and were then switched to the permissive temperature (32°C) for 16h to increase the expression of p53 target-genes (t = 0h). Cells were then returned to the restrictive temperature for 6h. RNA was collected at -16, 0 and 6h as indicated by the arrows. (B) Fold increase in expression at 6h (expression at 6h/expression at -16h) is expressed relative to the fold increase at 0h (expression at 0h/expression at -16h), as assessed by oligonucleotide microarray analysis. Values for 21 previously reported p53-induced genes are presented along with a line of best fit and 95% confidence intervals. (C) The relative expression of 8 previously characterized p53-regulated genes was monitored by quantitative RT-PCR to confirm the p53-dependent pattern of expression detected through microarray analysis. Transcripts are designated by official gene name except that SERPINB5 and CDKN1A are abbreviated SB5 and p21, respectively. Values in B were determined from 2 independent microarray experiments while the values in C represent the mean ± standard error of 3 independent experiments.

Figure 2. The effect of UV light on the decay of p53-regulated transcripts at the restrictive temperature. HT29-tsp53 cells were incubated at the permissive temperature for 16h, treated with 0 or 20 J/m^2 of UV light and returned to the restrictive temperature for 6h. RNA was collected at -16, 0 and 6h and samples were subjected to oligonucleotide microarray analysis as described in Figure 1. (A) Expression of 21 p53-regulated transcripts is expressed as fold change relative to the level of expression detected in samples collected at the restrictive temperature (-16 h). Each value represents the mean determined from two independent experiments (B) Fold change at 6 h (+/- UV light, as indicated in right and left panels) is plotted as a function of fold increase at the permissive temperature. The behaviour of 10 and 11 p53-regulated transcripts that appeared to exhibit differential responsiveness to UV light were plotted separately (open and closed circles). Expression values for each group of p53-regulated transcript were fit by linear regression and are plotted with 95% confidence intervals.

Figure 3. The effect of UV light on the decay of several p53-regulated transcripts was monitored in HT29-tsp53 cells. HT29-tsp53 cells were incubated at the permissive temperature for 16h, treated with 0 or 20 J/m^2 of UV light and returned to the restrictive temperature, as described in Figure 2. At the indicated times, total RNA was collected and subjected to quantitative RT-PCR analysis for p21^{WAF1} (A), FAS (B) and DDB2 (C). (D) DDB2 expression was similarly assessed in cells maintained at the restrictive temperature and mRNA expression was normalized to controls switched to the permissive temperature for 16h (t=0 h) (E) The half-life of p21^{WAF1}, FAS and DDB2 mRNAs was estimated from individual experiments like those presented in A-C. The half-life for DDB2 and p21^{WAF1} was significantly increased following UV exposure ($p=0.0015$ and $p<0.0001$, respectively as determined by Student *t* test). All values in A-E represent the mean ± standard error of at least 3 independent experiments. Significant differences between the indicated value and its respective control in (A-C) (*$p<0.05$) were determined using Student *t* test.

Figure 4. DDB2, p21^{WAF1} but not FAS mRNA is stabilized in a dose-dependent manner following exposure to UV light. HT29-tsp53 cells were grown at the restrictive temperature (38°C) and were then switched to the permissive temperature (32°C) for 16h to increase p53-dependent gene expression. Cells were treated with the indicated dose of UV light (at t=0h). They were subsequently switched back to the restrictive temperature to decrease p53 activity as described in Figure 1. RNA was collected at -16, 0, 3 (A) and 6h (B) relative to UV exposure. The relative expression of DDB2 (left panels), FAS (middle panels) and p21 ^{WAF1} (right panels) were analysed by quantitative RT-PCR. All values represent the mean ± standard error of 3 independent experiments. Significant differences (*$p<0.005$) between UV-treated samples and unirradiated samples collected at the same time were determined using Student *t* test.

Figure 5. Differential pattern of p53-dependent gene expression following UV exposure. HT29-tsp53 cells were treated with the indicated dose of UV light immediately before being placed at the permissive temperature for 6h. (A) The expression of MDM2, FAS, and DDB2 mRNAs was analysed by real-time quantitative RT-PCR and expressed as fold increase in expression. (B) The expression of DDB2, FAS and MDM2 is expressed relative to the induced level in unirradiated controls and is plotted as a function of UV dose. All values represent the mean ± standard error of 3 independent experiments.

Figure 6. UV light stabilizes DDB2 and p21 ^{WAF1} mRNA in the presence of actinomycin D. (A) As schematically represented in the upper panel, HT29-tsp53 cells were incubated at the permissive temperature (32°C) for 16h to increase p53-dependent gene expression. At time 0h, cells were treated with 0 or 20 J/m^2 and Act D (5μg/ml) was added to block nascent RNA synthesis. RNA was collected at the indicated times and relative mRNA expression is normalized to the induced level immediately prior to the addition of Act D (lower panels). (B) As schematically represented in the upper panel, HT29-tsp53 cells were incubated at the permissive temperature(32°C) for 16h to increase p53-dependent gene expression. Act D (5μg/ml) was added to block nascent RNA synthesis and cells were returned to the restrictive temperature (38°C). RNA was collected at the indicated times and relative mRNA expression is normalized to the induced level immediately prior to the addition of Act D (lower panels). Values in A and B represent the mean ± standard error of at least 3 independent experiments. * denotes that the value is significantly different from its repective control (* $p<0.05$) as determined using Student *t* test.

Figure 7. mRNA stability affects DDB2 protein levels. (A) HT29-tsp53 were treated as described in Figure 3 except that whole cell lysates were collected at the indicated times and subjected to immunoblot analysis for DDB2 and β actin. (B) Cells were treated as in A, except that cycloheximide (CHX) was added (50μg/ml) to inhibit *de novo* translation. Similar results were obtained in 3 independent experiments.

Table 1: p53-induced transcripts.

	Gene ontology[a]				Incubated for 16h at 32°C		
					t = 0h[b]	t = 6h[b]	
mRNA	1	2	3	4	**-UV**	**-UV**	**+UV**
TNFRSF10[c]	•				3.3[d]	1.1	1.0
DDIT4	•				3.7	1.0	1.1
SESN1		•	•		4.3	1.1	1.4
GADD45A	•	•	•		5.9	1.1	2.0
BTG2	•		•		6.0	1.1	1.5
FAS	•				6.2	1.2	1.4
GDF15					7.2	1.0	1.5
MDM2					7.9	1.0	2.6
CDKN1A	•	•	•		9.6	1.2	2.0
TP53INP1	•				11.6	1.1	3.4
CYFIP2[c]	•				3.0	1.5	2.2
CCNG1					3.1	1.3	2.0
SERPINB5					3.2	1.1	2.0
PRKAB1					3.5	1.0	1.8
C12orf5					4.1	1.0	1.8
POLH			•	•	4.2	1.0	1.8
DDB2			•	•	4.4	1.4	2.5
CES2					5.0	1.9	3.3
TP53I3	•				5.8	2.8	4.1
ZMAT3	•		•		6.3	1.3	3.3
RRM2B			•	•	6.8	1.6	4.1

[a] 1, 2, 3 and 4 represent apoptosis (GO: 0006915), cell cycle arrest (GO: 000750) , response to DNA damage (GO: 0006974) and DNA repair (GO: 0006281), respectively.

[b] Refer to figure 1A for a schematic representation of t=0 and t=6h.

[c] The p53 regulated transcripts are grouped into categories based on figure 2B. The upper and lower sections of the table correspond to UV_{low} and UV_{high} groups, respectively.

[d] Fold change is expressed relative to samples collected at -16 h (see Figure 1A).

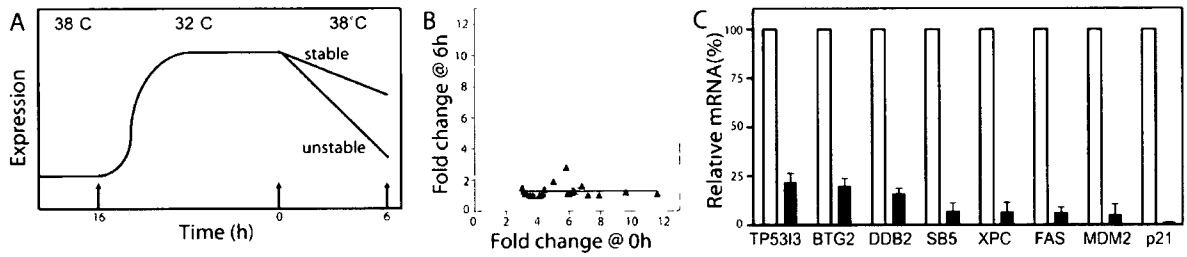
A
38 C
32 C
38°C
stable
unstable
Expression
16
0
6
Time (h)
B
Fold change @ 6h
Fold change @ 0h
C
Relative mRNA(%)
TP53I3
BTG2
DDB2
SB5
XPC
FAS
MDM2
p21

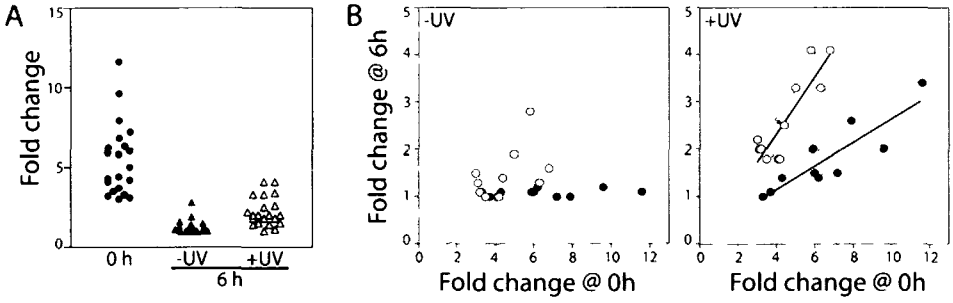
A
Fold change
15
10
5
0
0 h
-UV
+UV
6 h
B
-UV
+UV
Fold change @ 6h
Fold change @ 0h
Fold change @ 0h
0
1
2
3
4
5
0
2
4
6
8
10
12

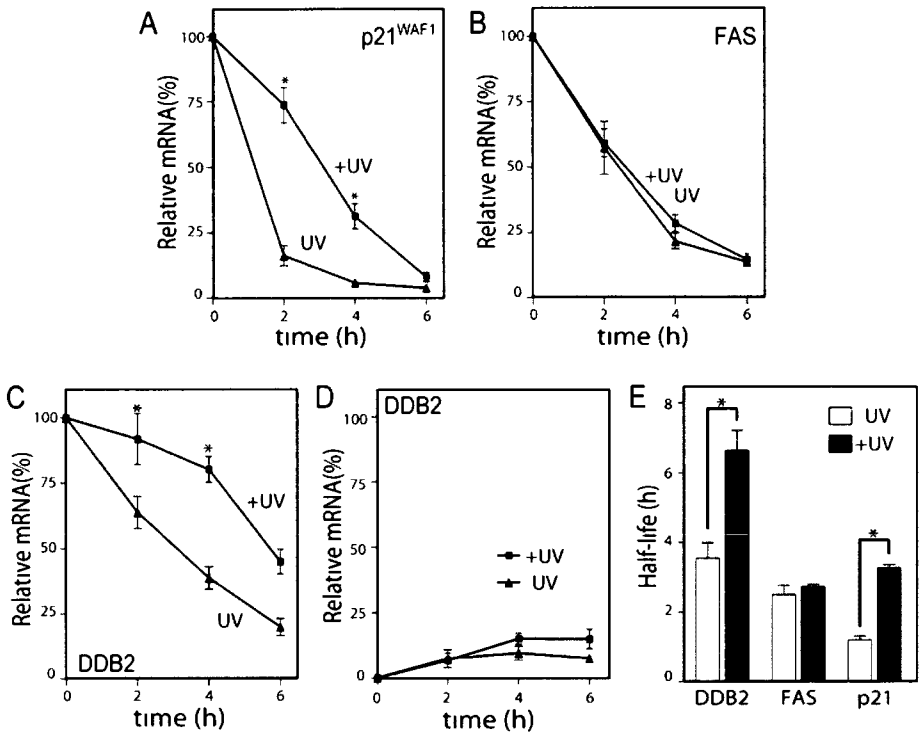
A
p21WAF1
Relative mRNA(%)
+UV
UV
time (h)
B
FAS
Relative mRNA(%)
+UV
UV
time (h)
C
Relative mRNA(%)
+UV
UV
DDB2
time (h)
D
DDB2
Relative mRNA(%)
+UV
UV
time (h)
E
UV
+UV
Half-life (h)
DDB2
FAS
p21

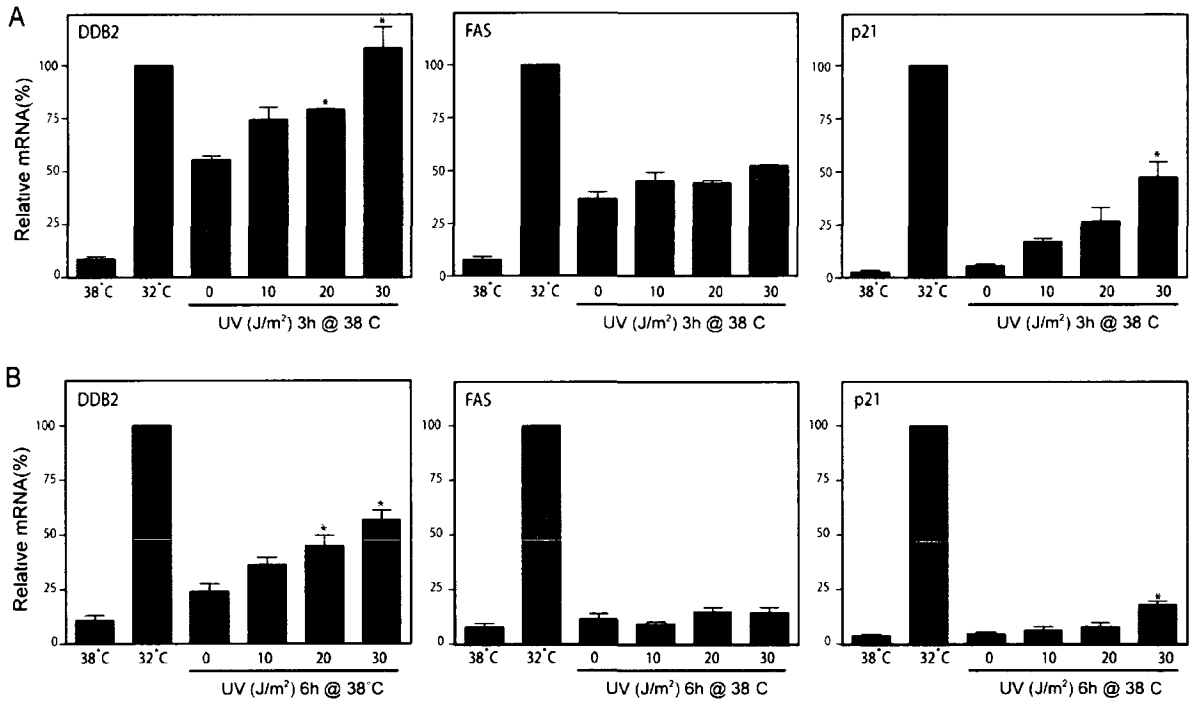
A
DDB2
FAS
p21
Relative mRNA(%)
100
75
50
25
0
38°C
32°C
0
10
20
30
UV (J/m²) 3h @ 38 C
B
DDB2
FAS
p21
Relative mRNA(%)
UV (J/m²) 6h @ 38°C
UV (J/m²) 6h @ 38 C

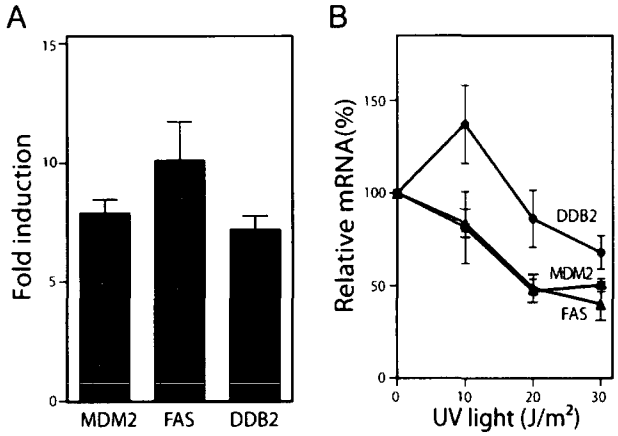
A
Fold induction
15
10
5
0
MDM2
FAS
DDB2
B
Relative mRNA(%)
150
100
50
0
DDB2
MDM2
FAS
0
10
20
30
UV light (J/m²)

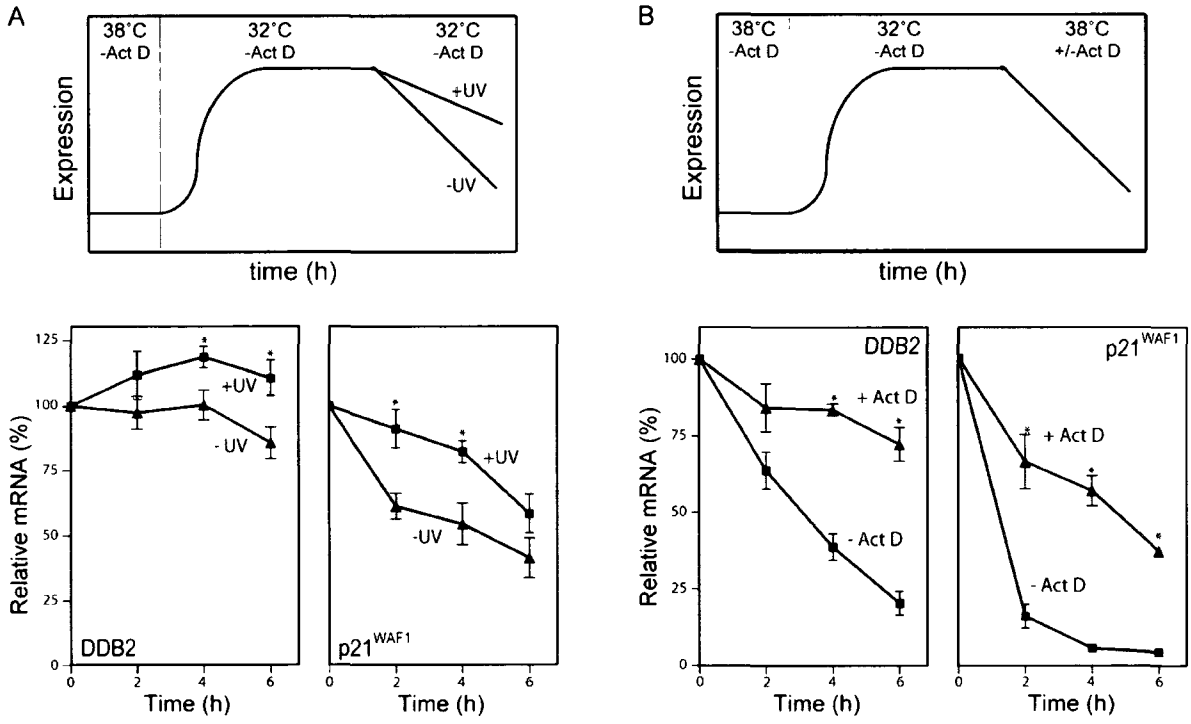
A
38°C
-Act D
32°C
-Act D
32°C
-Act D
+UV
-UV
Expression
time (h)
B
38°C
-Act D
32°C
-Act D
38°C
+/-Act D
Expression
time (h)
Relative mRNA (%)
DDB2
+UV
- UV
Time (h)
p21WAF1
+UV
-UV
Time (h)
DDB2
+ Act D
- Act D
Relative mRNA (%)
Time (h)
p21WAF1
+ Act D
- Act D
Time (h)

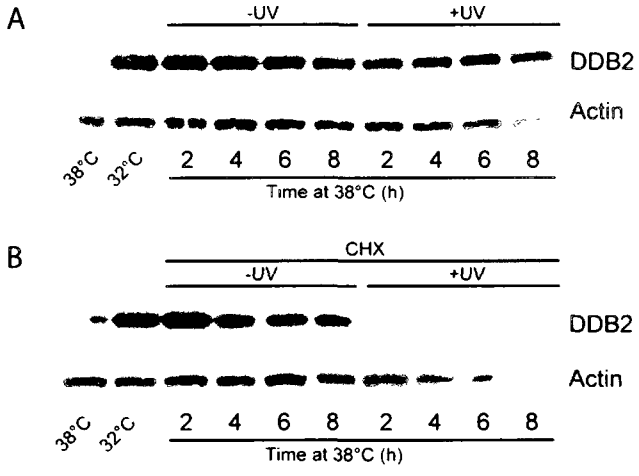
A
-UV
+UV
DDB2
Actin
38°C
32°C
2 4 6 8 2 4 6 8
Time at 38°C (h)
B
CHX
-UV
+UV
DDB2
Actin
38°C
32°C
2 4 6 8 2 4 6 8
Time at 38°C (h)

Supplementary Table 1: Transcripts induced three-fold or more at the permissive temperature.

Affymetrix cluster identifier	Official Gene Symbol	Entrez Gene ID #	p53 reg	0 h	Fold increase in expression 6 h	
					- UV	+ UV
7951662	CRYAB	1410		33.5	20.1	33.6
8066619	PLTP	5360		13.6	10.0	14.7
8151890	TP53INP1	94241	•	11.6	1.1	3.4
8119088	CDKN1A	1026	•	9.6	1.2	2.0
7956989	MDM2	4193	•	7.9	1.0	2.6
8027002	GDF15	9518	•	7.2	1.0	1.5
8152133	RRM2B	50484	•	6.8	1.6	4.1
8058708	ABCA12	26154		6.5	2.1	4.0
8092230	ZMAT3	64393	•	6.3	1.3	3.3
7929032	FAS	355	•	6.2	1.2	1.4
7908917	BTG2	7832	•	6.0	1.1	1.5
8073068	APOBEC3C APOBEC 3D	27350 140564		6.0	3.0	5.6
7902227	GADD45A	1647	•	5.9	1.1	2.0
8050702	TP53I3	9540	•	5.8	2.8	4.1
7940654	SCGB1A1	7356		5.6	3.7	6.3
8026490	UCA1	652995		5.1	2.4	6
7996345	CES2	8824	•	5.0	1.9	3
7952290	TRIM29	23650		4.6	2.0	3.6
7914270	LAPTM5	7805		4.6	3.2	4.6
7939738	DDB2	1643	•	4.4	1.4	2.5
8121257	PRDM1	639		4.3	1.0	1.2
7964183	GLS2	27165		4.3	1.8	2.8
8128698	SESN1	27244	•	4.3	1.1	4
8119858	POLH	5429	•	4.2	1.0	1.8
7935746	BLOC1S2	282991		4.1	1.0	2.4
7953211	C12orf5	57103	•	4.1	1.0	1.8
8091515	GPR87	53836		4.0	1.3	1.1
7935553	LOXL4	84171		4.0	2.0	2.5
8109926	GABRP	2568		3.9	2.1	3.1
8109344	GM2A	2760		3.9	2.2	3.8
7941761	RHOD	29984		3.9	1.8	2.5
7912343	CASZ1	54897		3.8	1.0	1.5
7958019	DRAM1	55332		3.7	1.0	1.9
8113790	c3hc4	115123		3.7	1.1	1.1
7928308	DDIT4	54541	•	3.7	1.0	1.1
7922976	PTGS2	5743		3.6	1.7	1.7
8072962	MICALL1	85377		3.5	1.2	1.7
7986446	ALDH1A3	220		3.5	1.6	2.6
7959123	PRKAB1	5564	•	3.5	1.0	1.8
7982985	MAPKBP1	23005		3.5	1.0	1.7
8053406	RETSAT	54884		3.4	1.8	3.5
7912347	CASZ1	54897		3.4	1.0	1.5
8092169	TNFSF10	8743	•	3.3	1.1	1.0
8057959	PGAP1	80055		3.2	1.2	2.2

8021584	SERPINB5	5268	•	3.2	1.1	2.0
8109697	CCNG1	900	•	3.1	1.2	2.0
	CTSD	1509				
7945663	LOC402778	402778		3.1	2.1	3.1
8005743	FLJ36000	284124		3.1	1.3	2.0
7956046	DGKA	1606		3.0	1.2	2.1
7969493	SCEL	8796		3.0	1.53	2.3
8119926	TMEM63B	55362		3.0		
7968883	C13orf31	144811		3.0	1.0	1.5
8109528	CYFIP2	26999	•	3.0	1.5	2.2